GABAergic Signalling in Temporal Lobe Epilepsy

Ruba Sayed Benini

Degree of Doctor of Philosophy

Department of Neurology & Neurosurgery

McGill University
Montreal, Quebec, Canada
January, 2006

A thesis submitted to the faculty of Graduate Studies and Research in partial fulfillment of the requirements of the degree of Doctor of Philosophy.

Your file Votre référence
ISBN: 978-0-494-25100-3
Our file Notre référence
ISBN: 978-0-494-25100-3

DEDICATION

"And of knowledge, you (mankind) have been given only a little"

(Translation of Qur'an 17:85)

This dissertation is dedicated to all those who attain humility during their quest for Knowledge and Truth.

ACKNOWLEDGMENTS

First and foremost, I would like to take this opportunity to thank my supervisor, Dr. Massimo Avoli, for allowing my graduate training at McGill University to be a truly enriching experience. His approach to research has played a crucial role not only in teaching me how to formulate the relevant scientific questions but also how to probe for the important answers. I am also truly grateful for his flexible and open-minded attitude which, during my studies, gave me the liberty to be scientifically creative in putting forth my hypotheses and designing my experiments. To say the least, it was truly a pleasure to work under the supervision of Dr. Avoli.

The next best thing to having a good supervisor is to have a good group to work with, which thankfully I did. My colleagues Philip de Guzman, Dr. Giulia Curia, Jessica Sudbury and Dr. Margherita D'Antuono were truly the best people I could ever imagine working with. Together, we wrestled perplexing scientific questions and frustrating technical problems (a common phenomenon in the field of electrophysiology!). The amicable personalities of each of them created such an enjoyable atmosphere within the lab that I always looked forward to coming in every morning. The impression that these individuals have made upon me leaves me hopeful that I get the opportunity to work with similar personalities in the future.

Working in Dr. Avoli's lab also gave me the rare opportunity to interact with a number of visiting scientists from different parts of the world. From Dr. Giuseppe Biagini (from Italy), Dr. Etienne Pralong (from Switzerland), Dr. Pierreangelo Cifelli (Italy), Dr. Toshi Kano (from Japan) and Dr. Yuji Inaba (from Japan) I learnt a lot of interesting facts not only about science and medicine but also about different cultures.

I am also indebted to my advisory committee members (Dr. François Dubeau, Dr. Jean-Claude Lacaille and Dr. Radan Čapek) and my mentor (Dr. David Ragsdale) for the invaluable advice and guidance they offered me during the course of my research.

I would like to express my gratitude to Ms. Toula Papadopoulus for her secretarial help with the articles as well as for her patience and readiness to assist whenever I came to her. Furthermore, I would also like to thank the MNI Animal Facility (Mrs. Janet Green and others); the Neurophotography crew (especially Susan Kaupp and Jean-Paul Acco) and the Neuroelectronics technicians (especially Pascal Lizotte and Jocelyn Roy) for all their help.

I would like to take this opportunity to thank all the graduate students and technicians that work in the labs of Dr. Philippe Seguela, Dr. David Ragsdale, and the late Dr. Angel Alonso for their help whenever I needed them. I would also like to especially thank Dr. Seguela for his help with the French translation of my PhD abstract.

I am grateful to Dr. Michael Poulter at Carleton University (Ottawa) for the two months I spent in his laboratory in the summer of 2003 to learn the patch-clamp technique. His kindness and patience are unforgettable.

I am indebted to the co-ordinators of the MD/PhD program (Dr. Jacquetta Trasler and Dr. Brian Collier) for their constant advice and support. I am also grateful to Fonds de la Recherche en Santé (FRSQ) for granting me the MD/PhD studentship.

Finally, I would like to take this opportunity to express my utmost gratitude to my family for their never-ending support and sacrifices. No acknowledgment section can ever express how importantly they have contributed to the furthering of my career. I am especially grateful to my mother (Sana), my father (Ramzi), my grandmother (Etaff) and my husband (Abdul Rahman) for their endless support and encouragements.

TABLE OF CONTENTS

LIST OF TABLES

LIST OF FIGURES

ABSTRACT

Earlier studies on temporal lobe epilepsy (TLE), by focusing on the anatomical and electrophysiological abnormalities of the hippocampus, have attributed a major role to this limbic structure in the process of epileptogenesis and seizure generation. Recently however, there has been increasing evidence from both animal and human studies that other limbic structures, including the subiculum, the entorhinal cortex (EC), perirhinal cortex (PC) as well as the amygdala, are possibly involved in the process of epileptogenesis. With the help of both acute and chronic models of limbic seizures, I have used an electrophysiological approach to gain more insight into the mechanisms through which these structures could participate in the establishment of hyperexcitable neuronal networks. Particularly, my investigations have focused on assessing the role played by the subiculum, the amygdala and the PC in epileptiform synchronization in vitro. My findings demonstrate that seizure-induced cell damage in chronically epileptic mice results in a change in limbic network interactions whereby EC ictogenesis is sustained via a reverberant EC-subiculum pathway (*Chapter 1*). Furthermore, I have discovered that the subiculum, which holds an anatomically strategic position within the hippocampus, is capable of gating hippocampal output activity via a $GABA_A$-receptor mediated mechanism (*Chapter 2*). My investigations in the amygdala have confirmed that this limbic structure contributes to epileptiform synchronization (*Chapter 3*). Moreover, using a chronic rat model of TLE, I have found novel evidence suggesting that alterations in inhibitory mechanisms play a role in the increased excitability of the lateral amygdalar nucleus (*Chapter 4*). Finally, my studies in chronically epileptic rats have also led to preliminary data signifying hyperexcitability of the PC as well alterations in the interactions between the amygdala and this cortical structure (*Chapter 5*).

ABRÉGÉ

Les anciennes études sur l'épilepsie du lobe temporal (ÉLT), en se consacrant à l'anatomie et à l'électrophysiologie anormale de l'hippocampe, ont attribué un rôle majeur à cette structure limbique dans le processus de l'épileptogénèse et de la génération de crises. Récemment, à partir d'études effectuées sur des animaux et des êtres humains, il est devenu évident que les autres structures limbiques, incluant le subiculum, le cortex entorhinal (CE), le cortex perirhinal (CP) et l'amygdale, sont probablement impliquées dans le processus de l'épileptogénèse. À l'aide des deux modèles animaux (aigue et chronique) de crises limbiques, j'ai utilisé une approche électrophysiologique pour en apprendre plus sur le mécanisme de participation de ces structures dans le développement de l'hyperexcitation du réseau neuronal. Plus précisément, mon enquête est centrée sur l'estimation du rôle joué par le subiculum, l'amygdale et le CP dans la synchronisation épileptiforme in vitro. Mes résultats démontrent que les crises induisant des dommages cellulaires dans l'épilepsie chronique chez le rat résultent de changements d'interactions dans le réseau limbique par lequel l'ictogénèse de CE est soutenue via un chemin CE-subiculum réverbérant (*Chapitre 1*). De plus, j'ai découvert que le subiculum, qui a une position anatomique stratégique par rapport à l'hippocampe, est capable de modifier le rendement d'activité de l'hippocampe via un mécanisme médié par les récepteurs $GABA_A$ (*Chapitre 2*). Ma recherche sur l'amygdale a confirmé que cette structure limbique contribue aussi à la synchronisation épileptiforme (*Chapitre 3*). De plus, en utilisant un modèle d'ÉLT chronique chez le rat, j'ai trouvé de nouveaux éléments suggérant que l'altération du mécanisme inhibiteur joue un rôle dans l'augmentation de l'excitabilité des noyaux latéraux de l'amygdale (*Chapitre 4*). Finalement, mes études sur l'épilepsie chronique du rat ont fourni des informations préliminaires précieuses sur une hyperexcitabilité significative du CP, tout comme sur l'altération des interactions entre l'amygdale et cette structure corticale (*Chapitre 5*).

CONTRIBUTION OF AUTHORS

The research presented in this thesis is grouped into five main chapters, each of which represents original work that was published or will be submitted for publication. The manuscripts for chapters 2, 4 and 5 were written by me whilst those for chapters 1 and 3 were written by Dr. Avoli.

Chapter 1:

D'Antuono M, **Benini R**, Biagini G, D'Arcangelo G, Barbarosie M, Tancredi V, Avoli M (2002) *Limbic network interactions leading to hyperexcitability in a model of temporal lobe epilepsy*. J Neurophysiol. 87:634-9.

The studies described in this chapter represent the collaborative efforts between members of Dr. Avoli's laboratory (D'Antuono M, myself and Barbarosie M) and Italian researchers (Biagini G, D'Arcangelo G, Tancredi V). My main contributions to this study involved carrying out electrophysiological recordings from both pilocarpine-treated and control tissue. The experiments I performed, in addition to others performed by M D'Antuono and M Barbarosie, were used to present the data reported in Figs 1-1 and 1-2. Biagini G, D'Arcangelo G and Tancredi V prepared the pilocarpine-treated mice and quantitated the cell loss in the Nissl stained tissue.

The results presented in this manuscript illustrate that seizure-induced cell damage leads to decreased control of hippocampal outputs over the excitability of the entorhinal cortex (EC). Furthermore, we report in this study that the resultant increased hyperexcitability of EC networks is sustained by reverberant interactions with the subiculum.

Chapter 2:

Benini R and Avoli M (2005) *Subicular networks gate hippocampal output activity in an in vitro model of limbic seizures*. J Physiol. 566:885-900.

I initiated this study upon the interesting observation that $GABA_A$ receptor blockade in our in vitro slice preparation leads to functional connectivity of hippocampal and

parahippocampal structures. Under the supervision of Dr. Avoli, I generated the ideas for this study, set out the hypotheses to be tested and analyzed all the data.

Although the subiculum is strategically positioned as an output structure, to our knowledge no previous studies had ever functionally assessed this role. I show in this manuscript, for the first time, evidence for the role of the subiculum as a gater of hippocampal outputs.

Chapter 3:

Benini R, D'Antuono M, Pralong E, Avoli M (2003) *Involvement of amygdala networks in epileptiform synchronization in vitro.* Neuroscience. 120:75-84.

The studies described in this chapter resulted from the collective efforts of members of Dr. Avoli's lab (myself and D'Antuono M) as well as those of Dr. Pralong, a visiting scientist from the University of Lausanne. My contributions to this work included carrying out the field potential experiments and analyzing the data presented in Figs. 3-2, 3-3 and 3-6. Dr. Pralong also performed some experiments that contributed to the data related to these figures. Dr. D'Antuono carried out the stimulation experiments that are presented in Fig 3-1, 3-4, 3-5 and 3-6.

The results presented in this study demonstrate the contribution of basolateral/lateral amygdalar networks to epileptiform synchronization in a combined slice preparation. We show, for the first time, the ability of CA3 networks to control electrographic activity generated within the amygdala.

Chapter 4:

Benini R and Avoli M (2006) *Altered inhibition in lateral amygdala networks in a rat model of temporal lobe epilepsy.* J Neurophysiol. 95:2143-54

I generated the ideas for this study under the supervision of Dr. Avoli. I set out the hypotheses to be tested, performed all the experiments and analyzed all the data presented.

For the first time, we report here functional changes in pre- and postsynaptic inhibitory mechanisms within the lateral nucleus of the amygdala in chronically epileptic rats.

Chapter 5:

Benini R and Avoli M. (manuscript in preparation) *Electrophysiology of deep layer perirhinal cortex in a model of temporal lobe epilepsy*

I generated the ideas for this study under the supervision of Dr. Avoli. I set out the hypotheses to be tested, performed all the experiments and analyzed all the data presented.

In this study, we provide evidence for hyperexcitability of the deep perirhinal cortex (PC) in chronically epileptic rats as well as alterations at the level of LA-PC interactions.

PRELUDE

0.1 Introduction

Affecting almost 1% of the population worldwide, epilepsy encompasses a set of chronic neurological disorders that are clinically associated with the occurrence of recurrent seizures and whose heterogeneous aetiologies include acquired, genetic and idiopathic factors (Blumcke et al., 1999; Engel, 1996, 2001). Among the variety of epileptic subtypes, temporal lobe epilepsy (TLE) is the most common form in humans (Wiebe, 2000). Patients suffering from this disorder present with seizures primarily involving the temporal neocortex as well as limbic areas such as the hippocampus and amygdala (Engel, 2001).

Significant progress has been made in the past two decade to try to elucidate the mechanisms underlying the pathophysiology of TLE. Imaging and histological studies have revealed that selective neuronal loss, gliosis and axonal sprouting are the pathological substrates underlying the hypersynchronicity of neuronal networks within the limbic system (Du et al., 1993; Gloor, 1997; Houser, 1999; Houser et al., 1990; Sutula et al., 1989; Yilmazer-Hanke et al., 2000). However, despite their implication in limbic network hyperexcitability, it remains unclear how these pathological processes interact to generate and propagate recurrent seizures in TLE.

0.2 Research Rationale of Thesis

Both acute convulsant models as well as chronic animal paradigms have played a crucial role in shedding more light onto the mechanisms underlying hyperexcitability of neuronal networks in focal epilepsy. Much of this work has focused on the hippocampus, specifically the CA3/CA1 subfields and dentate gyrus. Recently however, there has been increasing evidence from both animal and human studies that other limbic structures including the subiculum, the entorhinal cortex (EC), the perirhinal cortex (PC) as well as the amygdala are possibly involved in the process of epileptogenesis. The aim of my PhD project was to contribute to this newly emerging literature by investigating the participation of some of these understudied structures (namely subiculum, amygdala, and perirhinal cortex) in epileptiform synchronization

in vitro. My investigations, which are described in *Chapters 1* to *5* of this dissertation, have particularly focused on assessing GABAergic signalling within these brain regions in the context of hyperexcited neuronal networks.

The rationale for *Chapter 1* stemmed from previous in vitro investigations carried out in our laboratory illustrating that CA3 activity is capable of controlling the susceptibility of the EC for ictogenesis (Barbarosie and Avoli, 1997; Barbarosie et al., 2002). This evidence, taken together with the fact that MTLE patients present with severe cell loss in CA3/CA1 subfields (Houser, 1999), raised an interesting possibility that neuronal loss in these regions could potentially decrease control of hippocampal outputs over EC excitability and consequently lead to the limbic seizures observed in patients. This hypothesis was tested in *Chapter 1* where data obtained from pilocarpine-treated mice suggests that indeed, seizure-induced brain damage results in decreased hippocampal outputs and hyperexcitable EC networks that are in turn sustained by reverberant interactions with the subiculum.

The subiculum plays an important physiological role in learning and memory formation (O'Mara et al., 2001) but has also been implicated in the initiation and spread of seizures (Behr and Heineman, 1996; Cohen et al., 2002; D'Antuono et al., 2002; Wellmer et al., 2002; Wozny et al., 2003). To our knowledge, no previous investigations had addressed the role of the subiculum in controlling hippocampal outputs during epileptiform synchronization despite it being strategically positioned for doing so (Finch and Babb, 1981; Witter et al., 1989). The aim of *Chapter 2* was to explore the role of this structure in gating hippocampal output activity using the 4-aminopyridine (4AP) model of limbic seizures. Furthermore, since the subiculum is rich in GABAergic cells (Greene and Totterdell, 1997; Kawaguchi and Hama, 1987; Menendez de la Prida et al., 2003), the hypothesis that these inhibitory circuits probably participated in the gating mechanism was also tested in *Chapter 2*.

Chapters 3 to *5* describe studies pertaining to the amygdala-perirhinal system. Numerous investigations in the amygdala have examined the ability of the basolateral amygdala (BLA) to generate epileptiform activity (Gean, 1990; Gean and Shinnick-Gallagher, 1988; Kleuva et al., 2003). However, most of these studies had employed

the coronal slice preparation in which connections of the amygdala with the hippocampus and other limbic structures are not well preserved. In *Chapter 3*, we sought to identify the contribution of the basolateral/lateral amygdala nuclei (BLA/LA) to limbic network synchronization using a combined horizontal slice preparation in which the connections between the various structures are conserved. The interactions of the hippocampus, EC and BLA/LA were explored in this study using the 4AP model.

Finally, in spite of evidence from human studies implicating the LA (Hudson et al., 1993; Yilmazer-Hanke et al., 2000) and the PC (Bernasconi et al., 2003) in epilepsy, thorough electrophysiological evaluation of these structures using animal models remains sparse. In *Chapters 4* and *5*, the pilocarpine rat model of TLE was used to carry out an electrophysiological assessment of the cellular and network changes that occur within these structures in epileptic rats. Furthermore, since inhibitory responses are known to play an important role in controlling the excitability of LA neurons (Pitkanen and Amaral, 1994; Smith et al., 1998), GABA-mediated mechanisms were also investigated in more detail.

Below is a general introduction to familiarize the reader with the current state of knowledge in the field of TLE and set the stage for the main findings reported in Chapters 1-5.

0.3 Human TLE: Clinical and Neuropathological Findings

Retrospective studies have revealed that patients with TLE often present with a typical clinical history that involves an initial insult in early childhood such as birth trauma, complicated febrile convulsions, brain injury or meningitis (French et al., 1993; Salanova et al., 1994). Following this precipitating incident, a "latent" seizure-free period of a couple of years ensues and the development of recurring complex partial seizures only commences in adolescence or early adulthood (Engel, 1996, 2001).

Electroencephalographic (EEG) recordings from TLE patients reveals two main patterns of abnormal electrographic activity that signify the aberrant synchronization of neuronal networks and are classified as "interictal" and "ictal" discharges (Babb and Crandall, 1976; Babb et al., 1987; Cohen et al., 2002; Wyler et al., 1982). Interictal spikes represent short asymptomatic events that recur periodically between seizures and consist of high amplitude (> 50μV) spike-wave transients (de Curtis and Avanzini, 2001; Engel, 1996). Ictal discharges on the other hand are long events that manifest as behavioural seizures typically accompanied by staring and oroalimentary automatisms, and entail fast, low voltage spike discharges that initiate within the temporal lobe and can generalize to other structures (Engel, 1996). In the majority of patients, these debilitating seizures can be abolished with the use of antiepileptic drugs (AEDs) whose pharmacological mode of action commonly involves potentiation of GABAergic transmission or antagonism of voltage-gated sodium channels (Perucca, 2005). However, a third of cases are resistant to AEDs and for these intractable forms, surgical resection of the temporal lobe or selective amygdalohippocampectomy usually results in seizure relief (Engel, 2001; Engel et al., 2003; Wiebe et al., 2001)

Reduced hippocampal volumes are a characteristic hallmark of magnetic resonance images (MRI) obtained from TLE patients and are indicative of mesial temporal sclerosis (also known as Ammon's Horn sclerosis (AHS) or hippocampal sclerosis) (Jack, 1994; Watson et al., 1997). AHS, which is often associated with medical refractoriness, is the most common neuropathological finding in patients with TLE (Blumcke et al., 1999, 2002). Histologically, AHS denotes (i) selective neuronal loss and gliosis specifically within CA1/CA3/CA4 hippocampal subfields and dentate hilus; as well as (ii) axonal sprouting of dentate granule cells (Blumcke et al., 1999, 2002; Houser, 1999; Houser et al., 1990; Sutula et al., 1989). Despite these alterations, surgically-resected epileptic tissue reveals that not all hippocampal structures are involved and that areas such as the CA2 subfield, prosubiculum, subiculum and presubiculum do not disclose major cell damage (Blumcke et al., 2002; Dawodu and Thom, 2005; Gloor, 1997).

Remarkable advances in neuroimaging techniques over the past two decades have led to the realization that brain injury in TLE patients is more widespread than was originally believed. There is now increasing evidence from imaging and histological studies that damage is not restricted to the hippocampus but that extrahippocampal structures within the temporal lobe are also involved (Lee et al., 1998; Moran et al., 2001). For instance, recent MRI studies have demonstrated that volumetric reductions of the amygdala, entorhinal and perirhinal cortices do occur in a subset of TLE patients (Bernasconi et al., 1999, 2003; Cendes et al., 1993; Jutila et al., 2001; Salmenpera et al., 2000) in spite of normal hippocampal volumes (Bernasconi et al., 2001). Histopathological examination of human epileptic tissue corroborates these findings by demonstrating the presence of selective neuronal loss and synaptic reorganization within these structures (Aliashkevich et al., 2003; Du et al., 1993; Hudson et al., 1993; Mikkonen et al. 1998; Miller et al., 1994; Wolf et al., 1997) even in the absence of hippocampal sclerosis (Hudson et al., 1993; Miller et al., 1994; Yilmazer-Hanke et al., 2000).

The diffusiveness of the pathophysiological substrates underlying TLE is further substantiated by evidence of widespread MR volumetric reductions of extratemporal white matter (Seidenberg et al., 2005) as well as subtle abnormalities in structures such as the basal ganglia (Dreifuss et al., 2001), cerebellum (Sandok et al., 2000) and thalamus (DeCarli et al., 1998; Natsume et al., 2003).

0.4 Tools for Studying TLE: Acute and Chronic Models of Limbic Seizures

Ideally, research on human epileptic tissue would be expected to yield valuable information into the pathophysiology of TLE. However, such studies have been limited due to a number of reasons including (i) the invasiveness of in vivo depth-electrode recordings; (ii) the reality that surgically-resected epileptic tissue has usually been exposed to years of pharmacological regimes thereby making it almost impossible to differentiate between disease- and drug-induced changes, (iii) the lack of appropriate control tissue, and (iv) the fact that slices from human epileptic tissue rarely generate spontaneous activity perhaps as a consequence of extensive neuronal

loss (Avoli et al., 2005; Schwartzkroin, 1994). To avert these caveats, scientists have resorted to the use of animal tissue for studying TLE.

Acute treatment with convulsive agents can induce in cortical or hippocampal slices epileptiform activity analogous to the electrographic discharges recorded in the EEG of TLE patients (Avoli et al., 2002). These pharmacological agents, by shifting the balance between excitation and inhibition, increase cellular excitability and consequently lead to the synchronization of neuronal networks within the slice preparation. Some of the most commonly used convulsant models involve the depolarization of neuronal membranes through the alteration of ionic gradients (ex. high $[K^+]_o$ model); the augmentation of glutamatergic (ex. Mg^{2+}-free model) and cholinergic (ex. pilocarpine) transmission or the antagonism of GABAergic receptors (ex. picrotoxin; bicucullin) (Anderson et al., 1986; Avoli et al., 2002; Hablitz, 1984; Rutecki et al., 1985; Wong and Traub, 1983). Moreover, other convulsants are known to elicit their effect via a combination of mechanisms. For example, 4-aminopyridine (4AP) has been shown not only to block K^+ currents (Rudy, 1988) and interfere with Ca^{2+} channels (Segal and Barker, 1986), but also to facilitate neurotransmitter release at presynaptic terminals of both excitatory and inhibitory synapses (Aram et al., 1991; Rutecki et al, 1987; Thesleff, 1980).

Initially, studies employing convulsant models were carried out in isolated hippocampal slices maintained in vitro. Although this preparation takes advantage of the lamellar organization of the hippocampus, it does not provide access to other structures (such as the EC, PC, and amygdala) that are relevant to understanding the pathophysiogenesis of TLE. Furthermore, electrophysiological recordings from adult rodents have revealed that while interictal discharges can be induced in isolated hippocampal slices, ictal phenomena on the other hand are rarely observed (Anderson et al., 1986; Lothman et al., 1991; Rafiq et al., 1993). For these reasons, studies investigating network interactions have recently begun to use brain slice preparations with more than one interconnected limbic structure to reproduce the patterns of epileptiform activity observed in patients (Dreier and Heinemann, 1991; Jones and Lambert, 1990a, b; Nagao et al., 1996; Stoop and Pralong, 2000; Walther et al., 1986;

Wilson et al., 1988). For example, in reciprocally interconnected hippocampal-entorhinal cortex (EC) slices obtained from rodents, bath application of 4AP or Mg^{2+}-free medium has been shown to induce two main types of epileptic discharges: (1) fast interictal-like activity that originate in CA3 (Avoli et al., 1996; Barbarosie and Avoli, 1997; Dreier and Heinemann, 1991; Wilson et al., 1988), and (2) NMDA-receptor mediated ictal-like events that resemble electrographic limbic seizures seen in TLE patients (cf. Swartzwelder et al., 1987; Wilson et al., 1988); initiate in the EC and subsequently propagate to the hippocampus proper (Barbarosie and Avoli, 1997).

Despite the valuable insight that has been gained from brain tissue made epileptogenic by acute convulsant treatment, such investigations are nevertheless limited by their inability to reproduce in the slice preparation the scenario of chronic epilepsy and histopathological damage associated with the human condition. Fortunately, a variety of chronic animal models have been developed to complement these acute paradigms (Coulter et al., 2002; Loscher, 1997; Morimoto et al., 2004). The two most frequently-used models are the "kindling" and the "status epilepticus (SE)" models.

Kindling, first proposed as a physiological model for studying learning and memory processes, has since been used extensively as a chronic animal model of intractable TLE (Goddard, 1967; Goddard et al., 1969; Loscher, 2002; McIntyre et al., 2002; Morimoto et al., 2004; Racine, 1978). In this model, stimulating and recording electrodes are permanently implanted within one specific brain area such as the amygdala, perirhinal cortex or hippocampus. This structure is initially stimulated with a subconvulsive electrical current large enough to elicit in the locally recorded EEG a focal paroxysmal response (or "afterdischarge"), that progressively increases in amplitude and duration with subsequent stimulations (over days and weeks) (Racine, 1972a, b, 1975). The increased sensitivity to electrical stimulation attained in these animals over time is accompanied by the advanced severity of evoked seizures and denotes the kindling phenomenon. In amygdala kindling for example, evoked seizures progress in time through Racine's 1-5 grading of convulsive stages signifying the gradual recruitment of structures distant to the stimulating site (Racine, 1972b).

Interestingly, not all structures kindle at the same rate or in the same manner. For example, whereas the hippocampus kindles much more slowly than the amygdala (Coulter et al., 2002), the perirhinal cortex on the other hand has been shown to be the most easily kindled structure within the forebrain (McIntyre et al., 1993). Animals reaching stage 5 seizures are said to be fully-kindled and although they do not exhibit spontaneous seizures, the persistence of their convulsive responsiveness to electrical stimulation for several months is indicative of the underlying permanent changes induced within the brain during the kindling process (Sato et al., 1990). Persistent daily stimulations of fully-kindled animals for several weeks or months after they have attained stage 5 seizures can induce the development of spontaneous recurrent seizures in almost half of them (Michalakis et al., 1998; Pinel and Rovner, 1978). Notably, kindled animals exhibiting spontaneous seizures reveal minimal brain damage and thereby raise the interesting possibility that extensive injury is not an absolute criterion for instigating epileptogenesis (Michalakis et al., 1998).

In SE models, the epileptic state arises as a consequence of brain injury induced in the animal by an experimentally-provoked long-lasting seizure analogous to SE. This initial precipitating incident can be incited by injecting animals with high dosages of chemical convulsants, such as kainic acid or pilocarpine, either systemically (Ben-Ari, 1985; Liu et al., 1994; Turski et al., 1983) or directly into specific brain areas (Mathern et al., 1993; Tanaka et al., 1992). Alternatively, the acute SE can also be elicited via sustained electrical stimulation of limbic pathways such as the perforant path, ventral hippocampus or lateral amygdala (Du et al., 1995; Gorter et al., 2001; Nissinen et al., 2000; Sloviter, 1987). Similar to what occurs in humans, a "latent" period, ranging from weeks to months depending on the model, follows this initial insult. During this time, animals are behaviourally normal and only later in the chronic phase do they begin to exhibit spontaneous secondarily generalized seizures that persist throughout life and are usually of limbic origin (Coulter et al., 2002). Pathological investigations carried out in these SE models have revealed a pattern of brain injury analogous to the mesial temporal lobe sclerosis observed in humans thus rendering these animal paradigms attractive tools for studying TLE (Ben-Ari, 1985;

Cavalheiro et al., 1996; Liu et al., 1994; Mello et al., 1993; Sloviter, 1987; Tauck and Nadler, 1985; Turski et al., 1983).

Due to the difficulty in controlling the initial convulsive episode, the expression of spontaneous seizures in SE models tends to be unpredictable and the degree of brain damage more extensive than what is typically observed in humans (Sloviter, 2005). Moreover, although the pattern of damage tends to be comparable, differences in the severity of brain injury do exist between various models. For example, an investigation comparing two SE paradigms reveals that damage occurs at an earlier onset and tends to be more extensive in the pilocarpine versus kainate rodent model (Covolan and Mello, 2000).

In spite of this, the similarity in the temporal evolution of the epilepsy between the animal and human condition (i.e. the presence of acute, latent and chronic phases) renders SE models highly valuable tools for studying TLE. Exploitation of this latter characteristic has provided some insight into the type of alterations that occur within different brain structures soon after the initial insult, at a period that is often more difficult to study in humans (i.e. during the acute and latent phases). For example, recent MRI studies employing the pilocarpine-treated rodent model have illustrated that reactivity within the amygdala, EC and piriform cortex occurs as early as 24 hrs following SE (Roch et al., 2002a,b). Furthermore, combined MRI and histological results obtained from these investigations have also demonstrated that neuronal damage within these structures is complete at a much earlier stage than in the hippocampus, where the neuropathological progression tends to be delayed and more prolonged (Roch et al., 2002a).

0.5 The Pathophysiogenesis of MTLE: What has Research Taught us

Cellular, pharmacological and molecular studies have contributed remarkably to our understanding of the mechanisms leading to the hyperexcitability of neuronal networks in TLE. Unlike in other diseases where the cause-effect relationship is more apparent, the TLE scenario tends to be complicated not only by the diversity of the pathological factors involved but also by the ambiguity in the relationship between these phenomena and the seizures themselves. Below is a brief discussion of some of

the molecular, cellular and network changes that have been reported from human and animal epileptic tissue as well as the theories that have been proposed to explain how these alterations may contribute to the initiation and maintenance of seizures.

0.5.1 Enhanced Excitatory Transmission

Glutamate is the major excitatory neurotransmitter in the mammalian brain (Meldrum, 2000). It plays an important role in normal synaptic activity by binding to excitatory amino acid receptors to increase cationic ($Na^+/Ca^{2+}/K^+$) conductances and subsequently induce neuronal membrane depolarization (Collingridge and Lester, 1989; Mayer and Westbrook, 1987). Activation of glutamatergic receptors can also lead to a myriad of downstream effects involving interactions with other transmitter systems (Cartmell and Schoepp, 2000) as well as long-term alterations at the level of gene expression (Madison et al., 1991; Platenik et al., 2000). Glutamate acts on two main families of receptors namely: (1) the *ionotropic glutamate receptors* that comprise of NMDA, AMPA and kainate receptors; and (2) the G-protein-linked *metabotropic glutamate receptors* divided into Group I (mGluR1 and mGluR5), Group II (mGluR2 and mGluR3) and Group III (mGluR4, 6, 7 and 8) (Anwyl, 1999; Kew and Kemp, 2005; Mayer and Armstrong, 2004; Nakanishi, 1992; Seeburg, 1993). Due to its pivotal role in modulating the excitatory threshold of neuronal networks, glutamate has been implicated in the generation, spread and maintenance of seizures. Accordingly, alterations in glutamatergic mechanisms leading to increased extracellular glutamate concentrations and enhanced postsynaptic receptor sensitivity have been demonstrated in epileptic tissue (Chapman, 2000; Meldrum et al., 1999).

The extracellular concentration of glutamate is tightly regulated during synaptic activity to ensure a non-toxic milieu. Evidence from both human (During and Spencer, 1993; Ronne-Engstrom et al., 1992; Wilson et al., 1996) and animal (Kaura et al., 1995; Wilson et al., 1996; Zhang et al., 1991) epileptic tissue suggest that extracellular concentrations of glutamate are increased during spontaneous seizures, especially in the epileptogenic hippocampus. Notably, these increased glutamate levels persist even after the clinical seizures have subsided (During and Spencer, 1993), thereby suggesting a possible impairment in glutamate uptake mechanisms. Glutamate

transporters (also known as excitatory amino acid transporters or EAATs) are localized in the synaptic cleft where they regulate extracellular glutamate concentrations via Na^+-coupled uptake mechanisms (Bridges and Esslinger, 2005). To date, 5 human subtypes have been identified (EAAT 1-5) that differ in regional, cellular and developmental distribution (Danbolt, 2001; O'Shea, 2002). Whereas the astrocytic isoforms (EAAT1 and EAAT2) tend to be responsible for the majority of glutamate uptake during transmission, the neuronal subtypes (EAAT3) on the other hand tend to play a more subtle role (Amara and Fontana, 2002).

Despite the suggestion that glutamate transporters might be altered in TLE (During and Spencer, 1993), evidence thus far remains sparse and contradictory. For example, although mice lacking an EAAT1-related glial glutamate transporter have been shown to exhibit chronically elevated glutamate levels and increased seizure susceptibility (Tanaka et al., 1997; Watanabe et al., 1999), findings from acquired rodent models of epilepsy tend to be conflicting. Within the epileptogenic hippocampus of chronically epileptic animals evidence has been presented for (i) the absence of changes in both EAAT1- and EAAT2-related glial transporter subtypes (Akbar et al., 1997); (ii) a decrease in the EAAT1-related glial subtype and an increase in the EAAT3-related neuronal subtype (Miller et al., 1997); and (iii) an enhanced expression of both the EAAT1- and EAAT2-related glial transporter subtypes and a diminished expression of the EAAT3-related neuronal subtype (Nonaka et al., 1998; Simantov et al., 1999). The scenario in human epileptic tissue is no more demystified. Whereas evidence obtained from the hippocampus and temporal neocortex of tissue resected from TLE patients has illustrated the absence of changes in either neuronal or glial glutamate transporters (Tessler et al., 1999), other investigations have shown that modifications related to neuronal loss do indeed exist (Mathern et al., 1999; Proper et al., 2002). Altogether, the contribution of glutamate uptake mechanisms to the enhanced glutamate levels associated with epileptogenesis awaits further clarification.

The failure of presynaptic autoreceptors has also been proposed to account for the augmentation in extracellular glutamate levels. Both metabotropic glutamate (Group II/III) and $GABA_B$ receptors are known to play important physiological roles

in inhibiting the presynaptic release of glutamate (Cartmell and Schoepp, 2000; Miller, 1998; Thompson et al., 1993). Assessment of animal epileptic tissue suggests that a diminished efficacy of these presynaptic receptors occurs. Specifically, plastic changes leading to a failure in presynaptic $GABA_B$ receptor-mediated depression of glutamate release has been demonstrated at mossy fiber-CA3 synapses in chronically epileptic rats (Chandler et al., 2003). Moreover, in both kindled and pilocarpine-treated rodents, a decreased sensitivity of Group III metabotropic glutamate receptors has been identified in the lateral perforant path (Dietrich et al., 1999; Klapstein et al., 1999; Kral et al., 2003). Altogether, this data suggests that the increased release of glutamate observed at the onset of limbic seizures in the hippocampus of TLE patients may arise from the impaired sensitivity of presynaptic autoreceptors (During and Spencer, 1993).

Postsynaptic alterations in ionotropic glutamatergic receptors have also been implicated in TLE. Specifically, studies from human and animal epileptic tissue have demonstrated (i) an increase in the number of ionotropic receptors, namely NMDA and AMPA receptors (Kraus and McNamara, 1998; Mathern et al., 1997; Mikuni et al., 1999; Rafiki et al., 1998); (iii) changes in glutamate receptor subunit composition (Grigorenko et al., 1997) as well as (iii) enhanced activation of NMDA receptors, possibly due to posttranslational modifications (Kohr et al., 1993; Kojima et al., 1998; Lieberman and Mody, 1999; Mody, 1998; Mody and Heinemann, 1987; Sanchez et al., 2000; Turner and Wheal, 1991). These findings are relevant to understanding the contribution of glutamatergic mechanisms to epileptogenesis considering that NMDA and AMPA receptors have been shown to play an important role in the generation of epileptiform discharges in the hippocampus and neocortex (Avoli, 1991; Dingledine et al., 1990; Heinemann et al., 1991). The evidence of enhanced NMDA receptor activation in TLE is also noteworthy in view of the pivotal role of these receptors in eliciting downstream effects that alter gene expression and can perhaps lead to some of the long-term plastic changes associated with TLE (Platenik et al., 2000).

0.5.2 Dysfunctional GABAergic Signalling

γ-Aminobutyric acid (GABA) is the principal inhibitory neurotransmitter of the central nervous system (CNS). It is synthesized within the axon terminals of interneurons and released into the synapse from whence it acts at one of two types of receptors namely, $GABA_A$ and $GABA_B$ receptors. $GABA_A$ receptors are ligand-gated ion channels localized primarily on the postsynaptic membrane within the brain. GABA acting at these pentameric receptors induces an increased Cl^-/HCO^{3-} conductance that usually hyperpolarizes the membrane and mediates a fast inhibitory effect by driving its potential further away from firing threshold (Kaila, 1994; Macdonald and Olsen, 1994). $GABA_B$ receptors on the other hand are G-protein linked receptors that are localized pre- and postsynaptically and can be found on both excitatory and inhibitory axon terminals (Kerr and Ong, 1995; Macdonald and Olsen, 1994). Activation of these receptors results in an increased K^+ conductance that hyperpolarizes neurons, reduces Ca^{2+} entry and can decrease neurotransmitter release at the presynaptic terminal (Thompson et al., 1993).

A homeostatic balance between excitatory and inhibitory processes is essential for sustaining neuronal circuitry during normal physiological functions (Liu, 2004; Turrigiano and Nelson, 2004). Originally, research in TLE was overcome with the notion that a failure in GABA-mediated inhibition underlies hyperexcitability of the neuronal networks involved in seizure generation. In accordance with this concept, pharmacological drugs that enhance GABA-mediated inhibition are known to abolish seizures in TLE patients (Capek, 1997; Meldrum, 1999). Furthermore, extensive in vitro investigations have demonstrated that antagonism of GABAergic receptors unleashes excitatory interactions and consequently leads to the synchronization of neuronal networks (Dingledine and Gjerstad, 1980; Lebeda et al., 1982; Schwartzkroin and Prince, 1977). Additional support for the concept of diminished inhibition as an underlying mechanism leading to epileptogenesis stems from both human and animal epileptic tissue illustrating: (i) a decrease in the presynaptic pool of GABA (Hirsch et al., 1999); (ii) reduced expression of $GABA_A$ receptors (Johnson et al., 1992; McDonald et al., 1991; Olsen et al., 1992) (iii) alterations in the subunit composition

of $GABA_A$ receptors possibly accounting for their decreased sensitivity to agonists as well as reduced conductance (Brooks-Kayal et al., 1998; Buhl et al., 1996; Friedman et al., 1994; Henry et al., 1993; Rice et al., 1996; Savic et al., 1988); (iv) reduced efficiency of both pre- and postsynaptic $GABA_B$ receptors (Mangan and Lothman, 1996); (v) decreases in the number of GABA transporters (During et al., 1995); and (vi) loss of specific interneuronal subpopulations (Arellano et al., 2004; de Lanerolle et al., 1989; Houser et al., 1990; Robbins et al., 1991).

Despite these observations, it is becoming increasingly evident that GABAergic systems are more intricate than previously believed. Moreover, in epileptic tissue they undergo such complex transformations, at both the structural and functional level, that there is now a growing consensus that the older concept of decreased inhibition in epilepsy is oversimplified and needs to be reassessed (Bernard, 2005; Cossart et al., 2005). Importantly, there is an indication from epileptic tissue that GABAergic systems within various limbic regions are differentially affected. For example, whereas a decrease in the quantal release of GABA and a diminished conductance of $GABA_A$ receptors has been reported in the CA1 region (Gibbs et al., 1997; Hirsch et al., 1999), increased inhibition due to an enhancement in both the conductance and number of postsynaptic $GABA_A$ receptors has been identified in granule cells of the dentate gyrus (Brooks-Kayal et al., 1998; Gibbs et al., 1997; Nusser et al., 1998; Otis et al., 1994).

The implication of interneuronal loss in TLE is also being re-examined (Cossart et al., 2005). Recent investigations have demonstrated that interneurons within the hippocampus and neocortex are not a homogenous population of GABA-releasing cells but instead differ from each other in their morphological, neurochemical and electrophysiological constitution as well as in the variety of their connections with target cells (Freund and Buzsaki, 1996; Maccaferri and Lacaille, 2003). This diversity in interneuronal subtypes is physiologically relevant. By indicating that various interneuronal subpopulations may play different roles within the brain, it also implies that the outcome of interneuronal degeneration within a particular brain region would depend on the specific subpopulations affected.

Moreover, due to the increasing evidence suggesting that GABAergic neurons are not simply "inhibitory cells", the conventional association of interneuronal loss with decreased inhibition is no longer suitable. Specifically, investigations have demonstrated that in addition to their involvement in inhibitory processes, interneurons are also capable of synchronizing neuronal networks into the generation of high-frequency oscillations (Buzsaki et al., 1992; Cobb et al., 1995; Csicsvari et al., 1999; Whittington and Traub, 2003). Furthermore, interneurons have recently been shown to contribute to the interictal activity recorded in the subiculum of human epileptic tissue (Cohen et al., 2002).

Additional complexity to understanding the role of GABAergic signalling in TLE arises from evidence suggesting that GABA can paradoxically be "excitatory". As mentioned previously, GABA generally tends to induce hyperpolarization of neurons in the adult brain. However, there are several instances such as in the developing juvenile brain (Ben-Ari et al., 1989), in the adult brain under high frequency stimulation (Lamsa and Taira, 2003; Voipio and Kaila, 2000) or in the presence of 4AP (Perreault and Avoli, 1989), where the depolarizing effects of GABA are known to occur. This inhibitory-to-excitatory shift of GABA has been attributed to a number of factors including modification in Cl^- gradients due to a decreased expression of the K^+/Cl^- cotransporter KCC2 (Riviera et al., 1999) and deafferentiation (Vale and Sanes, 2000). Interestingly, there is now also evidence from human epileptic tissue for excitatory actions of GABA (Cohen et al., 2002).

Altogether, evidence from human and experimental epilepsy indicates that modifications in GABAergic signalling occur at all levels of processing, from receptor structure to wiring of interneuronal networks. The intricacy of these changes has led to a reformulation of the earlier concept that GABAergic signalling is reduced in TLE. Instead, the contemporary view is that alterations in GABAergic neurotransmission in TLE are region-specific and may take the form of decreased inhibition, increased inhibition or excitatory GABA action.

0.5.3 Neuronal loss and Network Rewiring

Selective neuronal loss and aberrant axonal sprouting within limbic structures are the pathological hallmarks of TLE (Blumcke et al., 1999, 2002; Houser, 1999; Houser et al., 1990; Sutula et al., 1989). The contribution of the former to the process of epileptogenesis depends on the normal functions of the damaged neurons and the context of their interactions within the network. In the dentate hilus for example, selective loss of excitatory mossy cells has been demonstrated in epileptic tissue and has led to the formulation of the "dormant basket cell" hypothesis (Bekenstein and Lothman, 1993; Sloviter, 1987, 1991). Mossy cells are known to receive glutamatergic inputs from dentate granule neurons and their activation has been demonstrated to lead to inhibition of dentate granule cells via a feedforward mechanism that involves excitation of basket cells (Scharfman, 1995; Scharfman et al., 1990). Thus, due to their role in this feedforward inhibition, loss of mossy cells in epileptic tissue has been associated with denervation of interneurons and subsequent disinhibition within the dentate gyrus, a structure that serves as the main input into the hippocampus and has been heavily implicated in the process of epileptogenesis (Heinemann et al., 1992; Lothman et al., 1992).

Additional outcomes of neuronal damage involve the loss of postsynaptic targets, axonal sprouting of surviving neurons and the consequent creation of aberrant circuits. The contribution of axonal reorganization to the process of epileptogenesis has been most studied within the dentate gyrus, where extensive restructuring of the mossy fiber pathway occurs in both human and animal epileptic tissue (Proper et al., 2000; Sutula et al., 1989; Tauck and Nadler, 1985). The mossy fiber tract, representing axonal collaterals of dentate gyrus granule cells, innervates the inner molecular layer of the dentate hilus as well area CA3 (Henze et al., 2000). Loss of hilar cells induces dentate granule neurons to redirect their axons to form aberrant recurrent excitatory connections with each other (Babb et al., 1991). These new circuits have been suggested to reduce the threshold for neuronal synchronization within this structure and possibly contribute to the sustenance of seizures (Nadler, 2003; Wuarin and Dudek, 1996). Despite this evidence, it has been argued that axonal sprouting,

although a phenomenon associated with epilepsy, is unlikely to be a major contributor to epileptogenesis. These arguments have been supported by temporal data illustrating that the epileptic state occurs well before considerable mossy fiber reorganization has taken place (Armitage et al., 1998; Ebert and Loscher, 1995). Furthermore, investigations employing SE animal models have demonstrated that preventing the occurrence of axonal sprouting with protein synthesis inhibitors does not avert the induction of spontaneous seizures (Longo and Mello, 1997, 1998).

Historically, studies investigating the role of axonal sprouting in epileptogenesis have focused on the zinc-rich mossy fiber pathway primarily due to easy visualization of this tract using the Timm staining technique. However, it is important to note that axonal sprouting in epileptic tissue has also been demonstrated in other pathways both within and outside the hippocampus, including CA3 (Siddiqui and Joseph, 2005), CA1 (Lehmann et al., 2001); CA1-subiculum region (Cavazos et al., 2004) as well as EC layer III (Mikkonen et al., 1998).

0.5.4 Other mechanisms – Alterations in Intrinsic Neuronal Properties

In addition to the above-mentioned modifications in synaptic mechanisms, there is emerging evidence that persistent changes in intrinsic neuronal properties also play an important role in epileptogenesis (Sanabria et al., 2001; Yaari and Beck, 2002; Yamada and Bilkey, 1991). This has been demonstrated by studies in the pilocarpine-treated rodent model illustrating a dramatic increase in the fraction of intrinsically bursting pyramidal cells in CA1 (Sanabria et al., 2001) and subiculum (Wellmer et al., 2002). Intrinsically bursting neurons are known to play an important role in entraining additional cells into synchronized network activity, which in turn can lead to the generation and/or amplification of seizures (McCormick and Contreras, 2001; Traub et al., 1987; Yaari and Beck, 2002). Thus, the up regulation of intrinsically bursting neurons in chronically epileptic tissue, which has been suggested to arise from a long-term enhancement in calcium currents, may play an essential role in the process of epileptogenesis (Sanabria et al., 2001).

In addition, down regulation of the A current in the dendrites of surviving hippocampal neurons from pilocarpine-treated rodents has also been recently

demonstrated (Bernard et al., 2004). The A current, mediated by voltage-gated A-type K^+ channels, is responsible for preventing the back propagation of action potentials from the soma to the dendrites (Hoffman et al., 1997; Johnston et al., 2000). Thus, by increasing the reverberation of action potentials between the soma and the dendrites, the loss of this inhibitory A current could potentially lead to the amplification of incoming synaptic inputs and consequently support seizure activity in an epileptic system where recurrent excitatory connections are known to occur (Staley, 2004).

0.6 Stepping Out of the Hippocampocentric Box

Historically, research in TLE has focused primarily on trying to understand the contribution of the hippocampus to epileptogenesis. This 'hippocampocentric' approach was justified due to the large body of evidence implicating this structure in epileptogenesis including (i) the fact that the most obvious and consistent neuropathological alterations are associated with this structure (Blumcke et al., 2002); (ii) EEG recordings often identify the hippocampus as an epileptogenic focus of seizure activity (Wieser et al., 1993); and (iii) in the majority of patients suffering from intractable TLE adequate seizure relief can be attained with surgical resection of the hippocampus (Spencer and Spencer, 1994a).

Despite these findings, recent evidence obtained from imaging, histological and electrophysiological studies has led to the realization that other structures within the limbic system contribute importantly to the process of epileptogenesis. My PhD studies have centred around three of these structures, namely the subiculum, amygdala and perirhinal cortex. The purpose of this section is to provide some background information about each of these brain regions, specifically by highlighting the evidence presented for their role in TLE.

0.6.1 Subiculum: Anatomy, Physiology and Role in TLE

The hippocampal formation consists of a number of subdivisions that include the dentate gyrus, the hippocampus proper (cornu ammonis areas CA1/CA3) and the subiculum (Amaral and Witter, 1989). Anatomically, the subiculum serves as the major output structure of the hippocampus, receiving extensive efferents from the hippocampal CA1 subfield (Finch and Babb, 1981; Witter et al., 1989) as well as

projecting to various limbic and extralimbic areas including EC layers IV and V (Swanson and Cowan, 1977; Witter et al., 1989), perirhinal cortex (Deacon et al., 1983; Swanson et al., 1978), amygdala (Canteras and Swanson, 1992) and thalamus (Canteras and Swanson, 1992; Witter et al., 1990) (see for review O'Mara et al., 2001).

The 'subicular complex', consisting of the subiculum proper, the presubiculum and the parasubiculum, is strategically positioned between the CA1 hippocampal subfield and the entorhinal cortex (Amaral and Witter, 1989; Lopes da Silva et al., 1990). As a transition zone between the hippocampus proper and the parahippocampal regions, it tends to share a number of characteristics with each of these two brain areas. Analogous to the three-layered allocortical hippocampus, the subiculum is cytoarchitectonically organized into a molecular, pyramidal and polymorphic layer (Lopes da Silva et al., 1990). Importantly however, the connectivity of this structure tends to be more comparable to the multilaminated parahippocampal regions in its multidirectionality and reciprocality. For example, the subiculum projects to the deep layers of the EC (IV/V) and in turn receives projections from the superficial layers (II/III) via the monosynaptic temporammonic pathway (Swanson and Cowan, 1977; Witter et al., 1989). This is in contrast to the other hippocampal subdivisions that are interconnected primarily via unidirectional pathways (i.e. the trisynaptic circuit consisting of the perforant, mossy fiber and Schaffer collateral pathways).

In vitro neurophysiological investigations have demonstrated that the subiculum is rich in large pyramidal neurons that are divided into two main groups based on their responses to intracellular current injection and orthodromic stimulation (Mattia et al., 1993; Staff et al., 2000; Stewart and Wong, 1993; Taube, 1993). Whereas 'regular spiking' neurons fire a regular train of action potentials in response to a depolarizing current pulse, 'intrinsic bursters' respond by firing an initial brief burst of 3-5 action potentials that is often followed by a short hyperpolarizing afterpotential. The ionic mechanisms underlying the bursting of these latter group of subicular cells is contentious and evidence indicates the involvement of both Ca^{2+} (Jung et al., 2001; Stewart and Wong, 1993) and persistent Na^{+} currents (Mattia et al.,

1993). Furthermore, although the absolute ratio of regular firing to intrinsically bursting neurons within the normal subiculum differs between various in vitro and in vivo studies, there is a general consensus that there are more bursting than non-bursting elements within this structure (O'Mara et al., 2001).

In addition to principal neurons, the subiculum is also equipped with several types of GABAergic cells (Greene and Totterdell, 1997; Kawaguchi and Hama, 1987; Menendez de la Prida et al., 2003). The functional significance of these fast-spiking inhibitory neurons has been established by electrophysiological studies demonstrating that subicular pyramidal cells are restrained by local GABAergic networks via both feedforward (Behr et al., 1998; Colino and Fernandez de Molina, 1986; Finch and Babb, 1980; Finch et al., 1988) and recurrent inhibitory mechanisms (Menendez de la Prida, 2003). Interestingly, intrinsically bursting neurons experience a greater degree of recurrent inhibition than regular spiking cells (Menendez de la Prida, 2003)

Within the normal brain, the subiculum appears to play an integral role in spatial encoding (Sharp and Green, 1994) and the retrieval of short-term memories (Gabrieli et al., 1997). Recently, it has also been implicated in TLE. Histological assessment of tissue resected from TLE patients reveals that minimal loss of principal cells occurs within the subiculum (Blumcke et al., 2002; Dawodu and Thom, 2005; Gloor, 1997). In spite of these findings, evidence from in vitro investigations strongly suggests that the subiculum may be involved in the initiation and spread of seizures. For example, various studies have demonstrated that under conditions of increased excitation (Mg^{2+}-free medium; NMDA) or reduced inhibition (picrotoxin), the subiculum is capable of generating robust interictal discharges that can initiate anywhere within the structure and spread to adjacent areas (Behr and Heinemann, 1996; Harris and Stewart, 2001). These reports have suggested that both the recurrent excitatory connections coupling subicular cells as well as the presence of intrinsically bursting pyramidal neurons within this structure may serve to amplify signals and synchronize neuronal networks into generating electrographic activity (Behr and Heinemann, 1996; Harris and Stewart, 2001). Recently, an enquiry into the contribution of different subicular neurons to the generation of epileptiform activity in

vitro revealed that whilst intrinsic bursters had the lowest firing threshold and appeared to initiate focal epileptic activity, local interneurons on the other hand were responsible for preventing this activity from becoming widespread (Menendez de la Prida and Gal, 2004).

Further evidence for the possible role of the subiculum in epileptogenesis stems from chronic animal models of MTLE demonstrating that despite the absence of neuronal loss, persistent alterations occur in both the intrinsic as well as network properties of principal neurons. Recent investigations assessing changes in the population of intrinsic bursters in the pilocarpine-treated subiculum indicate an increase (Wellmer et al., 2002), a reduction (Knopp et al., 2005) and no alterations in these subicular subtypes (de Guzman et al., submitted). However, synchronous subicular network hyperexcitability and enhanced sensitivity has been reported within the epileptic subiculum despite the population reduction of intrinsic bursters (Knopp et al., 2005; de Guzman et al., submitted). The hyperexcitable network interactions of the epileptic subiculum have also been attributed to a reduction in specific interneuronal subpopulations (van Vliet et al., 2004; de Guzman et al., submitted) and increased presynaptic sprouting (de Guzman et al., submitted). Furthermore, reduced expression of the KCC2 cotransporter in the subiculum of chronically epileptic animal tissue has also been suggested to account for the excitatory actions of GABA within this structure (de Guzman et al., submitted).

In parallel with the findings obtained from chronic animal models, recent in vitro studies in human epileptic tissue have demonstrated the presence of spontaneous interictal activity originating within the subiculum and spreading to adjacent hippocampal regions (Cohen et al., 2002; Wozny et al., 2003). Both pyramidal cells as well as interneurons were found to contribute to this electrographic activity, which upon further examination appeared to arise from perturbations in $GABA_A$ receptor mediated signalling (Cohen et al., 2002). Furthermore, decreased sensitivity of $GABA_A$ receptors to their ligand (Palma et al., 2005) and enhanced Na^+-persistent currents (Vreugdenhil et al., 2004) have also been identified in subicular cells of epileptic patients.

Altogether, increasing evidence is pointing towards an important role for the subiculum in the process of epileptogenesis. These findings are highly significant considering that the subiculum is strategically placed as the major output structure of the hippocampus and can thus possibly serve not only to initiate seizures, but also to amplify and relay this aberrant brain activity to other limbic and extralimbic structures.

0.6.2 Amygdala: Role of the Basolateral Complex in TLE

The amygdala, also referred to as the 'amygdaloid complex', is an almond-shaped structure located in the deep, anteromedial part of the temporal lobe. It is divided into various nuclei and cortical areas that differ from one another not only in their cytoarchitectonic and chemoarchitectonic constitution but also in their connectivity with other brain areas (Pitkanen et al., 1997, 2000a; Sims and Williams, 1990; Swanson and Petrovich, 1998). Typically, the amygdala can be divided into three main regions that include the basolateral complex, the cortical region, and the centromedial area, each of which can be further subdivided into various nuclei (Sims and Williams, 1990; Swanson and Petrovich, 1998). The basolateral complex for example is composed of three distinct structures namely the basal, lateral and accessory basal nuclei (Braak and Braak, 1983; Sims and Williams, 1990).

Recent studies carried out in humans have illustrated that the amygdala plays a crucial role not only in determining the emotional significance of sensory stimuli, but also in fear conditioning and emotional learning (Adolphs et al., 1994; LeDoux, 2000; Morris et al., 1996; Scott et al., 1997; Wilensky et al., 2000). The amygdala has also been implicated in a variety of brain disorders including Alzheimer's disease (Mori et al., 1999). Moreover, a large body of evidence suggests that the amygdala is a critical component of the hyperexcitable neuronal networks in TLE patients, where it is often the primary focus of seizure activity (Gloor 1992, 1997; Pitkanen et al., 1998; van Elst et al., 2000).

Extensive MRI studies have provided some insight into the importance of the amygdala in epilepsy by demonstrating unilateral or bilateral reductions in amygdalar volumes both in MTLE patients suffering from chronic epilepsy as well as in

individuals with a recent history of SE (Bernasconi et al., 2003; Bronen et al., 1995; Cendes et al., 1993; Pitkanen et al., 1998). Although in TLE patients this damage is commonly associated with AHS, isolated amygdalar pathology has also been detected in approximately 10% of patients who, interestingly, tend to present with more widespread EEG abnormalities and a greater predisposition for their seizures to become generalized (Gambardella et al., 1995; Hudson et al., 1993; Miller et al., 1994; Van Paesschen et al., 1996; Yilmazer-Hanke et al., 2000). Histochemistry of resected human epileptic tissue reveals that not all amygdalar nuclei are equally damaged but that the ventral regions of the amygdala, specifically the lateral and basal nuclei, are the most vulnerable to injury (Hudson et al., 1993; Miller et al., 1994; Pitkanen et al., 1998; Yilmazer-Hanke et al., 2000). Assessment of these nuclei discloses in addition to neuronal loss and gliosis the presence of synaptic alterations in the form of decreased dendritic branching of surviving cells also occurs (Aliashkevich et al., 2003).

Due to the overwhelming body of clinical evidence implicating the amygdala in the initiation and spread of limbic seizures, various studies have sought to identify the cellular and network mechanisms underlying the role of this structure in epileptogenesis. Earlier studies have shown that the amygdala has a low threshold for kindling (Goddard et al., 1969). In addition, in vitro investigations have demonstrated that in the presence of convulsive agents synaptic recruitment of amygdalar neurons via both excitatory and inhibitory mechanisms endows it with the ability to generate epileptic discharges and participate in epileptiform synchronization of limbic networks (Gean, 1990; Gean and Shinnick-Gallagher, 1988; Kleuva et al., 2003; Stoop and Pralong, 2000).

Neuropathological assessment of chronically epileptic animals has confirmed that damage to the amygdala is nucleus-specific and that some nuclei, specifically those of the basolateral complex, are more susceptible to injury than others (Nissinen et al., 2000; Tuunanen et al., 1996). Analogous to the pattern of damage observed in humans, loss of principal cells as well as decreased density of specific interneuronal populations has been documented in the lateral and basal amygdalar nuclei of

chronically epileptic animal tissue (Callahan et al., 1991; Tuunanen et al., 1996, 1997). Furthermore, combined MRI and histological studies carried out in pilocarpine-treated rodents have demonstrated that damage within the amygdala occurs at a much earlier time point in the disease process, shortly after SE (Roch et al., 2002a,b).

Further insight into the role of the amygdala in epileptogenesis stems from electrophysiological evaluation of chronically epileptic animal tissue demonstrating the presence of spontaneous bursting activity within the basal nucleus (Gean et al., 1989; Shoji et al., 1998). These studies, carried out in the lateral subdivision of the basal nucleus (i.e. the basolateral nucleus or BLA), have identified various mechanisms to account for neuronal network hyperexcitability including loss of spontaneously-occurring inhibitory postsynaptic potentials (IPSPs); loss of feedforward inhibition, as well as enhanced NMDA- and non-NMDA mediated excitation (Gean et al., 1989; Mangan et al., 2000; Rainnie et al., 1992; Shoji et al., 1998; Smith and Dudek, 1997). Unlike the BLA, electrophysiological assessment of the lateral nucleus (LA) in chronic animal models of TLE has been sparse (Niittykoski et al., 2004). Recently, a decrease in excitatory transmission, probably due to a decrease in glutamate release or neurodegeneration, has been reported within this nucleus in epileptic rodents (Niittykoski et al., 2004).

In conclusion, evidence from both human and experimental epilepsy suggests that synaptic alterations within the basolateral complex, specifically in the lateral and basal nuclei, render this amygdalar region hyperexcitable. These findings are increasingly relevant to understanding the role of the amygdala in the initiation and spread of seizures since the basolateral complex is densely interconnected with the hippocampus and parahippocampal cortices, structures that are highly implicated in TLE (Du et al, 1993; Pikkarainen and Pitkanen, 2001; Pitkanen et al., 1995, 2000b).

0.6.3 Perirhinal Cortex: Evidence for its Role in TLE

The perirhinal cortex (PC) is a parahippocampal structure that lies lateral to the rhinal fissure and has been established to play a crucial role in the limbic memory system (Buckley, 2005). It consists of two cytoarchitectonically distinct regions (areas 35 and 36) that receive prominent projections from both polymodal and unimodal cortices and

are also extensively interconnected with the hippocampus (via the lateral EC) and the amygdaloid complex (via the LA) (Burwell and Witter, 2002; Suzuki and Amaral, 1994a,b).

Despite the fact that MRI volumetric reductions occur within the PC of TLE patients (Bernasconi et al., 2000, 2003; Keller et al., 2004), the majority of evidence for the possible role of this structure in epilepsy stems from kindling studies. These elaborate investigations have demonstrated that both in vitro and in vivo, PC kindling occurs much faster and results in an earlier generalization of seizures than kindling of the amygdala, hippocampus and piriform cortex (McIntyre et al., 1993; McIntyre and Plant, 1989, 1993). Moreover, in addition to it being the most easily kindled structure within the mammalian forebrain, a pivotal role for the PC in the generalization of seizures has also been presented. For example, whereas local application of an NMDA receptor antagonist to the PC/insular cortex has been demonstrated to block amygdala-kindled seizures in rats (Holmes et al., 1992), lesional studies on the other hand have suggested that the PC is required for the generation of hippocampal motor seizures (Kelly and McIntyre, 1996; McIntyre and Kelly, 2000).

Further evidence implicating the PC in epileptogenesis arises from recent in vitro electrophysiological investigations carried out in combined hippocampal-parahippocampal slice preparations illustrating that the PC is capable of generating periodic oscillatory activity that depends on ionotropic glutamatergic receptors, GABAergic receptors and gap junctions (Kano et al., 2005). Furthermore, exposure of these brain slices to convulsive agents has been shown to induce seizure-like discharges that are more likely to initiate within the PC than within adjacent structures such as the EC and amygdala (de Guzman et al., 2004; Kleuva et al., 2003).

Despite these findings, extensive histological and electrophysiological assessment of the PC in chronically epileptic animals is still lacking. Although damage to the deep PC has been documented in pilocarpine-treated rodents (Covolan and Mello, 2000) the implications of these alterations to PC network excitability and ultimately to limbic network synchronization still needs to be determined.

0.7 Specific Objectives of Dissertation

The studies described herein employed the acute 4AP (*Chapters 1*, *2* and *3*) and chronic pilocarpine (*Chapters 1*, *4* and *5*) models of limbic seizures and were performed in combined horizontal slice preparations obtained mostly from rat tissue (except *Chapter 1*). Throughout the thesis, my work has centred around understanding the contribution of the subiculum, the amygdala (specifically the BLA and LA nuclei) and the PC to epileptogenesis. As mentioned previously, my investigations have particularly focused on assessing GABAergic signalling within these structures.

The specific questions addressed in my thesis are as follows: (1) Does an initial seizure-induced cell damage lead to decreased hippocampal output and increased EC ictogenecity in pilocarpine-treated mice? *(Chapter 1)* (2) Does the subiculum sustain EC hyperexcitability in epileptic mice through the temporoammonic pathway? *(Chapter 1)* (3) Can the subiculum gate hippocampal output activity? *(Chapter 2)* (4) Do GABAergic circuits within the subiculum play a role in its gating function? *(Chapter 2)* (5) What is the contribution of BLA/LA networks to 4AP-induced epileptiform synchronization in the combined slice preparation? *(Chapter 3)* (6) Do changes in inhibitory mechanisms within the LA and PC contribute to hyperexcitability of these structures in pilocarpine-treated rats? *(Chapters 4 and 5)* (7) Are LA-PC interactions altered in epileptic rats? *(Chapter 5).*

0.8 Functional Implications

The motivation behind the studies presented in this dissertation stems from the reality that despite the wealth of knowledge that has been acquired in the past few decades, the mechanisms underlying TLE remain to date elusive. By exploring limbic structures other than the extensively-studied hippocampus, my PhD studies will hopefully provide new answers that might not only deepen our current understanding of how neuronal network interactions contribute to epileptogenesis but also ultimately lead to improved medical treatments for patients with intractable TLE.

Chapter 1: Alterations in Limbic Network Interactions in a Mouse Model of Temporal Lobe Epilepsy

1.0 Linking Text & Information about publication

Previous investigations carried out in our laboratory using acute convulsant models strongly suggest that CA3-driven interictal activity exerts an important control over the propensity of the entorhinal cortex (EC) to generate ictal discharges (Avoli and Barbarosie, 1999; Barbarosie and Avoli, 1997; Barbarosie et al., 2002). These mouse studies have demonstrated that cutting the Schaffer collaterals to surgically isolate the EC from the hippocampus and in turn mimic the CA3/CA1 cell loss observed in human mesial temporal lobe sclerosis (MTS) results in two important observations: (i) increased EC ictogenesis; and (ii) enhanced activation of monosynaptic inputs from EC layer III to CA1/subiculum i.e. the temporammonic pathway (Avoli and Barbarosie, 1999; Barbarosie and Avoli, 1997; Barbarosie et al., 2000, 2002).

These findings led to the present study which was aimed at investigating whether the limbic network interactions established with the use of acute convulsant models could be reproduced in chronically epileptic mice. Specifically, the purpose of this investigation was to use the pilocarpine-treated mouse model of limbic seizures to determine whether neuronal loss in the hippocampus proper could potentially result in (i) a decreased control exerted by hippocampal outputs on the excitability of the EC; and (ii) increased activation of the temporoammonic pathway. The results of this study were published in the *Journal of Neurophysiology* in 2002 as a rapid communication entitled *"Limbic network interactions leading to hyperexcitability in a model of temporal lobe epilepsy"* (Authors: D'Antuono M, **Benini R**, Biagini G, D'Arcangelo G, Barbarosie M, Tancredi V and Avoli M). Permission granted by the journal to reproduce the contents of this manuscript can be found in Appendix A.

1.1 Abstract

In mouse brain slices that contain reciprocally connected hippocampus and entorhinal cortex (EC) networks, CA3 outputs control the EC propensity to generate experimentally induced ictal-like discharges resembling electrographic seizures.

Neuronal damage in limbic areas, such as CA3 and dentate hilus, occurs in patients with temporal lobe epilepsy and in animal models (e.g., pilocarpine- or kainate-treated rodents) mimicking this epileptic disorder. Hence, hippocampal damage in epileptic mice may lead to decreased CA3 output function that in turn would allow EC networks to generate ictal-like events. Here we tested this hypothesis and found that CA3-driven interictal discharges induced by 4-aminopyridine (4AP, 50μM) in hippocampus-EC slices from mice injected with pilocarpine 13-22 days earlier have a lower frequency than in age-matched control slices. Moreover, EC-driven ictal-like discharges in pilocarpine-treated slices occur throughout the experiment (≤6 h) and spread to the CA1/subicular area via the temporoammonic path; in contrast, they disappear in control slices within 2 h of 4AP application and propagate via the trisynaptic hippocampal circuit. Thus, different network interactions within the hippocampus-EC loop characterize control and pilocarpine-treated slices maintained in vitro. We propose that these functional changes, which are presumably caused by seizure-induced cell damage, lead to seizures in vivo. This process is facilitated by a decreased control of EC excitability by hippocampal outputs and possibly sustained by the reverberant activity between EC and CA1/subiculum networks that are excited via the temporoammonic path.

1.2 Introduction

Application of 4-aminopyridine (4AP) or Mg^{2+}-free medium to combined hippocampus-entorhinal cortex (EC) slices obtained from rodents induces ictal-like (thereafter termed ictal) epileptiform discharges that originate in EC and propagate to the hippocampus, as well as interictal activity initiating in CA3 (Avoli et al., 1996; Barbarosie and Avoli, 1997; Dreier and Heinemann, 1991; Wilson et al., 1988). CA3-driven interictal activity exerts an unexpected control on the EC propensity to generate ictal discharges. Accordingly, 1) interictal discharges occur throughout the experiment, but ictal activity disappears within 1-2 h; and 2) Schaffer collateral cut abolishes interictal activity in EC while making ictal discharge reappear in this structure (Barbarosie and Avoli, 1997).

Patients suffering from temporal lobe epilepsy present seizures involving the temporal cortex and limbic structures such as the hippocampus and the EC. These patients can manifest a pattern of brain damage (termed mesial temporal sclerosis) characterized by cell loss in CA3 and CA1 subfields and in the dentate hilus (Wieser et al., 1993). A similar pattern of brain damage is reproduced in laboratory animals by injecting kainic acid (Ben-Ari, 1985) or pilocarpine (Cavalheiro et al., 1996; Liu et al., 1994; Turski et al., 1984) that induces an initial status epilepticus followed 2-3 wk later by recurrent, limbic-type seizures.

Limbic network hyperexcitability in temporal lobe epileptic patients and in animal models mimicking this disorder may result from seizure-induced hippocampal damage leading to synaptic reorganization such as mossy fiber sprouting (Cavazos et al., 1991; Houser et al., 1990; Sutula et al., 1989). However, recurrent limbic seizures can occur in pilocarpine-treated rats when mossy fiber sprouting (but not neuronal damage) is abolished by inhibiting protein synthesis (Longo and Mello, 1997, 1998), thus suggesting that cell loss alone may cause a chronic epileptic condition. Since hippocampal output activity controls the EC propensity to generate electrographic seizures in control mouse slices (Barbarosie and Avoli, 1997), we predicted that a decrease in hippocampal network activity due to cell damage may lead per se to a chronic epileptic condition in pilocarpine-treated animals and perhaps in patients with temporal lobe epilepsy. Here, we tested this hypothesis by comparing the epileptiform patterns induced by 4AP in hippocampus-EC slices obtained from pilocarpine-treated and age-matched mice.

1.3 Method

Twenty-two CD-1 mice (29-42 days old) were used in this study. The procedures for injecting animals (n=12) with pilocarpine were similar to those used in our laboratories with rats (Liu et al., 1994). To prevent discomfort caused by stimulation of peripheral muscarinic receptors by pilocarpine (60-100 mg/kg), mice were pretreated with subcutaneous scopolamine methylnitrate (1 mg/kg). The animals' behavior was monitored $\leq$4 h after pilocarpine and scored according to Racine's classification (Racine et al., 1972b). Slices defined as "pilocarpine-treated" were

obtained 13-24 days following pilocarpine injection from mice with a behavioral response classified as stage 6 (i.e., tonic-clonic seizures occurring for ≥1 h). Control slices were obtained from age-matched mice. Animals were decapitated under halothane anesthesia; their brains were removed and placed in cold oxygenated artificial cerebrospinal fluid (ACSF) (Barbarosie and Avoli, 1997). Horizontal, hippocampus-EC slices (500μm thick) were cut with a vibratome and transferred to a tissue chamber where they lay between oxygenated ACSF and humidified gas (95% O_2-5% CO_2) at 32-34°C. ACSF composition was as follows (mM): 124 NaCl, 2 KCl, 1.25 KH_2PO_4, 2 $MgSO_4$, 2 $CaCl_2$, 26 $NaHCO_3$, and 10 glucose. 4AP (50 μM) was bath applied. Chemicals were acquired from Sigma.

Field potential recordings were made with ACSF-filled glass pipettes (tip diameter <10 μm; resistance <5-10 MΩ) positioned in EC, dentate gyrus, CA3 or CA1, and/or the subiculum. Signals were fed to high-impedance DC amplifiers and displayed on a Gould pen recorder. Field potential profiles of the ictal discharges recorded in the CA1/subiculum were performed with two recording electrodes. One electrode was maintained at a fixed position, while the other was moved in 100 μm stepwise increments along an axis normal to the alveus. Signals from the fixed electrode were used for temporal alignment of the field potentials obtained with the moving electrode. Field potential amplitudes at different latencies from the epileptiform discharge onset were calculated by averaging two to four events and plotted in a bidimensional fashion (i.e., amplitude versus space). In any given experiment, this type of analysis was restricted to ictal events that had similar electrographic characteristics (e.g., duration >20 s) when recorded from the fixed electrode. Time delays for discharge onset in different areas of the slice were calculated by taking as reference the first deflection from the baseline in expanded traces. Electrophysiological measurements are expressed as mean ± SD and n represents the number of slices studied. Data were compared with the Student's t-test or the analysis of variance (ANOVA) test and were considered significantly different if $p < 0.05$.

At the end of the experiments, some slices were fixed in 4% paraformaldehyde/100 mM phosphate-buffered solution overnight at 4°C and then rinsed several times in 15 and 30% sucrose-phosphate-buffered solutions for cryoprotection, and frozen at -80°C. Slices were cut with a cryostat into 14 μm thick sections and processed for Nissl staining. A blinded collaborator assessed the presence of tissue damage in various hippocampal regions. In pilocarpine-treated slices processed for histology (n = 7), we found a decrease of total neuron number that ranged 36-56 and 63-80% of controls in the CA1 and CA3 area, respectively. These data are in line with previous studies of the effects of ip pilocarpine in albino mice (Cavalheiro et al., 1996; Turski et al., 1984).

1.4 Results

Bath application of 4AP (50 μM) to combined hippocampus-EC slices (n = 8) obtained from control mice induced brief, interictal events at 0.5-1.1 Hz and prolonged ictal discharges with intervals of occurrence ranging 50-160 s. These two types of epileptiform activity were recorded in hippocampus and EC after 20-30 min of 4AP application (Fig. 1-1A). Time delay measurements and pathway cutting demonstrated that the interictal discharges originated in CA3 (Fig. 1-1A, inset), while the ictal events initiated in the EC (Barbarosie and Avoli, 1997). Moreover, ictal discharges disappeared in control slices within about 2 h of continuous 4AP application, while the interictal activity occurred throughout the experiment (Fig. 1-1, A and F).

Hippocampus-EC slices (n = 17) from pilocarpine-treated mice also responded to 4AP application by generating interictal and ictal discharges (Fig. 1-1B). However, the interictal activity observed in these experiments had a lower rate of occurrence and a longer duration than in control slices (Fig. 1-1, B, D, and E). Moreover, ictal discharges generated by pilocarpine-treated slices continued to occur throughout the experiment (≤6 h). Thus, the percentage of slices generating ictal discharges at different times of 4AP application was different when analyzed in control and pilocarpine-treated slices (Fig. 1-1F). As reported in control slices (Barbarosie and Avoli, 1997), ictal discharges in pilocarpine-treated slices initiated in EC (Fig. 1-1C).

Next, we analyzed the modalities of propagation of the interictal and ictal

discharges induced by 4AP in slices obtained from control and pilocarpine-treated mice. This was done by simultaneously recording the field potential activity in the EC, the dentate gyrus, and either the CA3 or the CA1/subiculum. The epileptiform activity occurring in control slices (n = 5) at the beginning of the experiment propagated as previously reported (Barbarosie and Avoli, 1997; Barbarosie et al., 2000). Namely, CA3-driven interictal discharges appeared to spread successively to CA1, subiculum, and EC from where they presumably re-entered the hippocampus via the perforant path (Fig. 1-2, A and C) (cf. Paré et al., 1992). Ictal discharges initiated in EC and propagated to the hippocampus through the perforant path with onset delays, suggesting the involvement of the classic trisynaptic hippocampal circuit (Fig. 1-2, A and D). CA3-driven interictal discharges in pilocarpine-treated slices (n = 10) also propagated to EC via the CA1-subiculum and re-entered the hippocampus via the perforant path (Fig. 1-2, B and C). In these experiments, however, ictal discharges initiating in EC were recorded in the dentate gyrus, CA1, and subiculum with similar time delays (Fig. 1-2, B and D). Hence, they presumably spread from the EC to the CA1/subiculum via the temporoammonic path.

Temporoammonic inputs to CA1/subicular neurons are localized more apically than those provided by the Schaffer collateral system (Soltesz and Jones, 1995). Therefore, we analyzed the depth profile characteristics of the ictal discharges recorded in the subiculum of control (n=5) and pilocarpine-treated slices (n=4). In both types of tissue, the steady shift associated with the ictal discharge was positive-going at or near the alveus, inverted in polarity when the electrode was moved toward the depth, and increased in amplitude as the electrode was further lowered toward the dentate upper blade (Fig. 1-3B). However, in pilocarpine-treated slices, it displayed maximal negative values at sites that were deeper (and thus more apical) than in control slices. Moreover, the peak-to-peak amplitude of the population spikes occurring during the ictal discharge attained maximal amplitude at approximately 500 and 700 μm in control and pilocarpine-treated slices, respectively. The depth-profile data obtained from three control and four pilocarpine-treated slices are summarized in Fig. 1-3, C and D.

1.5 Discussion

Hippocampal cell loss is found in patients with temporal lobe epilepsy (Wieser et al., 1993) and in laboratory animals treated with convulsants such as kainic acid (Ben Ari, 1985) or pilocarpine (Liu et al., 1994; Turski et al., 1983, 1984). The neuronal damage induced by the initial status epilepticus leads to sprouting along with synaptic reorganization (Cavazos et al., 1991; Gorter et al., 2001; Houser et al., 1990; Sutula et al., 1989). In addition, structural and functional impairment of GABA-mediated inhibition has been documented in these animal models (Doherty and Dingledine, 2001; Fountain et al., 1998; Gorter et al., 2001; Williams et al., 1993). However, it is unclear how these changes in network function produce a chronic epileptic condition.

Previous work performed in nonepileptic mouse hippocampus-EC slices has revealed that CA3-driven interictal activity controls the expression of ictal discharges in the EC, presumably by perturbing the ability of EC networks to reverberate (Barbarosie and Avoli, 1997). Here, we have found that CA3-driven interictal activity in pilocarpine-treated slices occurs at lower rates than in control tissue and that EC-driven ictal discharges persist throughout the experiment. Hence, we are inclined to propose that the cell damage and synapse loss seen in the CA3/CA1 areas of pilocarpine-treated slices (Cavalheiro et al., 1996; Turski et al., 1984), by reducing hippocampal output activity, may release its control on EC network excitability. In line with this view, similar data are obtained in control mouse slices by cutting the Schaffer collateral, a procedure that prevents CA3-driven interictal discharges from reaching the CA1/subiculum and thus from activating the EC (Barbarosie and Avoli, 1997).

We have also found that in intact, pilocarpine-treated slices the spread of ictal discharges from the EC to the CA1-subiculum occurs through the temporoammonic path (cf. Soltesz and Jones, 1995). In contrast, in control slices, this activity propagated to the CA1 through the classic trisynaptic circuit (cf. Paré et al., 1992). This conclusion is supported by the depth profile analysis of the ictal discharges recorded in the subiculum of control and pilocarpine-treated mice. We have previously shown in nonepileptic mouse slices that the temporoammonic path becomes involved

in the propagation of 4AP-induced ictal discharges after cutting the Schaffer collateral and thus after blocking the activation of CA1 and subicular networks (Barbarosie et al., 2000). Under normal conditions, depressing synaptic transmission between CA3 and CA1 makes the temporoammonic projection from the EC to CA1 operative (Maccaferri and McBain, 1995). In pilocarpine-treated tissue, this effect may also be contributed by a use-dependent reduction of the excitatory drive onto interneurons (Doherty and Dingledine, 2001). The functional consequence of this change in modality of propagation is that the ictal activity originating in the EC short-circuits the trisynaptic hippocampal route and thus can monosynaptically activate CA1 and subicular neurons, thus ensuring a high-fidelity synaptic transfer that increases epileptiform synchronization. Indeed, it may be hypothesized that in the pilocarpine-treated brain, subicular networks play a unique role in sustaining limbic seizures.

In conclusion, we have identified some differences in the way(s) limbic networks obtained from pilocarpine-treated and age-matched control mice interact in vitro during 4AP application. Our data provide some novel explanations for why pilocarpine-treated mice, and perhaps temporal lobe epilepsy patients, are susceptible to generating seizures in vivo. In particular, our findings emphasize the role played by cell loss in temporal lobe epilepsy that may hamper the control of EC excitability and also make the temporoammonic path operative.

1.6 Figures

Figure 1-1:

4-Aminopyridine (4AP)-induced epileptiform activities in control and pilocarpine-treated mouse hippocampus-entorhinal cortex (EC) slices. **A**: During the first hour of 4AP application, control slices generate spontaneous interictal and ictal discharges in CA3 and in EC. After 2h of 4AP treatment, the ictal discharges are no longer recorded, while the interictal activity continues to occur. Note in the inset that the interictal discharge recorded during the first hour starts in CA3 and spreads to the EC with a 75 ms latency. **B**: Similar experiment performed in a slice obtained from a pilocarpine-treated mouse. In this experiment as well both interictal and ictal discharges occur in CA3 and in EC. However, the interictal activity, which also initiates in CA3 and propagates to the EC with a 70 ms delay (inset), has a lower rate of occurrence and a longer duration than in the control slices. Note also that ictal discharges continue to occur after 2h of 4AP application. **C**: Expanded interictal-ictal discharge recorded in a pilocarpine-treated slice shows that the ictal event initiates in EC and propagates to CA3 with a 90 ms latency. **D** and **E**: Duration and rate of occurrence of interictal and ictal discharges in control (n=10) and pilocarpine-treated (n=11) slices. Values that were significantly different ($P<0.05$) are indicated by the asterisks. **F**: Percentage of slices generating ictal discharges at different times of 4AP application in control and pilocarpine-treated slices. Values were obtained from 6, 5, and 4 control slices for the periods of 1, 2-3, and 4-5 h, respectively, as well as from 8, 7, and 6 pilocarpine-treated slices for the periods of 1-3, 4, and 5 h, respectively.

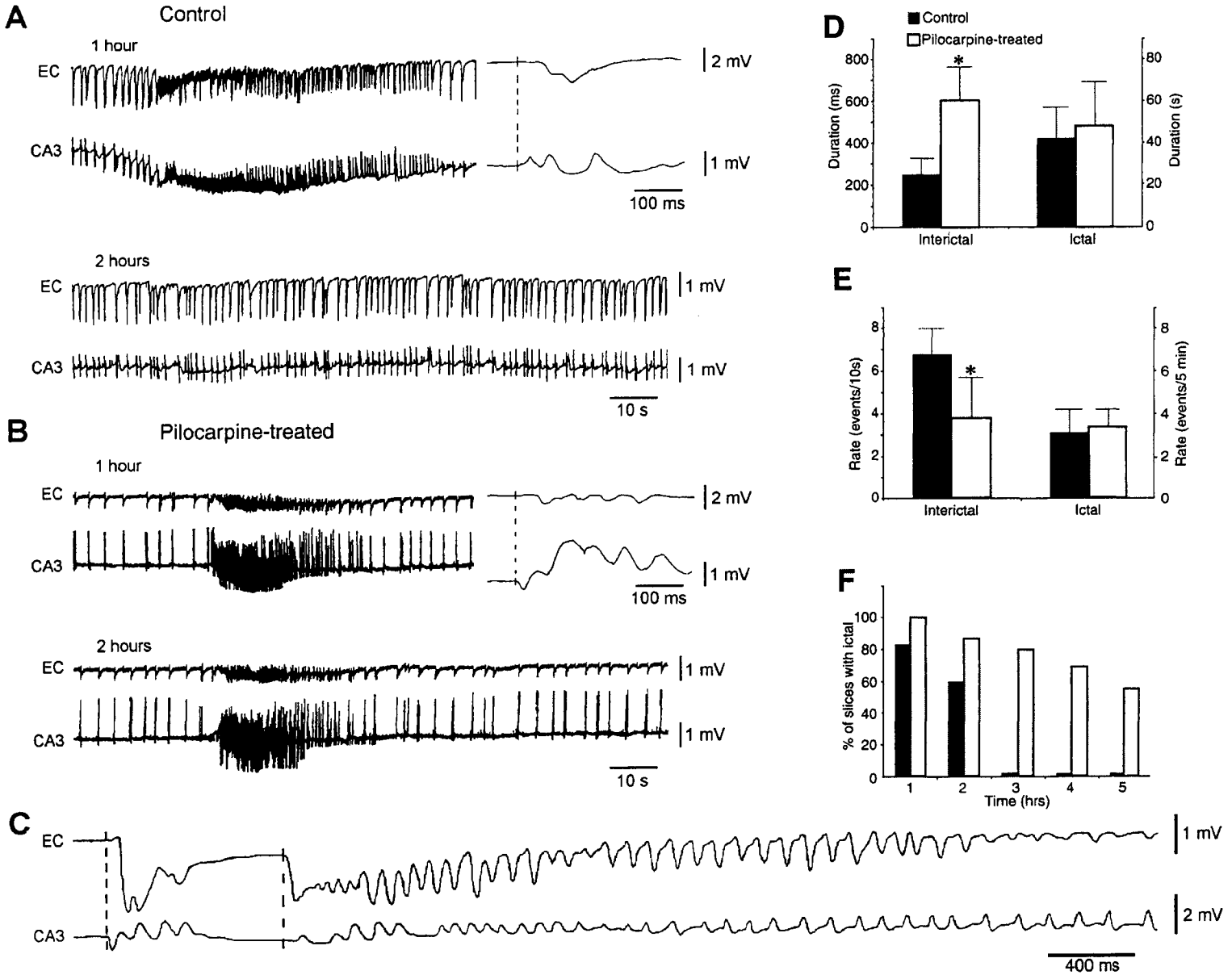
A
Control
1 hour
EC
CA3
2 mV
1 mV
100 ms
2 hours
EC
CA3
1 mV
1 mV
10 s
B
Pilocarpine-treated
1 hour
EC
CA3
2 mV
1 mV
100 ms
2 hours
EC
CA3
1 mV
1 mV
10 s
C
EC
CA3
1 mV
2 mV
400 ms
D
Control
Pilocarpine-treated
Duration (ms)
Duration (s)
Interictal
Ictal
E
Rate (events/10s)
Rate (events/5 min)
Interictal
Ictal
F
% of slices with ictal
Time (hrs)

Figure 1-2:

Propagation modalities of the 4AP-induced epileptiform activities in control and pilocarpine-treated slices. **A**: Simultaneous field potential recordings obtained from EC, dentate gyrus (DG), and CA1 in a control slice after 45 min of 4AP application. Both here and in **B**, the expanded traces in the bottom were triggered from the initial deflection seen in CA1 and in EC during the interictal and ictal discharge shown on the top recording. In this experiment, the differences in time onset suggest that interictal discharges occur first in CA1 and later spread to EC and DG, while the ictal discharges initiate in EC and spread successively to DG and to CA1. **B**: Similar experimental protocol performed in pilocarpine-treated slices. Note that in this experiment as well the interictal discharge is first seen in CA1 and propagates to the EC to re-enter the hippocampus via the perforant path. However, the ictal discharge initiating in EC appears in DG and in the CA1 with similar onset latencies. **C** and **D**: quantitative summary of the differences in time onset of interictal (**C**) and ictal (**D**) events recorded in different areas of control (n = 5) and pilocarpine-treated (n = 7). Note that the time lags between EC and CA1 or subiculum (SUB) for the ictal discharges are shorter in the pilocarpine-treated slices.

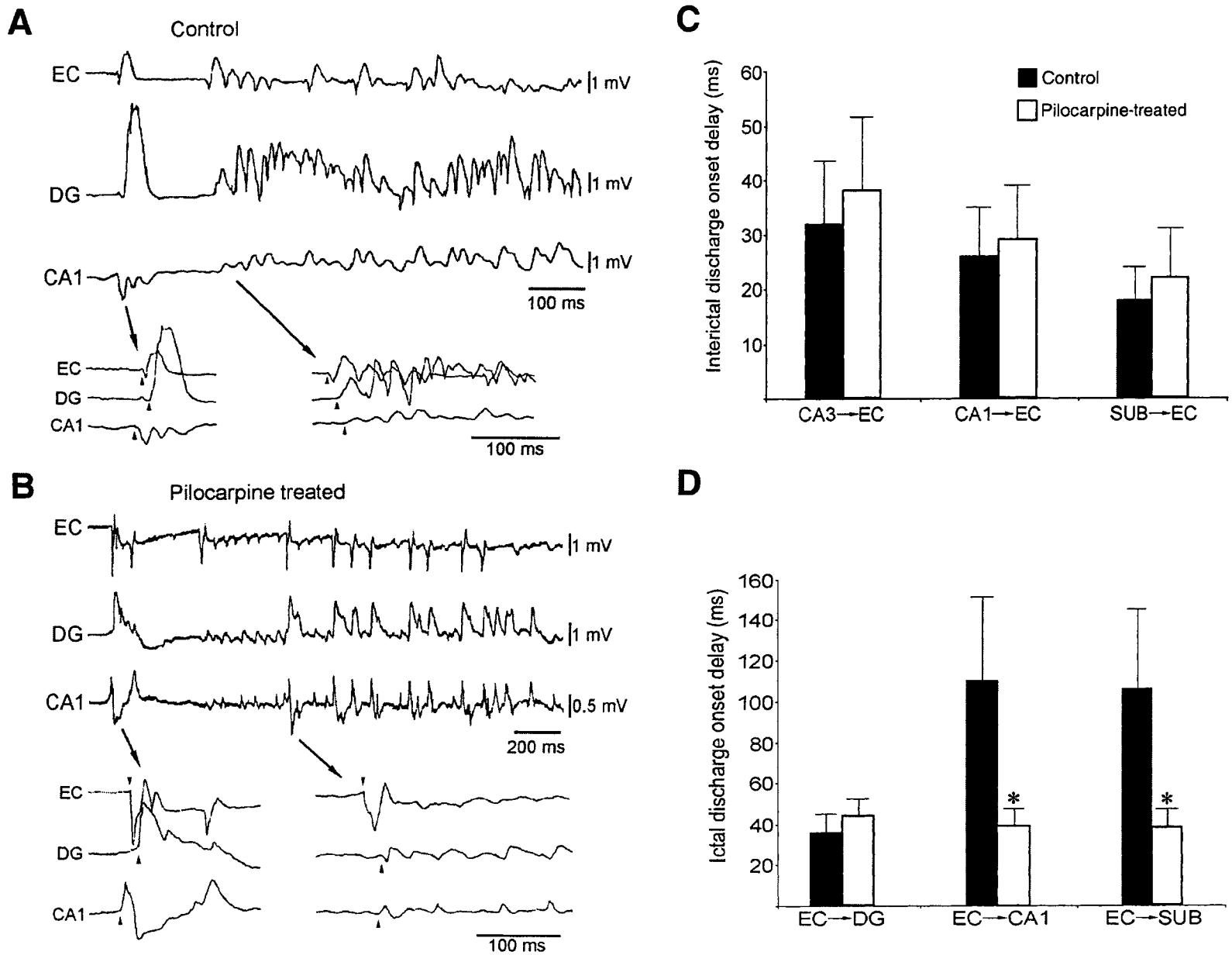
A
Control
EC
DG
CA1
1 mV
1 mV
1 mV
100 ms
EC
DG
CA1
100 ms
B
Pilocarpine treated
EC
DG
CA1
1 mV
1 mV
0.5 mV
200 ms
EC
DG
CA1
100 ms
C
Interictal discharge onset delay (ms)
60
50
40
30
20
10
Control
Pilocarpine-treated
CA3→EC
CA1→EC
SUB→EC
D
Ictal discharge onset delay (ms)
160
140
120
100
80
60
40
20
*
*
EC→DG
EC→CA1
EC→SUB

Figure 1-3:

Depth profile characteristics of the field potentials associated with the ictal discharges recorded in the CA1/subicular area of control and pilocarpine-treated slices. **A**: Schematic representation of the experimental procedure indicating the area where recordings were obtained with two microelectrodes: one was maintained at a fixed position, while the other was moved in 100 μm stepwise increments along an axis normal to the pial aspect of the subiculum. **B**: Field potential recordings obtained at different depths in control and pilocarpine-treated slices. Depth values were measured relative to the pia and are indicated on the left of each sample. Asterisks indicate the recording obtained from the stationary electrode in each of the two experiments. **C** and **D**: Depth distribution of the amplitudes of the fast events and of the DC shifts associated with the ictal discharges in control ($n = 3$) and pilocarpine-treated slices ($n = 4$). Values were grouped in increments of 100 μm. Note that the amplitudes of the fast transients in pilocarpine-treated slices attain maximal values at depths that are greater than control slices ($P < 0.05$). A similar pattern of distribution is also evident for the DC shift negative values.

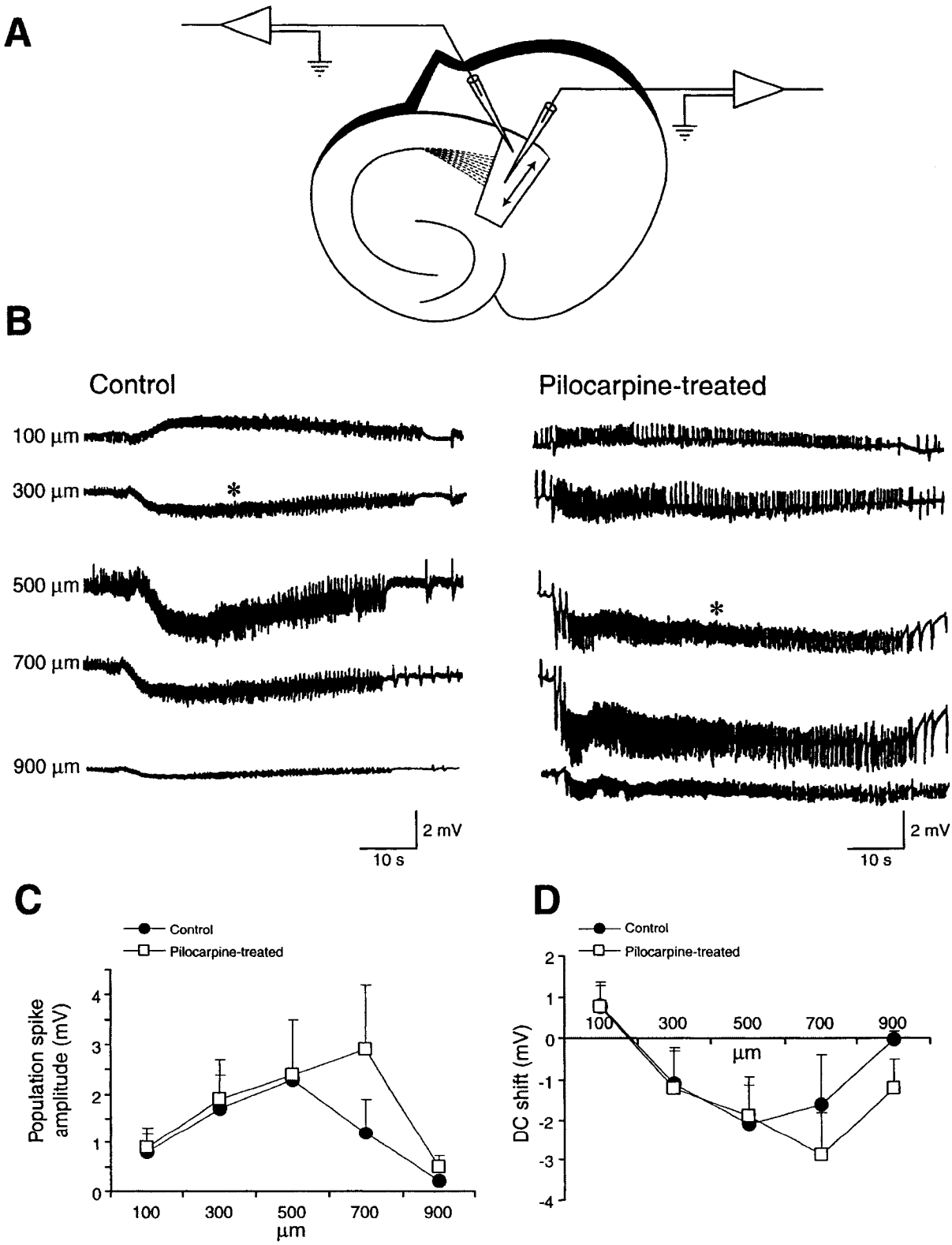
A
B
Control
Pilocarpine-treated
100 µm
300 µm
500 µm
700 µm
900 µm
*
*
2 mV
10 s
2 mV
10 s
C
Control
Pilocarpine-treated
Population spike amplitude (mV)
0
1
2
3
4
100
300
500
700
900
µm
D
Control
Pilocarpine-treated
DC shift (mV)
2
1
0
-1
-2
-3
-4
100
300
500
700
900
µm

Chapter 2: Investigating the Role of the Subiculum as a Gater of Hippocampal Output Activity

2.0 Linking Text & Information about publication

In the previous chapter, evidence from mouse epileptic tissue strongly suggested that the subiculum contributes to limbic seizure generation in vitro by sustaining reverberant interactions with the EC. These findings, together with observations made by other investigators, indicate that the subiculum plays an active role in TLE (Behr and Heinemann, 1996; Cohen et al., 2002; Wellmer et al., 2002; Wozny et al., 2003).

Elaborate anatomical data demonstrating that the subiculum is strategically positioned as the major output structure of the hippocampus exist. Interestingly however, an extensive search of the scientific literature revealed that no electrophysiological studies had functionally assessed the role of the subiculum in gating hippocampal output activity. Thus, in this study we sought to explore the role of the subiculum as a network filter of hippocampal outputs using the 4AP model. In addition, the contribution of local GABAergic circuits to this possible role was also examined in detail. The results presented in this chapter were published in the *Journal of Physiology* in 2005 in a manuscript entitled *"Rat subicular networks gate hippocampal output activity in an in vitro model of limbic seizures"* (Authors: **Benini R** and Avoli M). Permission granted by the journal to reproduce the contents of this manuscript can be found in Appendix B.

2.1 Abstract

Evidence obtained from human epileptic tissue maintained in vitro indicates that the subiculum may play a crucial role in initiating epileptiform discharges in patients with mesial temporal lobe epilepsy. Hence, we used rat hippocampus-entorhinal cortex (EC) slices to identify the role of subiculum in epileptiform synchronization during bath application of 4-aminopyridine (4AP, 50 μM). In these slices, fast CA3-driven interictal-like events were restricted to the hippocampal CA3/CA1 areas and failed to propagate to the EC where slow interictal-like and ictal-like epileptiform discharges were recorded. However, antagonizing $GABA_A$ receptors with picrotoxin (50 μM)

made CA3-driven interictal activity to spread to EC. Sequential field potential analysis along the CA3-CA1-subiculum axis revealed that the amplitude of CA3-driven interictal discharges recorded in the presence of 4AP only diminished within the subiculum. Furthermore, CA1 electrical stimulation under control conditions elicited little or no subicular activation and never any response in EC; in contrast, robust subicular discharges that spread to EC could be evoked after picrotoxin. Intracellular recordings indicated that potentiation by picrotoxin was associated with blockade of hyperpolarizing IPSPs in subicular cells. Finally, when surgically isolated from adjacent structures, the subiculum generated low-amplitude synchronous discharges that corresponded to an intracellular hyperpolarization-depolarization sequence, were resistant to glutamatergic antagonists, and represented the activity of synchronized interneuronal networks. Bath application of picrotoxin abolished these 4AP-induced events and in their place robust network bursting occurred. In conclusion, our study demonstrates that the subiculum plays a powerful gating role on hippocampal output activity. This function depends on $GABA_A$ receptor-mediated inhibition and controls hippocampal-parahippocampal interactions that are known to modulate limbic seizures.

2.2 Introduction

Mesial temporal lobe epilepsy (MTLE) is one of the most common types of partial epilepsy in humans (Wiebe, 2000). MRI images from MTLE patients are often characterized by hippocampal atrophy which, upon histological examination, reveals extensive neuronal loss and gliosis in the dentate hilus and CA3/CA1 areas along with synaptic reorganization (Houser et al., 1990; Sutula et al., 1989). In addition, neuronal damage in this epileptic disorder is seen in limbic areas such as the entorhinal cortex (EC) and the amygdala (Du et al., 1993; Gloor, 1997; Houser, 1999; Pitkanen et al., 1998; Yilmazer-Hanke et al., 2000). Histopathological analysis of human epileptic tissue has also shown that subicular principal cells are relatively unaffected in MTLE (Gloor, 1997). Nevertheless, the absence of neuronal loss in the subiculum does not exclude the possibility that this area may play an active role in MTLE. Indeed, recent studies in both human (Cohen et al., 2002; Wozny et al., 2003) and animal (Behr and

Heineman, 1996; D'Antuono et al., 2002; Wellmer et al., 2002) epileptic tissue suggest that cellular and synaptic reorganization in the subiculum contributes to limbic seizure generation.

The subiculum holds a strategic position within the limbic system. Not only does it serve as the major output structure of the hippocampus, getting extensive projections from the CA1 hippocampal region (Finch and Babb, 1981; Witter et al., 1989), but it also projects to various limbic and extralimbic areas including EC layers IV and V (Swanson and Cowan, 1977; Witter et al., 1989), perirhinal cortex (Deacon et al., 1983; Swanson et al., 1978), amygdala (Canteras and Swanson, 1992) and thalamus (Canteras and Swanson, 1992; Witter et al., 1990) (see for review O'Mara et al., 2001). In this study, we sought to identify the role played by the subiculum in intralimbic synchronization using the 4-aminopyridine (4AP) in vitro model of limbic seizures. Here, we report that $GABA_A$ receptor-mediated mechanisms confer the subiculum with the ability to gate hippocampal output activity, and thus to dictate the interactions between hippocampal and parahippocampal neuronal networks.

2.3 Methods

Male, adult Sprague-Dawley rats (150-200 g) were decapitated under halothane anesthesia according to the procedures established by the Canadian Council of Animal Care. The brain was quickly removed and a block of brain tissue containing the retrohippocampal region was placed in cold (1-3 °C), oxygenated artificial cerebrospinal fluid (ACSF). The brain's dorsal side was cut along a horizontal plane that was tilted by a 10° angle along a postero-superior-anteroinferior plane passing between the lateral olfactory tract and the base of the brain stem (Avoli et al., 1996). Horizontal slices (450-500 μm) containing the EC and the hippocampus were cut from this brain block using a vibratome. Subicular minislices were prepared from these horizontal slices by using microknife cuts to isolate the subiculum from the other hippocampal and parahippocampal structures (Fig. 2-7B). Slices were then transferred into a tissue chamber where they lay at the interface between ACSF and humidified gas (95% O_2, 5% CO_2) at a temperature of 34-35 °C and a pH of 7.4. ACSF composition was (in mM): NaCl 124, KCl 2, KH_2PO_4 1.25, $MgSO_4$ 2, $CaCl_2$ 2,

$NaHCO_3$ 26, and glucose 10. 4AP (50 μM), bicuculline methobromide (BMI, 10 μM), 6-cyano-7-nitroquinoxaline-2,3-dione (CNQX, 10 μM), 3,3-(2-carboxypiperazin-4-yl)-propyl-1-phosphonate (CPP, 10-30 μM), and picrotoxin (PTX, 50 uM) were applied to the bath. Chemicals were acquired from Sigma (St. Louis, MO, USA) with the exception of BMI, CNQX and CPP that were obtained from Tocris Cookson (Ellisville, MO, USA).

Field potential recordings were made with ACSF-filled, glass pipettes (resistance=2-10 MΩ) that were connected to high-impedance amplifiers. The location of the recording electrodes in the combined hippocampus-EC slice is shown in Fig. 2-2A. Field responses were induced by applying single shock electrical stimuli (50-100 μs; <200 μA) delivered through a bipolar, stainless steel electrode (Fig. 2-3A). Sharp-electrode intracellular recordings were performed in the subiculum with pipettes that were filled with 3M K-acetate (tip resistance= 70-120 MΩ). Intracellular signals were fed to a high-impedance amplifier with internal bridge circuit for intracellular current injection. The resistance compensation was monitored throughout the experiment and adjusted as required. The passive membrane properties of the subicular cells included in this study were measured as follows: (i) resting membrane potential (RMP) after cell withdrawal; (ii) apparent input resistance (Ri) from the maximum voltage change in response to a hyperpolarizing current pulse (100-200 ms, <-0.5 nA); (iii) action potential amplitude (APA) from the baseline and (iv) action potential duration (APD) at half-amplitude. Intrinsic firing patterns of subicular cells were determined from responses to depolarizing current pulses of 500-1000 ms duration. Three neuronal types could be distinguished in this study: strong bursters, weak bursters and regular firing (Staff et al., 2000). Since no differences were observed between these classes in terms of their 4AP-induced activity, strong and weak intrinsic bursters were put together in the "bursting" group (Fig. 2-5Ab) whilst regular firing cells were placed in the "non-bursting" category (Fig. 2-6Ab). No fast spiking cells were ever recorded in this study.

Field potential and intracellular signals were fed to a computer interface (Digidata 1322A, Axon Instruments) and acquired and stored using the pClamp 9

software (Axon Instruments). Subsequent analysis of these data was made with the Clampfit 9 software (Axon Instruments). For time-delay measurements, the onset of the field potential/intracellular signals was established as the time of the earliest deflection of the baseline recording (e.g., insert traces in Fig. 2-1A and B). Throughout this study we arbitrarily termed as "interictal" and "ictal" the synchronous epileptiform events with durations shorter or longer than 2 s, respectively (cf., Traub et al., 1996). Measurements in the text are expressed as mean ± SD and n indicates the number of slices or neurons studied under each specific protocol. Data were compared with the Student's t-test and were considered statistically significant if $p < 0.05$.

2.4 Results

2.4.1 Epileptiform activity induced by 4AP in combined hippocampus-EC slices

As illustrated in Figs. 2-1A (Control (4AP)) and 2-2A, the hippocampus-EC slices (n= 110) included in this study responded to 4AP application by generating three types of synchronous activities (cf., Avoli et al., 1996; Benini et al., 2003): (i) fast interictal discharges (interval of occurrence= 1.6±0.7 s; duration 139±65 ms; n= 25) that were restricted to the hippocampus proper (Fig. 2-1A, arrows); (ii) slow interictal events that were recorded in both hippocampal and EC regions and could initiate anywhere in the slice (interval of occurrence= 28±15 s; n= 25; Fig. 2-1A, asterisk) and (iii) long-lasting ictal discharges (interval of occurrence= 236±117 s; duration 64±56 s; n= 25) that originated in EC and could propagate to the hippocampus via the perforant pathway (Fig. 2-1A, bar). We termed these slices as functionally disconnected due to the lack of epileptiform activity propagation from the hippocampus to the EC.

2.4.2 Involvement of $GABA_A$ receptors in the epileptiform activity induced by 4AP

Next, we superfused these slices with the $GABA_A$ receptor antagonist picrotoxin (50 μM) to establish the role of $GABA_A$ receptor-mediated mechanisms in 4AP-induced epileptiform discharges. As shown in Fig. 2-1, picrotoxin application to these functionally disconnected slices (n= 45) resulted in a dramatic change in the 4AP-induced electrographic activity (Figs. 2-1 and 2-2). Exposure to this non-competitive $GABA_A$ receptor antagonist triggered an initial ictal burst in the EC (Fig. 2-2B,

+Picrotoxin) after which the activity was replaced by robust interictal discharges that initiated in CA3 and propagated sequentially to CA1 and EC (expanded trace in the insert of Fig. 2-1B, +Picrotoxin,). This phenomenon was reproduced with the competitive $GABA_A$ receptor antagonist BMI (10 μM, n= 4) thus suggesting that the effect observed was indeed due to hindrance of $GABA_A$ receptor function. Transformation of a functionally disconnected slice into one in which hippocampal-driven epileptiform activity could propagate to the EC was fully reversible upon washing out picrotoxin (n=6) for approx. 2 hr (not shown).

2.4.3 $GABA_A$ receptor antagonism potentiates interictal activity in the subiculum of functionally disconnected slices

To gain a better understanding of how $GABA_A$ receptor antagonism in functionally disconnected slices leads to synchronicity between hippocampus and EC, we analyzed the 4AP-induced activity in neuronal networks along the CA3-CA1-subiculum axis (n=14). This was achieved by obtaining simultaneous field potential recordings from CA3 and EC with two fixed electrodes while a third electrode was moved sequentially from the CA1-CA2 area towards the subiculum at the level of the stratum pyramidale. We found in 6 of these experiments that the CA3-driven interictal events had similar amplitudes up to the CA1-subiculum border (Fig. 2-2Ab, Control, +4AP) and then decreased as the recording electrode was placed in subiculum (Fig. 2-2Ac, Control, +4AP). Moreover, in the remaining experiments (n=8) interictal events were not recorded during 4AP application in the subiculum concomitant with those seen in the CA3 and CA1 areas (Fig. 2-4A).

Following picrotoxin application (Fig. 2-2B, +Picrotoxin), there was a potentiation in the amplitude of the epileptiform activity recorded within the subiculum. Moreover, such augmentation always occurred prior to the establishment of complete synchronization of the epileptiform activity between hippocampus and EC (Fig. 2-2B, +Picrotoxin, middle insert). Quantitative analysis of the picrotoxin-induced changes in field potential amplitudes in CA3, CA1 and subiculum revealed that the most drastic potentiation (314±163 %, n= 6) occurred within the last structure whereas the least augmentation took place in CA3 (31±8 %; n= 6) (Fig. 2-2C).

2.4.4 Stimulation of hippocampal networks elicits response in EC only under $GABA_A$ receptor antagonism.

To explore further the propagation of hippocampal-driven activity to the EC, we investigated the responses induced in the slice by focal electrical stimuli delivered in CA1, subiculum and EC: (i) in the absence of convulsants (i.e., normal ACSF); (ii) in the presence of 4AP and (iii) during application of 4AP + PTX (Fig. 2-3A, B and C, respectively). In these experiments, three recording electrodes were placed in CA1 stratum pyramidale, subiculum and EC deep layers while a stimulating electrode was used to sequentially activate each of these structures.

As expected, a local field response could be recorded in any of the stimulated structures during application of normal ACSF (Fig. 2-3Aa-c, arrows); in addition, EC stimulation could also elicit some responses in subiculum and CA1. Following 4AP application (Fig. 2-3B), the local responses increased in amplitude and duration while distant activation could be clearly identified when stimuli were delivered in subiculum and EC (Fig. 2-3Bb and c, respectively); in contrast, as seen in normal medium, CA1 single shock stimuli (Fig. 2-3Ba) failed in eliciting subicular (n=12) or EC responses (n=24). Finally, during concomitant application of 4AP and picrotoxin, electrical stimuli delivered in any area of the slice induced robust epileptiform discharges in all limbic structures (Fig. 2-3Ca-c, (4AP+PTX)). It should be emphasized that CA1 single-shock stimuli delivered during $GABA_A$-receptor antagonism (Fig. 2-3Ca) elicited an epileptiform response not only in subiculum, but also in EC (n=6). Therefore, these observations suggest that $GABA_A$ receptor-mediated mechanisms prevent the propagation of both stimulation- and 4AP-induced hippocampal activity to the EC, thereby confirming that the functional disconnectivity between the hippocampus proper and EC was not merely an artifact of the 4AP model itself. In addition, both the potentiation of subicular responses by picrotoxin and the subsequent ability of hippocampal-driven discharges to propagate to the EC suggest that these inhibitory restrictions are most likely at play in the subiculum itself.

2.4.5 Picrotoxin-induced changes in connectivity do not require NMDA receptor function

We also assessed whether NMDA receptors contributed to the changes in connectivity seen during picrotoxin application. To this end we applied high concentrations of the NMDA-receptor antagonist CPP to functionally disconnected slices. As shown in Fig. 2-4B (+30 μM CPP, n= 5) CPP abolished the 4AP-induced ictal events that initiated in EC (Avoli et al., 1996; de Guzman et al., 2004). However, further addition of picrotoxin could still cause an initial ictal event followed by interictal activity in all areas of the slice (Fig. 2-4C, +30 μM CPP + 50 μM Picrotoxin). Furthermore, NMDA receptor blockade did not avert the picrotoxin-induced potentiation of the interictal activity or its appearance in the subiculum. (Fig. 2-4C; n= 5).

2.4.6 Simultaneous field potential and intracellular recordings in the subiculum

The results obtained from the functionally disconnected slices during application of medium containing only 4AP suggest that the subiculum plays a role in gating hippocampal output activity. Furthermore, the ability of CA3-driven epileptiform discharges to propagate to the EC during picrotoxin suggests that GABAergic mechanisms in the subiculum might be involved in such a control. Hence, we recorded intracellularly subicular cells along with field potential activity in CA3 and EC in the presence of 4AP and following further addition of picrotoxin.

Two main modes of subicular activity were recorded from these slices during 4AP application. The first type was seen in 20 subicular cells and consisted of bursts of action potentials that followed the interictal discharges recorded in CA3 with time lags of 21±9 ms (n=7) (Fig. 2-5). Electrophysiological characterization of these neurons revealed that 9 out of 20 cells were intrinsic non-bursters (RMP= -62.9±7.2 mV, Ri= 66.4±16.3 MΩ, APA= 93.5±13.3 mV, APD= 1.0±0.2 ms; not shown) while the remaining 11 cells (RMP= -63.4±7.0 mV, Ri= 60.9±15.6 MΩ, APA= 94.5±6.8 mV, APD= 1.0±0.1 ms) discharged action potential bursts at the onset of an intracellular depolarizing pulse (Fig. 2-5Ab). Application of picrotoxin to these slices resulted in synchronous interictal discharges occurring in all areas. Furthermore, expanded traces demonstrated that these intracellular events followed CA3 field

activity and preceded that of the EC (Fig. 2-5B, Picrotoxin (late), insert). Intracellular injection of depolarizing pulses indicated that picrotoxin did not modify the intrinsic firing patterns of these cells (not shown).

In contrast, the second group of subicular cells (n=11) generated little or no spontaneous action potential firing, while producing robust post-synaptic potentials (PSPs) in association with the CA3-recorded interictal discharges (Fig. 2-6Aa, Control (4AP)). These PSPs were usually predominated by a hyperpolarizing component (Fig. 2-6A, Control (4AP), arrows in the lower insert) with a reversal value of approx. -71mV (not illustrated) suggesting that they were $GABA_A$ receptor mediated. In addition, these neurons also generated large isolated hyperpolarizing potentials (Fig. 2-6A, Control (4AP), asterix in the lower insert) with a similar reversal potential. Examination of the firing properties of these cells (Fig. 2-6Ab) revealed that 9 out of 11 were non-bursting elements (RMP= -67.7±5.1 mV, Ri= 57.2±14.3 MΩ, APA= 99.2±5.4 mV, APD= 1.2±0.1 ms). Superfusion of these slices with picrotoxin transformed the activity of these "silent" cells into synchronous burst firing (Fig. 2-6Aa, Picrotoxin). Monitoring the evolution in the intracellular activity of these neurons from the onset of picrotoxin application (Fig. 2-6Aa, Picrotoxin (transition)) until the complete synchronization between hippocampal areas and EC (Fig. 2-6Aa, Picrotoxin, late) revealed a gradual decrease in the frequency of occurrence and the eventual disappearance of the robust PSPs (Fig. 2-6Aa, Picrotoxin (transition) vs. Picrotoxin (late)) along with the complete blockade of the isolated hyperpolarizing potentials. As with the other group of subicular cells, the intrinsic firing patterns of these neurons were not changed by picrotoxin (not shown).

2.4.7 Picrotoxin-induced potentiation in subicular activity is not due to upstream effects

It has been well-documented that GABAergic circuits exert an important inhibitory control over local networks within CA3/CA1; in addition, loss of this restrain via $GABA_A$ receptor antagonism is sufficient to unmask polysynaptic glutamatergic excitation within these structures (Miles and Wong, 1987; Miles et al., 1988). Hence, it can be reasonably argued that the picrotoxin-induced potentiation of subicular

activity observed in our experiments might arise from enhanced, upstream hippocampal output rather than decreased gating within the subiculum. In order to clarify this issue, bath application of picrotoxin was investigated in slices in which the subiculum was isolated from CA3/CA1 by knife-cuts to the Schaffer collaterals (Fig. 2-7Aa). In this set of experiments, potentiation of subicular activity upon $GABA_A$ receptor antagonism was observed to occur in spite of the cut (n=6, Fig. 2-7Ab, +Picrotoxin). However, epileptiform discharges in this scenario appeared to initiate sometimes in the subiculum (n=3 slices) and at other times in the EC (n=3 slices) (Fig. 2-7Ab, insert).

The potential gating role of subicular networks was further addressed in isolated subicular minislices (Fig. 2-7B). In the presence of 4AP, low-amplitude synchronous discharges (interval of occurrence= 142±107 s; 55-450 s; n= 18) were observed to occur in all areas of the isolated subiculum and could initiate in the proximal, middle or distal regions (Fig. 2-7Ba, Control (4AP)). Subsequent addition of picrotoxin induced a drastic augmentation of activity in all subicular regions (n=13, Fig. 2-7Ba, +Picrotoxin) thereby providing conclusive evidence that during 4AP application subicular networks, both in the combined slice as well as the isolated minislice preparations, are under tight $GABA_A$ receptor-mediated control.

2.4.8 Slow 4AP-induced interictal discharges generated in the subiculum represent the activity of synchronized interneuronal networks

Intracellular characterization of the slow-interictal discharges recorded in subicular minislices revealed a sequence of an early hyperpolarizing IPSP followed by a long lasting depolarization that could at times trigger action potential firing (Fig. 2-8Aa,b and 8B, Control (4AP); n=20 neurons). Bath application of picrotoxin abolished these events and in their place robust network bursting was observed (n=6 neurons, Fig. 2-8Aa, +Picrotoxin).

To further investigate the mechanisms underlying the generation of these 4AP-induced slow events, glutamatergic antagonists were employed. Interestingly, CPP and CNQX could not abolish these low amplitude discharges (Fig. 2-8B, + (CPP+CNQX), n=8) while further application of picrotoxin resulted in their complete loss (n=4, not

shown). Thus, these results indicate that as in other cortical areas (Avoli et al., 1994, 1996; Perreault and Avoli, 1989, 1992) the synchronous potentials recorded in the subiculum in the presence of 4AP correspond to the responses of pyramidal cells to the synchronized interneuron activity.

2.5 Discussion

We have found here that decreasing $GABA_A$ receptor function facilitates communication within the limbic networks contained in a combined hippocampus-EC slice. Accordingly, picrotoxin transformed functionally disconnected slices into ones that were functionally connected. In addition, we have discovered that this effect is mainly caused by a gating function played by the subiculum on hippocampal outputs, thus indicating that this limbic structure modulates interactions between hippocampal and parahippocampal networks.

2.5.1 The 4AP model revisited in the light of different patterns of epileptiform activity

We have reported that in reciprocally interconnected hippocampal-EC slices obtained from adult rat (Benini et al., 2003) or mouse brains (Barbarosie and Avoli, 1997; Barbarosie et al., 2000), application of 4AP-containing or Mg^{2+}-free medium induces CA3-driven interictal events that propagate to the EC where they control the propensity of this latter structure to generate ictal discharges resembling those seen in MTLE patients (cf. Swartzwelder et al., 1987; Wilson et al., 1988). Accordingly, cutting the Schaffer collaterals in these functionally connected slices averts CA3 outputs and discloses NMDA receptor-mediated ictal events in the EC, thus leading to a pattern of epileptiform activity similar to what is recorded in functionally disconnected slices (Avoli et al., 1996; Benini et al., 2003).

Until now, we assumed that the inability of CA3-driven interictal activity to propagate to the EC was caused by the slicing procedure that had led to damaging the connections between hippocampus proper and EC. Contrary to this view, we have discovered here that $GABA_A$ receptor antagonism can reversibly transform a disconnected slice into one that appears to be functionally connected. Hence, these findings demonstrate that the two patterns of electrographic activity may not reflect

anatomical differences, but rather implicate a mechanism that rests on the gating role played by subicular networks on the propagation of epileptiform discharges originating in the hippocampus proper.

2.5.2 Subicular networks gate hippocampal outputs via $GABA_A$ receptor-mediated mechanisms in functionally disconnected slices

By using sequential recordings along the CA3-CA1-subiculum axis of functionally disconnected slices we have found that the amplitude of the 4AP-induced interictal activity decreases dramatically in the subiculum where it is often non-existent. Moreover, during $GABA_A$ receptor antagonism, the subiculum undergoes the most dramatic potentiation in field activity (150-550 %) signalling an increased recruitment of neurons.

It has been established that disinhibition unmasks polysynaptic excitation within CA3 neuronal networks (Miles and Wong, 1987; Miles et al., 1988) and it is possible that this improved synchronicity would consequently lead to an increased drive onto the subiculum. Local pharmacological activation of the subiculum would have been ideal for clarifying this issue. However, initial attempts at focal applications of picrotoxin were elusive due to the fact that in our horizontal slice preparation the subiculum lies critically close to other structures (CA1, dentate gyrus, and medial EC) and dispersion of the droplet to these areas could not be avoided. This being said, our observations strongly suggest that although increased presynaptic release of excitatory transmitters at CA1-subiculum synapses may occur, this mechanism is unlikely by itself to explain the amplification of subicular activity observed under $GABA_A$ receptor antagonism. First, potentiation of subicular activity upon $GABA_A$-receptor antagonism was observed even when the subiculum was separated from CA3/CA1 via microknife cuts to the Schaffer collaterals. Furthermore, significant augmentation in activity was demonstrated to occur in isolated subicular minislices in the absence of either upstream or downstream factors. Altogether this is conclusive evidence that the picrotoxin-induced effect in the subiculum is not due to enhanced output of upstream structures (i.e. CA3/CA1) but rather due to the decreased control of GABAergic circuits within the subiculum itself.

Investigation into the functional role of GABAergic circuits within the subiculum was made possible by the interesting property of the 4AP model used in our study. In addition to blocking K^+ currents (Rudy, 1988) and interfering with Ca^{2+} channels (Segal and Barker, 1986), 4AP has been shown to facilitate neurotransmitter release at presynaptic terminals of both excitatory and inhibitory synapses (Aram et al., 1991; Rutecki et al., 1987; Thesleff, 1980). Previous studies have shown that the subiculum is indeed capable of generating robust interictal discharges under conditions of decreased inhibition (Harris and Stewart, 2001) or increased excitation (Behr and Heineman, 1996; Harris and Stewart, 2001). Using our model we have however shown that the subiculum does not generate robust activity when both excitatory and inhibitory mechanisms are simultaneously altered. Furthermore, we found in the isolated subiculum that under such conditions, this structure is more likely to generate slow synchronous events that are resistant to glutamatergic antagonists but sensitive to $GABA_A$ receptor blockade. These synchronous potentials, which have been reported in other hippocampal structures as well as in the neocortex, represent the activity of highly synchronized interneuronal networks (Avoli et al., 1994, 1996; Lamsa and Kaila, 1997; Michelson and Wong, 1994; Perreault and Avoli, 1989, 1992). Altogether, these findings indicate that the overall activity of the subiculum in the presence of 4AP is predominated by inhibitory mechanisms that control hippocampal output propagation to the EC. Blockade of $GABA_A$ receptors hampers this inhibition (as suggested by the decrease in IPSPs recorded in "silent" subicular cells), allowing an increased recruitment of subicular networks and the consequent spread of both spontaneous and stimulus-induced activity from the hippocampus to the EC.

2.5.3 Subicular cells may be under a different degree of $GABA_A$ receptor-mediated control in the same functionally disconnected slice.

Neurophysiological investigations have shown that several types of GABAergic cells are present in the subiculum (Greene and Totterdell, 1997; Kawaguchi and Hama, 1987; Menendez de la Prida et al., 2003). We have found here that under control conditions (i.e., during application of medium containing 4AP only) subicular

pyramidal neurons generate two different patterns of intracellular activity in functionally disconnected slices: one group of cells fired action potentials in coincidence with CA3-driven interictal events whilst the other generated either EPSP-IPSP sequences or isolated IPSPs. These two behaviors of subicular cells, both of which could be found in the same slice, have also been reported in the human epileptic subiculum of MTLE patients where they reflect differences in the reversal potential of pyramidal cells for $GABA_A$ receptor-mediated conductances (Cohen et al., 2002).

The presence of "silent" subicular cells in functionally disconnected slices indicates that hippocampal activity may not propagate to the EC due to local inhibitory control exerted on a subset of projecting subicular cells. In line with this view, previous studies have demonstrated that subicular pyramidal cells are restrained by local GABAergic networks via feedforward (Behr et al., 1998; Colino and Fernandez De Molina, 1986; Finch and Babb, 1980; Finch et al., 1988) and recurrent inhibitory mechanisms (Menendez de la Prida, 2003; Menendez de la Prida and Gal, 2004). Accordingly, we have demonstrated that IPSP blockade by $GABA_A$ receptor antagonism coincides with the appearance of network-driven burst firing, thus implicating a role for subicular $GABA_A$ receptor-mediated inhibition in gating hippocampal output activity. Indeed, it has been reported that epileptiform discharges generated in the hippocampus can successfully propagate to the medial EC via the subicular complex under reduction of GABAergic mechanisms (Menendez de la Prida and Pozo, 2002).

2.6 Conclusions

Studies in various epilepsy models have identified the dentate gyrus as a gater for the spread of limbic seizures from the EC to the hippocampus proper (Collins et al., 1983; Heinemann et al., 1992). However, until this study, no investigation had addressed the role of the subiculum in controlling hippocampal outputs during epileptiform synchronization even though it was well established that this structure is in a strategic position for doing so. Our observations that blocking $GABA_A$ receptor-mediated mechanisms results in subicular hyperexcitability and subsequently intralimbic synchronization is relevant to pathological conditions such as epilepsy. Studies in

slices obtained from MTLE patients indicate that both bursting pyramidal cells and interneurons contribute to the interictal activity that occurs in the subiculum (Cohen et al., 2002; Wozny et al., 2003). In addition, in chronic animal models of MTLE, alterations at the level of intrinsic and network properties of principal cells (Knopp et al., 2005; Wellmer et al., 2002) as well as a reduction in specific interneuronal subpopulations (van Vliet et al., 2004) have been reported in this structure. Altogether, these findings suggest that synaptic reorganization and altered inhibition contributes to subicular network hyperexcitability that may in turn play a role in the generation and spread of convulsive activity.

2.7 Figures

Figure 2-1:

Effect of picrotoxin on 4AP-induced activity in a combined hippocampal-EC slice. A: Simultaneous field potential recordings obtained from EC, CA1 and CA3 during bath application of 4AP. Note that fast interictal discharges (arrows in the CA1 trace) are restricted to the hippocampus (CA3 and CA1) but that slow interictal events (asterix in the EC trace) are recorded in both hippocampus and EC. Note also the long-lasting ictal discharge (bar). **B**: Picrotoxin application causes loss of ictal discharge in the EC and the appearance of robust interictal discharges that initiate in CA3 and propagate sequentially to CA1 and EC (insert). The inserts in **A** and **B** show selected interictal events at faster time-bases and the dashed lines demonstrate that these discharges initiate in CA3.

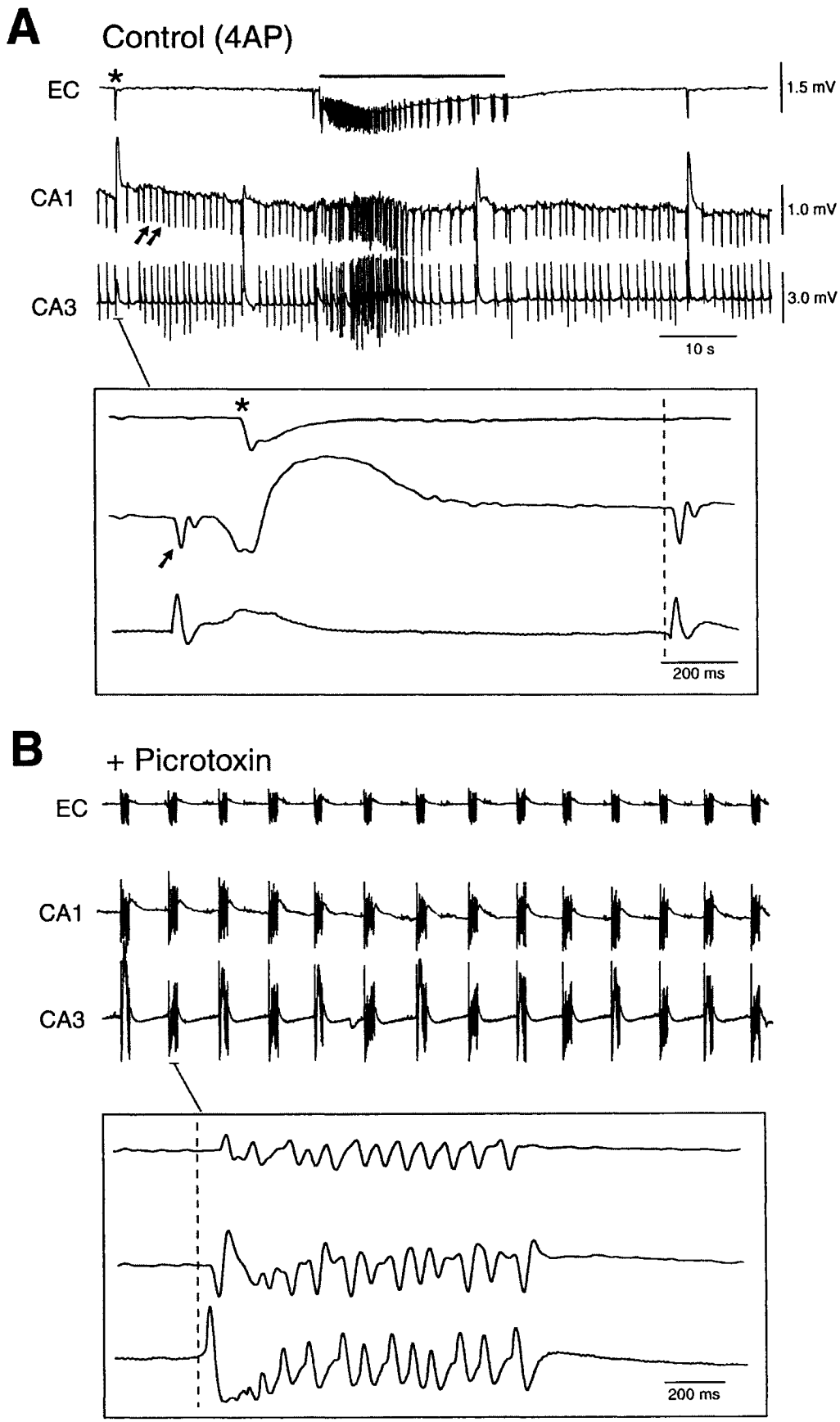
A
Control (4AP)
EC
CA1
CA3
1.5 mV
1.0 mV
3.0 mV
10 s
200 ms
B
+ Picrotoxin
EC
CA1
CA3
200 ms

Figure 2-2:

Picrotoxin-induced augmentation of field amplitudes in CA3, CA1 and subiculum. **A:** Sequential field potential recording along the CA3/CA1/Subiculim (Sub)/EC axis under control (4AP) conditions. Field electrodes in CA3 and EC were kept at the same position whilst a third electrode was moved along the stratum pyramidale to CA1 **(a)**, CA1-Sub border **(b)** and Sub **(c)**. Note the diminished field activity recorded in the subiculum as compared to CA1 and CA1-subiculum. **B**: Monitoring field potential activity in EC, subiculum and CA3 from the onset of picrotoxin application until complete synchronization of the limbic structures. Note that initially CA3-driven interictal discharges do not propagate to the EC (left lower insert), but that following potentiation of subicular network activity (arrow), CA3-driven interictal events can propagate to the EC (right lower insert). Also note that potentiation in subicular activity precedes hippocampus-EC synchronization (middle vs right insert). **C**: Histogram of the normalized increase in field potential amplitude recorded in different areas of the slice; note that the most drastic potentiation occurs in the subiculum.

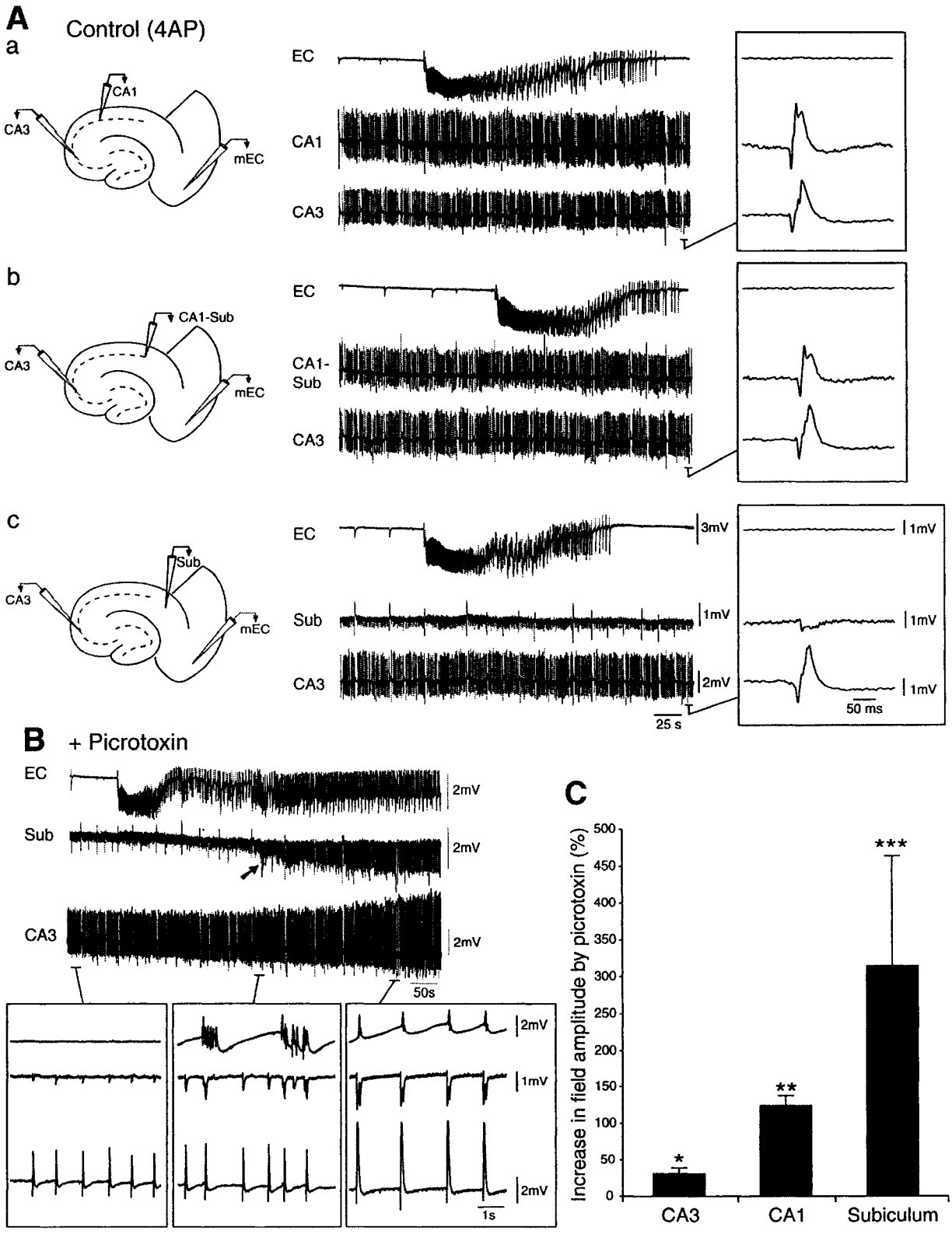
A
Control (4AP)
a
CA1
CA3
mEC
EC
CA1
CA3
b
CA1-Sub
CA3
mEC
EC
CA1-
Sub
CA3
c
Sub
CA3
mEC
EC
Sub
CA3
3mV
1mV
2mV
25 s
50 ms
B
+ Picrotoxin
EC
Sub
CA3
2mV
50s
1s
C
Increase in field amplitude by picrotoxin (%)
CA3
CA1
Subiculum

Figure 2-3:

Stimulation of hippocampal outputs activates EC only under conditions of $GABA_A$-receptor antagonism. Panels in the top row show the spontaneous field potential activity recorded simultaneously from CA1, subiculum and EC in the absence of convulsants (i.e. Normal ACSF) **(A)**, in the presence of 4AP **(B)**, and during 4AP+PTX **(C)**. Slice diagrams on the left column illustrate the positions of the stimulating bipolar electrode in CA1 **(a)**; subiculum **(b)** and deep EC layer **(c)**. Triangles indicate the structure stimulated in each set of recordings and arrows point to the subsequent response recorded. Note that single shock stimulation of CA1 networks both in the absence and presence of 4AP induces a small subicular response with no EC activation (**Aa**, **Ba**). Note in contrast the potentiated subicular response and the subsequent EC discharge (asterix) induced by hippocampal output stimulation under $GABA_A$-receptor antagonism (**Ca**).

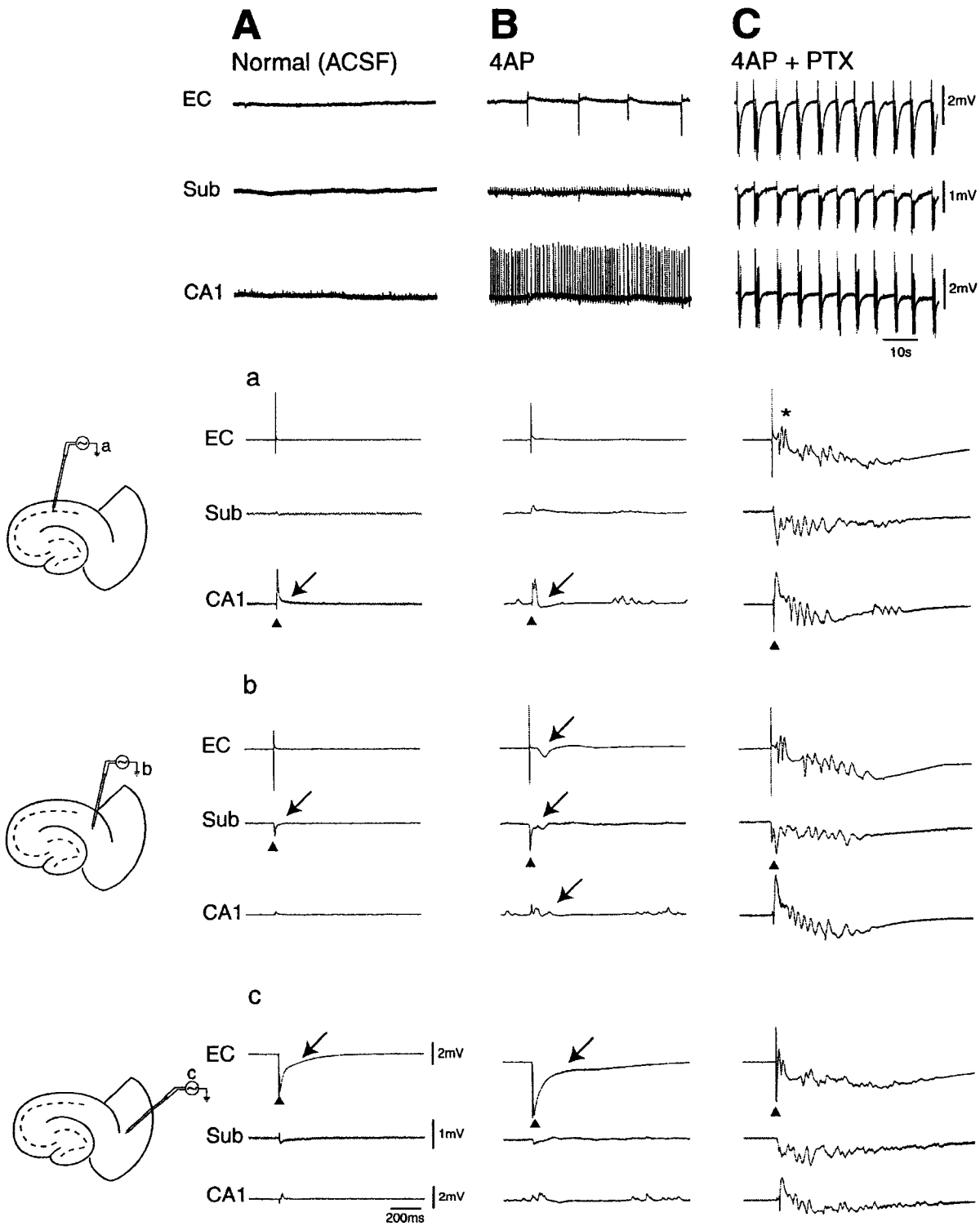
A
Normal (ACSF)
B
4AP
C
4AP + PTX
EC
Sub
CA1
2mV
1mV
2mV
10s
a
b
c
*
2mV
1mV
2mV
200ms

Figure 2-4:

NMDA receptors do not contribute to picrotoxin-induced synchronicity in a functionally disconnected slice. **A**: Simultaneous field potential recordings in EC, subiculum (Sub) and CA3 showing that interictal discharges initiating in CA3 do not propagate to the EC where activity is characterized by robust ictal discharges. Note that in this slice no field activity was recorded in the subiculum. **B**: Bath application of high concentrations of the NMDA-receptor antagonist CPP results in the loss of EC-driven ictal events. **C**: Subsequent application of picrotoxin results in an initial ictal discharge in EC that is followed by a pattern of interictal discharge in all limbic structures. **D**: CPP washout causes a prolongation of the interictal events and a slow down in their frequency of occurrence. These discharges continue to initiate in CA3 and propagate sequentially to the subiculum and EC (insert).

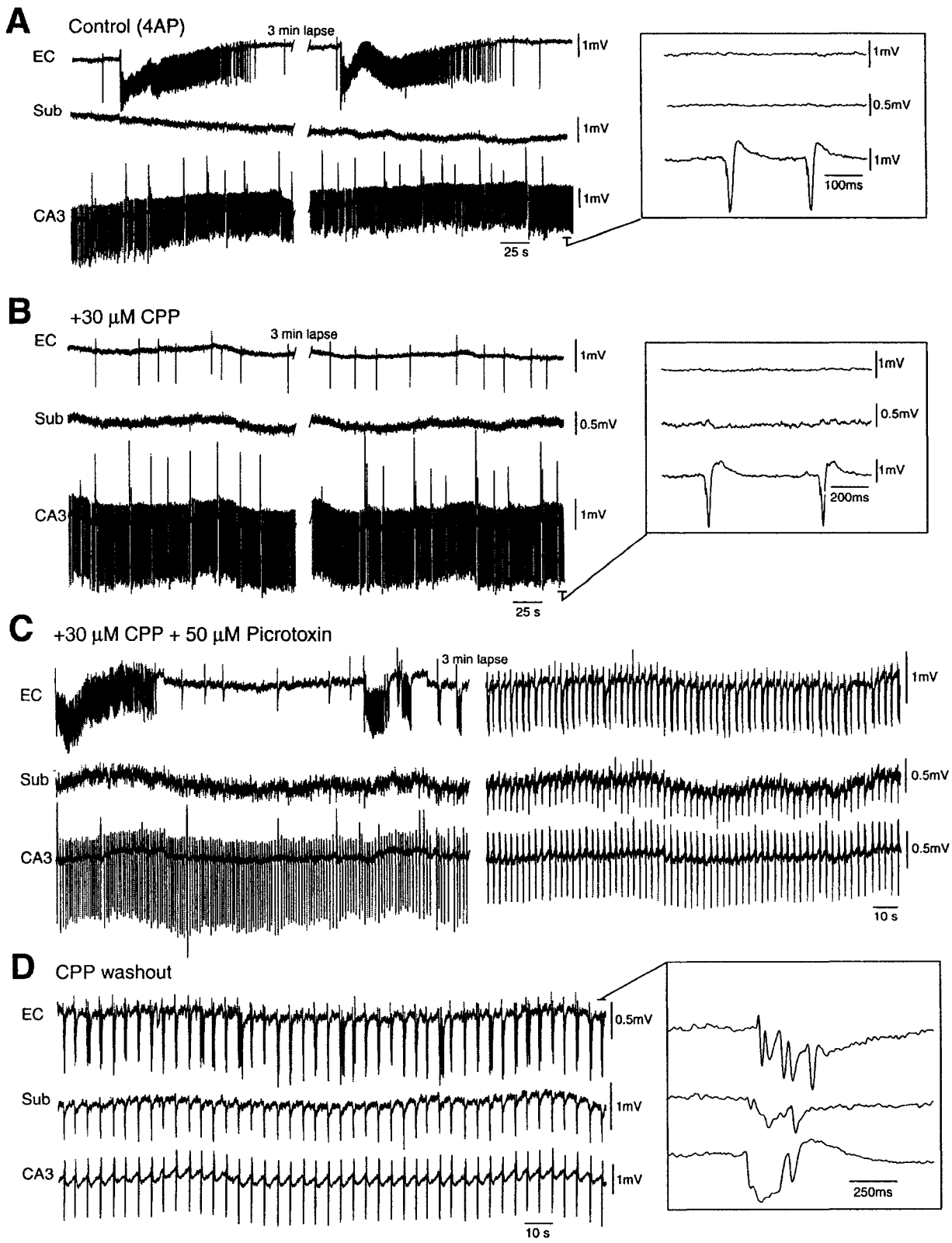
A
Control (4AP)
3 min lapse
EC
Sub
CA3
1mV
1mV
1mV
1mV
0.5mV
1mV
100ms
25 s
B
+30 μM CPP
3 min lapse
EC
Sub
CA3
1mV
0.5mV
1mV
1mV
0.5mV
1mV
200ms
25 s
C
+30 μM CPP + 50 μM Picrotoxin
3 min lapse
EC
Sub
CA3
1mV
0.5mV
0.5mV
10 s
D
CPP washout
EC
Sub
CA3
0.5mV
1mV
1mV
250ms
10 s

Figure 2-5:

Simultaneous field and intracellular recordings in functionally disconnected slice. **Aa**: Simultaneous field (EC, CA3) and intracellular (subiculum, -64 mV) recordings under control conditions (i.e., 4AP) reveal that this subicular cell is excitable at RMP. Note in the insert that the burst firing generated by this subicular neuron is synchronous with the interictal discharge recorded in CA3, but that no propagation occurs to EC. **Ab**: Responses to intracellular injection of depolarizing and hyperpolarizing current pulses; note that this neuron is an intrinsic burster. Depolarizing event during hyperpolarization represents a spontaneously-occurring EPSP (arrow) **B**: Picrotoxin application to another functionally disconnected slice results in an initial ictal event in EC (Picrotoxin (early)) followed by synchronization of all limbic networks (Picrotoxin (late)). Note in the expanded traces that the intracellularly recorded subicular bursts follow CA3 field activity and precede that of the EC.

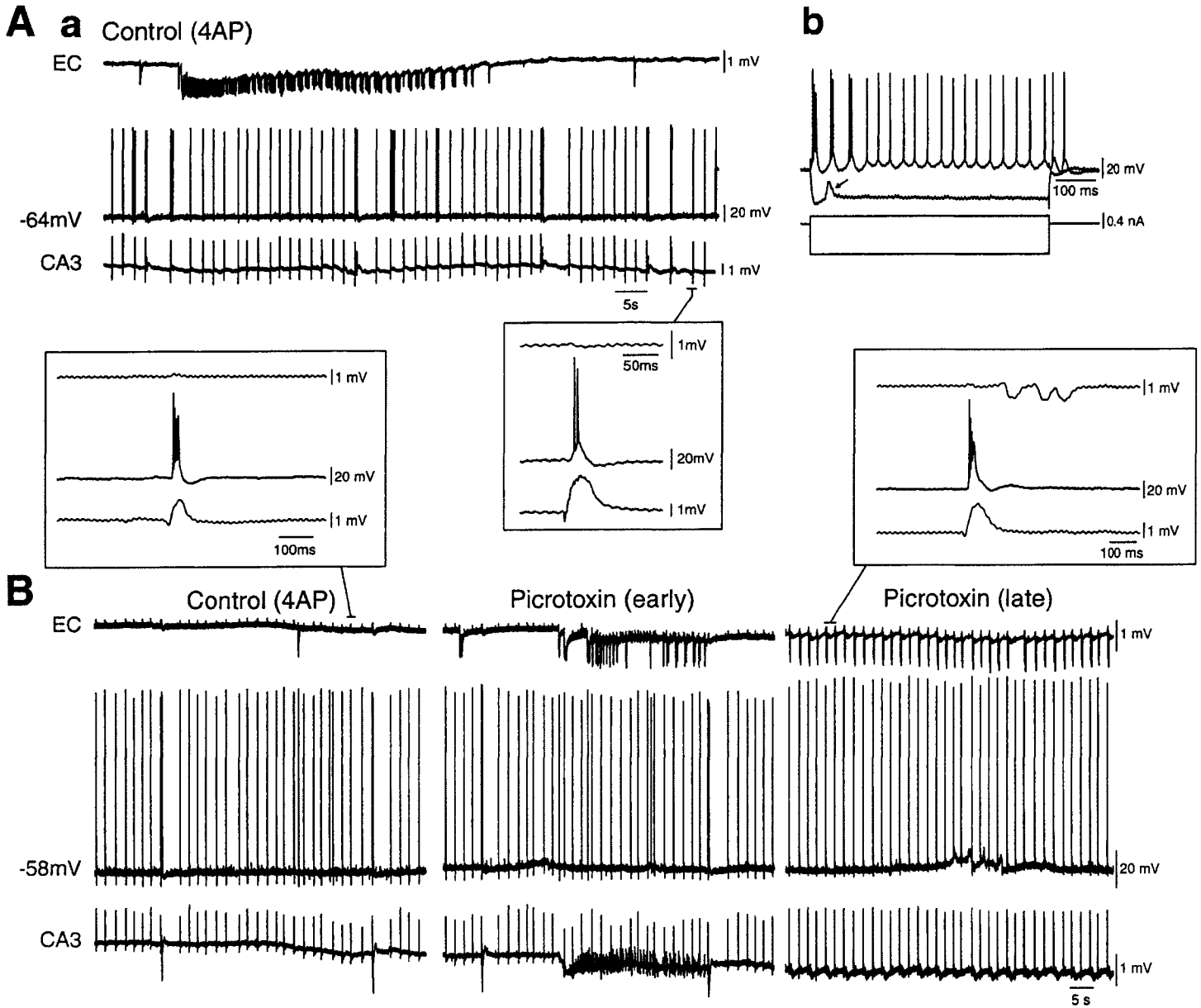
A
a
Control (4AP)
EC
1 mV
-64mV
20 mV
CA3
1 mV
5s
b
20 mV
100 ms
0.4 nA
1 mV
20 mV
100ms
1mV
50ms
20mV
1mV
1 mV
20 mV
1 mV
100 ms
B
Control (4AP)
Picrotoxin (early)
Picrotoxin (late)
EC
1 mV
-58mV
20 mV
CA3
1 mV
5 s

Figure 2-6:

Field and intracellular recordings in functionally disconnected slice. Aa: Simultaneous field (EC, CA3) and intracellular (subiculum, -60 mV) recordings during control (4AP) conditions reveals that this subicular cell is "silent" at RMP. Note the presence of PSPs that are coincident with CA3 discharges (arrows) and the large isolated inhibitory postsynaptic potentials (IPSPs) (Control (4AP), asterix). Superfusion of slices with picrotoxin discloses in these cells action potential discharges at RMP (Picrotoxin). Monitoring the evolution in the intracellular activity of these subicular neurons from the initial application of the $GABA_A$ receptor antagonist (Picrotoxin (transition)) until the complete synchronization between hippocampal and parahippocampal structures (Picrotoxin (late)) reveals IPSP disappearance. Inserts below traces demonstrate expansions of selected events. Note the presence of large IPSPs (asterix) and smaller PSPs (arrows) within the subiculum prior to complete synchronization of limbic structures. **Ab**: Firing properties of this cell reveal a nonbursting neuron.

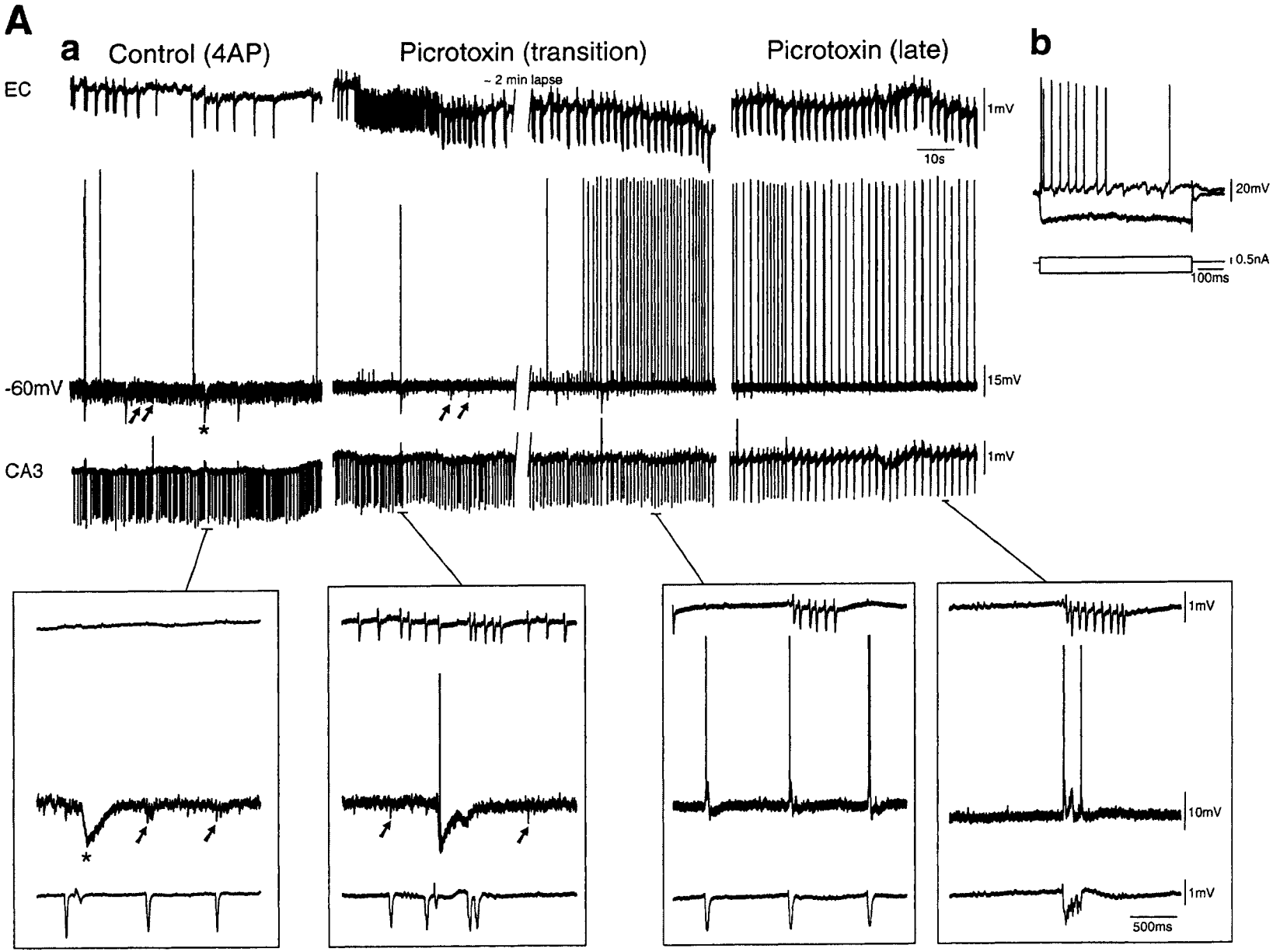
A
a
Control (4AP)
Picrotoxin (transition)
Picrotoxin (late)
b
EC
~ 2 min lapse
1mV
10s
20mV
0.5nA
100ms
-60mV
15mV
CA3
1mV
1mV
10mV
1mV
500ms

Figure 2-7:

Picrotoxin-induced potentiation of subicular activity is not due to upstream effects. **Aa**. Diagram illustrating a combined slice in which the Schaffer collaterals have been severed by a microknife cut at the level of CA1. **Ab** Simultaneous field potential recordings obtained from this slice preparation in EC, subiculum (Sub) and CA3 during bath application of 4AP and upon further addition of Picrotoxin. The slow interictal events observed in all structures in the presence of 4AP initiate in EC (bottom insert). Note the potentiation of subicular activity that occurs in the presence of the $GABA_A$ receptor antagonist (arrow). Also note that in the presence of picrotoxin, the epileptiform activity in this case initiates in EC and subsequently spreads to subiculum and CA3 (upper insert). **Ba** Simultaneous field potential recordings obtained from the proximal, middle and distal regions of an isolated subicular minislice preparation during 4AP application and upon further addition of Picrotoxin. Note that during 4AP, slow interictal-like events are generated in all regions of the subiculum (left insert). Also note that $GABA_A$ receptor antagonism induces potentiation of subicular activity in all regions (arrow indicates onset of picrotoxin-induced activity). Right insert illustrates expansion of picrotoxin-induced event. **Bb** Diagram illustrating the isolated minislice preparation and position of field electrodes.

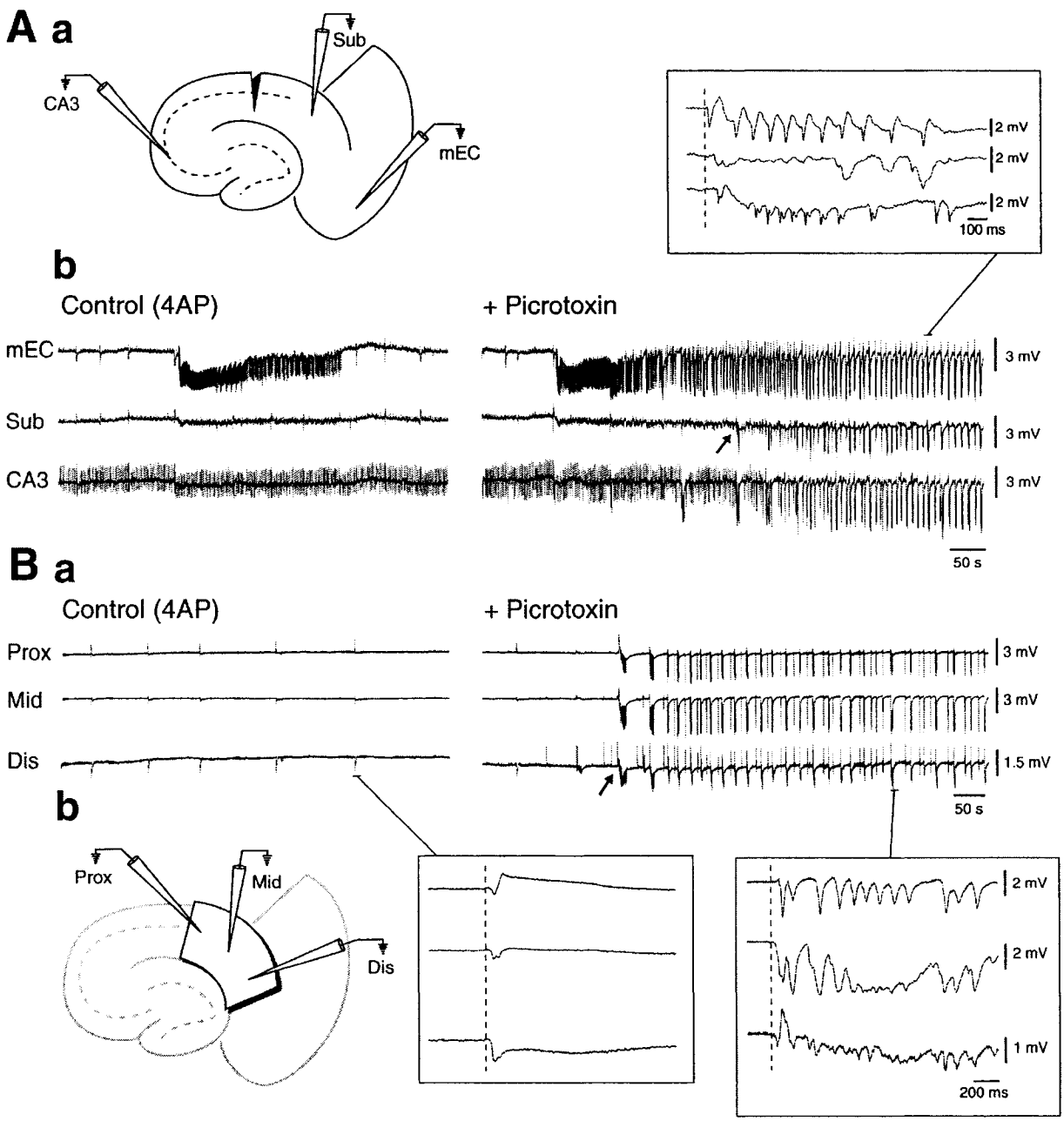
A a
Sub
CA3
mEC
2 mV
2 mV
2 mV
100 ms
b
Control (4AP)
+ Picrotoxin
mEC
Sub
CA3
3 mV
3 mV
3 mV
50 s
B a
Control (4AP)
+ Picrotoxin
Prox
Mid
Dis
3 mV
3 mV
1.5 mV
50 s
b
Prox
Mid
Dis
2 mV
2 mV
1 mV
200 ms

Figure 2-8:

Pharmacological characterization of 4AP-induced activity in isolated subicular minislices. **Aa**: Simultaneous field (Middle Subiculum, Distal subiculum) and intracellular (Middle subiculum, -66 mV) recordings during control (4AP) conditions reveals that the slow interictal-events correspond intracellularly to an early hyperpolarization followed by a sustained depolarization (left insert). In the presence of picrotoxin there is increased field activity in the isolated subiculum and robust network bursting can be recorded intracellularly (right insert). **Ab**: Firing properties of this cell reveals that it was an intrinsically bursting neuron. **Ac**: Intracellular traces of the 4AP-induced event at different membrane potentials reveals reversal of the hyperpolarizing component at negative membrane potentials (-73 mV and -76 mV). Note the truncated action potential riding on this reversed event at -76 mV. **Ba**: Simultaneous field (Middle Subiculum, Proximal Subiculum) and intracellular (Middle subiculum, -60 mV and -67 mV) recordings in control (4AP) and after 2hrs of further CPP+CNQX application. Note that intracellular recordings were carried out from two different cells within the same slice and in the same subicular region. Inserts demonstrate expansions of the slow synchronous event during both conditions.

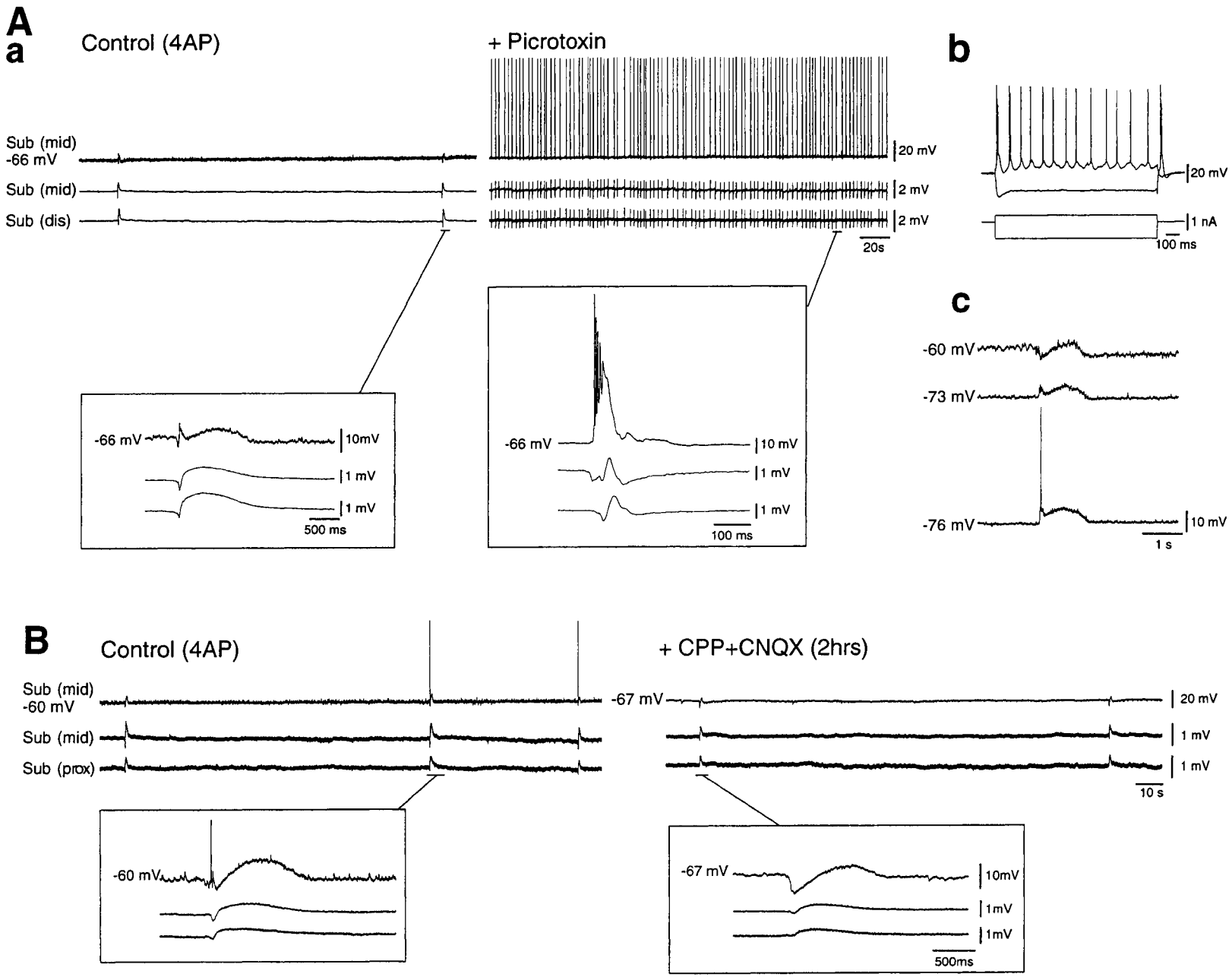
A
a
Control (4AP)
+ Picrotoxin
Sub (mid)
-66 mV
Sub (mid)
Sub (dis)
20 mV
2 mV
2 mV
20s
-66 mV
10mV
1 mV
1 mV
500 ms
-66 mV
10 mV
1 mV
1 mV
100 ms
b
20 mV
1 nA
100 ms
c
-60 mV
-73 mV
-76 mV
10 mV
1 s
B
Control (4AP)
+ CPP+CNQX (2hrs)
Sub (mid)
-60 mV
Sub (mid)
Sub (prox)
-67 mV
20 mV
1 mV
1 mV
10 s
-60 mV
-67 mV
10mV
1mV
1mV
500ms

Chapter 3: Involvement of Amygdala Networks in Epileptiform Synchronization In Vitro

3.0 Linking Text & Information about publication

In *Chapters 3* to *5*, the focus of my PhD studies shifts from the subiculum to the amygdala and perirhinal cortex. Previous electrophysiological studies have demonstrated that the basolateral amygdalar nucleus (BLA) is capable of generating interictal discharges in vitro (Gean, 1990; Gean and Shinnick-Gallagher, 1988). However, these investigations employed the use of coronal slices in which the connections of the BLA with other limbic structures are not maintained. Consequently, we sought to identify the role played by basolateral/lateral amygdalar networks to epileptiform synchronization using a combined horizontal slice preparation in which the connections between these amygdalar regions and the hippocampus-parahippocampus are preserved. Specifically, the 4AP model was employed to determine how amygdalar networks interacted with other limbic structures in brain slices obtained from adult rats. The study presented in this chapter summarizes the results published in *Neuroscience* in 2003 in a manuscript entitled *"Involvement of amygdala networks in epileptiform synchronization in vitro"* (Authors: **Benini R**, D'Antuono M, Pralong E, Avoli M). Permission granted by the journal to reproduce the contents of this manuscript can be found in Appendix C.

3.1 Abstract

We used field potential and intracellular recordings in rat brain slices that included the hippocampus, a portion of the basolateral/lateral nuclei of the amygdala (BLA) and the entorhinal cortex (EC). Bath application of the convulsant 4-aminopyridine (50 μM) to slices (n=12) with reciprocally connected areas, induced short-lasting interictal-like epileptiform discharges that (i) occurred at intervals of 1.2–2.8 s, (ii) originated in CA3, and (iii) spread to EC and BLA. Cutting the Schaffer collaterals abolished them in both parahippocampal areas where slower interictal-like (interval of occurrence =4–17 s) and prolonged ictal-like discharges (duration=15±6.9 s, mean±S.D., n=7) appeared. These new types of epileptiform activity originated in either EC or BLA.

Similar findings were obtained in slices (n=19) in which the hippocampus outputs were not connected with the EC and BLA under control conditions. Cutting the EC–BLA connections made independent slow interictal- and ictal-like activities appear in both areas (n=5). NMDA receptor antagonism (n=6) abolished ictal-like discharges and reduced the duration of the slow interictal-like events. Repetitive stimulation of BLA at 0.5–1 Hz in Schaffer collateral cut slices, induced interictal-like epileptiform depolarizations in EC and reversibly blocked ictal-like activity (n=14). Thus, CA3 outputs in intact slices entrain EC and BLA networks into an interictal-like pattern that inhibits the propensity of these parahippocampal areas to generate prolonged ictal-like paroxysms. Accordingly, NMDA receptor-dependent ictal-like events are initiated in BLA or EC once the propagation of CA3-driven interictal-like discharges to these areas is abated by cutting the Schaffer collaterals. Similar inhibitory effects also occur by activating BLA outputs directed to EC at rates that mimic the CA3-driven interictal-like pattern.

3.2 Introduction

The amygdala is located in the deep, anteromedial part of the temporal lobe and is connected with many brain regions including limbic structures such as the perirhinal, entorhinal and hippocampal cortices (Amaral et al., 1992; Amaral and Witter, 1995; Lopes da Silva et al., 1990; Pikkarainen and Pitkanen, 2001; Pitkanen et al., 2000b). The amygdala is involved in fear conditioning and emotional learning (Davis and Whalen, 2001; Gloor, 1992, 1997; LeDoux, 2000; Scott et al., 1997; Wilensky et al., 2000). Moreover, it is at the origin of some of the behavioral manifestations seen during seizures in mesial temporal lobe epilepsy patients where it is often a primary focus of seizure activity (Gloor, 1992, 1997; van Elst et al., 2000). The amygdala is also the limbic area most frequently used for kindling, which is an established animal model of mesial temporal lobe epilepsy (Goddard et al., 1969).

Several studies aimed at establishing the pathophysiogenesis of mesial temporal lobe epilepsy have been carried out in brain slices in which the connections between limbic structures were, at least partially, preserved. These experiments have shown that pharmacologically induced ictal-like (thereafter termed ictal) discharges

resembling electrographic limbic seizures, originate in the entorhinal cortex (EC) (Avoli et al., 1996; Bear and Lothman, 1993; Dreier and Heinemann, 1991; Nagao et al., 1996; Stanton et al., 1987; Wilson et al., 1988). In line with this evidence, clinical studies have demonstrated dysfunction of EC networks in patients presenting with temporal lobe epilepsy (Deutch et al., 1991; Rutecki et al., 1989; Spencer and Spencer, 1994b). In addition, we have found that CA3-driven interictal-like (thereafter termed interictal) activity in hippocampus–EC slices treated with the convulsant drug 4-aminopyridine (4AP) or with Mg^{2+}-free medium can control the EC propensity to generate ictal events (Barbarosie and Avoli, 1997; Barbarosie et al., 2000).

Coronal slices of the amygdala respond to application of 4AP or Mg^{2+}-free medium by generating interictal epileptiform discharges (Gean, 1990; Gean and Shinnick-Gallagher, 1988). However, little information is available on its participation in the epileptiform synchronization of limbic networks. In this study we addressed this issue by using horizontal, rat brain slices that contained the hippocampus proper along with the EC and a portion of the basolateral/lateral nuclei of the amygdala (thereafter referred for sake of simplicity as BLA). Recent data obtained in this in vitro preparation have demonstrated that interictal discharges induced by the $GABA_A$ receptor antagonist bicuculline are generated in the CA2/CA3 region of the hippocampus from where they spread to EC and BLA (Stoop and Pralong, 2000). It is however known that decreasing or abolishing $GABA_A$ receptor-mediated function, reduces the ability of limbic networks to express ictal activity, at least in the in vitro slice preparation (Avoli et al., 1996; Köhling et al., 2000; Lopantsev and Avoli, 1998a). Therefore, we have analyzed here the role of BLA networks in the generation and in the control of epileptiform activity induced by 4AP. This drug does not interfere with GABAergic inhibition (Perreault and Avoli, 1991; Rutecki et al., 1987) and allows the appearance of both interictal and ictal discharges in combined hippocampus-EC slices obtained from rodents (Avoli et al., 1996; Barbarosie and Avoli, 1997; Barbarosie et al., 2000; Lopantsev and Avoli, 1998a,b).

3.3 Experimental Procedures

Male, adult Sprague–Dawley rats (200–250 g) were decapitated under halothane anesthesia according to the procedures established by the Canadian Council of Animal Care. All efforts were made to minimize the number of animals used and their suffering. The brain was quickly removed and a block of brain tissue containing the retrohippocampal region was placed in cold (1–3°C), oxygenated artificial cerebrospinal fluid (ACSF). The brain dorsal side was cut along a horizontal plane that was tilted by a 10° angle along a posterosuperior–anteroinferior plane passing between the lateral olfactory tract and the base of the brain stem (Stoop and Pralong, 2000). Horizontal slices (500 μm thick) were cut from this brain block using a vibratome and were transferred into a tissue chamber where they lay at the interface between ACSF and humidified gas (95% O_2, 5% CO_2) at a temperature of 34–35 °C and a pH of 7.4. We focused in this study on the most ventral slices that were comprised between −8.6 to −7.6 mm from the bregma (Paxinos and Watson, 1998). These slices contained the EC, the hippocampus and the BLA (Fig. 3-1A). Two to three of such slices could be obtained from each hemisphere. ACSF composition was (in mM): NaCl 124, KCl 2, KH_2PO_4 1.25, $MgSO_4$ 2, $CaCl_2$ 2, $NaHCO_3$ 26, and glucose 10. 4AP (50 μM), 6-cyano-7-nitroquinoxaline-2,3-dione (CNQX, 10 μM) and 3,3-(2-carboxypiperazin-4-yl)-propyl-1-phosphonate (CPP, 10 μM) were applied to the bath. Chemicals were acquired from Sigma (St. Louis, MO, USA) with the exception of CNQX and CPP that were obtained from Tocris Cookson (Langford, UK).

Field potential recordings were made with ACSF-filled, glass pipettes (resistance=2–10 MΩ) that were connected to high-impedance amplifiers. Signals were at times processed with high-pass filters set at 0.1 Hz. The location of these recording electrodes is shown in Fig. 3-1A. Sharp-electrode, intracellular recordings were performed in the EC with pipettes that were filled with 3 M K-acetate (tip resistance=70–120 MΩ) and were aimed at depths ranging 600–900 μM from the pia. Intracellular signals were fed to a high-impedance amplifier with internal bridge circuit for intracellular current injection. The resistance compensation was monitored throughout the experiment and adjusted as required. The fundamental

electrophysiological parameters of the EC neurons included in this study were measured as follows: (i) resting membrane potential (RMP) after cell withdrawal; (ii) apparent input resistance (Ri) from the maximum voltage change in response to a hyperpolarizing current pulse (100–200 ms, <−0.5 nA); (iii) action potential amplitude from the baseline. The electrophysiological properties recorded in a representative group of EC neurons (n=18) during application of 4AP were: RMP=−65±12 mV (mean±S.D.), Ri=30±7.2 MΩ, and action potential amplitude=92.3±8.2 mV.

Field potential signals were displayed on a GOULD Windograf (Gould Instruments, Valley View, OH, USA) and stored on videotape. Time-delay measurements were obtained with a digital oscilloscope. For each trace the onset of the 4AP-induced synchronous potentials was determined as the time of the earliest deflection of the baseline recording (e.g. insert traces in Fig. 3-2). Intracellular signals were fed to a computer interface (Digidata 1200B, Axon Instruments, Union City, CA, USA) and were acquired and stored by using the pClamp 8 software (Axon Instruments). Subsequent analysis of these data was made with the Clampfit8 software (Axon Instruments).

Cut of the Schaffer collateral pathway or of selected areas in the slice was accomplished under visual control with a razor blade mounted on a micromanipulator (cf, Barbarosie and Avoli, 1997). The location of these cuts is illustrated in Fig. 3-1B. At the beginning of each experiment (i.e. before applying 4AP), we verified the reciprocal connectivity between different structures of the slice by analyzing the field potential responses induced by single-shock, electrical stimuli (10–150 μs; <200 μA) that were delivered through bipolar, stainless steel electrodes in appropriate areas. As illustrated in Fig. 3-1C–F, field potential responses, with latencies ranging from 6 to 14 ms, were recorded in the dentate gyrus, subiculum (SUB) and deep or superficial EC layers following electrical stimulation of the EC, CA1 stratum radiatum and SUB, respectively. Field and intracellular responses could also be obtained under control conditions in the EC in response to single-shock electrical stimulation of the BLA (not illustrated).

Throughout this study we termed interictal and ictal discharges the synchronous epileptiform events with durations shorter or longer than 3 s, respectively. In doing so, we included the afterdischarge that could at times occur with both types of activity (e.g. BLA trace in Fig. 3-3, Control). Measurements in the text are expressed as mean ± S.D. and n indicates the number of slices or neurons studied under each specific protocol. The results obtained were compared with the Student's t-test or the ANOVA test and were considered statistically significant if $P<0.05$.

3.4 Results

3.4.1 Epileptiform activity induced by 4AP in combined hippocampus–EC–amygdala slices

A pattern of continuous interictal activity occurred synchronously in CA3, EC and BLA during steady, bath application of 4AP to 12 slices (Fig. 3-2A). These interictal discharges could be recorded throughout each experiment (up to 4 h) and had intervals ranging between 1.2 and 2.8 s and durations of 180–650 ms when measured in the CA3 subfield. Time-delay measurements of the onset of these interictal events demonstrated that they always initiated in CA3 from where they first spread to the EC and then to BLA with latencies of 93±8 ms and 137±44 ms (n=12), respectively (Fig. 3-2A, inset). Moreover, these epileptiform discharges could often re-enter the CA3 network as indicated by the occurrence of late population spikes at this recording site (Fig. 3-2B, arrows in the bottom, left inset; cf. Paré et al., 1992).

A similar pattern of interictal activity occurs in reciprocally connected, mouse hippocampus–EC slices treated with 4AP or Mg^{2+}-free medium (Barbarosie and Avoli, 1997; Barbarosie et al., 2000). We have reported there that the CA3-driven interictal activity can inhibit the expression of ictal discharges in the EC. Hence, we investigated the effects induced by cutting the Schaffer collateral, a procedure that would selectively abolish the propagation of CA3 activity to CA1 and SUB, thus preventing hippocampal output activity from reaching the EC and BLA. As illustrated in Fig. 3-2B, cutting the Schaffer collaterals abolished the propagation of CA3-driven interictal activity (arrows in the CA3 trace of the panel '+Schaffer collateral cut') to the EC and BLA and disclosed in both structures ictal (duration=15±6.9 s; interval of

occurrence =75–300 s, n=6; continuous line in Fig. 3-2B '+Schaffer collateral cut' panel) and interictal discharges (duration=240–2100 ms; interval of occurrence =4–17 s, n=11; asterisks in Fig. 3-2B '+Schaffer collateral cut' panel). Thereafter, this interictal activity will be termed slow interictal discharge. It should be also noted that cutting the Schaffer collaterals also reduced the late population spikes associated with the CA3-driven interictal discharges in this area further suggesting that these population events reflect re-entry of activity from the EC (not shown, but see Barbarosie and Avoli, 1997)

Both ictal and slow interictal discharges recorded in EC and BLA after cutting the Schaffer collateral propagated to CA3 (Fig. 3-2B). Moreover, ictal events had always similar durations in BLA and EC, while the slower interictal discharges could display different durations in these two limbic areas. In any given experiment the two new types of epileptiform activity disclosed by cutting the Schaffer collaterals could initiate in either EC or BLA and spread to the other parahippocampal area with similar time delays ranging between 15 and 70 ms (Fig. 3-2C). Further lesion of the connections between EC and BLA (n=5) caused the appearance of independent slow interictal and ictal discharges in these two limbic areas (Fig. 3-2B, '+BLA/EC separation' panel), thus indicating that both EC and BLA networks can generate per se these two types of epileptiform synchronization.

As shown in Figs. 3-2B ('+BLA/EC separation' panel) and 3-3, only the epileptiform activity that was present in the EC did propagate to the CA3 subfield after separation of the BLA from the EC, presumably through the perforant path–dentate gyrus route. This way of propagation was further demonstrated by cutting the perforant path, a procedure that made slow interictal and ictal discharges disappear in CA3, but not in the EC (n=3; not illustrated). Findings similar to those seen after cutting the Schaffer collateral in reciprocally connected hippocampus–EC–BLA slices were obtained in 19 additional experiments in which the hippocampus outputs were not functionally connected with the EC-BLA networks under control conditions (cf. Avoli et al., 1996).

3.4.2 Involvement of NMDA receptors in epileptiform activity induced by 4AP

Next we analyzed the involvement of NMDA receptor-mediated transmission in the generation of the slow interictal and ictal discharges recorded in the EC and BLA after Schaffer collateral cut (n=6). Three of these slices had undergone a further lesion of the EC–BLA connections, and thus they generated independent epileptiform activity in these two areas.

Bath application of the NMDA receptor antagonist CPP (10 μM) abolished ictal discharges in all limbic structures (Fig. 3-3). This effect was accompanied by a block of the afterdischarges seen in BLA during each interictal event. Interestingly the rate of occurrence of CA3-driven interictal events increased during CPP application (from 0.9±0.3–1.1±0.3 Hz, n=4). The ictal discharges as well as the afterdischarges associated with the slow interictal events generated in BLA and EC reappeared during CPP washout with control medium containing 4AP only (Fig. 3-3, Wash). In three additional experiments we found that all epileptiform discharges (including those originating in CA3) were abolished by bath applying the non-NMDA receptor antagonist CNQX (10 μM; not illustrated, but cf. Avoli et al., 1996).

3.4.3 Slow frequency amygdala stimulation can control ictal discharges

We have previously shown that repetitive electrical stimulation of hippocampal outputs at 0.5–1 Hz reversibly blocks the occurrence of ictal discharges induced by 4AP or by Mg^{2+}-free ACSF in Schaffer collateral cut hippocampus–EC slices obtained from mice (Barbarosie and Avoli, 1997). Here, we have found that CA3-driven interictal discharges entrain both EC and BLA networks and inhibit the occurrence of ictal discharges that are otherwise seen after cutting the Schaffer collaterals. Hence, we tested whether under these experimental conditions (i.e. after lesioning the Schaffer collaterals), low-frequency (i.e. 0.1–1 Hz) stimulation of BLA, which projects to the EC (Finch et al., 1986; Pikkarainen and Pitkanen, 2001), can control 4AP-induced ictal discharges in a way similar to what was previously reported with hippocampal output stimulation.

Spontaneous ictal discharges, which were recorded extracellularly in these experiments, corresponded intracellularly to sustained membrane depolarizations that

were capped by repetitive action potential bursts (Fig. 3-4A). As shown in the inset of Fig. 3-4A (asterisk), the onset of these discharges was often characterized by a sustained depolarization that triggered minimal action potential firing and led, within a few hundreds of milliseconds, to the development of repetitive action potential bursting at 9–15 Hz. This modality of firing, which identified the initial 'tonic' phase of the ictal event, was followed by recurrent 'clonic' discharges that progressively slowed down during the membrane repolarization. These characteristics were remarkably similar to those reported in previous intracellular studies of the ictal activity generated by 'isolated' rat EC network during application of 4AP (Lopantsev and Avoli, 1998a, b).

The ictal discharges generated spontaneously by limbic networks in these slices were decreased and eventually abolished during repetitive stimulation of BLA. As shown in Fig. 3-4B, the first stimulus of the sequence could at times trigger an ictal-like response, but successive stimuli only elicited short-lasting (<1 s) epileptiform discharges that closely resembled the paroxysmal depolarizing shifts that are the typical intracellular correlate of the CA3-driven interictal activity induced by a variety of epileptogenic procedures (Perreault and Avoli, 1991; Rutecki et al., 1987, 1990; Schwartzkroin and Prince, 1980; Tancredi et al., 1990).

The short-lasting epileptiform responses induced by BLA stimuli displayed latencies that were quite variable and could range between 60 and 180 ms (Fig. 3-5A). Moreover, these latency values could be decreased in the same experiment by augmenting the stimulus intensity (Fig. 3-5B). Such a procedure could eventually induce an epileptiform response that was initiated by an EPSP with latency ranging between 6 and 10 ms (arrowhead in Fig. 3-5C). As shown in Fig. 3-5D, modifying the membrane potential with intracellular injection of steady depolarizing or hyperpolarizing current caused a decrease or an increase of the intracellular epileptiform responses, respectively (n=6 cells). These changes, which are quantitatively illustrated in the plot of Fig. 3-5Db, indicated an extrapolated reversal potential of these epileptiform depolarizations at approximately −35 mV. These values suggested that, as reported in CA3 pyramidal cells (Perreault and Avoli, 1991; Rutecki

et al., 1987), $GABA_A$ receptor-mediated, inhibitory conductances contributed to the paroxysmal depolarizing shifts generated by EC neurons in response to stimuli delivered in BLA.

Fig. 3-6 illustrates the effects induced on the occurrence of ictal discharge by repetitive stimuli delivered at rates between 0.2 and 1 Hz in the BLA. At 0.2 Hz, EC networks responded to BLA stimuli by generating epileptiform discharges that lasted less than 2 s; however, at this rate of stimulation, ictal discharges (i.e. periods of epileptiform synchronization lasting over 3 s) continued to occur (Fig. 3-6, asterisk in the 0.2 Hz trace). When repetitive stimuli were delivered at 0.5 or 1 Hz, ictal discharges did not occur during the period of stimulation (with the exception of the ictal-like response that was at times seen at the stimulation onset). As illustrated in Fig. 3-6, stimuli at 0.5 or 1 Hz elicited paroxysmal depolarizing shifts that had shorter duration than at 0.2 Hz. Data obtained in 14 experiments indicated that repetitive stimulation at 0.2 Hz had no effect on the occurrence of ictal discharges, while it completely suppressed them at 0.5 and 1 Hz. It must be emphasized that in all cases the effects induced by BLA repetitive stimulation on ictal discharge occurrence was assessed by delivering periods of stimulation that were in any given experiment at least twice as long as the interval of occurrence of the spontaneous ictal events. Ictal discharges that were similar both in duration and in shape to those seen during the prestimulus period, reappeared in all experiments upon termination of the stimulating protocol (Fig. 3-4B).

3.5 Discussion

Reciprocal functional connectivity between hippocampus and EC in mouse combined slices makes CA3-driven interictal discharges restrain the propensity of EC networks to generate prolonged ictal discharges resembling the electrographic limbic seizures seen in patients presenting with mesial temporal lobe epilepsy (Barbarosie and Avoli, 1997; Barbarosie et al., 2000). This characteristic, which underscores an important mechanism for activity-dependent control of limbic network excitability, was not so far obtained in rat combined slices in which only EC to hippocampus connections remained preserved after slicing (Avoli et al., 1996; Dreier and Heinemann, 1991). In

this study, we have found that the hippocampus–EC loop (cf. Paré et al., 1992) can also be maintained in slices obtained from the most ventral portion of the rat brain (i.e. comprised between −8.6 and −7.6 mm from the bregma; (Paxinos and Watson, 1998). In addition, these slices contained a connected portion of the BLA.

By employing such an in vitro preparation we have discovered that CA3 outputs can entrain EC and BLA networks into a pattern of interictal activity that restrains the propensity of these parahippocampal areas to generate ictal activity. Accordingly, cutting the Schaffer collaterals prevented CA3-driven output activity from reaching the CA1 area and the SUB (and thus from leaving the hippocampus), and disclosed ictal discharges in EC and BLA. This ictal activity depended on the function of the NMDA receptor, could initiate in either BLA or EC networks, and could be sustained by either structure independently. In addition, we have demonstrated that activation of BLA outputs directed to the EC at a frequency that mimics that of CA3-driven interictal activity, can effectively depress ictal discharges in limbic networks. It should however, be emphasized that our findings were obtained from normal tissue to which 4AP was applied in order to disclose epileptiform synchronization. Such a situation is certainly different from what is encountered in patients with mesial temporal lobe epilepsy or in animal models mimicking this disorder.

3.5.1 CA3 networks as pacers of limbic network activity

We have found that 4AP treatment in extended brain slices that include the hippocampus proper, the EC and the BLA, induces CA3-driven interictal activity that spread to the EC and BLA. All these limbic regions are densely interconnected (cf. Amaral and Witter, 1995; Finch et al. 1986; Pikkarainen and Pitkanen, 2001; Pitkanen et al., 2000b). Moreover, preservation of connections between the amygdala and other limbic areas has been anatomically documented in a horizontal, brain slice preparation by (von Bohlen und Halbach and Albrecht, 1998).

The CA3 area in isolated hippocampal slices responds readily to a variety of epileptogenic treatments by generating epileptiform discharges recurring at frequencies comprised between 0.5 and 1 Hz (Perreault and Avoli, 1991; Rutecki et

al., 1987, 1990; Schwartzkroin and Prince, 1980; Tancredi et al., 1990). This pattern of interictal discharge reflects the presence of recurrent excitatory, glutamatergic synapses on neighboring CA3 pyramidal cells along with the ability of these neurons to generate dendritic Ca^{2+} spikes (Miles and Wong, 1986, 1987; for review see Traub and Jefferys, 1994). Thus, the ability of CA3 networks to generate interictal discharges is not unexpected. However, it is surprising that in intact, interconnected slices this type of epileptiform activity can consistently entrain BLA and EC networks, even though the fiber paths directed from these two parahippocampal area to CA3 area are functional, as demonstrated by the re-entry of interictal activity to CA3. Indeed, we have found here that even when BLA networks are included in the slice preparation, CA3-driven interictal discharges control rather than facilitate the occurrence of limbic seizures.

3.5.2 BLA and EC networks as generators of electrographic limbic seizures

When set free from the interictal activity originating from the hippocampus, EC and BLA networks generate ictal discharges, along with slow interictal events. This observation is in keeping with previous experiments in extended hippocampus–EC slices, where ictogenesis occurred in EC networks that did not receive hippocampal output activity, or it appeared after separation from the hippocampus proper (Avoli et al., 1996; Barbarosie and Avoli, 1997; Dreier and Heinemann, 1991; Wilson et al, 1988).

We have also found that the ictal activity recorded in slices after cutting the Schaffer collaterals, can originate in either EC or BLA (even in the same experiment), and propagate to the other limbic area with time delays of 15–70 ms. Similar characteristics were seen with the slow interictal events. Such a large variability in onset delay suggests that these epileptiform events may also initiate from limbic areas (e.g. the perirhinal cortex) located in between the EC and BLA. This type of initiation has been documented in preliminary experiments in which simultaneous field potential recordings were obtained from the EC, the perirhinal cortex and the BLA (de Guzman et al., unpublished data).

The evidence obtained by surgically separating the EC from the BLA, demonstrates that both limbic areas are endowed with the ability to produce similar periods of prolonged epileptiform synchronization. Interestingly, BLA and EC networks under 4AP treatment were unable per se to generate the pattern of frequent interictal discharge seen in the CA3 area. Previous studies (Gean, 1990; Gean and Shinnick-Gallagher, 1988) have shown that the epileptiform activity induced by 4AP or Mg^{2+}-free medium in coronal slices of the amygdala, consists of interictal events that recur at intervals longer than 7 s.

We have also provided evidence for a role played by NMDA receptors in the generation of ictal discharges in BLA or EC. Similar conclusions have been reached with the ictal activity recorded in the EC during several epileptogenic procedures (Avoli et al., 1996; Dreier and Heinemann, 1991; Nagao et al., 1996; Stanton et al., 1987). In addition, NMDA receptor antagonism reduced the amount of afterdischarge associated with the slow interictal activity (cf. Gean and Shinnick-Gallagher, 1988), but it failed in blocking fast CA3-driven interictal discharges (Perreault and Avoli, 1991). In line with several studies performed in limbic structures treated with convulsant drugs (Avoli et al., 1996; Gean, 1990; Nagao et al., 1996), all types of epileptiform discharge were abolished by the non-NMDA receptor antagonist CNQX.

3.5.3 BLA outputs can control electrographic limbic seizures

The EC and the amygdala are interconnected components of the limbic system as documented by several anatomical studies (Amaral and Witter; 1995; Finch et al, 1986; Lopes da Silva et al., 1990; Swanson and Kohler, 1986). We have found here that repetitive BLA stimulation at frequencies of 0.5–1 Hz reversibly block ictal discharge generation in limbic networks. This activity-dependent effect may result from several mechanisms that include the activation of presynaptic metabotropic receptors inhibiting glutamate release (Burke and Hablitz, 1994; Scanziani et al., 1997), or extracellular alkalization leading to a reduction of NMDA transmission (de Curtis et al., 1998). Moreover, the stimulus frequency effective in inhibiting ictal discharges is close to what is used for eliciting long term depression of synaptic transmission in the hippocampus (Kimura and Pavlides, 2000). However, ictal

discharges in our experiments reappeared shortly after the termination of the stimulating procedure thus suggesting that long-term depression was presumably not involved in this inhibitory action.

The field potential characteristics of the responses generated by EC neurons during repetitive stimuli delivered at frequencies >0.5 Hz were similar to those of the CA3-driven interictal discharges recorded in intact slices, in which ictogenesis does not occur. By employing intracellular recordings we have also found that the interictal-like responses to repetitive stimuli are characterized by depolarizing bursts that are presumably contributed by $GABA_A$ receptor-mediated conductances. Hence, repetitive stimulation may also lead to an increased release of GABA that in turn activates presynaptic $GABA_B$ receptors thus reducing glutamate release. Such a mechanism has been recently proposed to contribute to the control of ictogenesis by interictal activity (de Curtis and Avanzini, 2001). Interestingly, the latencies of the interictal-like responses induced in the EC by BLA stimulation were longer than what seen with stimulus-induced EPSPs (i.e. approximately 30 ms versus 10 ms). Further analysis is required to establish why a different latency characterizes EC neuron activation following stimulation of the same pathway. However, it is attractive to speculate that this phenomenon reflects the time required by EC networks to elaborate the synaptic interactions that lead to the interictal discharge.

3.5.4 Relevance for identifying the mechanisms of temporal lobe epilepsy

Mesial temporal lobe epilepsy is characterized both in humans and in animal models by a reduction in neuronal population in limbic structures such as the CA3 area of the hippocampus and the amygdala (Liu et al., 1994; Miller et al., 1994; Tuunanen et al., 1999; van Elst et al., 2000; Yilmazer-Hanke et al., 2000). The results obtained by cutting the Schaffer collaterals support the hypothesis that a decreased excitatory drive from the hippocampus onto EC or BLA may lead to ictogenesis (Barbarosie and Avoli, 1997; Barbarosie et al., 2000). Such a mechanism has been recently demonstrated to occur in slices obtained from pilocarpine-treated epileptic mice in which the increased occurrence of ictal events in vitro is paralleled by decreased CA3-

driven output activity and presumably sustained by interactions between the EC and SUB (D'Antuono et al., 2002).

Likewise, the results obtained by stimulating the BLA indicate that a reduction of amygdala output activity, as a result of the neuronal damage associated with mesial temporal lobe epilepsy, may contribute to ictogenesis. However, evidence obtained with depth electrode EEG recordings in epileptic patients indicates that the damaged amygdala can generate (and at times initiate) electrographic discharges (Gloor, 1992). These conflicting data indicate that further experiments in animal models of mesial temporal lobe epilepsy are required in order to identify the relative contribution of cell damage versus intrinsic epileptogenicity of amygdala networks.

3.6 Figures

Figure 3-1:

Schematic drawings of the combined slice used in this study. Abbreviations in this and the following figures are CA1-3, Ammon's horn area 1–3; DG, dentate gyrus. (**A**) Position of the recording and stimulating electrodes that were placed in CA3, the middle layers of the medial EC and BLA. (**B**) Location and extension of the cuts used to lesion the Schaffer collaterals or to separate BLA from EC. (**C–F**) Field potential responses induced by stimuli delivered in EC (**C**), CA1 stratum radiatum (**D**) and SUB (**E** and **F**) and recorded in DG, SUB and deep or superficial EC layers, respectively. The responses illustrated in each panel were induced by stimuli of increasing strength (as obtained by changing the stimulus duration).

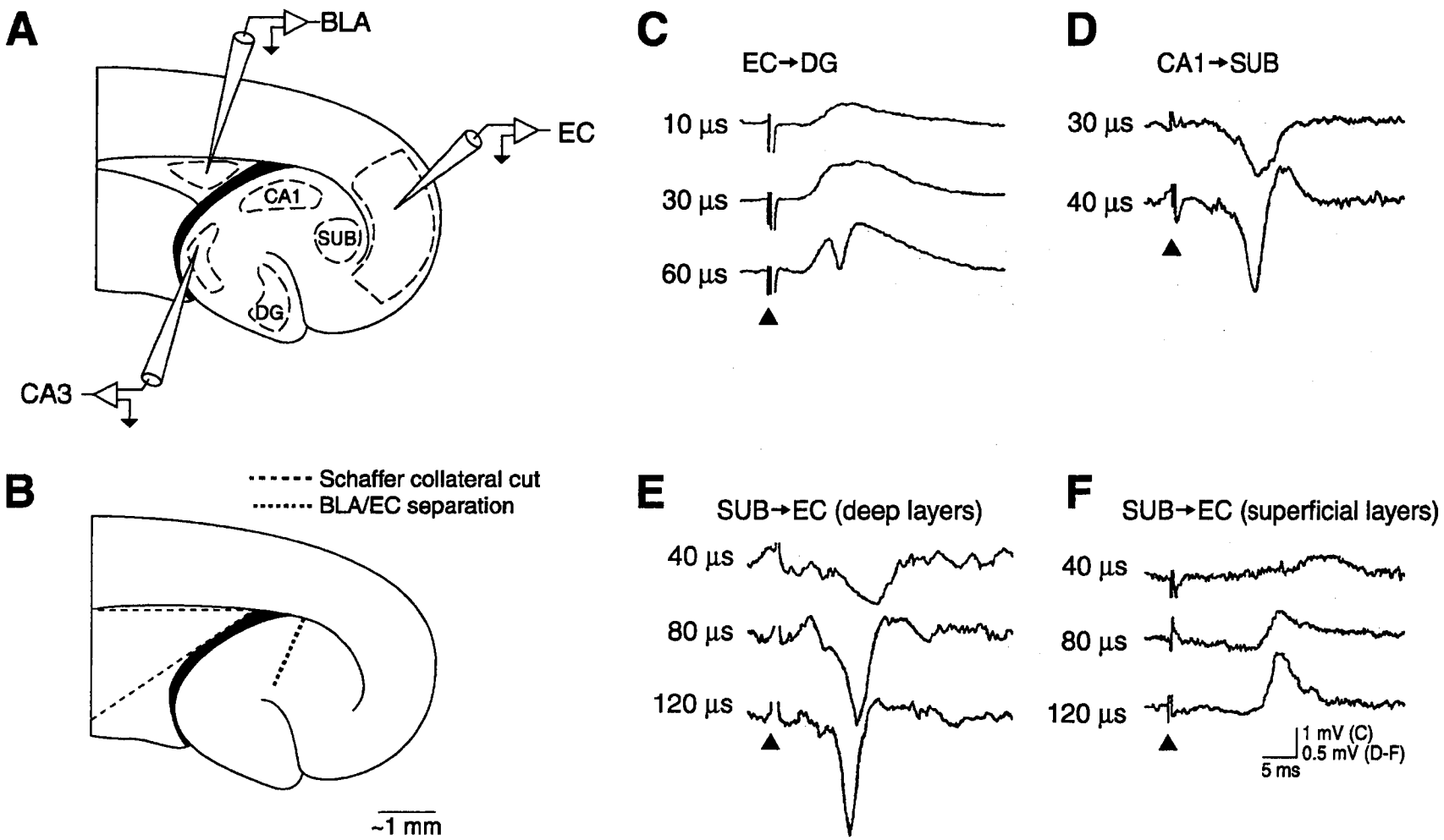
A
BLA
EC
CA1
SUB
DG
CA3
B
Schaffer collateral cut
BLA/EC separation
~1 mm
C
EC→DG
10 µs
30 µs
60 µs
D
CA1→SUB
30 µs
40 µs
E
SUB→EC (deep layers)
40 µs
80 µs
120 µs
F
SUB→EC (superficial layers)
40 µs
80 µs
120 µs
1 mV (C)
0.5 mV (D-F)
5 ms

Figure 3-2:

(A) Simultaneous field potential recordings obtained from EC, BLA and CA3 during bath application of 4AP (50 μM). Signals in this experiment were processed with a high-pass filter at 0.1 Hz. Note that the interictal discharges occur in apparent synchronicity in all limbic areas, but when displayed at faster time base (inset) they are characterized by onset in CA3 and propagation to the EC and BLA. In this and the following insets, interrupted lines point to the time of the earliest deflection of the baseline recording, which in this case occurs in CA3. **(B)** Effects induced by cutting the Schaffer collaterals and the BLA–EC connections during application of 4AP; note that cutting the Schaffer collaterals abolishes the propagation of CA3-driven interictal discharges (arrows in the CA3 trace) to the EC and BLA where a new type of slow interictal activity (asterisks) along with ictal discharges (continuous line) appear; note also that both types of epileptiform activity propagate to CA3. Subsequent separation of the EC from BLA makes independent interictal and ictal discharges occur in both structures. Insets show (i) expanded traces of a CA3-driven interictal discharge under control conditions in which the CA3 origin and the population activity re-entry (arrows) can be appreciated; and (ii) expanded traces of a slow interictal discharge after the Schaffer collateral cut, originating in BLA and spreading to EC and CA3. Note also in the '+BLA/EC separation' panel that only the ictal discharge occurring in EC propagates to CA3. **(C)** Column histogram of the time differences in the onset of slow interictal and ictal discharges measured in EC and BLA. Data were obtained from five slices and segregated according to their site of origin (i.e. BLA or EC). Values represent the mean ± S.D. of onset latency of 28 and 47 slow interictal discharges for BLA→ EC and EC→ BLA propagation, and seven and 12 ictal discharges for BLA→ EC and EC→ BLA propagation, respectively. Differences were not statistically significant.

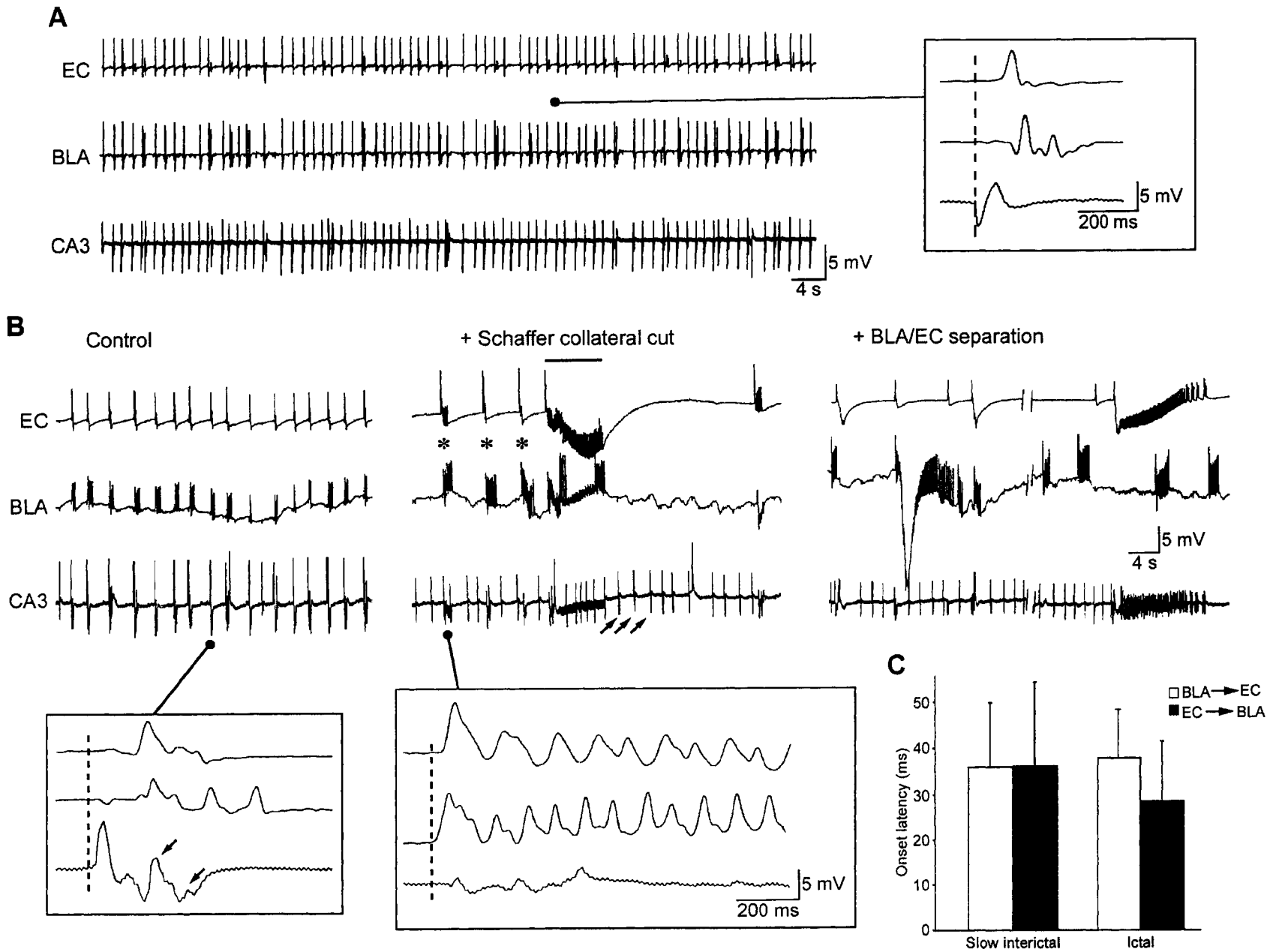
A
EC
BLA
CA3
5 mV
4 s
5 mV
200 ms
B
Control
+ Schaffer collateral cut
+ BLA/EC separation
EC
BLA
CA3
*
*
*
5 mV
4 s
5 mV
200 ms
C
BLA → EC
EC → BLA
Onset latency (ms)
0
10
20
30
40
50
Slow interictal
Ictal

Figure 3-3:

Application of the NMDA receptor antagonist CPP (10 μM) reversibly blocks the ictal discharges recorded in a combined slice after Schaffer collateral cut and separation of the BLA from the EC. Note that this NMDA receptor antagonist also reduces the amount of fast events associated with each interictal event in the BLA, while the rate of occurrence of CA3-driven interictal activity increases. Note also that in the Control and Wash panels only the slow interictal and ictal discharges generated by EC networks propagate to CA3.

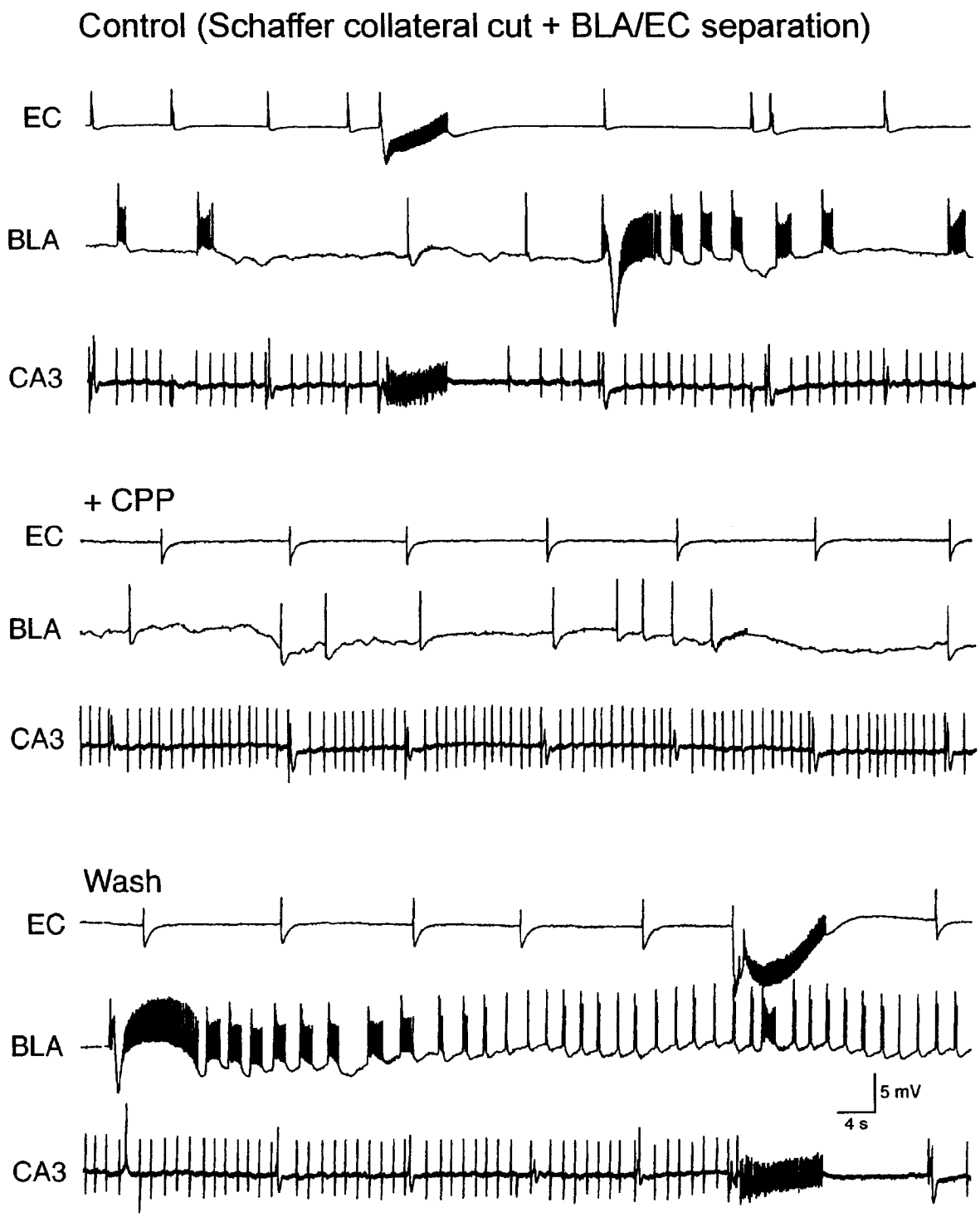
Control (Schaffer collateral cut + BLA/EC separation)
EC
BLA
CA3
+ CPP
EC
BLA
CA3
Wash
EC
BLA
5 mV
4 s
CA3

Figure 3-4:

Simultaneous intracellular (−69 mV) and field potential (Field) recordings obtained in the EC of a Schaffer collateral cut slice during 4AP application. **A** and **B** are continuous recordings. Note that ictal discharges are generated spontaneously under control conditions **(A)** as well as that repetitive stimuli delivered in BLA at 0.5 Hz induce an initial sustained response similar to the spontaneous ictal discharges, followed by a continuous pattern of interictal responses with disappearance of the ictal events. Note also that the interictal responses were barely visible in the field potential recording due to the low gain of the amplification. **(B)** These reappear within 40 s upon termination of repetitive stimulation. The expanded traces show the onset of an ictal discharge during the prestimulus period, the first stimulus-induced response (triangles point at the stimulus artifacts), and the ictal discharge seen at the end of the stimulation period.

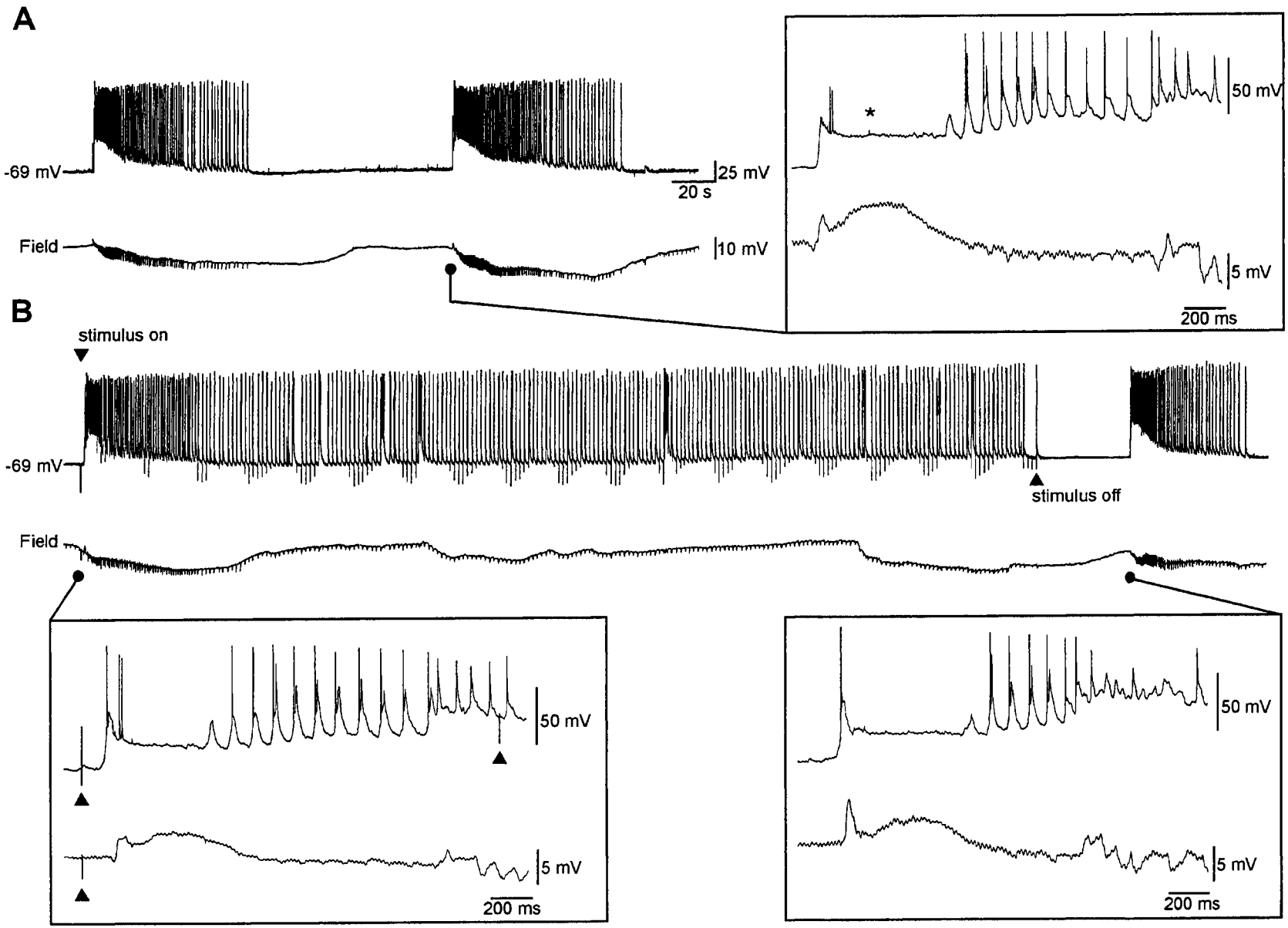
A
-69 mV
25 mV
20 s
Field
10 mV
*
50 mV
5 mV
200 ms
B
stimulus on
-69 mV
stimulus off
Field
50 mV
5 mV
200 ms
50 mV
5 mV
200 ms

Figure 3-5:

Interictal-like responses induced in an EC cell by repetitive stimuli delivered at 0.5 Hz to the BLA. Triangles below each set of traces point at the stimulus. **(A)** Expanded intracellular (−65 mV) and field potential (Field) traces reveal that the stimulus-induced epileptiform responses have variable latency. **(B)** Effects induced by increasing the stimulus strength (which was varied by increasing the stimulus duration from 20 to 90 μs) on the latency of the epileptiform depolarization; note that the delay time decreases suggesting the activation of polysynaptic pathways. **(C)** Intracellular responses induced by stimuli delivered at low (10 μs) and high (90 μs) strength. Note that in the latter case the interictal-like response is initiated by an EPSP (arrow-head). **(D)** Intracellular recordings made during steady injection of depolarizing and hyperpolarizing current. In **a**, intracellular responses at depolarized (−58 mV), hyperpolarized (−84 mV) and RMP (−65 mV) are shown. In **b**, plot of the values of the epileptiform depolarizations obtained at different values of the membrane potential. These values were measured at approx. 300 ms from the stimulus during a period of the interictal depolarization that was not associated with action potential, as shown by the stars in sample **a**.

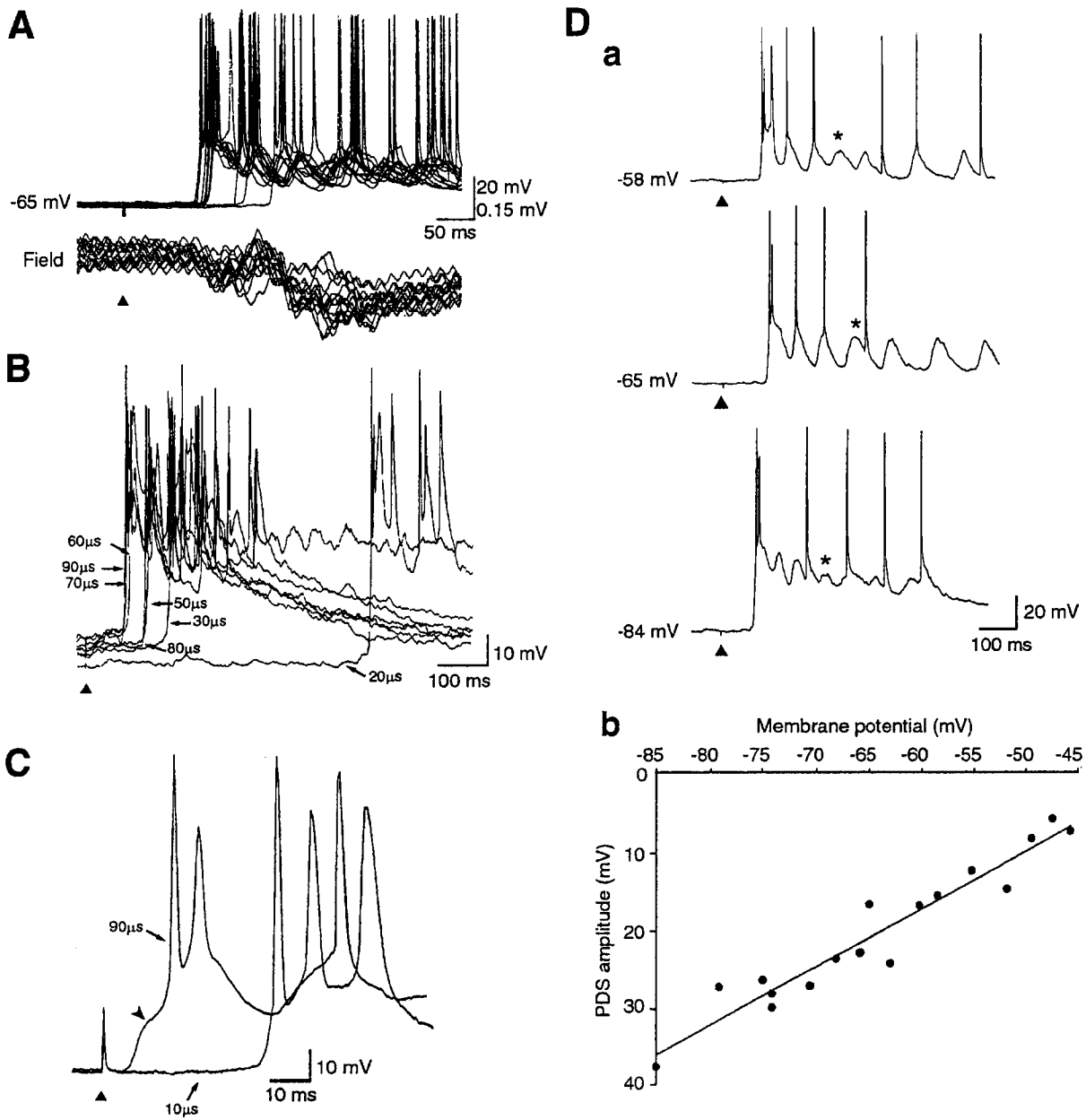
A
-65 mV
20 mV
0.15 mV
50 ms
Field
B
60μs
90μs
70μs
50μs
30μs
80μs
20μs
10 mV
100 ms
C
90μs
10 mV
10 ms
10μs
D
a
-58 mV
-65 mV
-84 mV
20 mV
100 ms
b
Membrane potential (mV)
-85 -80 -75 -70 -65 -60 -55 -50 -45
0
10
20
30
40
PDS amplitude (mV)

Figure 3-6:

Effects induced by different rates of repetitive stimuli delivered in BLA on the spontaneous ictal discharges recorded simultaneously with field potential and intracellular microelectrodes in the EC of a slice in which the Schaffer collaterals have been cut. Data were obtained during the steady state response (i.e. at least 10 s after the onset of repetitive stimulation). Note that stimuli delivered at 0.2 Hz are unable to abolish the occurrence of ictal discharges (asterisk). In contrast, repetitive stimuli at 0.5 and 1 Hz can inhibit the ictal discharges. Note also that the interictal-like responses induced by 0.2 Hz stimulation are longer than those seen with either 0.5 or 1 Hz rates.

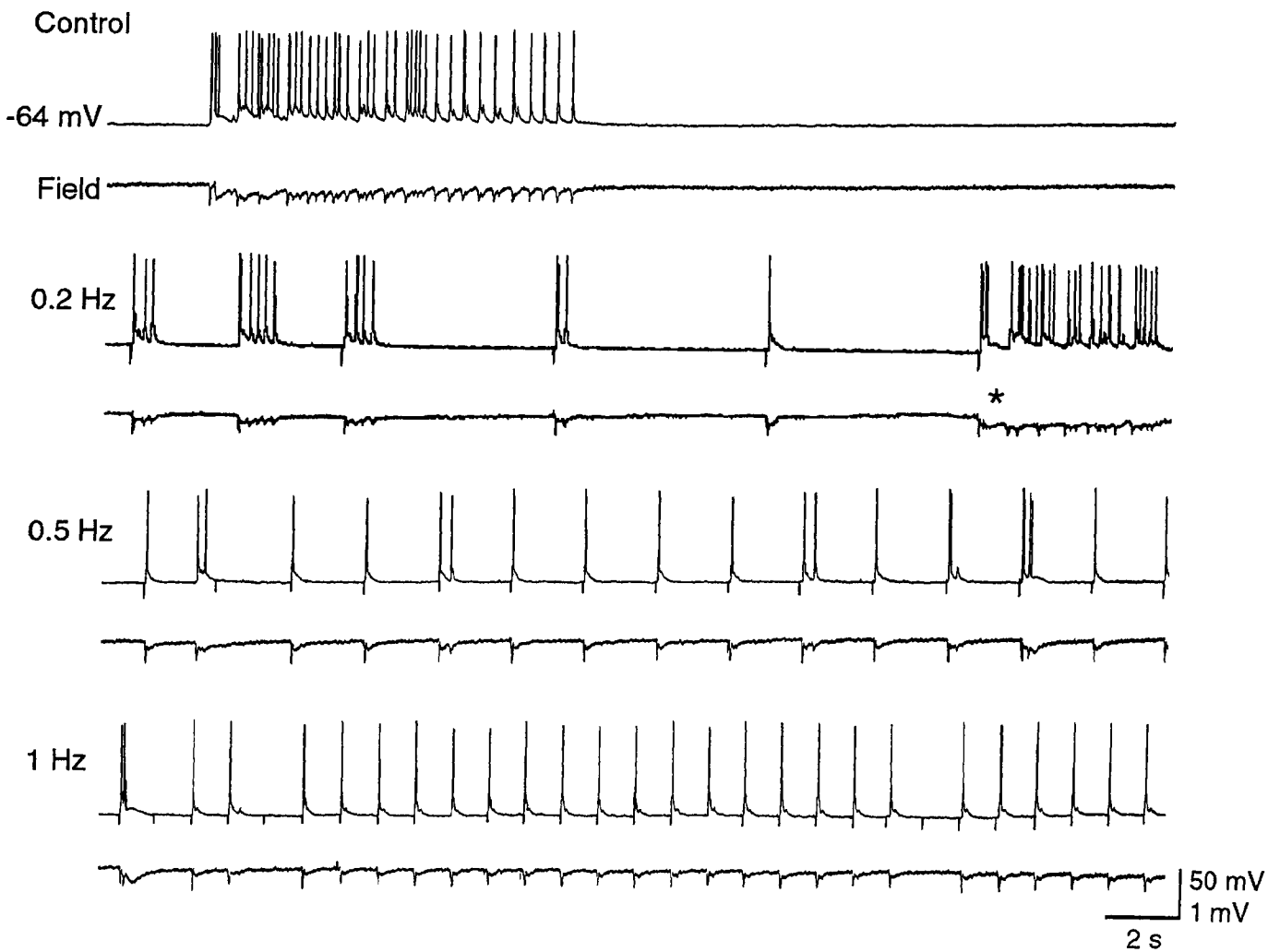
Control
-64 mV
Field
0.2 Hz
*
0.5 Hz
1 Hz
50 mV
1 mV
2 s

Chapter 4: Altered Inhibition in Lateral Amygdala Networks in a Rat Model of Temporal Lobe Epilepsy

4.0 Linking Text and Information about manuscript

In *Chapter 3* exploration of the 4AP-induced activity in a combined slice preparation demonstrated that when connections are preserved, CA3 network activity paces both EC and BLA/LA networks and prevents ictogenesis in these structures. Moreover, evidence was also provided for the ability of BLA/LA networks to generate both interictal- and ictal-like activity, independent of inputs from adjacent structures.

In *Chapter 4*, we sought to identify what changes occur within the amygdala in chronically epileptic rats. A literature search revealed that although such an assessment in the BLA had already been carried out by other investigators, surprisingly detailed electrophysiological evaluation of the LA using chronic animal models of TLE is sparse. We thus addressed this issue in *Chapter 4*. The results of this study were published in the *Journal of Neurophysiology* in 2006 as a manuscript entitled *"Altered inhibition in lateral amygdala networks in a rat model of temporal lobe epilepsy"* (Authors: **Benini R** and Avoli M). Permission granted by the journal to reproduce the contents of this manuscript can be found in Appendix D.

4.1 Abstract

Clinical and experimental evidence indicates that the amygdala is involved in limbic seizures observed in patients with temporal lobe epilepsy. Here, we used simultaneous field and intracellular recordings from horizontal brain slices obtained from pilocarpine-treated rats and age-matched non-epileptic controls (NEC) to shed light on the electrophysiological changes that occur within the lateral nucleus (LA) of the amygdala. No significant differences in LA neuronal intrinsic properties were observed between pilocarpine-treated and NEC tissue. However, spontaneous field activity could be recorded in the LA of 21% of pilocarpine-treated slices but never from NECs. At the intracellular level, this network activity was characterized by robust neuronal firing and was abolished by glutamatergic antagonists. In addition, we could identify in all pilocarpine-treated LA neurons: (i) large amplitude depolarizing

postsynaptic potentials (PSPs), and (ii) a lower incidence of spontaneous hyperpolarizing PSPs as compared with NECs. Single-shock stimulation of LA networks in the presence of glutamatergic antagonists revealed a biphasic IPSP in both NEC and pilocarpine-treated tissue. The reversal potential of the early $GABA_A$-receptor mediated component, but not of the late $GABA_B$-receptor mediated component, was significantly more depolarized in pilocarpine-treated slices. Furthermore, the peak conductance of both fast and late IPSP components had significantly lower values in pilocarpine-treated LA cells. Finally, paired-pulse stimulation protocols in the presence of glutamatergic antagonists revealed a less pronounced depression of the second IPSP in pilocarpine-treated slices as compared to NEC. Altogether, these findings suggest that alterations in both pre- and postsynaptic inhibitory mechanisms contribute to synaptic hyperexcitability of LA networks in epileptic rats.

4.2 Introduction

The amygdalar complex, located in the deep anteromedial part of the temporal lobe, is composed of several nuclei that are interconnected with cortical and subcortical regions in a specific manner (Lopes da Silva et al., 1990; Pitkanen et al., 2000a,b). Under normal physiological conditions, the amygdala is involved in fear conditioning and emotional learning (LeDoux, 2000; Paré et al., 2004; Scott et al., 1997; Stork and Pape, 2002; Wilensky et al., 2000). The amygdala is also known to be at the origin of some of the behavioral manifestations observed during seizures in temporal lobe epilepsy (TLE) patients where it is often the primary focus of seizure activity (Gloor, 1992, 1997; van Elst et al., 2000). Patients with TLE can present with unilateral or bilateral damage to this structure, and in certain instances, isolated amygdalar pathology occurs in the absence of hippocampal sclerosis (reviewed by Pitkanen et al., 1998). Histochemistry of resected human epileptic tissue has revealed that the lateral and basal nuclei are the most vulnerable to injury (Yilmazer-Hanke et al., 2000). Assessment of these nuclei has disclosed that in addition to neuronal loss and gliosis, synaptic alterations - in the form of decreased dendritic branching of surviving cells - also take place (Aliashkevich et al., 2003).

Histological examination of chronically epileptic animal tissue has confirmed an overlap with the pattern of cell loss detected in humans. Specifically, these studies have confirmed that amygdala damage is nucleus-specific and that some nuclei are more resistant to injury than others (Nissinen et al., 2000; Tuunanen et al., 1996). Furthermore, in addition to loss of principal cells, decreased density of specific interneuronal populations has been documented in chronically epileptic animals (Tuunanen, 1996, 1997). The basolateral amygdalar nucleus (BLA) has been the primary focus of electrophysiological evaluation of the amygdala in chronic animal models of TLE. These studies have identified various mechanisms to account for the hyperexcitability of BLA networks observed in epileptic animals including loss of spontaneously-occurring inhibitory postsynaptic potentials (IPSPs), loss of feedforward inhibition, and enhanced NMDA- and non-NMDA mediated excitation (Gean et al., 1989; Mangan et al., 2000; Rainnie et al., 1992; Shoji et al., 1998; Smith and Dudek, 1997).

Despite such an extensive assessment of the BLA, relatively few electrophysiological studies have carefully examined other amygdalar nuclei using chronic animal models of TLE. For instance, little is known about the functional changes that take place within the lateral nucleus of the amygdala (LA) where neuronal loss and gliosis have been identified in subjects with intractable TLE (Yilmazer-Hanke et al., 2000). A recent study reported that decreased excitatory transmission occurs in the LA of epileptic rodents probably due to a decrease in glutamate release or neurodegeneration (Niittykoski et al., 2004). However, much information is still needed to fully understand the contribution of this structure to epileptogenesis. For example, although previous investigations have illustrated the essential role of local GABAergic circuits in controlling LA excitability (Callahan et al., 1991; Lang and Paré, 1997, 1998), a detailed electrophysiological examination of how these inhibitory networks are affected in epileptic animals is still lacking.

Assessing the contribution of the LA to hyperexcitability of limbic neuronal networks becomes essential when one considers its dense reciprocal interconnections with the hippocampus and parahippocampal cortices, structures that are highly

implicated in TLE (Du et al., 1993; Pikkarainen and Pitkanen, 2001; Pitkanen et al., 1995, 2000b). In this study we assessed the electrophysiological changes that occur in the LA of epileptic rats by using the pilocarpine chronic animal model of TLE where damage to this amygdala nucleus has been reported (Cavalheiro et al., 1987; Fujikawa, 1996). Our investigations were specifically aimed at assessing the functional characteristics of inhibition within this structure.

4.3 Methods

Animal preparation - Procedures approved by the Canadian Council of Animal Care were used to induce status epilepticus (SE) in adult male Sprague-Dawley rats weighing 150-200g at the time of injection. All efforts were made to minimize the number of animals used and their suffering. Briefly, rats were injected with a single dose of pilocarpine hydrochloride (380-400 mg/Kg, i.p). In order to reduce the discomforts caused by peripheral activation of muscarinic receptors, methyl scopolamine (1 mg/Kg i.p) was administered 30 min prior to the pilocarpine injection. The animals' behavior was monitored for approx. 4 h following pilocarpine and scored according to Racine's classification (Racine et al., 1972b). Only rats that experienced SE (stage 3-5) for more than 30 minutes (53.1±9.3 min, mean±SEM; n=35 rats) were included in the pilocarpine group and used for in vitro electrophysiological studies approx. 4 months (18±1 week; n=35 rats) following pilocarpine injection. Since it has been previously established that all adult rats experiencing pilocarpine-induced SE will later exhibit spontaneous recurrent seizures (Cavalheiro et al., 1991; Priel et al., 1996), only a subset of pilocarpine-treated animals were video-monitored and the presence of spontaneous behavioral seizures was confirmed in virtually all of them (n= 14/15). In this study, rats receiving a saline injection instead of pilocarpine were used as age-matched non-epileptic controls (NEC).

Slice preparation and maintenance - Adult rats were decapitated under halothane anesthesia; the brain was quickly removed and a block of brain tissue containing the retrohippocampal region was placed in cold (1-3°C), oxygenated artificial cerebrospinal fluid (ACSF). The brain dorsal side was cut along a horizontal plane that was tilted by a 10° angle along a postero-superior-anteroinferior plane passing

between the lateral olfactory tract and the base of the brain stem (Benini et al., 2003). Horizontal slices (400-450 μm thick) were cut from this brain block using a vibratome and slices were then transferred into a tissue chamber where they lay at the interface between ACSF and humidified gas (95% O_2, 5% CO_2) at a temperature of 34-35 °C and a pH of 7.4. We focused in this study on the most ventral slices that were comprised between -8.6mm to -7.6mm from the bregma (Paxinos and Watson, 1998). These slices contained the hippocampus proper, the parahippocampal cortices as well as the lateral nucleus of the amygdala (LA) (Fig. 4-1A). Two to three of such slices could be obtained from each hemisphere. ACSF composition was (in mM): NaCl 124, KCl 2, KH_2PO_4 1.25, $MgSO_4$ 2, $CaCl_2$ 2, $NaHCO_3$ 26, and glucose 10. (2S)-3-[[(1S)-1-(3,4-Dichlorophenyl)ethyl]amino-2-hydroxypropyl](phenyl-ethyl)phosphinic acid (CGP 55845A, 10 μM), 6-cyano-7-nitroquinoxaline-2,3-dione (CNQX, 10 μM), 3,3-(2-carboxypiperazin-4-yl)-propyl-1-phosphonate (CPP, 10 μM), and picrotoxin (PTX, 50 μM) were applied to the bath. Chemicals were acquired from Sigma (St. Louis, MO, USA) with the exception of CGP 55845A, CNQX and CPP that were obtained from Tocris Cookson (Ellisville, MO, USA).

Electrophysiological recordings and stimulation protocols - Field potential recordings were made from the LA and deep layers of the perirhinal cortex (PC) with ACSF-filled, glass pipettes (resistance=2-10 MΩ) that were connected to high-impedance amplifiers (Fig. 4-1A). Sharp-electrode intracellular recordings were performed in LA with pipettes that were filled with 3M K-acetate or with 3M K-Acetate/75 mM lidocaine,N-ethyl bromide (QX314) (tip resistance= 70-120 MΩ in both cases). Intracellular signals were fed to a high-impedance amplifier with internal bridge circuit for intracellular current injection. The resistance compensation was monitored throughout the experiment and adjusted as required. The passive membrane properties of LA cells included in this study were measured as follows: (i) resting membrane potential (RMP) after cell withdrawal; (ii) apparent input resistance (Ri) from the maximum voltage change in response to a hyperpolarizing current pulse (100-200 ms, <-0.6 nA); (iii) action potential amplitude (APA) from the baseline and (iv) action potential duration (APD) at half-amplitude. Intrinsic firing patterns of LA

cells were classified from responses to depolarizing current pulses of 1000-2500 ms duration. The adaptation ratio (AR), defined as the ratio of the last interspike interval (ISI) to the first ISI, was used to quantitatively compare the firing properties of cells from pilocarpine (n=30) and NEC groups (n=30) (cf., Takazawa et al., 2004). For each cell, AR was obtained from a 1200 ms depolarizing pulse at a current intensity 0.2 nA larger than that which induced threshold action potential firing.

Synaptic responses to single shock stimulation (50-100 μs; < 350 μA) of local LA networks was assessed using a bipolar, stainless steel electrode placed < 500 μm from the recording electrodes. "Monosynaptic" IPSPs were evoked in the presence of glutamatergic antagonists (10 μM CPP+10 μM CNQX). The stimulation parameters used to elicit these responses were not significantly different ($p>0.05$) between pilocarpine (stimulus intensity= 203±21 μA; duration= 100 μs; n=22) and NEC (stimulus intensity= 175±17 μA; duration= 100 μs; n=16) groups. Reversal potential and peak conductance values for the early and late components of the IPSPs were obtained from a series of responses evoked at membrane potentials set to different levels by intracellular current injection. Reversal potentials were computed from regression plots of response amplitude vs membrane potential. Peak conductance values were estimated using the parallel conductance model (cf., Williams et al., 1993). Briefly, the membrane potential vs intensity of injected current was plotted (i) before the stimulation and (ii) at the peak of the IPSP response. The slopes of these two regression lines were then used to yield the input resistance at rest (i.e. before the stimulation) and during the response respectively, and to ultimately determine the change in resistance that occurred during the IPSP (ΔR_{IPSP}). ΔR_{IPSP} was then translated to peak conductance changes (ΔG_{IPSP}) using the formula: $\Delta G_{IPSP} = 1/\Delta R_{IPSP}$.

Paired stimuli (100 μs duration) at intervals from 50-1600 ms were used to assess changes in synaptic depression of "monosynaptic" $GABA_A$-receptor mediated IPSPs by using K-Acetate/QX314-filled electrodes. For the paired pulse protocols, the stimulus current strength giving >50% maximal response was used to stimulate LA interneuronal networks. Furthermore, cells were hyperpolarized by current injection to obtain depolarizing IPSPs. The membrane potential at which the test was conducted

was not significantly different ($p>0.05$) between the two experimental groups (pilocarpine-treated= -102±2 mV, n=10 and NEC= -105±3 mV; n=10); in addition, the absolute amplitude of the first response (P1) evoked at this membrane potential was not different in pilocarpine-treated (9±0.5 mV, n=10) and NEC (10±0.5 mV, n=10) neurons.

Field potential and intracellular signals were fed to a computer interface (Digidata 1322A; Axon Instruments Inc) and were acquired and stored using the pClamp 9 software (Axon Instruments Inc., Foster City, CA, USA). Subsequent data analysis was made with the Clampfit 9 software (Axon Instruments). For time-delay measurements, the onset of the field potential/intracellular signals was determined as the time of the earliest deflection of the baseline recording (e.g., insert trace in Fig. 4-2Ca). Measurements in the text are expressed as mean±SEM and n indicates the number of slices or neurons studied under each specific protocol. Data were compared with the Student's t-test and were considered statistically significant if $p<0.05$.

Neuronal labelling - Electrodes for intracellular labeling were filled with 2% neurobiotin dissolved in 2M K-acetate. Intracellular injection of neurobiotin was accomplished by passing pulses of depolarizing current (0.5-1nA, 3.3Hz, 150ms) through the recording electrode for 2-10 min. Neurobiotin injection did not have any appreciable effect on RMP, Ri and evoked action potential properties (cf., Xi and Xu, 1996). Only one neuron was filled in each slice. Following the electrophysiological characterization of these neurons, slices were removed from the recording chamber and fixed in 4% paraformaldehyde, 100 mM phosphate-buffered solution overnight at 4°C. Slices were then rinsed in phosphate buffered saline (PBS) and the endogenous peroxidase activity extinguished by incubating them in 0.1% phenylhydrazine for 20 min. After several rinses in PBS, the slices were incubated for 2 h in 1% Triton X-100 and then in vectastain ABC reagent comprising the avidin-biotinylated horseradish peroxidase complex in PBS for at least 4h. After wash in PBS, the sections were reacted with 0.5% 3,3'-diaminobenzidine tetrahydrochloride and 0.003% hydrogen peroxide in PBS, mounted on slides, dehydrated and covered (Kita and Armstrong, 1991). The intracellularly stained neurons were photographed using the Nomarski

optics or a Zeiss Axiophot microscope. Neurobiotin and vectastain ABC were obtained from Vector Laboratories.

4.4 Results

4.4.1 Intrinsic electrophysiological properties and morphology of lateral amygdala neurons

Intracellular recordings were carried out in the LA of brain slices obtained from pilocarpine-treated rats (n= 83 cells from 66 slices) and age-matched non-epileptic controls (NECs) (n=54 cells from 41 slices). Morphological identification with intracellular injection of neurobiotin was also carried out in some neurons (n= 17 and 11 in pilocarpine and NEC slices, respectively). Based on a gross visual examination of cell body shape and dendrite distribution, three main types of principal spiny neurons could be distinguished in both epileptic and NEC tissue: (i) stellate-like elements (8/17 and 6/11 of pilocarpine and NEC neurons, respectively) (Fig. 4-1Ba); (ii) bipolar-shaped cells (2/17 and 0/11 of pilocarpine and NEC neurons, respectively) (Fig. 4-1Bb) ; and (iii) pyramidal-like neurons (7/17 and 5/11 of pilocarpine and NEC cells, respectively) (Fig. 4-1Bc).

Analysis of the intrinsic properties of cells recorded in the two types of tissue revealed no significant differences in RMP, Ri, APD and APA (Table 4-1). Moreover, as previously reported by other investigators (Faber et al., 2001; Faulkner and Brown, 1999) the regular firing characteristics of LA neurons consisted of a spectrum of different spike adaptations (Fig. 4-1Ca-c). The range of adaptation ratios (AR, see Methods) varied between 1.1 and 69.0 in pilocarpine and between 1.3 and 43.5 in NEC neurons, with no significant difference in the AR distribution between the two groups (p= 0.2). Thus no disparity in the expression of the different modalities of repetitive firing could be identified between NEC and pilocarpine-treated neurons.

4.4.2 Spontaneous synaptic activity in LA of pilocarpine-treated rats is altered

Field potential recordings obtained during application of normal ACSF from the LA and the PC of NEC slices (n= 41) demonstrated the absence of any spontaneous activity (Fig. 4-2Aa, bottom field traces). Moreover, when analyzed with intracellular recordings, all neurons from this group exhibited at RMP depolarizing postsynaptic

potentials (PSPs) with amplitudes of 1.71±0.03 mV (range= 0.5-8.4 mV, n=26) and rates of occurrence of 0.72±0.04 s (range= 0.01-13.5 s, n=26) (Fig. 4-2Aa, arrows) (Table 4-2). In addition, spontaneous hyperpolarizing PSPs (sIPSPs) (amplitude: -3.4±0.2 mV; rate of occurrence: 18±5 s, range= 0.2-140 s, n=14) could be recorded in 53% of NEC LA neurons (n=25/47) (Fig. 4-2Aa, asterix) (Table 4-2). Steady hyperpolarization and depolarization of the membrane potential altered the amplitude of these two types of spontaneous activities without influencing their rate of occurrence, thereby confirming their synaptic nature (Fig. 4-2Ab).

Spontaneous field activity was also absent from the majority of pilocarpine-treated slices (n= 52/66) (Fig. 4-2B, Pilocarpine-treated tissue (no field activity)). As in NEC tissue, neurons recorded intracellularly from pilocarpine-treated slices also exhibited spontaneous depolarizing PSPs with amplitudes of 2.73±0.05 mV (range= 0.7-16.6 mV, n=33) and rates of occurrence of 1.02±0.07 s (range= 0.01-21.8s, n=33) (Fig. 4-2B, arrows, insert) (Table 4-2). Distribution analysis revealed that although there was no significant difference between the two groups in their rate of occurrence, depolarizing PSPs recorded from pilocarpine-treated slices skewed towards larger amplitudes (Fig. 4-3A, $p<0.001$) (Table 4-2). Furthermore, in contrast to the NEC group, an appreciably lower proportion (31%) of cells (n=21/68) in the epileptic group displayed sIPSPs at RMP (amplitude: -3.0±0.1 mV; rate of occurrence: 22±4 s, range= 1-210 s, n=16) (Fig. 4-3B, RMP) (Table 4-2). This difference in the expression of sIPSPs between the two experimental groups was evident even when neurons were depolarized to ~ - 60 mV to unmask any reversed inhibitory potentials (Fig. 4-3B, Depolarized MP). Thus, these results suggest that pilocarpine-treated LA cells display subtle differences in synaptic activity. These alterations include the presence of larger amplitude depolarizing PSPs (Fig. 4-2A-B and Fig. 4-3A) and reduced incidence of sIPSPs (Fig. 4-3B).

In addition to these differences, more significant changes were observed in 21% of slices from the pilocarpine-treated group (n=14/66, Fig. 4-2Ca and Fig. 4-3Da, Pilocarpine-treated tissue (with field activity)). In these slices, spontaneous field activity (duration: 786±514 ms, range: 190-2100 ms; rate of occurrence: 13.1±10.7 s,

7-41 s; Table 4-2) could be recorded in the LA and at times could spread to the deep layers of the PC (n=3) (Fig. 4-2Ca). Intracellularly, this network activity corresponded to robust neuronal firing at RMP (n=14 cells) and in the majority of these cells (n=11/14) no sIPSPs could be recorded (Fig. 4-2Ca and 4-3Da, Control). The increasing amplitude of the underlying excitatory postsynaptic potential with hyperpolarization of the membrane potential confirmed the synaptic nature of these events (Fig. 4-2Cb, arrows).

4.4.3 Pharmacology of spontaneous activity

The NMDA-receptor antagonist CPP reduced the frequency of occurrence of spontaneous depolarizing PSPs in both NEC (n=7) and pilocarpine-treated tissue (n=4). Further treatment with the non-NMDA receptor antagonist CNQX abolished these PSPs (n=10 and 11 in pilocarpine and NEC slices, respectively) without affecting the occurrence of hyperpolarizing sIPSPs that were often biphasic (Fig. 4-3C, +CPP+CNQX, insert) and reduced by the $GABA_A$ receptor antagonist picrotoxin (n=4, not shown). CPP+CNQX application to pilocarpine-treated slices exhibiting spontaneous field events completely abolished this network activity (Fig. 4-3Da, +CPP+CNQX) and uncovered biphasic sIPSPs (Fig. 4-3Da,b) that were diminished with picrotoxin addition.

4.4.4 Evidence for alterations in inhibitory networks of LA

The incidence of sIPSPs at RMP was lower in LA neurons recorded from pilocarpine-treated slices as compared with those of the NEC group (Fig. 4-3B, RMP). This difference was also evident even when the membrane potential was depolarized to ~ -60mV to unmask any reversed sIPSPs (Fig. 4-3B, Depolarized MP). This observation suggested that altered inhibition occurred in the LA of pilocarpine-treated animals.

To isolate and assess the activity of local inhibitory networks within the LA of NEC and pilocarpine-treated rats, we analyzed the intracellular responses of LA neurons to single-shock stimulation in the presence of glutamatergic antagonists (CPP+CNQX). As reported by previous studies (Heinbockel and Pape, 1999), these "monosynaptic" stimulus-evoked IPSPs in the NEC group (n=13) were biphasic in nature, with an early $GABA_A$-receptor mediated component (Fig. 4-4A, NEC, Early)

and a late $GABA_B$-receptor component (Fig. 4-4A, NEC, Late). Similar observations were made in the pilocarpine group (n=13, Pilocarpine-treated) thereby suggesting that post-synaptic $GABA_A$- and $GABA_B$-receptor mechanisms remained intact. However, comparison of the reversal potentials of the early IPSP component revealed a significantly ($p<0.002$) more depolarized value in pilocarpine-treated neurons (-65.9±1.5 mV, n=13) than NEC cells (-74.5±0.7 mV, n=13) (Fig. 4-4B, Early Phase). Peak conductance of the early IPSP component was also different ($p<0.05$) between the two groups, with a lower peak conductance in the pilocarpine-treated tissue (7.3±1.1nS, n= 15) as compared to NEC (12.1±1.6nS, n=15) (Fig. 4-4C).

Similar assessment of the late $GABA_B$-receptor mediated component of the IPSP revealed no difference in reversal potentials between pilocarpine-treated (-95.7±1.9 mV, n=13) and NEC cells (-93.3±2.0 mV, n=11) (Fig. 4-4B, Late Phase). However, the peak conductance of this late IPSP component was slightly lower in pilocarpine (2.2±0.4nS, n=14) vs NEC neurons (4.6±0.7nS, n=11) (Fig. 4-4C, Late Phase). Altogether, these results indicate that alterations in postsynaptic GABAergic mechanisms, specifically in $GABA_A$ receptor-mediated inhibition, occur in the LA of epileptic rats.

4.4.5 Functional changes also involve presynaptic alterations

To determine whether modifications in presynaptic mechanisms occurred in the LA of pilocarpine-treated rats, we delivered paired stimuli (100 μs duration; <350 μA intensity) at intervals of 50-1600 ms with a stimulating electrode placed within 500 μm from the recording electrode. Recordings were carried out with QX-314-filled microelectrodes in the presence of CPP+CNQX. In addition to its well-known effects on voltage-gated sodium channels (Connors and Prince, 1982) QX-314 blocks $GABA_B$-receptors (Nathan et al., 1990) thus allowing the isolation of the fast $GABA_A$-receptor mediated component of the IPSP. Furthermore, due to the ability of this lidocaine derivative to attenuate I_h (Perkins and Wong, 1995), the corresponding IPSPs could be assessed more easily in their reversed form at hyperpolarized membrane potentials (Fig. 4-5A, B).

In NEC slices, paired-pulse stimulation protocols revealed a marked depression in the amplitude of the second stimulus-induced IPSP (P2) with respect to the first (P1) at interstimulus intervals between 50 and 1000 ms (Fig. 4-5A, C, n=10). The second IPSP amplitudes recovered to initial values at intervals of ≥1,200 ms (Fig. 4-5C). In contrast, paired IPSPs in LA neurons recorded from pilocarpine-treated tissue tended to exhibit a less pronounced depression at interstimulus intervals between 50 and 1600 ms as compared to NEC, thereby suggesting a failure in presynaptic GABAergic interneuron autoreceptors (Fig. 4-5B, C, n= 10). The difference between NEC and pilocarpine-treated groups was statistically different ($p<0.05$) at interstimulus intervals between 200 and 1000 ms (Fig. 4-5C, asterisk).

Presynaptic $GABA_B$ receptors have been shown to contribute to the paired-pulse depression of $GABA_A$-receptor mediated inhibitory postsynaptic currents (IPSCs) induced in the LA by paired stimulation of cortical and thalamic inputs in the presence of glutamatergic transmission (Szinyei et al., 2000). To determine whether the same was true for the monosynaptic IPSPs induced in our experimental paradigm (i.e. in the absence of glutamatergic transmission), the effect of the $GABA_B$ receptor antagonist CGP 55845A on the magnitude of the IPSP paired-pulse depression (PPD) was tested at an interstimulus interval yielding maximal depressant effects (400ms). In NEC tissue, CGP 55845A increased the P2/P1 ratio by 24.7±4.7% in 6 out of 12 neurons (Fig. 4-5D). On the other hand, PPD in pilocarpine-treated cells tended to be less affected by $GABA_B$ receptor antagonism which increased the P2/P1 ratio in only 3 of 9 neurons by 11.7±0.9% (Fig. 4-5D). The difference in the extent of PPD attenuation by CGP 55845A was marginally significant between the NEC (24.7±4.7%, n=6) and pilocarpine-treated cells (11.7±0.9%, n=3) at $p=0.05$. Altogether, these results suggest that presynaptic $GABA_B$ receptors may contribute to controlling neurotransmitter release from LA interneurons and point towards the possibility of altered presynaptic $GABA_B$ receptor-mediated mechanisms in chronically epileptic animals.

4.5 Discussion

In this study, we sought to identify the functional changes that occur within the LA using the pilocarpine rodent model of TLE. The results obtained demonstrate that alterations in LA network excitability occur in chronically epileptic rats. Specifically, LA neurons exhibit larger PSPs and a lower incidence of hyperpolarizing sIPSPs than those observed in NEC animals. Moreover, in contrast to NEC, a subset of slices from the pilocarpine group displayed intense network bursting in LA. Finally, in addition to the lower incidence of sIPSPs observed in the epileptic group, we provide for the first time evidence for both postsynaptic and, presumably, presynaptic modifications in GABA receptor-mediated mechanisms.

4.5.1 Synaptic alterations in LA of epileptic rats

Due to the overwhelming body of clinical evidence implicating the amygdala in the initiation and spread of limbic seizures, various studies have sought to identify the cellular and network mechanisms underlying the role of this nucleated structure in epileptogenesis. In vitro investigations have shown that in the presence of convulsive agents, synaptic recruitment of amygdalar neurons via both excitatory and inhibitory mechanisms endows it with the ability to generate epileptic discharges and participate in epileptiform synchronization of limbic networks (Benini et al., 2003; Gean, 1990; Gean and Shinnick-Gallagher, 1988; Kleuva et al., 2003; Stoop and Pralong, 2000). Furthermore, studies carried out in the BLA of kindled (Gean et al., 1989; Mangan et al., 2000; Rainnie et al., 1992; Shoji et al., 1998) and kainate-treated rodents (Smith and Dudek, 1997) have demonstrated that in addition to cellular loss and gliosis, permanent changes in synaptic transmission render this amygdaloid region epileptic. We report here similar results in the LA of pilocarpine-treated rats where spontaneous NMDA/non-NMDA sensitive epileptiform bursting and large amplitude depolarizing PSPs occurred.

Interestingly, a reduced incidence of sIPSPs was also evident in pilocarpine-treated tissue as compared to non-epileptic controls, thereby suggesting that alterations in inhibitory mechanisms had also taken place. This finding is relevant considering the extensive immunohistochemical and electrophysiological data illustrating that the

amygdala is rich in GABAergic cells and that inhibitory processes play an underlining role in controlling the excitability of the LA (Pitkanen and Amaral, 1994; Smith et al., 1998). For instance, stimulation of various afferents in vivo results in mainly inhibitory responses within the LA (Lang and Pare, 1997, 1998; Le Gal La Salle, 1976). Furthermore, as demonstrated here and by other investigators, in vitro stimulation of LA networks yields biphasic IPSP responses that are mediated by $GABA_A$ and $GABA_B$ receptors (Danober and Pape, 1998; Martina et al., 2001; Sugita et al., 1992). Moreover, we have found that the majority of LA neurons in NEC tissue exhibit robust spontaneously-occurring IPSPs that are resistant to glutamatergic antagonists but are sensitive to $GABA_A$-receptor antagonism, thus further substantiating a significant role for inhibitory networks within this nucleus.

Histological examination of epileptic tissue has demonstrated a reduction of GABAergic neurons within the LA (Tuunanen, 1996, 1997), possibly accounting for the reduced incidence of sIPSPs observed in our pilocarpine-treated tissue. It is noteworthy to mention that in contrast to studies reporting a complete loss of sIPSPs in the BLA of epileptic animals (Gean et al., 1989; Rainnie et al., 1992), we have shown here that inhibitory inputs onto principal cells are not completely lost in the LA of pilocarpine-treated tissue. This is evident by the continued presence of sIPSPs in epileptic tissue, albeit in a smaller proportion of cells. Our findings are in line with previous reports that illustrate a partial loss of interneurons within the LA of chronically epileptic rats, with some studies even reporting > 50% of surviving interneurons (Tuunanen et al., 1996, 1997). Finally, decreased dendritic branching of surviving principal cells in the epileptic amygdala (Aliashkevich et al., 2003) also raises the possibility that interneurons make fewer contacts onto pyramidal cells and could perhaps contribute to the reduced incidence of sIPSPs in pilocarpine-treated slices. Hence, our findings suggest that in epileptic rats, alterations in both excitatory and inhibitory synaptic transmission contribute to the hyperexcitability of LA neuronal networks.

4.5.2 Altered postsynaptic $GABA_A$ receptor-mediated inhibition

In order to further assess the changes in inhibitory inputs onto LA principal cells, IPSPs induced in the presence of glutamatergic antagonists were studied in pilocarpine-treated and NEC tissue. Interestingly, we were able to record biphasic IPSPs in the LA of both types of tissue thereby indicating that $GABA_A$- and $GABA_B$ receptor-mediated mechanisms were present in the epileptic group. However, notable differences were observed in the reversal potential of the fast component of the IPSP. Specifically, the reversal potential of this $GABA_A$ receptor-mediated component was found to be significantly more depolarized in the pilocarpine-treated tissue as compared to NEC. In fact, the reversal potential in the epileptic tissue was more positive than the mean resting membrane potential by approx. 6mV. Altogether, this signifies that postsynaptic $GABA_A$ receptor-mediated potentials have a greater chance to be depolarizing at resting levels in the pilocarpine-treated group as compared to NEC where the reversal potential is more negative than RMP.

GABA generally tends to induce hyperpolarization of neurons in the adult brain. However, there are several instances such as in the developing juvenile brain (Ben-Ari et al., 1989) or in the adult brain under high frequency stimulation (Lamsa and Taira, 2003; Voipio and Kaila, 2000) where depolarizing effects of GABA are known to occur. Furthermore, the excitatory actions of GABA have also been documented under pathological conditions such as epilepsy (Cohen et al., 2002), pain (Coull et al., 2003) and ischemia (Schwartz-Bloom and Sah, 2001). Several mechanisms have been proposed to account for this polarity switch in GABA action including modified Cl^- gradients due to a decreased expression of the K^+/Cl^- cotransporter KCC2 (Riviera et al., 1999) and deafferentiation (Vale and Sanes, 2000).

Thus, the more depolarized reversal potential and the lower peak conductance of the $GABA_A$-mediated IPSP denotes an excitatory effect of GABA in the LA of pilocarpine-treated tissue. These changes may potentially reduce the hyperpolarizing effect of inhibitory inputs onto principal cells, bring LA neurons closer to firing threshold, and consequently facilitate epileptiform synchronization.

4.5.3 Reduced presynaptic depression of GABA release

Alterations in presynaptic release of neurotransmitters are known to contribute to hyperexcitability of different neuronal networks (Asprodini et al., 1992; Behr et al., 2002; Jarvie et al., 1990; Kamphuis et al., 1990). In this study, we employed paired-pulse stimulation protocols in the absence of glutamatergic transmission to indirectly assess whether there were any changes in the release of GABA from LA interneurons of epileptic rats. Interneuronal inputs onto pyramidal cells generally show a frequency-dependent depression (Gupta et al., 2000). A pronounced depression in the second IPSP as compared to the first would indicate that presynaptic autoreceptors are at play in controlling the release of GABA. Alternatively, additional mechanisms could include a depletion in the presynaptic vesicle pool (von Gersdoff and Borst, 2002), presynaptic metabotropic receptors (Cartmell and Schoepp, 2000) or even postsynaptic effects such as desensitization of receptors (Jones and Westbrook, 1996) and shifts in Cl- gradients (Kaila, 1994; Thompson and Gahwiler, 1989). Interestingly, we found in NEC tissue a pronounced PPD of $GABA_A$-mediated responses that was partially reduced by $GABA_B$ receptor antagonism. This evidence suggests that these G-protein linked receptors might play a role in controlling neurotransmitter release from LA interneurons (Miller, 1998).

In contrast, we found in pilocarpine-treated tissue a depression in the paired IPSP ratio that was less pronounced and less affected by $GABA_B$-receptor antagonism as compared to NEC. Altogether, these observations suggest that presynaptic $GABA_B$ receptors might be less efficient in controlling the release of GABA from LA interneurons of epileptic rodents. At first glance, these results are by themselves peculiar since less PPD in an excitatory network may imply more excitation but in an inhibitory context may mean more inhibition due to increased GABA at the synapse, specifically at high frequency stimulation. However, the reduced PPD combined with the data suggesting a depolarizing effect of GABA could conceivably lead to hyperexcitability of LA neuronal networks in epileptic tissue.

4.6 Conclusions

Until recently, most electrophysiological assessments of the amygdala and specifically of the BLA were carried out in coronal slices in which connections with other limbic structures are not maintained (Gean et al., 1989; Mangan et al., 2000; Rainnie et al., 1992; Shoji et al., 1998; Smith and Dudek, 1997). However, the advent of the combined horizontal slice preparation (Stoop and Pralong, 2000; von Bohlen und Halbach and Albrecht, 2002) has enabled evaluation of the amygdala's participation in intralimbic synchronization of epileptiform activity (Benini et al., 2003; Kleuva et al., 2003; Stoop and Pralong, 2000). The LA is heavily interconnected with hippocampal and parahippocampal structures that are highly implicated in TLE and it would be of crucial importance to determine what significance the alterations presented in our study have on the interactions of the LA with other structures like the perirhinal and entorhinal cortices.

4.7 Tables:

Table 4-1:

Intrinsic and regular firing properties of LA neurons in non-epileptic control (NEC) and pilocarpine-treated rats

	NEC (n=46)	Pilocarpine (n=68)
RMP (mV)	-70.7 ± 1.0	-71.9 ± 0.9
Ri (MΩ)	46.6 ± 1.3	47.7 ± 1.2
APA (mV)	98.5 ± 1.3	99.3 ± 0.9
APD (ms)	1.5 ± 0.03	1.6 ± 0.03
AR*	9.1 ± 1.8	13.5 ± 3.0

RMP, resting membrane potential; Ri, input resistance; APA, action potential amplitude; APD, action potential duration at half amplitude; AR, adaptation ratio. *AR values were calculated for n=30 cells from each group. Data are provided as mean ± SEM.

Table 4-2:

Spontaneous synaptic activity recorded at rest from LA neurons in non-epileptic control (NEC) and pilocarpine-treated rats

	NEC	Pilocarpine
Spontaneous Bursting Activity*		*(n=14)*
Duration (ms)	–	786 ± 514
Rate of occurrence (s)	–	13.1 ± 10.7
Depolarizing PSPs	*(n=26)*	*(n=33)*
Amplitude (mV)	1.71 ± 0.03	**2.73 ± 0.05
Rate of occurrence (s)	0.72 ± 0.04	1.02 ± 0.07
Hyperpolarizing PSPs	*(n=14)*	*(n=16)*
Amplitude (mV)	-3.4 ± 0.2	-3.0 ± 0.1
Rate of occurrence (s)	18.0 ± 5.0	22.0 ± 4.0

Data are provided as mean ± SEM. n represents number of neurons.
*These events were only observed in a subset of pilocarpine-treated tissue but never in NEC.
**Indicates values significantly different ($p < 0.05$) from NEC.

4.8 Figures:

Figure 4-1:

Slice preparation and sites of recording. A: Diagram of typical combined horizontal slice preparation illustrating the position of the field (fd), intracellular (in) and stimulating (stim) electrodes placed within the lateral amygdala (LA) and perirhinal cortex (PC). **B**: Neurobiotin-staining identifies stellate (**a**), bipolar (**b**) and pyramidal-like (**c**) cells in pilocarpine-treated tissue. The respective firing properties of these cells are illustrated in C (**a-c**). Note that LA neurons show a range of spike frequency adaptation. The magnitude of the current pulses injected include -1.0, 0, and +0.6 nA in **a** and -1.0, 0, and +0.8 nA in both **b** and **c**.

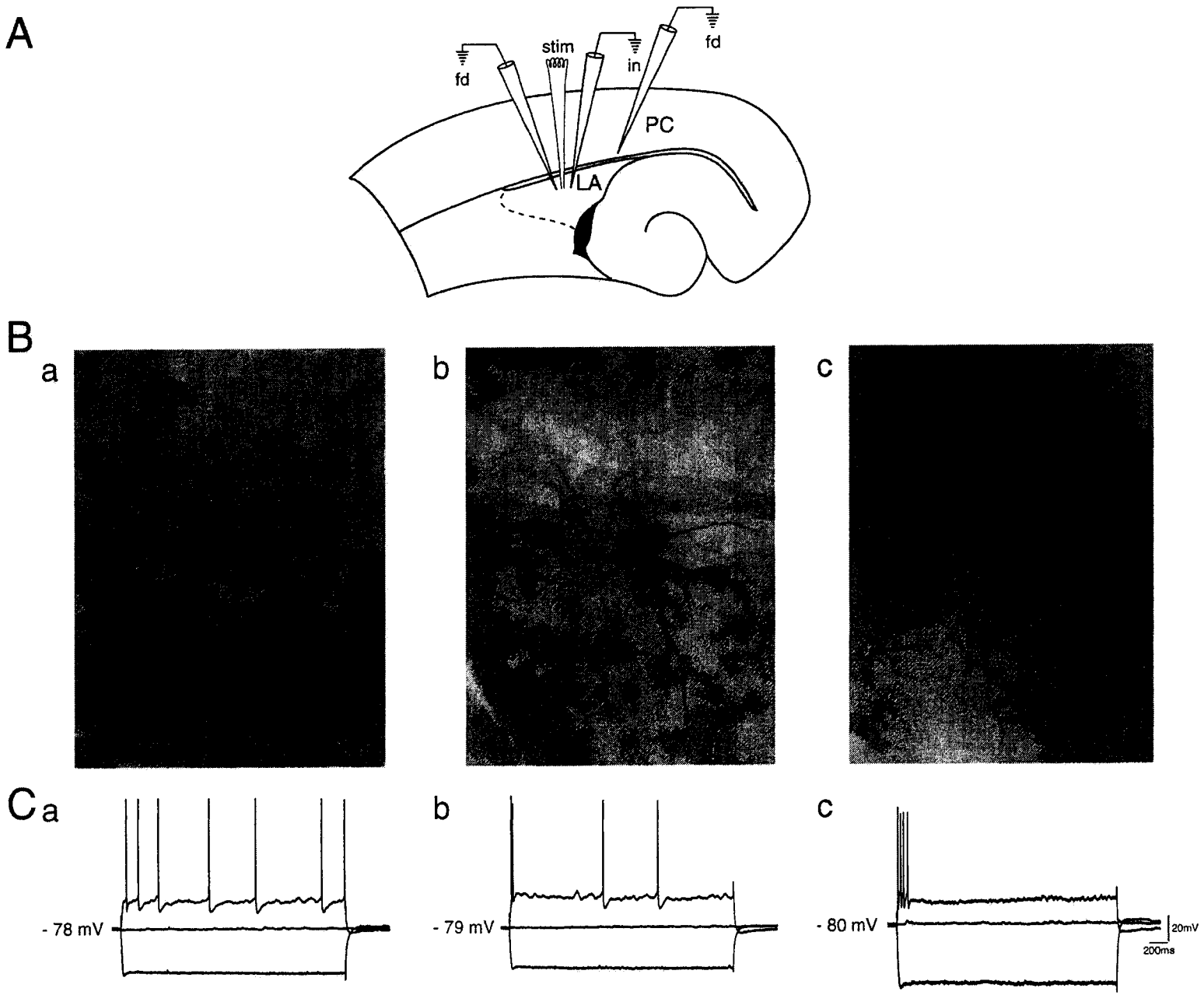
A
fd
stim
in
fd
PC
LA
B
a
b
c
C a
b
c
- 78 mV
- 79 mV
- 80 mV
20mV
200ms

Figure 4-2:

Spontaneous synaptic activity in NEC and Pilocarpine-treated tissue. **A**: **(a)** Simultaneous field (LA_f, deep perirhinal cortex (PC_f)) and intracellular recording (-72 mV) in NEC tissue reveals (i) depolarizing postsynaptic potentials (PSPs) indicated by arrows and (ii) robust spontaneous hyperpolarizing inhibitory postsynaptic potentials (sIPSP) indicated by asterix. **(b)** Spontaneous synaptic activity recorded during depolarization and hyperpolarization of the membrane potential by steady current injection of +0.2, +0.1, -0.1 and -0.2 nA (from top to bottom trace respectively). Note the larger amplitude and biphasic nature of sIPSPs at more depolarized levels (-61 mV to -76 mV). **B**: Simultaneous field (LA_f, PC_f) and intracellular activity (-76 mV) recorded in the majority of pilocarpine-treated tissue. Note the absence of field activity (LA_f, PC_f) and the presence of large depolarizing postsynaptic potentials (PSPs) indicated by arrows in the intracellular trace. Expansion of these events is depicted in the right upper insert. **C**: **(a)** Simultaneous field (LA_f, PC_f) and intracellular activity (-60 mV) recorded in a subset of pilocarpine-treated slices reveals robust network activity (LAf, PCf). Expansion of an event demonstrates initiation in LA (arrow) and spread to PC (right upper insert). **(b)** Steady hyperpolarization and depolarization of the membrane potential with current injections of +0.2, -0.2 and -0.8 nA (from top to bottom trace respectively) alters the amplitude of the underlying EPSP (arrow) thereby confirming the synaptic nature of the event.

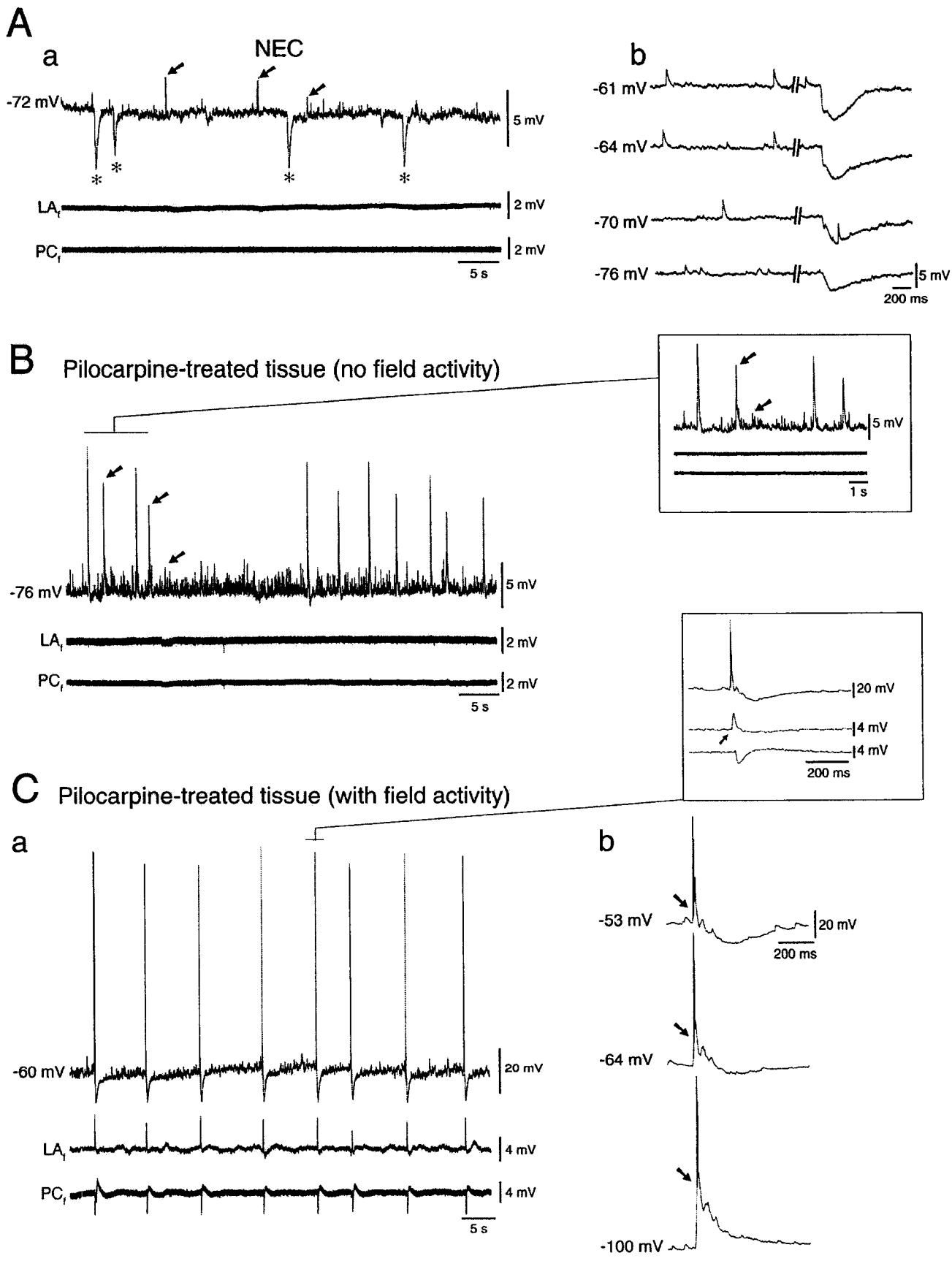
A
a
NEC
-72 mV
5 mV
LA$_f$
2 mV
PC$_f$
2 mV
5 s
b
-61 mV
-64 mV
-70 mV
-76 mV
5 mV
200 ms
B
Pilocarpine-treated tissue (no field activity)
5 mV
1 s
-76 mV
5 mV
LA$_f$
2 mV
PC$_f$
2 mV
5 s
20 mV
4 mV
4 mV
200 ms
C
Pilocarpine-treated tissue (with field activity)
a
b
-53 mV
20 mV
200 ms
-64 mV
-100 mV
-60 mV
20 mV
LA$_f$
4 mV
PC$_f$
4 mV
5 s

Figure 4-3:

Distribution and pharmacology of spontaneous activity. **A**: Distribution histogram of the amplitude of depolarizing PSP events pooled from pilocarpine-treated (n=33 neurons, 1000 events) and NEC (n= 26 neurons, 1000 events) groups at resting levels. Note that in pilocarpine-treated tissue these events distribute at higher amplitudes. **B**: Histogram comparing the incidence of hyperpolarizing sIPSPs in NEC (n=47 cells) versus pilocarpine-treated tissue (n=68 cells) at resting levels (RMP) and more depolarized membrane potentials (Depolarized MP). Note the lower incidence of sIPSPs in pilocarpine-treated tissue. **C**: Bath application of glutamatergic antagonists (+CPP+CNQX) to NEC tissue abolishes depolarizing PSPs but does not affect sIPSPs. Lower inserts depict expansion of sIPSP events. **D**: (**a**) In pilocarpine-treated tissue exhibiting field activity in LA (Control), bath application of glutamatergic antagonists (+CPP+CNQX) abolishes spontaneously-occurring network bursting (expansion in lower left trace) and uncovers biphasic sIPSPs (expansion in right lower insert). (**b**) Depolarizing the membrane to -56 mV with a steady current injection of +0.5 nA increases the amplitude of these sIPSPs.

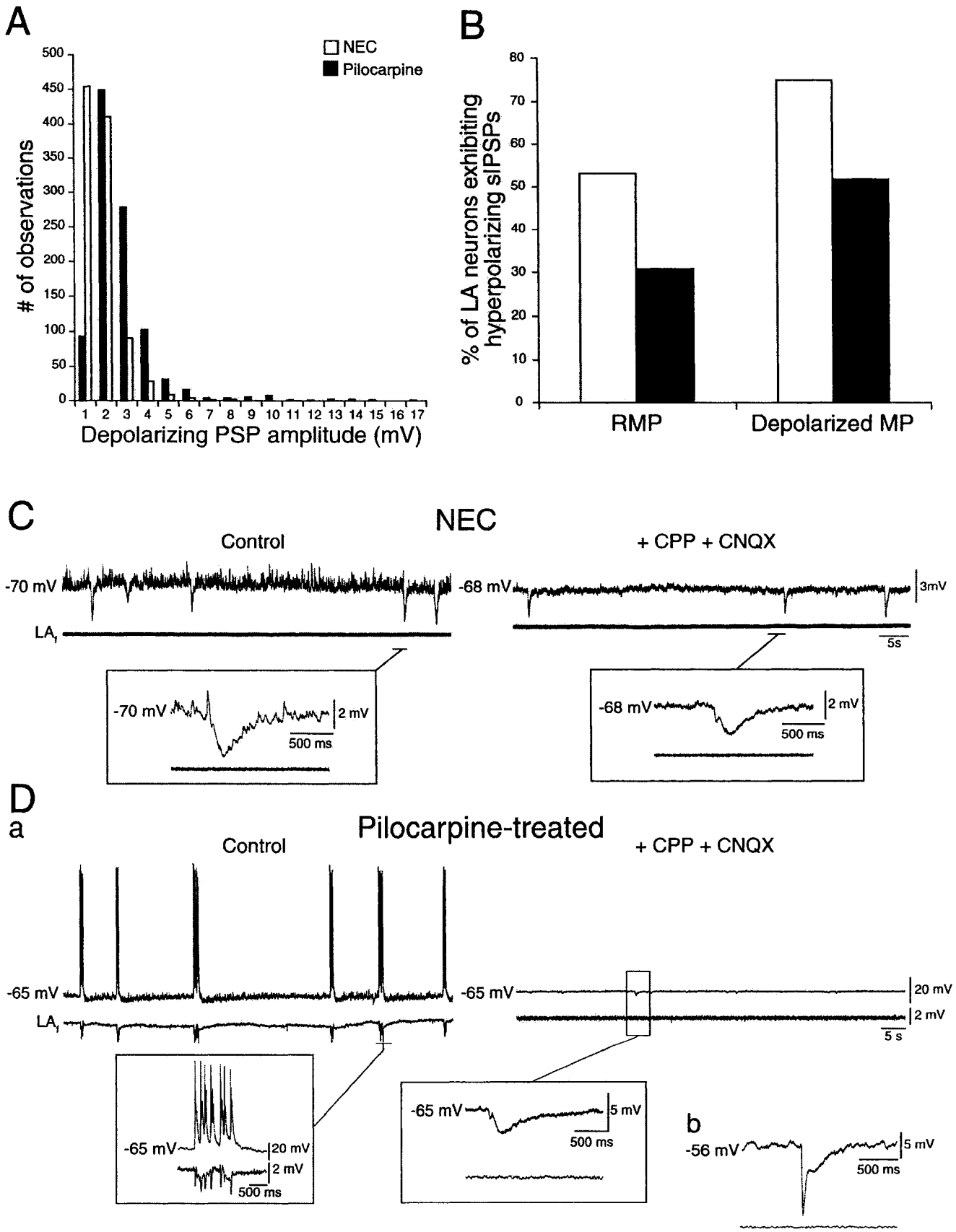
A
NEC
Pilocarpine
# of observations
Depolarizing PSP amplitude (mV)
B
% of LA neurons exhibiting hyperpolarizing sIPSPs
RMP
Depolarized MP
C
NEC
Control
+ CPP + CNQX
-70 mV
-68 mV
LA
2 mV
500 ms
3mV
5s
D
a
Pilocarpine-treated
Control
+ CPP + CNQX
-65 mV
20 mV
5 mV
5 s
b
-56 mV

Figure 4-4:

$GABA_A$-mediated component of evoked IPSP in Pilocarpine-treated tissue exhibits a more depolarized reversal potential and a smaller peak conductance. **A**: Comparison of the monosynaptic IPSPs evoked in the presence of CPP+CNQX in NEC and pilocarpine-treated tissue at membrane potentials set to different levels by intracellular current injection (-0.6 to +0.6nA in NEC and -0.8 to +0.6 nA in Pilocarpine-treated). Note the biphasic nature of these IPSPs (Early and Late components). Also note that the reversal potential of the early component (arrow) is more depolarized in NEC versus pilocarpine-treated tissue. Triangles indicate stimulus artifact. **B**: Histogram comparing reversal potential of both early and late IPSP components in NEC versus pilocarpine-treated group. Asterix indicates significance at $p<0.002$. **C**: Histogram comparing peak conductance of both early and late IPSP components in NEC versus pilocarpine-treated group. Asterix indicates significance at $p<0.05$; n represents number of neurons. Error bars: means±SEM.

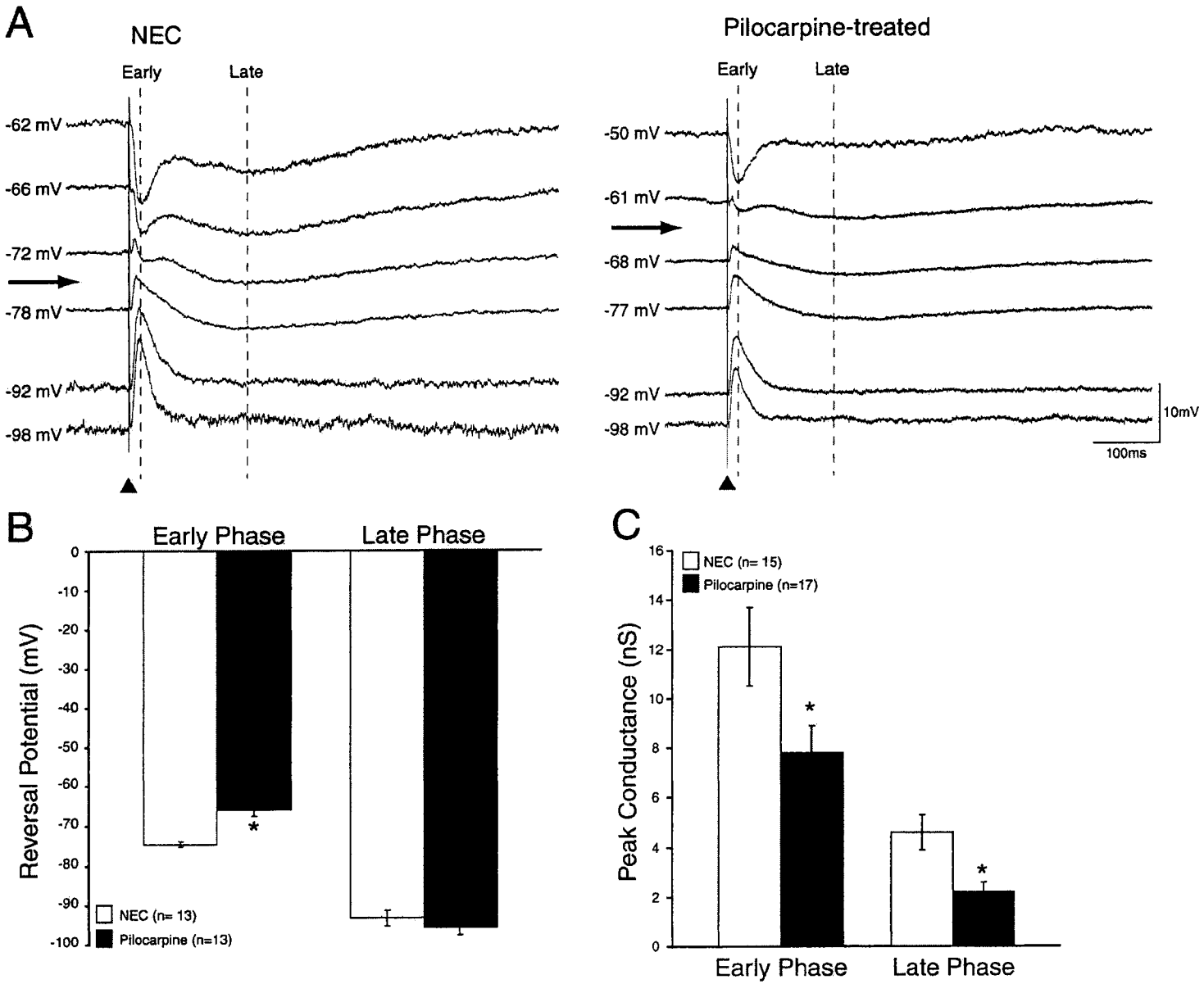
A
NEC
Early
Late
-62 mV
-66 mV
-72 mV
-78 mV
-92 mV
-98 mV
Pilocarpine-treated
Early
Late
-50 mV
-61 mV
-68 mV
-77 mV
-92 mV
-98 mV
10mV
100ms
B
Early Phase
Late Phase
Reversal Potential (mV)
0
-10
-20
-30
-40
-50
-60
-70
-80
-90
-100
NEC (n= 13)
Pilocarpine (n=13)
C
NEC (n= 15)
Pilocarpine (n=17)
Peak Conductance (nS)
16
14
12
10
8
6
4
2
0
Early Phase
Late Phase

Figure 4-5:

Pilocarpine-treated tissue exhibits a less pronounced paired-pulse depression of 'monosynaptically'-evoked IPSP. **A**: Intracellular recording from a hyperpolarized LA neuron (-105 mV, -0.4 nA injected current) in NEC tissue showing paired IPSPs (P1 and P2) at interstimulus intervals of (**a**) 200 ms and (**b**) 600 ms. Note marked depression of P2 relative to P1 at both intervals. **B**: Intracellular recording from a hyperpolarized LA cell (-102 mV, -0.8 nA injected current) in pilocarpine-treated tissue showing paired IPSPs (P1 and P2) at interstimulus intervals of (**a**) 200 ms and (**b**) 600 ms. Note that at both intervals, there is less paired-pulse depression of the second response with respect to the first. **C**: Plot of P2/P1 ratios for interstimulus intervals between 50 ms and 1600 ms. Note that pilocarpine-treated tissue exhibits less PPD than NEC. Asterix indicate interstimulus intervals at which the two groups were significantly different from each other ($p < 0.05$). **D**: Effect of CGP 55845A on the normalized P2/P1 ratio in NEC (n=6) and pilocarpine-treated tissue (n=3). Note the less pronounced effect of $GABA_B$ receptor antagonism in the pilocarpine-treated group (p=0.05). n represents number of neurons. Error bars: means±SEM.

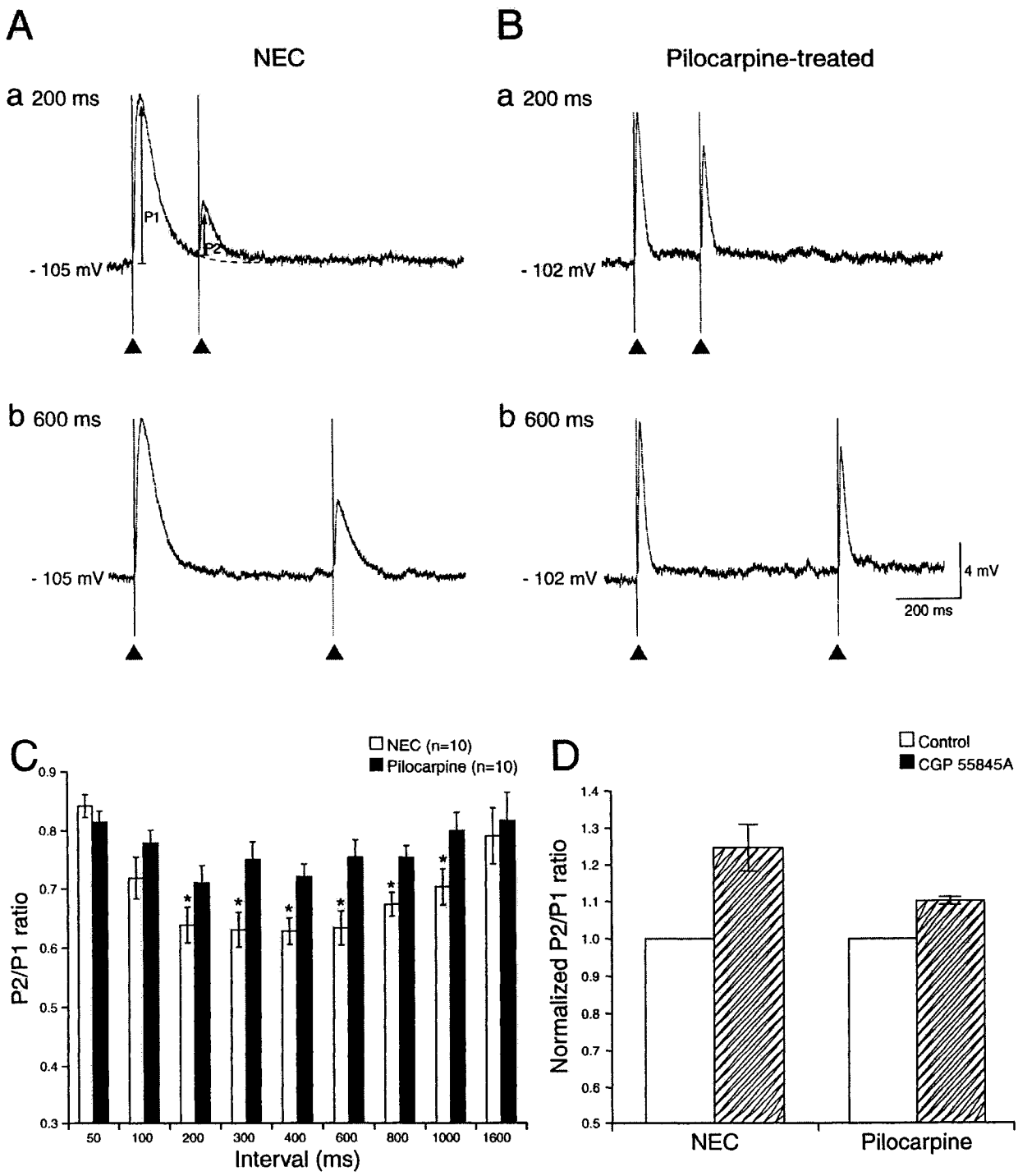
A
NEC
a 200 ms
P1
P2
- 105 mV
b 600 ms
- 105 mV
B
Pilocarpine-treated
a 200 ms
- 102 mV
b 600 ms
- 102 mV
4 mV
200 ms
C
NEC (n=10)
Pilocarpine (n=10)
P2/P1 ratio
0.9
0.8
0.7
0.6
0.5
0.4
0.3
50
100
200
300
400
600
800
1000
1600
Interval (ms)
D
Control
CGP 55845A
Normalized P2/P1 ratio
1.4
1.3
1.2
1.1
1.0
0.9
0.8
0.7
0.6
0.5
NEC
Pilocarpine

Chapter 5: Electrophysiology of Deep Layer Perirhinal Cortex in a Model of Temporal Lobe Epilepsy

5.0 Linking Text

Using the pilocarpine model of TLE, I reported in *Chapter 4* that alterations at the level of GABAergic signalling contribute to LA network hyperexcitability in chronically epileptic rats. The next step in my investigations was to determine whether these modifications could affect the interactions of the LA with other limbic structures such as the perirhinal cortex (PC), a structure that has also been implicated in TLE.

Despite the elaborate information presented from kindling studies, electrophysiological assessment of the PC in chronically epileptic animals remains sparse. Thus, prior to addressing the question of how LA-PC interactions are altered in TLE, we decided it was more appropriate to first assess the changes that occur within the PC in pilocarpine-treated rats. The findings obtained from such an electrophysiological study in chronically epileptic rats are presented in this final *Chapter 5*, where data suggesting altered LA-PC interactions are shown. *Chapter 5* represents a manuscript in preparation entitled *"Electrophysiology of deep layer perirhinal cortex in a model of temporal lobe epilepsy"* (Authors: **Benini R** and Avoli M).

5.1 Abstract

The perirhinal cortex (PC) may play an important role in the generation and spread of seizures. Here, we used simultaneous field and intracellular recordings from horizontal brain slices obtained from pilocarpine-treated rats and age-matched non-epileptic controls (NEC) to shed light on the electrophysiological changes that occur within the deep layers of the PC. No significant differences in PC neuronal intrinsic properties were observed between pilocarpine-treated and NEC tissue. We could identify in PC neurons spontaneous depolarizing and hyperpolarizing postsynaptic potentials that were not significantly different in duration and amplitude between the two experimental groups. However, spontaneous field activity could be recorded in the PC of 21% of pilocarpine-treated slices but never from NECs. At the intracellular level,

this network activity was characterized by robust neuronal firing that was sensitive to glutamatergic antagonists. In the absence of glutamatergic transmission, PC neurons in both NEC and pilocarpine-treated tissue generated biphasic IPSPs in response to single-shock stimulation of local networks. The reversal potential of the early $GABA_A$-receptor mediated component, but not of the late $GABA_B$-receptor mediated component, was significantly more depolarized in pilocarpine-treated slices. Finally, stimulation of LA networks revealed that LA inputs onto deep PC cells are predominantly inhibitory in nature in NEC tissue but become more excitatory in chronically epileptic rats. Altogether, these preliminary findings suggest that deep layer PC networks are hyperexcitable in a subset of tissue obtained from chronically epileptic rats where alterations in LA-PC interactions also occur.

5.2 Introduction

As a result of the surging interest in identifying the functions played by extrahippocampal structures in temporal lobe epilepsy (TLE), an important role for the parahippocampal cortices, including the perirhinal cortex (PC), has been recognized (Avoli et al., 2002). Accordingly, magnetic resonance imaging studies have revealed that volumetric reductions occur within the PC of TLE patients (Bernasconi et al., 2000, 2003; Keller et al., 2004). Furthermore, evidence from experimental epilepsy has demonstrated that not only is the PC the most easily kindled structure within the mammalian forebrain (McIntyre et al., 1993; McIntyre and Plant, 1989, 1993), but that it is also more likely to generate electrographic seizures in vitro than adjacent limbic structures such as the entorhinal cortex (EC), hippocampus or amygdala (de Guzman et al., 2004; Kleuva et al., 2003). Moreover, a pivotal role for this cortical region in the generalization of seizures has also been presented (Holmes et al., 1992; Kelly and McIntyre, 1996; McIntyre and Kelly, 2000).

Despite these findings, extensive histological and electrophysiological assessment of the PC in chronically epileptic animals is still lacking. Although damage to the deep PC has been documented in pilocarpine-treated rodents (Covolan and Mello, 2000), the implications of these alterations to PC network excitability and ultimately to limbic network synchronization still needs to be determined. Thus, the

aim of our study was to use an electrophysiological approach to assess the intrinsic and network changes that occur within the deep layers of the PC in epileptic rats by using the pilocarpine chronic animal model of TLE. Furthermore, since the PC is known to be extensively interconnected with the amygdaloid complex via the lateral nucleus (LA) (Burwell and Witter, 2002; Suzuki and Amaral, 1994a,b), we also sought to identify whether there were any changes in the interactions between these two limbic structures in chronically epileptic rats. This latter question might be relevant to understanding the spread of limbic seizures across temporal lobe structures specifically since it has recently been reported that under conditions of reduced inhibition, LA inputs can promote the spread of activity from the PC to the EC and hippocampus (Kajiwara et al., 2003).

5.3 Methods

Animal preparation - Procedures approved by the Canadian Council of Animal Care were used to induce status epilepticus (SE) in adult male Sprague-Dawley rats weighing 150-200g at the time of injection. All efforts were made to minimize the number of animals used and their suffering. Briefly, rats were injected with a single dose of pilocarpine hydrochloride (380-400mg/Kg, i.p). In order to reduce the discomforts caused by peripheral activation of muscarinic receptors, methyl scopolamine (1mg/Kg i.p) was administered 30 min prior to the pilocarpine injection. The animals' behaviour was monitored for approx. 4 h following pilocarpine and scored according to Racine's classification (Racine et al., 1972b). Only rats that experienced SE (stage 3-5) for 30 minutes or more (48±6 min, mean±SEM; n=21 rats) were included in the pilocarpine group and used for in vitro electrophysiological studies approximately 4 months (17±1week; n=21 rats) following the pilocarpine injection. The presence of spontaneous behavioural seizures was confirmed with video-monitoring in a subset of pilocarpine-treated rats (n= 14). In this study, rats receiving a saline injection instead of pilocarpine were used as age-matched nonepileptic controls (NEC).

Slice preparation and maintenance - Adult rats were decapitated under halothane anesthesia; the brain was quickly removed and a block of brain tissue containing the

retrohippocampal region was placed in cold (1-3 °C), oxygenated artificial cerebrospinal fluid (ACSF). The brain dorsal side was cut along a horizontal plane that was tilted by a 10° angle along a postero-superior-anteroinferior plane passing between the lateral olfactory tract and the base of the brain stem (Benini et al., 2003). Horizontal slices (400-450 μm thick) were cut from this brain block using a vibratome and slices were then transferred into a tissue chamber where they lay at the interface between ACSF and humidified gas (95% O_2, 5% CO_2) at a temperature of 34-35 °C and a pH of 7.4. We focused in this study on the most ventral slices that were comprised between -8.6mm to -7.6mm from the bregma (Paxinos and Watson, 1998). These slices contained the hippocampus proper, the parahippocampal cortices as well as the lateral nucleus of the amygdala (LA) (Fig. 4-1A). Two to three of such slices could be obtained from each hemisphere. ACSF composition was (in mM): NaCl 124, KCl 2, KH_2PO_4 1.25, $MgSO_4$ 2, $CaCl_2$ 2, $NaHCO_3$ 26, and glucose 10. (2S)-3-[[(1S)-1-(3,4-Dichlorophenyl)ethyl]amino-2-hydroxypropyl](phenylmethyl) phosphinic acid (CGP 55845A, 10μM), 6-cyano-7-nitroquinoxaline-2,3-dione (CNQX, 10μM), 3,3-(2-carboxypiperazin-4-yl)-propyl-1-phosphonate (CPP, 10μM), and picrotoxin (PTX, 50uM) were applied to the bath. Chemicals were acquired from Sigma (St. Louis, MO, USA) with the exception of CGP 55845A, CNQX and CPP that were obtained from Tocris Cookson (Ellisville, MO, USA).

Electrophysiological recordings and stimulation protocols - Field potential recordings were made from the deep layers of the perirhinal cortex (PC) and the lateral nucleus of the amygdala (LA) with ACSF-filled, glass pipettes (resistance=2-10 MΩ) that were connected to high-impedance amplifiers. Sharp-electrode intracellular recordings were performed in PC with pipettes that were filled with 3M K-acetate (tip resistance= 70-120 MΩ in both cases). Intracellular signals were fed to a high-impedance amplifier with internal bridge circuit for intracellular current injection. The resistance compensation was monitored throughout the experiment and adjusted as required. The passive membrane properties of PC cells included in this study were measured as follows: (i) resting membrane potential (RMP) after cell withdrawal; (ii) apparent input resistance (Ri) from the maximum voltage change in response to a

hyperpolarizing current pulse (100-200 ms, <-0.6 nA); (iii) action potential amplitude (APA) from the baseline and (iv) action potential duration (APD) at half-amplitude. Intrinsic firing patterns of PC cells were classified from responses to depolarizing current pulses of 1000-2500 ms duration.

Synaptic responses of PC networks to local single shock stimulation or stimulation of LA (100 μs; <350 μA) was assessed using a bipolar, stainless steel electrode placed < 500 μm from the recording electrodes. "Monosynaptic" IPSPs were evoked in the presence of glutamatergic antagonists (10μM CPP and 10μM CNQX). Reversal potential and peak conductance values for the early and late components of the IPSPs were obtained from a series of responses evoked at membrane potentials set to different levels by intracellular current injection. Reversal potentials were computed from regression plots of amplitude of response vs membrane potential. Peak conductance values on the other hand were estimated using the parallel conductance model (cf. Williams et al., 1993). Briefly, the membrane potential vs intensity of injected current was plotted before the stimulation and at the peak of the IPSP response. The slopes of these regression lines were then used to yield the input resistance at rest (i.e. before the stimulation) and during the response respectively, and to ultimately determine the change in resistance that occurred during the IPSP (ΔR_{IPSP}). ΔR_{IPSP} was then translated to peak conductance changes (ΔG_{IPSP}) using the formula: $\Delta G_{IPSP} = 1/\Delta R_{IPSP}$.

Field potential and intracellular signals were fed to a computer interface (Digidata 1322A, Axon Instruments) and were acquired and stored using the pClamp 9 software (Axon Instruments). Subsequent data analysis was made with the Clampfit 9 software (Axon Instruments). For time-delay measurements, the onset of the field potential/intracellular signals was determined as the time of the earliest deflection of the baseline recording (e.g., insert trace in Fig. 5-1Ca). Measurements in the text are expressed as mean±SEM and n indicates the number of slices or neurons studied under each specific protocol. Data were compared with the Student's t-test and were considered statistically significant if $p<0.05$.

5.4 Results

5.4.1 Intrinsic electrophysiological properties of deep PC neurons

Simultaneous field and intracellular recordings were carried out in the deep perirhinal cortex (PC) of brain slices obtained from pilocarpine-treated rats (n= 63 cells from 47 slices) and age-matched non-epileptic controls (NECs) (n=29 cells from 26 slices). As reported by other groups (D'Antuono et al., 2001; Faulkner and Brown 1999; Martina et al., 2001), neurons from this PC layer could be characterized either as 'bursting' or 'regular firing' depending on their responses to intracellular depolarizing pulses. Whereas bursting neurons exhibited a high-frequency burst of action potentials (APs) at the beginning of the pulse, regular spiking cells on the other hand fired APs throughout the pulse at different spike adaptations (Fig. 5-1Ab, Bb, Cb). Both intrinsically bursting and regular firing neurons could be observed in the pilocarpine-treated and NEC groups (Table 5-1). No fast spiking interneurons were ever recorded in this study.

Comparison of RMP, Ri, APD and APA revealed no significant differences between the NEC and pilocarpine-treated groups thereby suggesting that the intrinsic properties of PC cells were unchanged in chronically epileptic rats (Table 5-1).

5.4.2 Spontaneous synaptic activity in the PC of pilocarpine-treated rats is altered

Simultaneous field potential recordings obtained from the PC and LA during bath application of normal ACSF demonstrated the absence of any spontaneous activity in NEC slices (n= 18) (Fig. 5-1Aa, bottom field traces). When analyzed with intracellular recordings, all neurons from this group exhibited at RMP depolarizing postsynaptic potentials (PSPs) with amplitudes of 1.6±0.1 mV and interval of occurrence of 2.4±0.4 s (n=19) (Fig. 5-1Aa, arrows) (Table 5-2). In addition, spontaneous hyperpolarizing PSPs (sIPSPs) (amplitude: -2.9±0.5 mV; interval of occurrence: 11.5±1.8 s) could be recorded in 58% of PC neurons (n=11/19 cells) (Fig. 5-1Aa, asterix, insert) (Table 5-2). Steady hyperpolarization and depolarization of the membrane potential altered the amplitude of these two types of spontaneous activities without influencing their rate of occurrence, thereby confirming their synaptic nature (not shown).

Based on the pattern of spontaneous field activity, pilocarpine-treated tissue could be divided into two main groups. In the first set, which constituted the majority of slices (n=37/47) and were classified as "Pilocarpine (no field activity)", no spontaneous field events could ever be detected in either the PC or LA (Fig. 5-1Ba, Pilocarpine (no field activity)). As in NEC, neurons recorded intracellularly from these pilocarpine-treated slices exhibited spontaneous depolarizing PSPs (amplitudes= 1.8±0.1 mV; interval of occurrence= 1.02±0.07 s; n=21; Fig. 5-1Ba, arrows, insert) and could at times display sIPSPs at RMP (amplitude: -3.6±0.6 mV; interval of occurrence: 28.6±6.9 s, n= 6/21 neurons) (Table 5-2). The amplitudes and rates of occurrence of both the depolarizing PSPs and sIPSPs were not statistically different between NEC tissue and this pilocarpine-treated group (Table 5-2).

In the second group of pilocarpine-treated tissue, classified as "Pilocarpine (with field activity)", spontaneous field events could be recorded in the PC (n=10 slices, 15 neurons) (Fig. 5-1Ca, bottom field traces). Analysis of field events at different recording sites revealed that these discharges could initiate in the deep layers and subsequently spread to the middle and superficial layers of the PC as well as to the LA (Fig. 5-1Ca, insert, arrow; n=5 slices). Intracellularly, this network activity corresponded to robust neuronal firing at RMP (duration: 1199±315 ms; interval of occurrence: 39.2±15.2 s; n=15 cells) interspaced by depolarizing PSPs (amplitude: 2.0±0.2 mV; interval of occurrence: 2.0±0.2 s; n=15 cells) (Table 5-1). sIPSPs could also be recorded in a subset of these cells (n=7/15 cells).

Altogether, these results suggest that increased PC network excitability resulting in the generation of robust epileptiform-like activity characterizes a subset of slices obtained from pilocarpine-treated rats.

5.4.3 Pharmacology of spontaneous synaptic activity in deep layer PC cells

In order to assess the contribution of glutamatergic transmission to the three types of spontaneous synaptic activity recorded intracellularly, NMDA- and non-NMDA receptor antagonists (CPP and CNQX respectively) were employed.

Bath application of both CPP and CNQX completely abolished the spontaneous depolarizing PSPs in NEC (n=6) and pilocarpine-treated tissue (n=9). In pilocarpine-treated slices (with field activity), the spontaneous bursting events associated with field activity were reduced in duration (926±64 ms to 120±39 ms; n=3 cells) by application of CPP only and completely abolished with further application of CNQX (n=4). Finally, sIPSPs were found to be resistant to glutamatergic antagonists in both NEC (n=6) and pilocarpine-treated cells (n=7), thereby suggesting that they were presumably mediated by GABAergic receptors.

5.4.4 Stimulus-evoked responses of PC neurons

Response of PC neurons to single-shock stimulation was investigated with the help of a bipolar stimulating electrode placed within 500 μm from the recording electrode. In NEC slices, responses to stimulation of local PC networks resulted primarily in sequential EPSP-IPSP responses (n=10/12; Fig. 5-2Aa, NEC, insert) and at higher stimulation intensities were characterized by single AP firing (Fig. 5-2Aa, NEC). Pure subthreshold EPSP responses could also be recorded in some cells (n=2/11, not shown). Bath application of CPP/CNQX abolished the EPSP and AP component of the evoked PC response and disclosed a biphasic IPSP (Fig. 5-2Ba).

Similar responses could be recorded in pilocarpine-treated tissue with no field activity (n= 21; Fig. 5-2Ab, Bb, Pilocarpine (no field activity)). As in the case of NEC cells (Fig. 5-2Aa), both EPSP (n= 8/21, not shown) and EPSP-IPSP (13/21, Fig. 5-2Ab, insert) responses could be recorded in PC cells at subthreshold stimulation intensities. In pilocarpine-treated slices with field activity however, single shock stimulation could elicit only pure EPSP responses in PC cells (Fig. 5-2Ac, Pilocarpine (with field activity), insert) and at higher stimulation intensities resulted in longer duration discharges characterized by robust APs riding on depolarizing envelopes (Fig. 5-2Ac, Pilocarpine (with field activity); n= 6/6). CPP reduced the duration of these afterdischarges (n=3, not shown), whilst further application of CNQX revealed an underlying IPSP (Fig. 5-2Bc, +CPP+CNQX; n=3).

Altogether, stimulation of local PC networks demonstrates that pilocarpine-treated tissue was more likely to generate in this structure epileptiform-like activity

that was dependent on glutamatergic transmission. Interestingly, the exposure of an underlying IPSP during bath application of glutamatergic antagonists suggests that this increased excitability of PC cells was not due to the absence of inhibitory inputs.

5.4.5 Evoked "monosynaptic" IPSP responses of PC neurons

To isolate and assess the activity of local inhibitory networks within the PC of NEC and pilocarpine-treated rats, we analyzed the intracellular responses of LA neurons to single-shock stimulation in the presence of glutamatergic antagonists (CPP+CNQX). In the presence of CPP+CNQX, pure biphasic IPSP responses could be elicited in both NEC (n= 9) and pilocarpine-treated tissue (n=12) (Fig. 5-3A). The early phase of this evoked IPSP was greatly reduced by the $GABA_A$ receptor antagonist picrotoxin (n=6) whereas the late phase was sensitive to CGP 88485A, a $GABA_B$ receptor antagonist (n= 3). Quantitative comparison of these "monosynaptically-evoked" IPSPs revealed that the reversal potential of the early $GABA_A$-receptor mediated component, but not of the late $GABA_B$-receptor mediated component, was more depolarized ($p< 0.05$) in pilocarpine-treated tissue (-69.6±1.0 mV, n= 12) as compared with NEC (-74.9±1.7 mV, n= 9) (Table 5-3, Fig. 5-3B). No differences in the peak conductance of both the early and late IPSP components were observed between the two groups (Table 5-3, Fig. 5-3C).

5.4.6 Evidence for altered LA-PC interactions

Previous investigations carried out in our laboratory suggested that changes in network excitability do occur in the LA of chronically epileptic rats (Benini and Avoli, 2005). Since the LA is reciprocally interconnected with the PC, we sought to examine whether PC responses to stimulation of LA networks were altered in pilocarpine-treated rats.

To study this, responses of deep PC neurons to LA stimulation was compared in NEC and pilocarpine-treated tissue. Briefly, single shock stimulation of LA networks in NEC slices resulted in pure IPSP responses in PC neurons (Fig. 5-4, NEC; Table 5; n=8/8). The IPSP response was found to be abolished by application of CPP/CNQX (n=3). Single-shock stimulation applied at high frequencies (1Hz-10Hz) did not attenuate these responses (n= 5).

Interestingly, LA-induced synaptic responses of PC neurons in pilocarpine-treated tissue were somewhat different. In pilocarpine tissue (no field activity), LA stimulation could elicit (i) a pure EPSP response (n=2/11, not shown), (ii) an EPSP-IPSP response (Fig. 5-4, Pilocarpine (no field activity); n=4/11) as well as (iii) a pure IPSP response (n=5/11, not shown). Furthermore, in pilocarpine tissue (with field activity), stimulation of LA networks resulted in robust burst discharges in the PC (n=5/5), which at more depolarized levels appeared to be preceded by a hyperpolarizing component (Fig. 5-4, Pilocarpine (with field activity), -54 mV trace, asterix).

Altogether, these results suggest that whereas in NEC tissue LA inputs to deep PC cells are predominantly inhibitory in nature they become more excitatory in chronically epileptic rats.

5.5 Discussion

In this study, we sought to identify the functional changes that occur within the deep PC using the pilocarpine rodent model of TLE. The results obtained demonstrate that the intrinsic properties of PC neurons are not altered in chronically epileptic rats. Furthermore, the expression of spontaneous synaptic potentials (both depolarizing and hyperpolarizing) was not significantly different between the two experimental groups. However, in contrast to NEC, a subset of slices from the pilocarpine group displayed intense network bursting within the PC and responded with robust epileptiform-like discharges to local network stimulation. Furthermore, alteration in $GABA_A$-receptor mediated mechanisms was also evident in pilocarpine-treated tissue. Finally, evidence for a shift from inhibitory to excitatory responses of PC cells to stimulation of LA inputs was also demonstrated in tissue obtained from chronically epileptic rats.

5.5.1 Evidence for hyperexcitability of PC networks

In vitro investigations carried out in brain slices made epileptogenic by pharmacological treatment with convulsants have demonstrated that PC circuitry is more likely to initiate seizure-like discharges than adjacent structures such as the amygdala, piriform cortex and EC (de Guzman et al., 2004; Kleuva et al., 2003; McIntyre and Plant, 1993). This propensity of the PC to develop and sustain

epileptiform activity is further collaborated by studies demonstrating that PC kindling occurs much faster and results in an earlier generalization of seizures than kindling of the amygdala, hippocampus and piriform cortex (McIntyre et al., 1993; McIntyre and Plant, 1989, 1993). Moreover, in addition to it being the most easily kindled structure within the mammalian forebrain, a pivotal role for the PC in the generalization of seizures has also been presented. For example, whereas local application of an NMDA receptor antagonist to the PC/insular cortex has been demonstrated to block amygdala-kindled seizures in rats (Holmes et al., 1992), lesional studies have suggested that the PC is required for the generation of hippocampal motor seizures (Kelly and McIntyre, 1996; McIntyre and Kelly, 2000). Altogether, these investigations strongly suggest that the PC plays an important role in the initiation and spread of seizures. In accordance with these reports, we demonstrate here the presence of glutamate-mediated spontaneous bursting activity within the deep PC in a subset of brain slices obtained from chronically epileptic rats.

Recent data suggests that intrinsic inhibitory networks within the PC and EC confer these structures with the ability to actively gate signal transmission between the neocortex and the hippocampus (Biella et al., 2002; de Curtis and Pare, 2004; Pelletier et al., 2004). Conceivably, this propensity of the rhinal cortices to control the propagation of neural activity might be highly relevant to understanding the spread of epileptiform activity within the limbic system. Moreover, it raises the interesting question as to whether inhibition within the PC is reduced in epileptic rats. In this study, assessment of inhibitory transmission within the deep PC revealed no significant differences between NEC and pilocarpine-treated rodents in the expression of either spontaneously-occurring IPSPs or in the presence of evoked IPSPs. Even in pilocarpine-treated tissue that exhibited spontaneous field events, IPSP responses could still be evoked by single-shock stimulation of local networks although only in the presence of glutamatergic antagonists. These observations indicate that inhibitory inputs of local interneurons onto principal cells may not be lost in epileptic rats. The only observable difference between the two experimental groups was a more depolarized $GABA_A$ receptor mediated response in the pilocarpine-treated tissue. The

relevance of this finding is yet to be determined. Moreover, more detailed investigations are required to determine whether the inhibitory gating of neural activity across the PC is altered in chronically epileptic rats and how this relates to the role of the PC in seizure propagation. Histological evaluation of chronically epileptic tissue for reductions in interneuronal subpopulations might prove useful in addressing this question.

5.5.2 Preliminary evidence for decreased inhibitory drive of LA inputs onto PC neurons in pilocarpine-treated tissue

The PC is known to be extensively and reciprocally interconnected with the amygdaloid complex via the lateral nucleus (LA) (Burwell and Witter, 2002; Suzuki and Amaral, 1994a,b). Although these projections have been established to play an important role in the transfer of sensory information and in emotional learning, assessment of LA-PC interactions in chronically epileptic tissue is virtually non-existent. Here, we provide evidence demonstrating that in NEC tissue, stimulation of LA networks results in primarily inhibitory responses within the deep PC. These results are somewhat in conflict with previous reports illustrating that in vivo stimulation of the LA results in both excitatory and inhibitory responses within the PC (Pelletier et al., 2005). One explanation that might account for this discrepancy might be that in this latter study, recordings were carried out from layers I-V whilst our study focused on only deep layer PC cells.

Interestingly, we have found here that stimulation of LA networks in pilocarpine-treated tissue results in more excitatory than inhibitory responses within the PC. Although the relevance of these findings still needs to be determined by further investigations, they are by themselves noteworthy considering that a recent imaging study revealed that LA inputs can facilitate the spread of excitatory activity from the PC to the EC and hippocampus under conditions of reduced inhibition (Kajiwara et al., 2003). Thus, further assessment of LA-PC interactions in chronically epileptic rats might provide some answers about the role of these structures in seizure propagation to the hippocampus.

5.6 Tables

Table 5-1:

Intrinsic membrane properties of PC neurons from Pilocarpine-treated and Non-Epileptic Control (NEC) tissue.

	Pilocarpine *(with field activity)* *n=14*	**Pilocarpine** *(no field activity)* *n= 42*	**NEC** *n= 26*
RMP (mV)	-65.5 (± 1.9)	-65.7 (± 1.4)	-64.6 (± 1.5)
R_i (MΩ)	47.8 (± 4.1)	54.8 (± 1.8)	58.5 (± 3.2)
APD (ms)	1.2 (± 0.1)	1.4 (± 0.1)	1.4 (± 0.1)
APA (mV)	86.2 (± 1.7)	88.8 (± 1.2)	88.7 (± 1.6)
Burst Firing*	1/14	8/42	7/26
Regular Firing*	13/14	34/42	19/26

RMP, resting membrane potential; R_i, input resistance; APD, action potential duration; APA, action potential amplitude. n represents number of neurons recorded in each group. Data are provided as mean (±SEM). Comparison of the three groups revealed no statistical significance ($p>0.05$).

*PC neurons were classified as 'burst firing' or 'regular firing' depending on their response to a depolarizing current pulse.

Table 5-2:

Spontaneous synaptic activity of PC neurons from Non-Epileptic Controls (NEC) and Pilocarpine-treated tissue.

	Pilocarpine *(with field activity)*	**Pilocarpine** *(no field activity)*	**NEC**
	n=15	*n= 21*	*n= 19*
Spontaneous Bursting Activity*			
Duration (ms)	1199±315	-	-
Interval of occurrence (s)	39.2±15.2	-	-
Depolarizing PSPs			
Amplitude (mV)	2.0±0.2	1.8±0.1	1.6±0.1
Interval of occurrence (s)	2.0±0.8	2.4±0.6	2.4±0.4
Hyperpolaring PSPs			
Amplitude (mV)	-3.2±0.4	-3.6±0.6	-2.9±0.5
Interval of occurrence (s)	12.5±2.0	28.6±6.9	11.5±1.8

Data are provided as mean (±SEM). Comparison of the three groups revealed no statistical significance ($p>0.05$).

*These events were only observed in a subset of Pilocarpine-treated tissue but never in NEC.

Table 5-3:

'Monosynaptically' evoked IPSPs in PC neurons from NEC and Pilocarpine-treated tissue.

	Pilocarpine	**NEC**
	n=12	*n= 9*
Early Component		
Reversal potential (mV)	-69.6±1.0*	-74.9±1.7
Peak Conductance (nS)	13.2±1.9	12.5±3.1
Late Component		
Reversal potential (mV)	-92.5±5.7	-97.9±2.91
Peak Conductance (nS)	2.4±0.7	4.7±2.6

Data are provided as mean (±SEM).

*These values are significantly different ($p<0.05$) from NEC.

5.7 Figures

Figure 5-1:

Spontaneous synaptic activity in NEC and Pilocarpine-treated tissue. **A**: (**a**) Simultaneous field (deep perirhinal cortex (PC_f) and lateral amygdalar nucleus (LA_f)) and intracellular recording (-68 mV, PC) in NEC tissue reveals (i) depolarizing postsynaptic potentials (PSPs) indicated by arrows in insert and (ii) robust spontaneous hyperpolarizing inhibitory postsynaptic potentials (sIPSP) indicated by asterix. Expansion of these events is depicted in the right lower insert. (**b**) Response of PC neuron to intracellular current injection. **B**: Simultaneous field (PC_f, LA_f) and intracellular activity (-68 mV, PC) recorded in the majority of pilocarpine-treated tissue. Note the absence of field activity (PC_f, LA_f). PSPs are indicated by arrows in the intracellular trace and in the expansion in the right lower insert. (**b**) Response of PC neuron to intracellular current injection. **C**: (**a**) Simultaneous field (PC_f, LA_f) and intracellular activity (-65 mV) recorded in a subset of pilocarpine-treated slices reveals robust network activity (PC_f, LA_f). Expansion of an event demonstrates initiation in PC (arrow) and spread to LA (right lower insert). (**b**) Response of PC neuron to intracellular current injection.

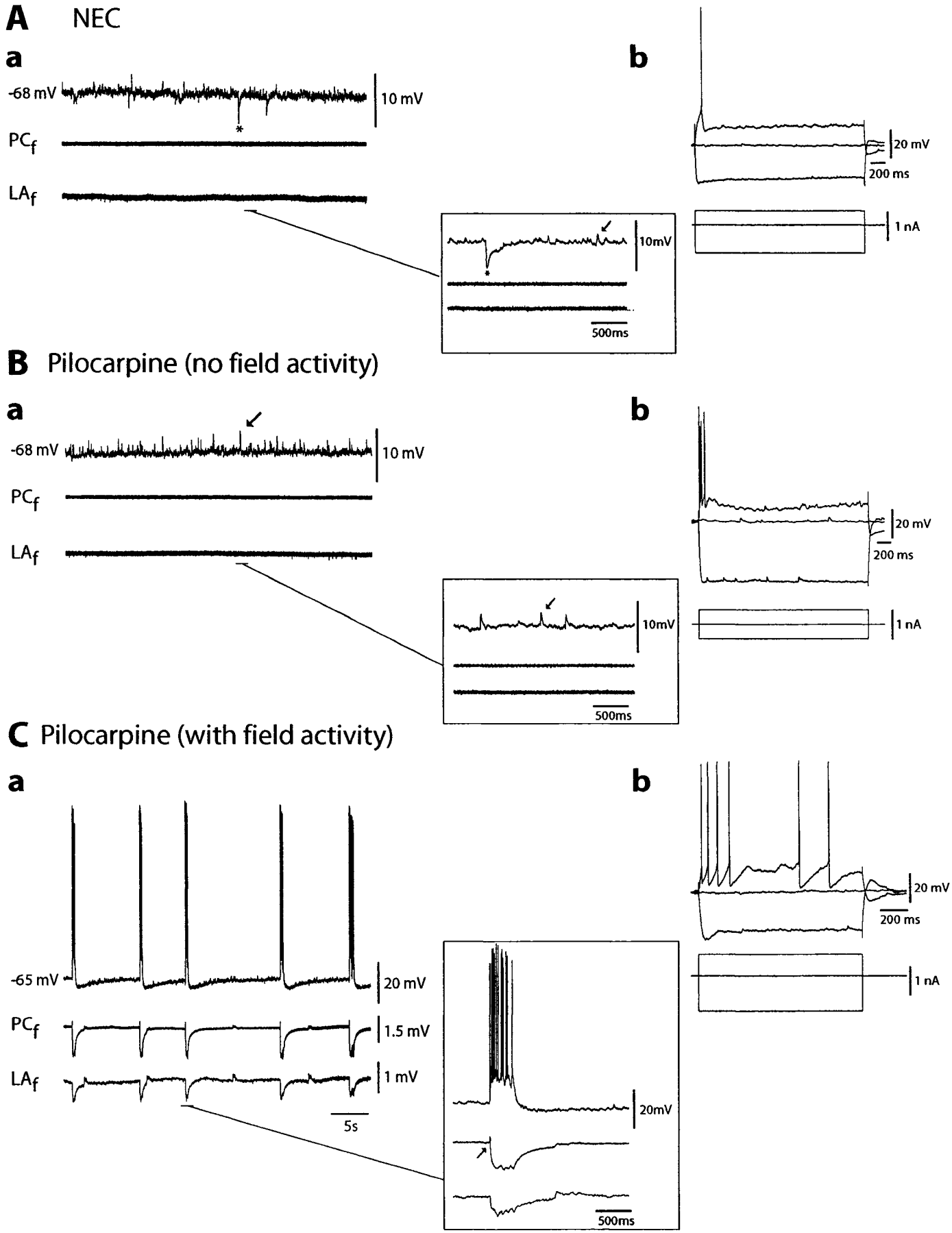
A NEC
a
-68 mV
10 mV
PCf
LAf
10mV
500ms
b
20 mV
200 ms
1 nA
B Pilocarpine (no field activity)
a
-68 mV
10 mV
PCf
LAf
10mV
500ms
b
20 mV
200 ms
1 nA
C Pilocarpine (with field activity)
a
-65 mV
20 mV
PCf
1.5 mV
LAf
1 mV
5s
20mV
500ms
b
20 mV
200 ms
1 nA

Figure 5-2:

Responses of PC neurons to local single shock stimulation. **A**: Sub- and suprathreshold responses of PC neurons in (**a**) NEC, (**b**) Pilocarpine (no field activity) and (**c**) Pilocarpine (with field activity) recorded in 'Control' conditions (i.e. ACSF only). Note the absence of an inhibitory response (insert) and the evoked epileptiform-like activity in (**c**) Pilocarpine (with field activity). **B**: Responses of PC neurons in (**a**) NEC, (**b**) Pilocarpine (no field activity) and (**c**) Pilocarpine (with field activity) in the presence of glutamatergic antagonists (+CPP+CNQX). Note the biphasic IPSP responses specifically at more depolarized membrane potentials (inserts). ▲ represent stimulation artifact.

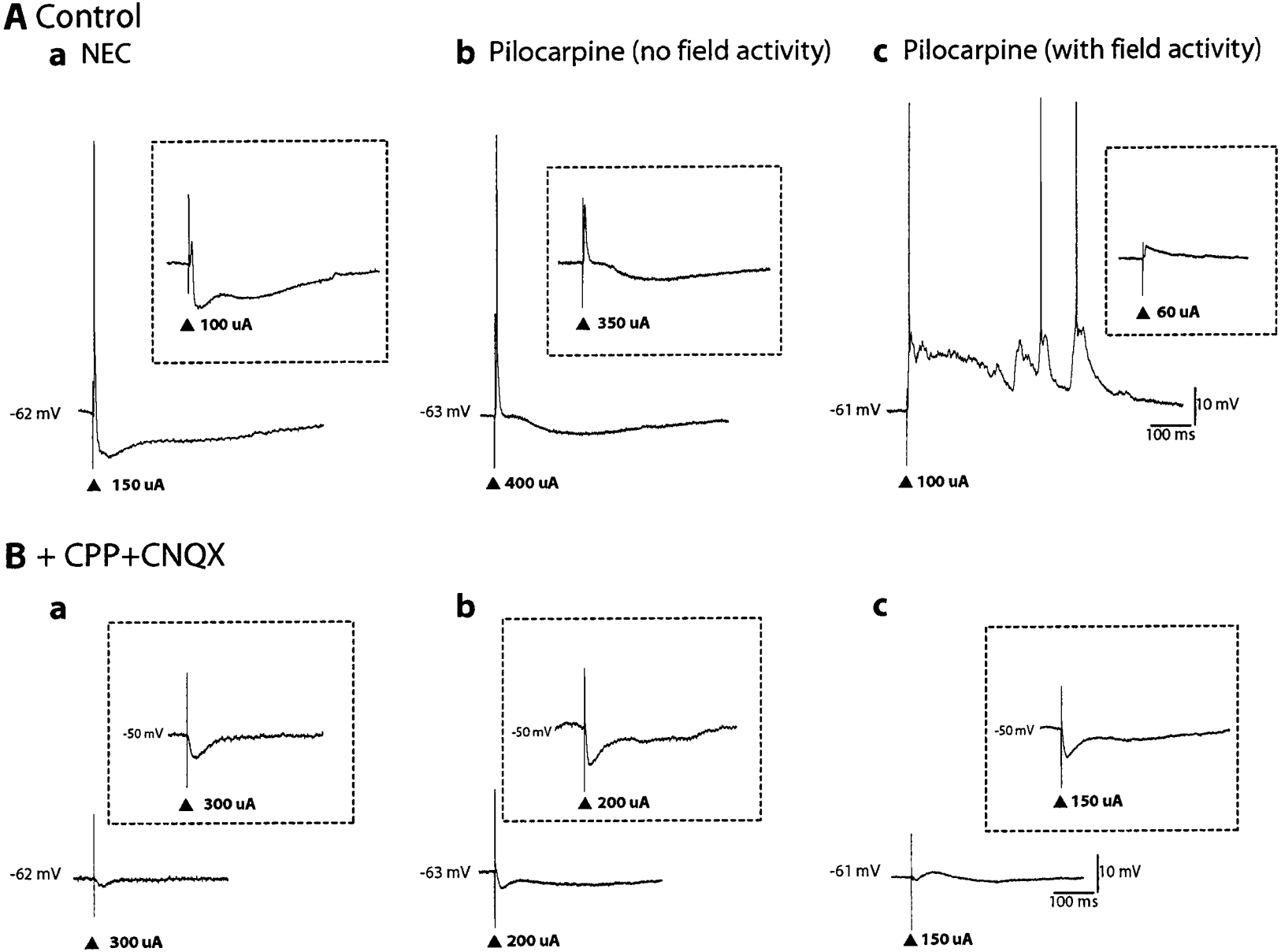
A Control
a NEC
b Pilocarpine (no field activity)
c Pilocarpine (with field activity)
100 uA
-62 mV
150 uA
350 uA
-63 mV
400 uA
60 uA
-61 mV
10 mV
100 ms
100 uA
B + CPP+CNQX
a
b
c
-50 mV
300 uA
-62 mV
300 uA
200 uA
-63 mV
200 uA
150 uA
-61 mV
10 mV
100 ms
150 uA

Figure 5-3:

$GABA_A$-mediated component of evoked IPSP in PC of Pilocarpine-treated tissue exhibits a more depolarized reversal potential **A**: Comparison of the monosynaptic IPSPs evoked in the presence of CPP+CNQX in NEC and pilocarpine-treated tissue at membrane potentials set to different levels by intracellular current injection. Note that the reversal potential of the early component is more depolarized in NEC (Erev = -74.7 mV) versus pilocarpine-treated tissue (Erev = -69.5 mV). **B**: Histogram comparing reversal potential of both early and late IPSP components in NEC versus pilocarpine-treated group. Asterix indicates significance at $p<0.02$. **C**: Histogram comparing peak conductance of both early and late IPSP components in NEC versus pilocarpine-treated group. n represents number of neurons. Error bars: means±SEM.

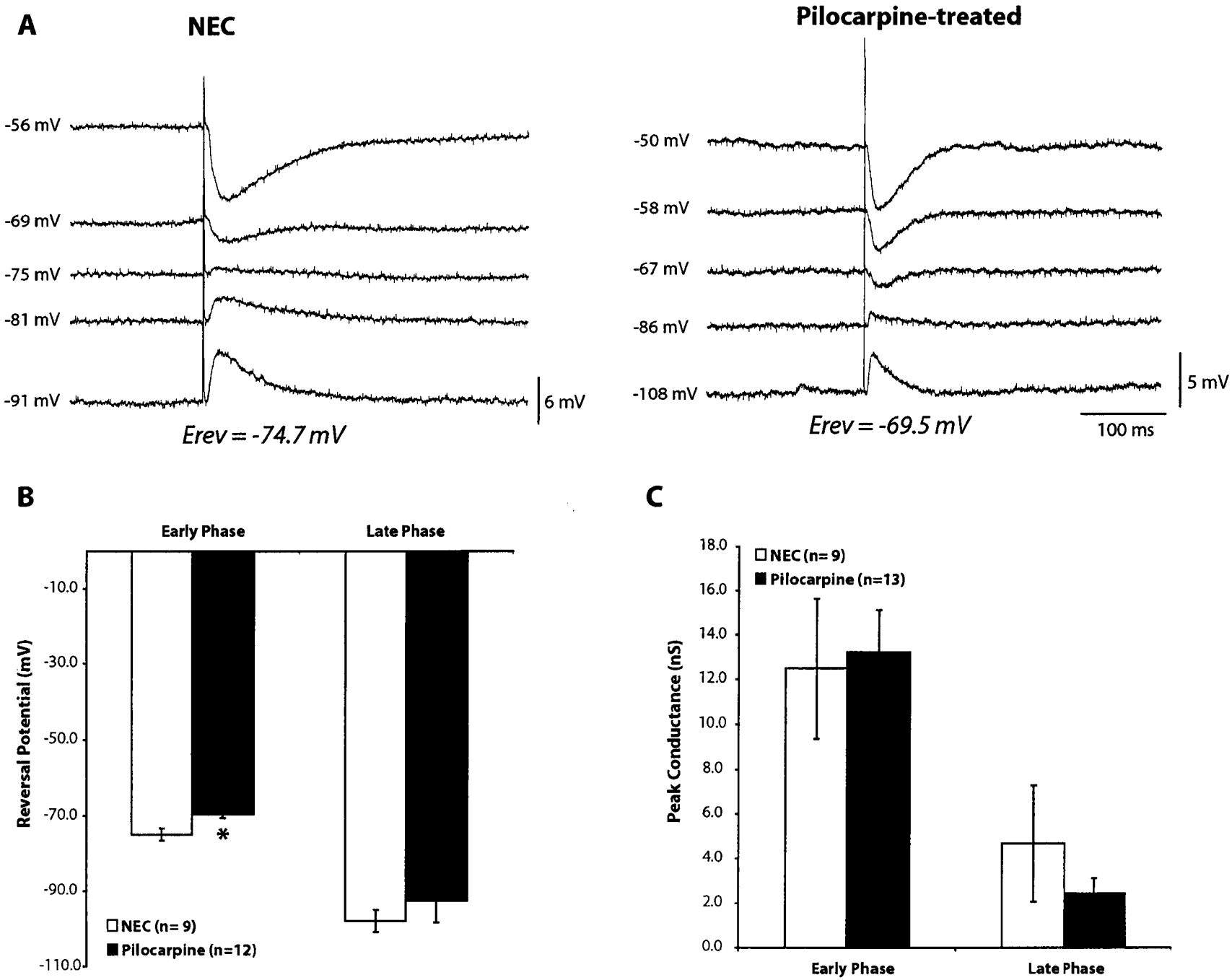
A
NEC
-56 mV
-69 mV
-75 mV
-81 mV
-91 mV
6 mV
Erev = -74.7 mV
Pilocarpine-treated
-50 mV
-58 mV
-67 mV
-86 mV
-108 mV
5 mV
Erev = -69.5 mV
100 ms
B
Early Phase
Late Phase
Reversal Potential (mV)
-10.0
-30.0
-50.0
-70.0
-90.0
-110.0
*
NEC (n= 9)
Pilocarpine (n=12)
C
NEC (n= 9)
Pilocarpine (n=13)
Peak Conductance (nS)
18.0
16.0
14.0
12.0
10.0
8.0
6.0
4.0
2.0
0.0
Early Phase
Late Phase

Figure 5-4:

Responses of PC neurons to single shock stimulation of LA networks. Comparison of PC responses evoked by single shock stimulation of LA networks in NEC, Pilocarpine (no field activity) and Pilocarpine (with field activity). In each cell, responses are recorded at membrane potentials set to different levels by intracellular current injection. Note that in NEC, LA stimulation results in pure IPSP responses whilst EPSP-IPSP responses can be recorded in Pilocarpine (no field activity). Also note that LA stimulation in Pilocarpine (with field activity) results in robust discharges in PC cells which at more depolarized membrane levels appear to be preceded by a hyperpolarizing component (-54 mV). ▲ represent stimulation artifact.

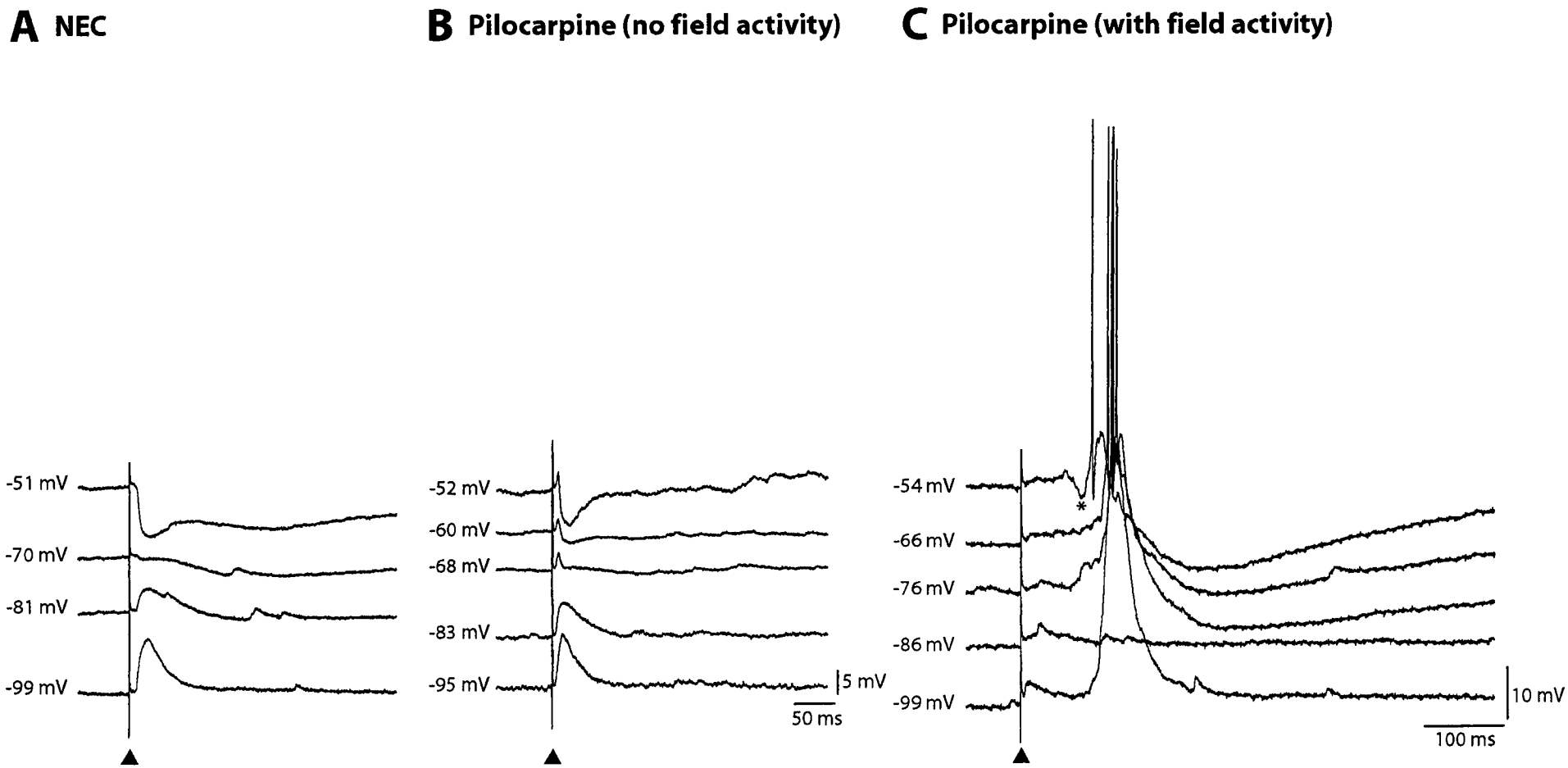
A NEC
B Pilocarpine (no field activity)
C Pilocarpine (with field activity)
-51 mV
-70 mV
-81 mV
-99 mV
-52 mV
-60 mV
-68 mV
-83 mV
-95 mV
5 mV
50 ms
-54 mV
-66 mV
-76 mV
-86 mV
-99 mV
10 mV
100 ms

FINALE

0.1 Summary of Research Findings

The main findings of my PhD studies can summarized as follows:

1. Seizure-induced cell damage results in the decreased ability of CA3/CA1 outputs to control the excitability of the EC where the consequent ictogenesis is sustained via reverberant interactions of this structure with the subiculum (*Chapter 1*).

2. For the first time, evidence is provided demonstrating that GABAergic circuits confer the subiculum with the ability to gate hippocampal output activity (*Chapter 2*).

3. CA3-driven interictal events are capable of controlling not only the ability of the EC for ictogenesis, but also that of BLA/LA networks. Furthermore, in the absence of inputs from adjacent structures, these latter amygdalar nuclei are capable of contributing to epileptiform synchronization by generating both interictal- and ictal-like activity (*Chapter 3*).

4. Novel findings suggest that alterations in both pre- and postsynaptic GABAergic mechanisms play a role in the increased excitability of the LA in chronically epileptic rats (*Chapter 4*).

5. Finally, data indicate that hyperexcitability of the PC as well alterations in the interactions between the amygdala and this parahippocampal structure can occur in chronically epileptic rats (*Chapter 5*).

0.2 CA3-driven interictal activity – A possible anticonvulsive role?

Earlier studies in isolated hippocampal slices have demonstrated that the CA3 area responds readily to a variety of epileptogenic treatments by generating epileptiform discharges recurring at frequencies comprised between 0.5 and 1 Hz (Perreault and Avoli, 1991; Rutecki et al., 1987, 1990; Schwartzkroin and Prince, 1980; Tancredi et al., 1990). Intracellularly, these interictal-like events correspond to action potential bursts and resemble the paroxysmal depolarizing shifts (PDS) described both in vivo and in vitro under various experimental conditions (Avoli et al., 2002; de Curtis and Avanzini, 2001). The propensity of the CA3 region to generate these synchronous interictal discharges is due to the presence of recurrent excitatory, glutamatergic

synapses that couple neighbouring CA3 pyramidal cells along with the ability of these neurons to generate dendritic Ca^{2+} spikes (Miles and Wong, 1986, 1987; for review see Traub and Jefferys, 1994).

The ability of CA3 networks to generate interictal discharges is therefore not unexpected. However, it is surprising that this type of epileptiform activity can consistently entrain downstream networks in intact, interconnected slices. Previous studies carried out in hippocampal-EC slices obtained from rodents have shown that in the presence of convulsive agents: (i) fast interictal activity almost always initiates in the CA3 region, (ii) subsequently propagates to CA1, subiculum and EC, (iii) can re-enter the hippocampus through the perforant path; and importantly (iv) can control ictogenesis within the EC (Avoli and Barbarosie, 1999; Barbarosie and Avoli, 1997; Barbarosie et al., 2002). Extension of the slice preparation in my studies to include BLA/LA networks has not only confirmed the above observations, but has further illustrated that CA3-driven interictal discharges can pace epileptiform activity generated by amygdalar networks (*Chapter 3*). The significance of CA3-generated interictal discharges in entraining other limbic structures is conveyed further in chronically epileptic mice where hippocampal output activity compromised by neuronal loss consequently leads to seizure generation in the downstream EC (*Chapter 1*). Finally, I have demonstrated that even in the absence of neuronal loss in the CA3 region, inhibitory processes at the level of the subiculum can prevent CA3-driven interictal activity from reaching the EC where ictal discharges consequently appear (*Chapter 2*).

Altogether, my observations confirm that CA3-driven interictal activity control rather than facilitate the occurrence of limbic seizures. In thus doing, they raise the fascinating and much debated question of interictal-ictal interactions within the epileptic brain. One notion is that the asymptomatic interictal events are proconvulsive and can lead to seizure onset in a process known as interictal-to-ictal transition (Ayala et al., 1973; Dzhala and Staley, 2003). This hypothesis is further substantiated by reports from kindling studies demonstrating that interictal spiking becomes more frequent as kindling progresses as well as prior to the appearance of spontaneous

seizures (Pinel and Rovner, 1978; Wada et al., 1974). In contrast, my observations are in line with the majority of experimental and clinical evidence suggesting that interictal spikes most probably protect against the occurrence of ictal discharges by maintaining a low level of excitation (for review see de Curtis and Avanzini, 2001). These studies have established that the rate of interictal spikes does not change and can sometimes even decrease before the onset of limbic seizures in epileptic patients (for review see de Curtis and Avanzini, 2001). Moreover, sustained interictal spiking has been demonstrated to reduce the probability of ictal events whereas suppression of interictal discharges has been shown to lead to seizures (for review see de Curtis and Avanzini, 2001).

Overall, further validation of this anticonvulsive role of CA3-driven interictal discharges may lead to dramatic changes in the management of epileptic patients. Specifically, it suggests that a paradigmatic shift in the development of antiepileptic therapies may be needed to exploit strategies that enhance rather than suppress interictal-like activity. Examples of such therapies may involve new AEDs that selectively increase CA3 function in patients with severe hippocampal atrophy. Alternatively, surgical implantation of pacemakers that can deliver rhythmic, low-frequency stimulation of hippocampal outputs to mimic CA3-driven interictal activity may also decrease the propensity of the EC or other downstream structures from generating seizures, and may prove to be an effective alternative to surgical resection.

0.3 The subiculum – Unscathed bystander or culprit?

Until recently, the subiculum has received little attention in epileptology. This could perhaps have been due to earlier histological reports demonstrating that no significant cell loss occurs within this hippocampal region (Blumcke et al., 2002; Dawodu and Thom, 2005; Gloor 1997). However, despite the absence of neuronal loss, increasing evidence suggests that the subiculum may be intricately involved in the process of epileptogenesis (for review see Stafstrom, 2005). My studies have demonstrated that in slices obtained from chronically epileptic mice, the subiculum not only supports EC ictogenesis but can also provide a monosynaptic bypass for seizure activity to enter the hippocampus via the temporammonic pathway (*Chapter 1*).

These observations are significant on two levels. First, considering the strategic position of the subiculum within the limbic system and its dense interconnections with cortical and subcortical regions, the increased activation of the monosynaptic temporoammonic pathway can provide a more efficient way for EC-generated seizures to generalize, via the subiculum, to other brain structures. Secondly, the absence of neuronal loss within this region may in fact be playing an important role in rendering this structure capable of sustaining and perhaps amplifying seizures. Recent evidence suggests that although loss of principal cells is minimal, cellular and network reorganization within the epileptic subiculum confers this structure with the propensity to sustain abnormal synchrony and hyperexcitability (Knopp et al., 2005; Wellmer et al., 2002; de Guzman et al., submitted). Accordingly, in vitro studies in human epileptic tissue have demonstrated the presence of spontaneous interictal activity originating within the subiculum and spreading to adjacent hippocampal regions (Cohen et al., 2002; Wozny et al., 2003). Altogether, my observations are in line with the increasing realization that the subiculum might be more actively involved in epileptogenesis than previously believed.

In addition to its suggested role in sustaining seizures in chronically epileptic mice, my studies have also demonstrated that GABAergic circuits within the subiculum are capable of gating hippocampal output activity (*Chapter 2*). These latter findings are significant in illustrating that the subiculum is not merely the anatomical exit of the hippocampus but rather a structure that is capable of dynamically processing and modifying inputs in such a way so as to modify the activity of downstream structures (such as the EC). This characteristic of the subiculum might be relevant to understanding its role in the spread of seizures. For example, in patients where the epileptogenic focus has been localized to the hippocampus, any reduction in subicular inhibitory networks could provide a way for hippocampal seizures to generalize. Alternatively, if CA3-driven activity is indeed anticonvulsive as previously discussed, then inhibition at the level of the subiculum might prevent these discharges from spreading and controlling EC ictogenesis, even in patients without obvious CA3/CA1 sclerosis.

0.4 The importance of stepping out of the "hippocampocentric" box

Perhaps one of the most essential developments in TLE research in the past decade has been the important recognition that the pathophysiological substrates underlying this neurological disorder extend beyond the hippocampus to involve not only extrahippocampal but extratemporal structures as well (DeCarli et al., 1998; Dreifuss et al., 2001; Lee et al., 1998; Moran et al., 2001; Natsume et al., 2003; Sandok et al., 2000; Seidenberg et al., 2005). Advances in neuroimaging techniques have revealed that volumetric reductions of the amygdala, entorhinal and perirhinal cortices do occur in a subset of TLE patients in spite of normal hippocampal volumes (Bernasconi et al., 1999, 2001, 2003; Cendes et al., 1993; Jutila et al., 2001; Salmenpera et al., 2000). Histopathological examination of human epileptic tissue have corroborated these findings by demonstrating the presence of selective neuronal loss and synaptic reorganization within these structures even in the absence of hippocampal sclerosis (Aliashkevich et al., 2003; Du et al., 1993; Hudson et al., 1993; Mikkonen et al., 1998; Miller et al., 1994; Wolf et al., 1997; Yilmazer-Hanke et al., 2000).

By investigating the amygdala (specifically the LA) and the PC in chronically epileptic rats, I have provided evidence that supports the above reports and further implicates these extrahippocampal structures in the process of epileptogenesis (*Chapter 4 and 5*). My findings of altered GABAergic signalling and hyperexcitability of LA networks are specifically noteworthy considering that this amygdalar nuclei is importantly interconnected with other structures that are also implicated in TLE. Nevertheless, further exploration of this brain region is necessary for identifying the exact role played by the LA in the initiation and spread of seizures within the epileptic brain. Interestingly, clinical studies have reported that epileptic patients that present with isolated amygdalar pathology tend to exhibit more widespread EEG abnormalities and a greater predisposition for their seizures to become generalized (Gambardella et al., 1995; Hudson et al., 1993; Miller et al., 1994; Van Paesschen et al., 1996; Yilmazer-Hanke et al., 2000). Furthermore, the cytoarchitectonic construction of the amygdala and the extensive intrinsic interconnectivity between its various nuclei confer this structure with the propensity to amplify and generalize

seizures (for review see Pitkanen et al., 1998). Additional to understanding its role in seizure generalization, it would be essential to identify how dysfunctional inhibition of LA networks modifies the amygdalar's interactions with the PC, EC and hippocampus. Preliminary evidence suggests that decreased inhibitory input of LA neurons onto PC cells occurs in chronically epileptic rats (*Chapter 5*). However, the nature and relevance of this finding to epileptogenesis is yet to be determined.

Finally, it is worthwhile to mention that thorough assessment of extrahippocampal structures might help increase our understanding of the mechanisms underlying the pathophysiology of TLE. For example, histopathological, molecular and electrophysiological assessment of structures such as the PC in chronically epileptic tissue are currently sparse. Understanding the functional changes that occur within this structure in the epileptic brain might provide valuable information about its role in epileptogenesis.

0.5 Concluding Remarks

Although I find myself at the end of my graduate training left with more questions than when I first begun, my PhD studies have helped me appreciate the complexity of the CNS and the diversity of the pathological factors involved in TLE. I have come to realize that neuronal loss, synaptic reorganization, alterations in inhibitory and excitatory processes are all phenomena that, albeit important, need to be understood in the context of specific limbic structures. My amateur conclusion is that in order to get closer to resolving the ambiguity in the relationship between these phenomena and the seizures themselves, we need to be more daring in our scientific explorations.

Due to obvious ethical reasons, depth electrode recordings in epileptic patients, although valuable, tend to be greatly limited. Nevertheless, chronic animal models offer us a unique opportunity to investigate questions that might prove beneficial to the management of refractory epileptic patients. For example, a comprehensive study employing multiple depth electrode recordings in epileptic animals coupled with MRI imaging, surgical resection, histopathological and molecular studies, as well as in vitro electrophysiological recordings might conceivably be technically challenging and overtly ambitious. However, such a study could perhaps provide some clues to

pertinent questions including: (i) How does the temporal evolution of electrographic seizures, MRI changes and histopathological damage following SE compare in various structures (such as hippocampus proper, subiculum, EC, PC or amygdala)? (ii) Can surgical resection or pharmacological intervention during the early stages of the disease process prevent the occurrence of chronic epilepsy? (iii) Which structures are more likely to be the 'ictal-onset' versus the 'irritative' areas within the epileptogenic focus? (iv) How can we improve localization of the epileptogenic region(s)? (v) How do the various structures interact within the epileptic brain? (vi) Is surgical resection or disconnection of one structure more efficient at controlling seizures than others? (vii) Can implantation of pacemakers within the hippocampus reduce seizures in these epileptic animals (i.e. can the anticonvulsive role of CA3-driven interictal activity be validated)?

On a final note, it is indisputable that the technological advancements of the past three decades have contributed importantly to our understanding of the pathophysiology of TLE. In order to achieve better therapeutic management of TLE patients, it is perhaps necessary to re-evaluate our current experimental paradigms and reformulate some of the questions that guide research in this important medical field.

REFERENCES

Adolphs R, Tranel D, Damasio H and Damasio A (1994) Impaired recognition of emotion in facial expressions following bilateral damage to the human amygdala. Nature. 372:669-72.

Akbar MT, Torp R, Danbolt NC, Levy LM, Meldrum BS and Ottersen OP (1997) Expression of glial glutamate transporters GLT-1 and GLAST is unchanged in the hippocampus in fully kindled rats. Neuroscience. 78:351-9.

Aliashkevich AF, Yilmazer-Hanke D, Van Roost D, Mundhenk B, Schramm J and Blumcke I (2003) Cellular pathology of amygdala neurons in human temporal lobe epilepsy. Acta Neuropathol (Berl). 106, 99-106.

Amara SG and Fontana AC (2002) Excitatory amino acid transporters: keeping up with glutamate. Neurochem Int. 41:313-8.

Amaral DG, Price JL, Pitkänen A and Carmichael TS (1992) Anatomical organization of the primate amygdaloid complex. In: The amygdala: neurobiological aspects of emotion, memory and mental dysfunction (Aggleton JP, ed), pp. 1–66. New York: Wiley-Liss.

Amaral DG and Witter MP (1989) The three-dimensional organization of the hippocampal formation: a review of anatomical data. Neuroscience. 31:571-91.

Amaral DG and Witter MP (1995) Hippocampal formation. In: The rat nervous system (Paxinos G, ed), pp. 443–493., San Diego: Academic Press.

Anderson WW, Lewis DV, Swartzwelder HS and Wilson WA (1986) Magnesium-free medium activates seizure-like events in the rat hippocampal slice. Brain Res. 398:215-9.

Anwyl R (1999) Metabotropic glutamate receptors: electrophysiological properties and role in plasticity. Brain Res Brain Res Rev. 29:83-120.

Aram JA, Michelson HB and Wong RK (1991) Synchronized GABAergic IPSPs recorded in the neocortex after blockade of synaptic transmission mediated by excitatory amino acids. J Neurophysiol. 65, 1034-41.

Arellano JI, Munoz A, Ballesteros-Yanez I, Sola RG and DeFelipe J (2004) Histopathology and reorganization of chandelier cells in the human epileptic sclerotic hippocampus. Brain. 127:45-64.

Armitage LL, Mohapel P, Jenkins EM, Hannesson DK and Corcoran ME (1998) Dissociation between mossy fiber sprouting and rapid kindling with low-frequency stimulation of the amygdala. Brain Res. 781:37-44.

Asprodini EK, Rainnie DG and Shinnick-Gallagher P (1992) Epileptogenesis reduces the sensitivity of presynaptic gamma-aminobutyric acidB receptors on glutamatergic afferents in the amygdala. J Pharmacol Exp Ther. 262:1011-21.

Avoli M (1991) Excitatory amino acid receptors in the human epileptogenic neocortex. Epilepsy Res. 10:33-40.

Avoli M and Barbarosie M (1999) Interictal-ictal interactions and limbic seizure generation. Rev Neurol (Paris). 155:468-71.

Avoli M, Barbarosie M, Lücke A, Nagao T, Lopantsev V and Köhling R (1996) Synchronous GABA-mediated potentials and epileptiform discharges in the rat limbic system in vitro. J. Neurosci. 16: 3912-3924

Avoli M, D'Antuono M, Louvel J, Kohling R, Biagini G, Pumain R, D'Arcangelo G and Tancredi V (2002) Network and pharmacological mechanisms leading to epileptiform synchronization in the limbic system in vitro. Prog Neurobiol. 68:167-207.

Avoli M, Louvel J, Pumain R and Kohling R (2005) Cellular and molecular mechanisms of epilepsy in the human brain. Prog Neurobiol. (epub).

Avoli M, Mattia D, Siniscalchi A, Perreault P and Tomaiuolo F (1994) Pharmacology and electrophysiology of a synchronous GABA-mediated potential in the human neocortex. Neuroscience. 62, 655-666.

Ayala GF, Dichter M, Gumnit RJ, Matsumoto H and Spencer WA (1973) Genesis of epileptic interictal spikes. New knowledge of cortical feedback systems suggests a neurophysiological explanation of brief paroxysms. Brain Res. 52: 1-17.

Barbarosie M and Avoli M (1997) CA3-driven hippocampal-entorhinal loop controls rather than sustains in vitro limbic seizures. J. Neurosci. 17: 9308-9314.

Barbarosie M, Louvel J, Kurcewicz I, and Avoli M (2000) CA3-released entorhinal seizures disclose dentate gyrus epileptogenicity and unmask a temporoammonic pathway. J Neurophysiol 83: 1115-1124.

Barbarosie M, Louvel J, D'Antuono M, Kurcewicz I and Avoli M (2002) Masking synchronous GABA-mediated potentials controls limbic seizures. Epilepsia. 43, 1469-79.

Babb TL and Crandall PH (1976) Epileptogenesis of human limbic neurons in psychomotor epileptics. Electroencephalogr Clin Neurophysiol. 40:225-43.

Babb TL, Kupfer WR, Pretorius JK, Crandall PH and Levesque MF (1991) Synaptic reorganization by mossy fibers in human epileptic fascia dentata. Neuroscience. 42:351-63.

Babb TL, Wilson CL and Isokawa-Akesson M (1987) Firing patterns of human limbic neurons during stereoencephalography (SEEG) and clinical temporal lobe seizures. Electroencephalogr Clin Neurophysiol. 66:467-82.

Bear J and Lothman EW (1993) An in vitro study of focal epileptogenesis in combined hippocampal-parahippocampal slices. Epilepsy Res 14: 183–193.

Behr J, Gebhardt C, Heinemann U, and Mody I (2002) Kindling enhances kainate receptor-mediated depression of GABAergic inhibition in rat granule cells. Eur J Neurosci. 16:861-7.

Behr J, Gloveli T and Heinemann U (1998) The perforant path projection from the medial entorhinal cortex layer III to the subiculum in the rat combined hippocampal-entorhinal cortex slice. Eur J Neurosci. 10, 1011-1018.

Behr J and Heinemann U (1996) Low Mg2+ induced epileptiform activity in the subiculum before and after disconnection from rat hippocampal and entorhinal cortex slices. Neurosci. Lett. 205, 25-28.

Bekenstein JW and Lothman EW (1993) Dormancy of inhibitory interneurons in a model of temporal lobe epilepsy. Science. 259:97-100.

Ben-Ari Y (1985) Limbic seizure and brain damage produced by kainic acid: mechanisms and relevance to human temporal lobe epilepsy. Neuroscience. 14:375-403.

Ben-Ari Y, Cherubini E, Corradetti R and Gaiarsa JL (1989) Giant synaptic potentials in immature rat CA3 hippocampal neurones. J Physiol. 416:303-25, 1989.

Benini R, D'Antuono M, Pralong E and Avoli M (2003) Involvement of amygdala networks in epileptiform synchronization in vitro. Neuroscience. 120, 75-84.

Bernard C (2005) Dogma and dreams: experimental lessons for epilepsy mechanism chasers. Cell Mol Life Sci. 62:1177-81.

Bernard C, Anderson A, Becker A, Poolos NP, Beck H and Johnston D (2004) Acquired dendritic channelopathy in temporal lobe epilepsy. Science. 305:532-5

Bernasconi N, Bernasconi A, Andermann F, Dubeau F, Feindel W and Reutens DC (1999) Entorhinal cortex in temporal lobe epilepsy: a quantitative MRI study. Neurology. 52:1870-6.

Bernasconi N, Bernasconi A, Caramanos Z, Andermann F, Dubeau F and Arnold DL (2000) Morphometric MRI analysis of the parahippocampal region in temporal lobe epilepsy. Ann N Y Acad Sci. 911:495-500.

Bernasconi N, Bernasconi A, Caramanos Z, Dubeau F, Richardson J, Andermann F and Arnold DL (2001) Entorhinal cortex atrophy in epilepsy patients exhibiting normal hippocampal volumes. Neurology.56:1335-9.

Bernasconi N, Bernasconi A, Caramanos Z, Antel SB, Andermann F and Arnold DL (2003) Mesial temporal damage in temporal lobe epilepsy: a volumetric MRI study of the hippocampus, amygdala and parahippocampal region. Brain. 126:462-9.

Biella G, Uva L and de Curtis M (2002) Propagation of neuronal activity along the neocortical-perirhinal-entorhinal pathway in the guinea pig. J Neurosci. 22:9972-9.

Blumcke I, Beck H, Lie AA and Wiestler OD (1999) Molecular neuropathology of human mesial temporal lobe epilepsy. Epilepsy Res. 36:205-23.

Blumcke I, Thom M and Wiestler OD (2002) Ammon's horn sclerosis: a maldevelopmental disorder associated with temporal lobe epilepsy. Brain Pathol. 12:199-211.

Bridges RJ and Esslinger CS (2005) The excitatory amino acid transporters: pharmacological insights on substrate and inhibitor specificity of the EAAT subtypes. Pharmacol Ther. 107:271-85.

Braak H and Braak E (1983) Neuronal types in the basolateral amygdaloid nuclei of man. Brain Res Bull. 11:349-65.

Bronen RA, Fulbright RK, Kim JH, Spencer SS, Spencer DD and al-Rodhan NR (1995) Regional distribution of MR findings in hippocampal sclerosis. AJNR Am J Neuroradiol. 16:1193-200

Brooks-Kayal AR, Shumate MD, Jin H, Rikhter TY and Coulter DA (1998) Selective changes in single cell GABA(A) receptor subunit expression and function in temporal lobe epilepsy. Nat Med. 4:1166-72.

Buckley MJ (2005) The role of the perirhinal cortex and hippocampus in learning, memory, and perception. Q J Exp Psychol B. 58:246-68.

Buhl EH, Otis TS and Mody I (1996) Zinc-induced collapse of augmented inhibition by GABA in a temporal lobe epilepsy model. Science. 271: 369-73.

Burke JP and Hablitz JJ (1994) Presynaptic depression of the synaptic transmission mediated by activation of metabotropic glutamate receptors in the rat neocortex. J Neurosci 4: 5120–5130.

Burwell RDB and Witter MP (2002) Perirhinal structure and connectivity. In: The parahippocampal region. Editors: Witter MP and Wouterlood F. Oxford University Press. pp 42-45.

Buzsaki G, Horvath Z, Urioste R, Hetke J and Wise K (1992) High-frequency network oscillation in the hippocampus. Science. 256:1025-7.

Callahan PM, Paris JM, Cunningham KA and Shinnick-Gallagher P (1991) Decrease of GABA-immunoreactive neurons in the amygdala after electrical kindling in the rat. Brain Res. 555:335-9.

Canteras NS and Swanson LW (1992) Projections of the ventral subiculum to the amygdala, septum, and hypothalamus: a PHAL anterograde tract-tracing study in the rat. J Comp Neurol. 324, 180-194.

Capek R (1997) Multiple targets of anti-epileptic drugs at GABAergic synapses. In: Molecular and cellular targets of antiepileptic drugs. Editors: Avanzini G, Regesta G, Tanganelli G, et al. London: Jon Libbey, pp 163-182.

Cartmell J and Schoepp DD (2000) Regulation of neurotransmitter release by metabotropic glutamate receptors. J Neurochem. 75:889-907.

Cavalheiro EA, Leite JP, Bortolotto ZA, Turski WA, Ikonomidou C, and Turski L (1991) Long-term effects of pilocarpine in rats: structural damage of the brain triggers kindling and spontaneous recurrent seizures. Epilepsia. 32:778-82.

Cavalheiro EA, Santos NF and Priel MR (1996) The pilocarpine model of epilepsy in mice. Epilepsia. 37:1015-9.

Cavalheiro EA, Silva DF, Turski WA, Calderazzo-Filho LS, Bortolotto ZA, and Turski L (1987) The susceptibility of rats to pilocarpine-induced seizures is age-dependent. Brain Res. 465:43-58.

Cavazos JE, Golarai G, and Sutula TP (1991) Mossy fiber synaptic reorganization induced by kindling: time course of development, progression, and permanence. J Neurosci 11: 2795-2803.

Cavazos JE, Jones SM and Cross DJ (2004) Sprouting and synaptic reorganization in the subiculum and CA1 region of the hippocampus in acute and chronic models of partial-onset epilepsy. Neuroscience. 126:677-88.

Cendes F, Andermann F, Gloor P, Evans A, Jones-Gotman M, Watson C, Melanson D, Olivier A, Peters T, Lopes-Cendes I, et al. (1993) MRI volumetric measurement of amygdala and hippocampus in temporal lobe epilepsy. Neurology. 43:719-25.

Chandler KE, Princivalle AP, Fabian-Fine R, Bowery NG, Kullmann DM and Walker MC (2003) Plasticity of GABA(B) receptor-mediated heterosynaptic interactions at mossy fibers after status epilepticus. J Neurosci. 23:11382-91.

Chapman AG (2000) Glutamate and epilepsy. J Nutr. 130:1043S-5S.

Cobb SR, Buhl EH, Halasy K, Paulsen O and Somogyi P (1995) Synchronization of neuronal activity in hippocampus by individual GABAergic interneurons. Nature. 378:75-8.

Cohen I, Navarro V, Clemenceau S, Baulac M and Miles R (2002) On the origin of interictal activity in human temporal lobe epilepsy in vitro. Science 298, 1418-1421.

Colino A and Fernandez de Molina A (1986) Inhibitory response in entorhinal and subicular cortices after electrical stimulation of the lateral and basolateral amygdala of the rat. Brain Res. 378, 416-419.

Collingridge GL and Lester RA (1989) Excitatory amino acid receptors in the vertebrate central nervous system. Pharmacol Rev. 41:143-210.

Collins RC, Tearse RG and Lothman EW (1983) Functional anatomy of limbic seizures: Focal discharges from medial entorhinal cortex in rat. Brain Res. 280, 25-40.

Connors BW and Prince DA (1982) Effects of local anesthetic QX-314 on the membrane properties of hippocampal pyramidal neurons. J Pharmacol Exp Ther. 220:476-81.

Cossart R, Bernard C and Ben-Ari Y (2005) Multiple facets of GABAergic neurons and synapses: multiple fates of GABA signalling in epilepsies. Trends Neurosci. 28:108-15.

Coull JA, Boudreau D, Bachand K, Prescott SA, Nault F, Sik A, De Koninck P and De Koninck Y (2003) Trans-synaptic shift in anion gradient in spinal lamina I neurons as a mechanism of neuropathic pain. Nature. 424:938-42.

Coulter DA, McIntyre DC and Loscher W (2002) Animal models of limbic epilepsies: what can they tell us? Brain Pathol. 12:240-56.

Covolan L and Mello LE (2000) Temporal profile of neuronal injury following pilocarpine or kainic acid-induced status epilepticus. Epilepsy Res. 39:133-52.

Csicsvari J, Hirase H, Czurko A, Mamiya A and Buzsaki G (1999) Oscillatory coupling of hippocampal pyramidal cells and interneurons in the behaving Rat. J Neurosci. 19:274-87.

Danbolt NC (2001) Glutamate uptake. Prog Neurobiol. 65:1-105.

Danober L and Pape HC (1998) Mechanisms and functional significance of a slow inhibitory potential in neurons of the lateral amygdala. Eur J Neurosci. 10:853-67.

D'Antuono M, Benini R, Biagini G, D'Arcangelo G, Barbarosie M, Tancredi V et al. (2002) Limbic network interactions leading to hyperexcitability in a model of temporal lobe epilepsy. J. Neurophysiol. 87, 634-639.

D'Antuono M, Biagini G, Tancredi V and Avoli M (2001) Electrophysiology of regular firing cells in the rat perirhinal cortex. Hippocampus. 11:662-72.

Davis M and Whalen PJ (2001) The amygdala: vigilance and emotion. Mol Psychiatry 6: 13–34.

Dawodu S and Thom M (2005) Quantitative neuropathology of the entorhinal cortex region in patients with hippocampal sclerosis and temporal lobe epilepsy. Epilepsia. 46:23-30.

Deacon TW, Eichenbaum H, Rosenberg P and Eckmann KW (1983) Afferent connections of the perirhinal cortex in the rat. J. Comp. Neurol. 220, 168-190.

DeCarli C, Hatta J, Fazilat S, Fazilat S, Gaillard WD and Theodore WH (1998) Extratemporal atrophy in patients with complex partial seizures of left temporal origin. Ann Neurol. 43:41-5.

de Curtis M and Avanzini G (2001) Interictal spikes in focal epileptogenesis. Prog Neurobiol. 63:541-67.

de Curtis M and Pare D (2004) The rhinal cortices: a wall of inhibition between the neocortex and the hippocampus. Prog Neurobiol. 74:101-10.

de Curtis M, Manfridi A and Biella G (1998) Activity-dependent pH shifts and periodic recurrence of spontaneous interictal spikes in a model of focal epileptogenesis. J Neurosci 18: 7543–7551.

de Guzman P, D'Antuono M and Avoli M (2004) Initiation of electrographic seizures by neuronal networks in entorhinal and perirhinal cortices in vitro. Neuroscience. 123:875-86.

de Guzman P, Inaba Y, Biagini G, Baldelli E, Mollinari C, Merlo D and Avoli M (submitted) Subiculum network excitability is increased in a rodent model of temporal lobe epilepsy.

de Lanerolle NC, Kim JH, Robbins RJ and Spencer DD (1989) Hippocampal interneuron loss and plasticity in human temporal lobe epilepsy. Brain Res. 495:387-95.

Deutch C, Spencer S, Robbins R, Cicchetti D and Spencer D (1991) Interictal spikes and hippocampal somatostatin levels in temporal lobe epilepsy. Epilepsia 32: 174–178.

Dietrich D, Kral T, Clusmann H, Friedl M and Schramm J (1999) Reduced function of L-AP4-sensitive metabotropic glutamate receptors in human epileptic sclerotic hippocampus. Eur J Neurosci. 11:1109-13.

Dingledine R and Gjerstad L (1980) Reduced inhibition during epileptiform activity in the in vitro hippocampal slice. J Physiol. 305:297-313.

Dingledine R, McBain CJ and McNamara JO (1990) Excitatory amino acid receptors in epilepsy. Trends Pharmacol Sci. 11:334-8.

Doherty J and Dingledine R (2001) Reduced excitatory drive onto interneurons in the dentate gyrus after status epilepticus. J Neurosci. 21, 2048-57.

Dreier JP and Heinemann U (1991) Regional and time dependent variations of low Mg2+ induced epileptiform activity in rat temporal cortex slices. Exp Brain Res. 87, 581-96.

Dreifuss S, Vingerhoets FJ, Lazeyras F, Andino SG, Spinelli L, Delavelle J and Seeck M (2001) Volumetric measurements of subcortical nuclei in patients with temporal lobe epilepsy. Neurology. 57:1636-41.

Du F, Eid T, Lothman EW, Kohler C and Schwarcz R (1995) Preferential neuronal loss in layer III of the medial entorhinal cortex in rat models of temporal lobe epilepsy. J Neurosci. 15:6301-13.

Du F, Whetsell WO Jr, Abou-Khalil B, Blumenkopf B, Lothman EW and Schwarcz R (1993) Preferential neuronal loss in layer III of the entorhinal cortex in patients with temporal lobe epilepsy. Epilepsy Res. 16, 223-233.

During MJ, Ryder KM and Spencer DD (1995) Hippocampal GABA transporter function in temporal-lobe epilepsy. Nature. 376:174-7.

During MJ and Spencer DD (1993) Extracellular hippocampal glutamate and spontaneous seizure in the conscious human brain. Lancet. 341:1607-10.

Dzhala VI and Staley KJ (2003) Transition from interictal to ictal activity in limbic networks in vitro. J Neurosci. 23:7873-80.

Ebert U and Loscher W (1995) Differences in mossy fibre sprouting during conventional and rapid amygdala kindling of the rat. Neurosci Lett. 190:199-202.

Engel J Jr (1996) Introduction to temporal lobe epilepsy. Epilepsy Res. 26, 141-150.

Engel J Jr (2001) Intractable epilepsy: definition and neurobiology. Epilepsia. 42 Suppl 6:3.

Engel J Jr, Wiebe S, French J, Sperling M, Williamson P, Spencer D, Gumnit R, Zahn C, Westbrook E and Enos B (2003) Practice parameter: temporal lobe and localized neocortical resections for epilepsy. Epilepsia. 44:741-51.

Faber ES, Callister RJ and Sah P (2001) Morphological and electrophysiological properties of principal neurons in the rat lateral amygdala in vitro. J Neurophysiol. 85:714-23.

Faulkner B and Brown TH (1999) Morphology and physiology of neurons in the rat perirhinal-lateral amygdala area. J Comp Neurol. 411:613-42.

Finch DM and Babb TL (1980) Inhibition in subicular and entorhinal principal neurons in response to electrical stimulation of the fornix and hippocampus. Brain Res. 196, 89-98.

Finch DM and Babb TL (1981). Demonstration of caudally directed hippocampal efferents in the rat by intracellular injection of horseradish peroxidase. Brain Res. 214, 405-410.

Finch DM, Tan AM and Isokawa-Akesson M (1988) Feedforward inhibition of the rat entorhinal cortex and subicular complex. J Neurosci. 8, 2213-2226.

Finch DM, Wong EE, Derian EL, Chen XH, Nowlin-Finch NL and Brothers LA (1986) Neurophysiology of limbic system pathways in the rat: projections from the amygdala to the entorhinal cortex. Brain Res 370: 273–284.

Fountain NB, Bear J, Bertram EH 3rd and Lothman EW (1998) Responses of deep entorhinal cortex are epileptiform in an electrogenic rat model of chronic temporal lobe epilepsy. J Neurophysiol 80: 230-240.

French JA, Williamson PD, Thadani VM, Darcey TM, Mattson RH, Spencer SS and Spencer DD (1993) Characteristics of medial temporal lobe epilepsy: I. Results of history and physical examination. Ann Neurol. 34:774-80.

Freund TF and Buzsaki G (1996) Interneurons of the hippocampus. Hippocampus. 6:347-470.

Friedman LK, Pellegrini-Giampietro DE, Sperber EF, Bennett MV, Moshe SL and Zukin RS (1994) Kainate-induced status epilepticus alters glutamate and $GABA_A$ receptor gene expression in adult rat hippocampus: an in situ hybridization study. J Neurosci. 14:2697-707.

Fujikawa DG (1996) The temporal evolution of neuronal damage from pilocarpine-induced status epilepticus. Brain Res. 725:11-22.

Gabrieli JD, Brewer JB, Desmond JE and Glover GH (1997) Separate neural bases of two fundamental memory processes in the human medial temporal lobe. Science. 276:264-6.

Gambardella A, Gotman J, Cendes F and Andermann F (1995) The relationship of spike foci and of clinical seizure characteristics to different patterns of mesial temporal atrophy. Arch. Neurol. 52, pp. 287–293.

Gean PW (1990) The epileptiform activity induced by 4-aminopyridine in rat amygdala slices: antagonism by non-N-methyl-D-aspartate receptor antagonists. Brain Res 530: 251–256.

Gean PW and Shinnick-Gallagher P (1988) Epileptiform activity induced by magnesium-free solution in slices of rat amygdala: antagonism by N-methyl-D-aspartate receptor antagonists. Neuropharmacology 27: 557–562.

Gean PW, Shinnick-Gallagher P and Anderson AC (1989) Spontaneous epileptiform activity and alteration of GABA- and of NMDA-mediated neurotransmission in amygdala neurons kindled in vivo. Brain Res. 494:177-81.

Gibbs JW 3rd, Shumate MD and Coulter DA (1997) Differential epilepsy-associated alterations in postsynaptic GABA(A) receptor function in dentate granule and CA1 neurons. J Neurophysiol. 77:1924-38.

Gloor P (1992) Role of the amygdala in temporal lobe epilepsy. In: J. Aggleton, Editor, The amygdala: neurobiological aspects of emotion, memory and mental dysfunction. New York: Wiley-Liss, pp. 505–538.

Gloor P (1997) The temporal lobe and limbic system. New York: Oxford University Press.

Goddard GV (1967) Development of epileptic seizures through brain stimulation at low intensity. Nature. 214:1020-1.

Goddard GV, McIntyre DC and Leech CK (1969) A permanent change in brain function resulting from daily electrical stimulation. Exp Neurol. 25:295-330.

Gorter JA, van Vliet EA, Aronica E and Lopes da Silva FH (2001) Progression of spontaneous seizures after status epilepticus is associated with mossy fibre sprouting and extensive bilateral loss of hilar parvalbumin and somatostatin-immunoreactive neurons. Eur J Neurosci. 13:657-69.

Greene JR and Totterdell S (1997) Morphology and distribution of electrophysiologically defined classes of pyramidal and nonpyramidal neurons in rat ventral subiculum in vitro. J. Comp. Neurol. 380, 395-408.

Grigorenko E, Glazier S, Bell W, Tytell M, Nosel E, Pons T and Deadwyler SA (1997) Changes in glutamate receptor subunit composition in hippocampus and cortex in patients with refractory epilepsy. J Neurol Sci. 153:35-45.

Gupta A, Wang Y and Markram H (2000) Organizing principles for a diversity of GABAergic interneurons and synapses in the neocortex. Science. 287:273-8.

Hablitz JJ (1984) Picrotoxin-induced epileptiform activity in hippocampus: role of endogenous versus synaptic factors. J Neurophysiol. 51:1011-27.

Harris E and Stewart M (2001) Intrinsic connectivity of the rat subiculum: II. Properties of synchronous spontaneous activity and a demonstration of multiple generator regions. J Comp Neurol. 435, 506-518.

Heinbockel T and Pape HC (1999) Modulatory effects of adenosine on inhibitory postsynaptic potentials in the lateral amygdala of the rat. Br J Pharmacol. 128:190-6.

Heinemann U, Arens J, Dreier JP, Stabel J and Zhang CL (1991) In vitro epileptiform activity: role of excitatory amino acids. Epilepsy Res. 10:18-23.

Heinemann U, Beck H, Dreier JP, Ficker E, Stabel J and Zhang CL (1992) The dentate gyrus as a regulated gate for the propagation of epileptiform activity. Epilepsy Res Suppl. 7, 273-280.

Henry TR, Frey KA, Sackellares JC, Gilman S, Koeppe RA, Brunberg JA, Ross DA, Berent S, Young AB and Kuhl DE (1993) In vivo cerebral metabolism and central benzodiazepine-receptor binding in temporal lobe epilepsy. Neurology. 43:1998-2006.

Henze DA, Urban NN and Barrionuevo G (2000) The multifarious hippocampal mossy fiber pathway: a review. Neuroscience. 98:407-27

Hirsch JC, Agassandian C, Merchan-Perez A, Ben-Ari Y, DeFelipe J, Esclapez M and Bernard C (1999) Deficit of quantal release of GABA in experimental models of temporal lobe epilepsy. Nat Neurosci. 2:499-500.

Hoffman DA, Magee JC, Colbert CM and Johnston D (1997) K+ channel regulation of signal propagation in dendrites of hippocampal pyramidal neurons. Nature. 387:869-75.

Holmes KH, Bilkey DK and Laverty R (1992) The infusion of an NMDA antagonist into perirhinal cortex suppresses amygdala-kindled seizures. Brain Res. 587:285-90.

Houser CR (1999) Neuronal loss and synaptic reorganization in temporal lobe epilepsy. Adv. Neurol. 79, 743-761.

Houser CR, Miyashiro JE, Swartz BE, Walsh GO, Rich JR and Delgado-Escueta AV (1990) Altered patterns of dynorphin immunoreactivity suggest mossy fiber reorganization in human hippocampal epilepsy. J. Neurosci. 10, 267-282.

Hudson LP, Munoz DG, Miller L, McLachlan RS, Girvin JP and Blume WT (1993) Amygdaloid sclerosis in temporal lobe epilepsy. Ann Neurol. 33:622-31.

Jack CR Jr (1994) MRI-based hippocampal volume measurements in epilepsy. Epilepsia. 35 Suppl 6:S21-9.

Jarvie PA, Logan TC, Geula C and Slevin JT (1990) Entorhinal kindling permanently enhances Ca2+-dependent -glutamate release in regio inferior of rat hippocampus. Brain Res. 508, pp. 188–193.

Johnson EW, de Lanerolle NC, Kim JH, Sundaresan S, Spencer DD, Mattson RH, Zoghbi SS, Baldwin RM, Hoffer PB, Seibyl JP, et al. (1992) "Central" and "peripheral" benzodiazepine receptors: opposite changes in human epileptogenic tissue. Neurology. 42:811-5.

Johnston D, Hoffman DA, Magee JC, Poolos NP, Watanabe S, Colbert CM and Migliore M (2000) Dendritic potassium channels in hippocampal pyramidal neurons. J Physiol. 525:75-81.

Jones RS and Lambert JD (1990a) Synchronous discharges in the rat entorhinal cortex in vitro: site of initiation and the role of excitatory amino acid receptors. Neuroscience. 34:657-70.

Jones RS and Lambert JD (1990b) The role of excitatory amino acid receptors in the propagation of epileptiform discharges from the entorhinal cortex to the dentate gyrus in vitro. Exp Brain Res. 80:310-22.

Jones MV and Westbrook GL (1996) The impact of receptor desensitization on fast synaptic transmission. Trends Neurosci. 19:96-101.

Jung HY, Staff NP and Spruston N (2001) Action potential bursting in subicular pyramidal neurons is driven by a calcium tail current. J Neurosci. 21:3312-21.

Jutila L, Ylinen A, Partanen K, Alafuzoff I, Mervaala E, Partanen J, Vapalahti M, Vainio P and Pitkanen A (2001) MR volumetry of the entorhinal, perirhinal, and temporopolar cortices in drug-refractory temporal lobe epilepsy. AJNR Am J Neuroradiol. 22:1490-501.

Kaila K (1994) Ionic basis of $GABA_A$ receptor channel function in the nervous system. Prog Neurobiol. 42:489-537

Kajiwara R, Takashima I, Mimura Y, Witter MP and Iijima T (2003) Amygdala input promotes spread of excitatory neural activity from perirhinal cortex to the entorhinal-hippocampal circuit. J Neurophysiol. 89:2176-84.

Kamphuis W, Huisman E, Dreijer AM, Ghijsen WE, Verhage M and Lopes da Silva FH (1990) Kindling increases the K(+)-evoked Ca2(+)-dependent release of endogenous GABA in area CA1 of rat hippocampus. Brain Res. 511:63-70.

Kano T, Inaba Y and Avoli M (2005) Periodic oscillatory activity in parahippocampal slices maintained in vitro. Neuroscience. 130:1041-53.

Kaura S, Bradford HF, Young AM, Croucher MJ and Hughes PD (1995) Effect of amygdaloid kindling on the content and release of amino acids from the amygdaloid complex: in vivo and in vitro studies. J Neurochem. 65:1240-9.

Kawaguchi Y and Hama K (1987) Fast-spiking non-pyramidal cells in the hippocampal CA3 region, dentate gyrus and subiculum of rats. Brain Res. 425, 351-355.

Keller SS, Wilke M, Wieshmann UC, Sluming VA and Roberts N (2004) Comparison of standard and optimized voxel-based morphometry for analysis of brain changes associated with temporal lobe epilepsy. Neuroimage. 23:860-8

Kelly ME and McIntyre DC (1996) Perirhinal cortex involvement in limbic kindled seizures. Epilepsy Res. 26:233-43.

Kerr DI and Ong J (1995) $GABA_B$ receptors. Pharmacol Ther. 67:187-246.

Kew JN and Kemp JA (2005) Ionotropic and metabotropic glutamate receptor structure and pharmacology. Psychopharmacology (Berl). 179:4-29

Kimura A and Pavlides C (2000) Long-term potentiation/depotentiation are accompanied by complex changes in spontaneous unit activity in the hippocampus. J Neurophysiol 84: 1894–1906.

Kita H and Armstrong W (1991) A biotin-containing compound N-(2-aminoethyl)biotinamide for intracellular labeling and neuronal tracing studies: comparison with biocytin. J Neurosci Methods. 37:141-50.

Klapstein GJ, Meldrum BS and Mody I (1999) Decreased sensitivity to Group III mGluR agonists in the lateral perforant path following kindling. Neuropharmacology. 38:927-33.

Klueva J, Munsch T, Albrecht D and Pape HC (2003) Synaptic and non-synaptic mechanisms of amygdala recruitment into temporolimbic epileptiform activities. Eur J Neurosci. 18:2779-91.

Knopp A, Kivi A, Wozny C, Heinemann U and Behr J (2005) Cellular and network properties of the subiculum in the pilocarpine model of temporal lobe epilepsy. J Comp Neurol. 483:476-88.

Köhling R, Vreugdenhil M, Bracci E and Jefferys JG (2000) Ictal epileptiform activity is facilitated by hippocampal $GABA_A$ receptor-mediated oscillations. J Neurosci 20: 6820–6829.

Kohr G, De Koninck Y and Mody I (1993) Properties of NMDA receptor channels in neurons acutely isolated from epileptic (kindled) rats. J Neurosci. 13:3612-27.

Kojima N, Ishibashi H, Obata K and Kandel ER (1998) Higher seizure susceptibility and enhanced tyrosine phosphorylation of N-methyl-D-aspartate receptor subunit 2B in fyn transgenic mice. Learn Mem. 5:429-45.

Kral T, Erdmann E, Sochivko D, Clusmann H, Schramm J and Dietrich D (2003) Down-regulation of mGluR8 in pilocarpine epileptic rats. Synapse. 47:278-84.

Kraus JE and McNamara JO (1998) Measurement of NMDA receptor protein subunits in discrete hippocampal regions of kindled animals. Brain Res Mol Brain Res. 61:114-20.

Lamsa K and Kaila K (1997) Ionic mechanisms of spontaneous GABAergic events in rat hippocampal slices exposed to 4-aminopyridine. J Neurophysiol. 78, 2582-2591.

Lamsa K and Taira T (2003) Use-dependent shift from inhibitory to excitatory $GABA_A$ receptor action in SP-O interneurons in the rat hippocampal CA3 area. J Neurophysiol. 90:1983-95.

Lang EJ and Pare D (1997) Similar inhibitory processes dominate the responses of cat lateral amygdaloid projection neurons to their various afferents. J Neurophysiol. 77:341-52.

Lang EJ and Pare D (1998) Synaptic responsiveness of interneurons of the cat lateral amygdaloid nucleus. Neuroscience. 83:877-89.

Lebeda FJ, Hablitz JJ and Johnston D (1982) Antagonism of GABA-mediated responses by d-tubocurarine in hippocampal neurons. J Neurophysiol. 48:622-32.

LeDoux JE (2000) Emotion circuits in the brain. Annu Rev Neurosci 23: 155–184.

Lee JW, Andermann F, Dubeau F, Bernasconi A, MacDonald D, Evans A and Reutens DC (1998) Morphometric analysis of the temporal lobe in temporal lobe epilepsy. Epilepsia. 39:727-36.

Le Gal La Salle G (1976) Unitary responses in the amygdaloid complex following stimulation of various diencephalic structures. Brain Res. 118:475-8.

Lehmann TN, Gabriel S, Eilers A, Njunting M, Kovacs R, Schulze K, Lanksch WR and Heinemann U (2001) Fluorescent tracer in pilocarpine-treated rats shows widespread aberrant hippocampal neuronal connectivity. Eur J Neurosci. 14:83-95.

Lieberman DN and Mody I (1999) Properties of single NMDA receptor channels in human dentate gyrus granule cells. J Physiol. 518:55-70.

Liu G (2004) Local structural balance and functional interaction of excitatory and inhibitory synapses in hippocampal dendrites. Nat Neurosci. 7:373-9.

Liu Z, Nagao T, Desjardins GC, Gloor P and Avoli M (1994) Quantitative evaluation of neuronal loss in the dorsal hippocampus in rats with long-term pilocarpine seizures. Epilepsy Res. 17, 237-47.

Longo BM and Mello LE (1997) Blockade of pilocarpine- or kainate-induced mossy fiber sprouting by cycloheximide does not prevent subsequent epileptogenesis in rats. Neurosci Lett. 226:163-6.

Longo BM and Mello LE (1998) Supragranular mossy fiber sprouting is not necessary for spontaneous seizures in the intrahippocampal kainate model of epilepsy in the rat. Epilepsy Res. 32:172-82.

Lopantsev V and Avoli M (1998a) Participation of $GABA_A$-mediated inhibition in ictal-like discharges in the rat entorhinal cortex. J Neurophysiol 79: 352–360.

Lopantsev V and Avoli M (1998b) Laminar organization of epileptiform discharges in the rat entorhinal cortex in vitro. J Physiol (Lond) 509: 785–796.

Lopes da Silva FH, Witter MP, Boeijinga PH and Lohman AH (1990) Anatomic organization and physiology of the limbic cortex. Physiol Rev. 70:453-511.

Loscher W (1997) Animal models of intractable epilepsy. Prog Neurobiol. 53:239-58.

Loscher W (2002) Animal models of epilepsy for the development of antiepileptogenic and disease-modifying drugs. A comparison of the pharmacology of kindling and post-status epilepticus models of temporal lobe epilepsy. Epilepsy Res. 50:105-23.

Lothman EW, Bertram EH 3rd and Stringer JL (1991) Functional anatomy of hippocampal seizures. Prog Neurobiol. 37:1-82.

Lothman EW, Stringer JL and Bertram EH (1992) The dentate gyrus as a control point for seizures in the hippocampus and beyond. Epilepsy Res Suppl. 7:301-13.

Maccaferri G and Lacaille JC (2003) Interneuron Diversity series: Hippocampal interneuron classifications--making things as simple as possible, not simpler. Trends Neurosci. 26:564-71.

Maccaferri G and McBain CJ (1995) Passive propagation of LTD to stratum oriens-alveus inhibitory neurons modulates the temporoammonic input to the hippocampal CA1 region. Neuron 15: 137-145.

Macdonald RL and Olsen RW (1994) $GABA_A$ receptor channels. Annu Rev Neurosci. 17:569-602.

Madison DV, Malenka RC and Nicoll RA (1991) Mechanisms underlying long-term potentiation of synaptic transmission. Annu Rev Neurosci. 14:379-97.

Mangan PS and Lothman EW (1996) Profound disturbances of pre- and postsynaptic $GABA_B$-receptor-mediated processes in region CA1 in a chronic model of temporal lobe epilepsy. J Neurophysiol. 76:1282-96.

Mangan PS, Scott CA, Williamson JM and Bertram EH (2000) Aberrant neuronal physiology in the basal nucleus of the amygdala in a model of chronic limbic epilepsy. Neuroscience. 101:377-91.

Martina M, Royer S and Pare D (2001) Cell-type-specific GABA responses and chloride homeostasis in the cortex and amygdala. J Neurophysiol. 86:2887-95.

Mathern GW, Cifuentes F, Leite JP, Pretorius JK and Babb TL (1993) Hippocampal EEG excitability and chronic spontaneous seizures are associated with aberrant synaptic reorganization in the rat intrahippocampal kainate model. Electroencephalogr Clin Neurophysiol. 87:326-39.

Mathern GW, Mendoza D, Lozada A, Pretorius JK, Dehnes Y, Danbolt NC, Nelson N, Leite JP, Chimelli L, Born DE, Sakamoto AC, Assirati JA, Fried I, Peacock WJ, Ojemann GA and Adelson PD (1999) Hippocampal GABA and glutamate transporter immunoreactivity in patients with temporal lobe epilepsy. Neurology. 52:453-72.

Mathern GW, Pretorius JK, Kornblum HI, Mendoza D, Lozada A, Leite JP, Chimelli LM, Fried I, Sakamoto AC, Assirati JA, Levesque MF, Adelson PD and Peacock WJ (1997) Human hippocampal AMPA and NMDA mRNA levels in temporal lobe epilepsy patients. Brain. 120:1937-59.

Mattia D, Hwa GG and Avoli M (1993) Membrane properties of rat subicular neurons in vitro. J Neurophysiol. 70:1244-8.

Mayer ML and Armstrong N (2004) Structure and function of glutamate receptor ion channels. Annu Rev Physiol. 66:161-81.

Mayer ML and Westbrook GL (1987) The physiology of excitatory amino acids in the vertebrate central nervous system. Prog Neurobiol. 28:197-276.

McCormick DA and Contreras D (2001) On the cellular and network bases of epileptic seizures. Annu Rev Physiol. 63:815-46.

McDonald JW, Garofalo EA, Hood T, Sackellares JC, Gilman S, McKeever PE, Troncoso JC and Johnston MV (1991) Altered excitatory and inhibitory amino acid receptor binding in hippocampus of patients with temporal lobe epilepsy. Ann Neurol. 29:529-41.

McIntyre DC and Kelly ME (2000) The parahippocampal cortices and kindling. Ann N Y Acad Sci. 911:343-54.

McIntyre DC, Kelly ME and Armstrong JN (1993) Kindling in the perirhinal cortex. Brain Res. 615:1-6.

McIntyre DC and Plant JR (1989) Pyriform cortex involvement in kindling. Neurosci Biobehav Rev. 13:277-80.

McIntyre DC and Plant JR (1993) Long-lasting changes in the origin of spontaneous discharges from amygdala-kindled rats: piriform vs. perirhinal cortex in vitro. Brain Res. 624:268-76.

McIntyre DC, Poulter MO and Gilby K (2002) Kindling: some old and some new. Epilepsy Res. 50:79-92.

Meldrum BS (1999) Antiepileptic drugs potentiating GABA. Electroencephalogr Clin Neurophysiol Suppl. 50:450-7.

Meldrum BS (2000) Glutamate as a neurotransmitter in the brain: review of physiology and pathology. J Nutr. 130(4S Suppl):1007S-15S.

Meldrum BS, Akbar MT and Chapman AG (1999) Glutamate receptors and transporters in genetic and acquired models of epilepsy. Epilepsy Res. 36:189-204.

Mello LE, Cavalheiro EA, Tan AM, Kupfer WR, Pretorius JK, Babb TL and Finch DM (1993) Circuit mechanisms of seizures in the pilocarpine model of chronic epilepsy: cell loss and mossy fiber sprouting. Epilepsia. 34:985-95.

Menendez de la Prida L (2003) Control of bursting by local inhibition in the rat subiculum in vitro. J Physiol. 549, 219-230.

Menendez de la Prida L and Gal B (2004) Synaptic contributions to focal and widespread spatiotemporal dynamics in the isolated rat subiculum in vitro. J Neurosci. 24, 5525-5536.

Menendez de la Prida L and Pozo MA (2002) Excitatory and inhibitory control of epileptiform discharges in combined hippocampal/entorhinal cortical slices. Brain Res. 940, 27-35.

Menendez de la Prida L, Suarez F and Pozo MA (2003) Electrophysiological and morphological diversity of neurons from the rat subicular complex in vitro. Hippocampus 13, 728-744.

Michalakis M, Holsinger D, Ikeda-Douglas C, Cammisuli S, Ferbinteanu J, DeSouza C, DeSouza S, Fecteau J, Racine RJ and Milgram NW (1998) Development of spontaneous seizures over extended electrical kindling. I. Electrographic, behavioral, and transfer kindling correlates. Brain Res. 793:197-211.

Michelson HB and Wong RK (1994) Synchronization of inhibitory neurones in the guinea-pig hippocampus in vitro. J Physiol. 477, 35-45.

Mikkonen M, Soininen H, Kalvianen R, Tapiola T, Ylinen A, Vapalahti M, Paljarvi L and Pitkanen A (1998) Remodeling of neuronal circuitries in human temporal lobe epilepsy: increased expression of highly polysialylated neural cell adhesion molecule in the hippocampus and the entorhinal cortex. Ann Neurol. 44:923-34.

Mikuni N, Babb TL and Christi W (1999) Increased NR1-NR2A/B coassembly as a mechanism for rat chronic hippocampal epilepsy. Neurosci Lett. 267:165-8.

Miles R and Wong RK (1986) Excitatory synaptic interactions between CA3 neurons in the guinea-pig hippocampus. J Physiol 373: 397–418.

Miles R and Wong RK (1987) Inhibitory control of local excitatory circuits in the guinea-pig hippocampus. J Physiol. 388, 611-629.

Miles R, Traub RD and Wong RK (1988) Spread of synchronous firing in longitudinal slices from the CA3 region of the hippocampus. J Neurophysiol. 60, 1481-96.

Miller RJ (1998) Presynaptic receptors. Annu Rev Pharmacol Toxicol. 38:201-27.

Miller HP, Levey AI, Rothstein JD, Tzingounis AV and Conn PJ (1997) Alterations in glutamate transporter protein levels in kindling-induced epilepsy. J Neurochem. 68:1564-70.

Miller LA, McLachlan RS, Bouwer MS, Hudson LP and Munoz DG (1994) Amygdalar sclerosis: preoperative indicators and outcome after temporal lobectomy. J Neurol Neurosurg Psychiatry. 57:1099-105.

Mody I (1998) Ion channels in epilepsy. Int Rev Neurobiol. 42:199-226

Mody I and Heinemann U (1987) NMDA receptors of dentate gyrus granule cells participate in synaptic transmission following kindling. Nature. 326:701-4.

Moran NF, Lemieux L, Kitchen ND, Fish DR and Shorvon SD (2001) Extrahippocampal temporal lobe atrophy in temporal lobe epilepsy and mesial temporal sclerosis. Brain. 124:167-75.

Mori E, Ikeda M, Hirono N, Kitagaki H, Imamura T and Shimomura T (1999) Amygdalar volume and emotional memory in Alzheimer's disease. Am J Psychiatry. 156:216-22.

Morimoto K, Fahnestock M and Racine RJ (2004) Kindling and status epilepticus models of epilepsy: rewiring the brain. Prog Neurobiol. 73:1-60.

Morris JS, Frith CD, Perrett DI, Rowland D, Young AW, Calder AJ and Dolan RJ (1996) A differential neural response in the human amygdala to fearful and happy facial expressions. Nature. 383:812-5.

Nadler JV (2003) The recurrent mossy fiber pathway of the epileptic brain. Neurochem Res. 28:1649-58

Nagao T, Alonso A and Avoli M (1996) Epileptiform activity induced by pilocarpine in the rat hippocampal-entorhinal slice preparation. Neuroscience 72: 399–408.

Nakanishi S (1992) Molecular diversity of glutamate receptors and implications for brain function. Science. 258:597-603.

Nathan T, Jensen MS and Lambert JD (1990) The slow inhibitory postsynaptic potential in rat hippocampal CA1 neurones is blocked by intracellular injection of QX-314. Neurosci Lett. 110:309-13.

Natsume J, Bernasconi N, Andermann F and Bernasconi A (2003) MRI volumetry of the thalamus in temporal, extratemporal, and idiopathic generalized epilepsy. Neurology. 60:1296-300.

Nissinen J, Halonen T, Koivisto E and Pitkanen A (2000) A new model of chronic temporal lobe epilepsy induced by electrical stimulation of the amygdala in rat. Epilepsy Res. 38:177-205.

Niittykoski M, Nissinen J, Penttonen M and Pitkanen A (2004) Electrophysiologic changes in the lateral and basal amygdaloid nuclei in temporal lobe epilepsy: an in vitro study in epileptic rats. Neuroscience. 124:269-81.

Nonaka M, Kohmura E, Yamashita T, Shimada S, Tanaka K, Yoshimine T, Tohyama M and Hayakawa T (1998) Increased transcription of glutamate-aspartate transporter (GLAST/GluT-1) mRNA following kainic acid-induced limbic seizure. Brain Res Mol Brain Res. 55:54-60.

Nusser Z, Hajos N, Somogyi P and Mody I (1998) Increased number of synaptic GABA(A) receptors underlies potentiation at hippocampal inhibitory synapses. Nature. 395:172-7.

Olsen RW, Bureau M, Houser CR, Delgado-Escueta AV, Richards JG and Mohler H (1992) GABA/benzodiazepine receptors in human focal epilepsy. Epilepsy Res Suppl. 8:383-91.

O'Mara SM, Commins S, Anderson M and Gigg J (2001) The subiculum: a review of form, physiology and function. Prog Neurobiol. 64, 129-155.

O'Shea RD (2002) Roles and regulation of glutamate transporters in the central nervous system. Clin Exp Pharmacol Physiol. 29:1018-23

Otis TS, De Koninck Y and Mody I (1994) Lasting potentiation of inhibition is associated with an increased number of gamma-aminobutyric acid type A receptors activated during miniature inhibitory postsynaptic currents. Proc Natl Acad Sci U S A. 91:7698-702.

Palma E, Spinelli G, Torchia G, Martinez-Torres A, Ragozzino D, Miledi R and Eusebi F (2005) Abnormal $GABA_A$ receptors from the human epileptic hippocampal subiculum microtransplanted to Xenopus oocytes. Proc Natl Acad Sci U S A. 102:2514-8.

Paré D, de Curtis M, and Llinás R (1992) Role of hippocampal-entorhinal loop in temporal lobe epilepsy: extra- and intracellular study in the isolated guinea pig brain in vitro. J Neurosci 12: 1857-1881.

Paré D, Quirk GJ and Ledoux JE (2004) New vistas on amygdala networks in conditioned fear. J Neurophysiol. 92:1-9.

Paxinos G and Watson C (1998) The rat brain in stereotaxic coordinates, 4th edition. San Diego, CA, USA: Academic Press

Pelletier JG, Apergis J and Pare D (2004) Low-probability transmission of neocortical and entorhinal impulses through the perirhinal cortex. J Neurophysiol. 91: 2079-89.

Pelletier JG, Apergis-Schoute J and Pare D (2005) Interaction between amygdala and neocortical inputs in the perirhinal cortex. J Neurophysiol. 94:1837-48.

Perkins KL and Wong RK (1995) Intracellular QX-314 blocks the hyperpolarization-activated inward current Iq in hippocampal CA1 pyramidal cells. J Neurophysiol. 73:911-5.

Perreault P and Avoli M (1989) Effects of low concentrations of 4-aminopyridine on CA1 pyramidal cells of the hippocampus. J Neurophysiol. 61, 953-970.

Perreault P and Avoli M (1991) Physiology and pharmacology of epileptiform activity induced by 4-aminopyridine in rat hippocampal slices. J Neurophysiol 65: 771–785.

Perreault P and Avoli M (1992) 4-aminopyridine-induced epileptiform activity and a GABA-mediated long-lasting depolarization in the rat hippocampus. J Neurosci. 12, 104-115.

Perucca E (2005) An introduction to antiepileptic drugs. Epilepsia. 46 Suppl 4:31-7.

Pikkarainen M and Pitkanen A (2001) Projections from the lateral, basal and accessory basal nuclei of the amygdala to the perirhinal and postrhinal cortices in rat. Cereb Cortex. 11:1064-82.

Pinel JP and Rovner LI (1978) Experimental epileptogenesis: kindling-induced epilepsy in rats. Exp Neurol. 58:190-202.

Pitkanen A and Amaral DG (1994) The distribution of GABAergic cells, fibers, and terminals in the monkey amygdaloid complex: an immunohistochemical and in situ hybridization study. J Neurosci. 14:2200-24.

Pitkanen A, Jolkkonen E and Kemppainen S (2000a) Anatomic heterogeneity of the rat amygdaloid complex. Folia Morphol (Warsz). 59(1):1-23.

Pitkanen A, Pikkarainen M, Nurminen N and Ylinen A (2000b) Reciprocal connections between the amygdala and the hippocampal formation, perirhinal cortex, and postrhinal cortex in rat. A review. Ann N Y Acad Sci. 911:369-91

Pitkanen A, Savander V and LeDoux JE (1997) Organization of intra-amygdaloid circuitries in the rat: an emerging framework for understanding functions of the amygdala. Trends Neurosci. 20:517-23.

Pitkanen A, Stefanacci L, Farb CR, Go GG, LeDoux JE and Amaral DG (1995) Intrinsic connections of the rat amygdaloid complex: projections originating in the lateral nucleus. J Comp Neurol. 356:288-310

Pitkanen A, Tuunanen J, Kalviainen R, Partanen K and Salmenpera T (1998) Amygdala damage in experimental and human temporal lobe epilepsy. Epilepsy Res. 32:233-53.

Platenik J, Kuramoto N and Yoneda Y (2000) Molecular mechanisms associated with long-term consolidation of the NMDA signals. Life Sci. 67:335-64.

Priel MR, dos Santos NF and Cavalheiro EA (1996) Developmental aspects of the pilocarpine model of epilepsy. Epilepsy Res. 26:115-21.

Proper EA, Hoogland G, Kappen SM, Jansen GH, Rensen MG, Schrama LH, van Veelen CW, van Rijen PC, van Nieuwenhuizen O, Gispen WH and de Graan PN (2002) Distribution of glutamate transporters in the hippocampus of patients with pharmaco-resistant temporal lobe epilepsy. Brain. 125:32-43.

Proper EA, Oestreicher AB, Jansen GH, Veelen CW, van Rijen PC, Gispen WH and de Graan PN (2000) Immunohistochemical characterization of mossy fibre sprouting in the hippocampus of patients with pharmaco-resistant temporal lobe epilepsy. Brain. 123:19-30.

Racine RJ (1972a) Modification of seizure activity by electrical stimulation. I. After-discharge threshold. Electroencephalogr Clin Neurophysiol. 32:269-79.

Racine RJ (1972b) Modification of seizure activity by electrical stimulation. II. Motor seizure. Electroencephalogr Clin Neurophysiol. 32:281-94.

Racine RJ (1975) Modification of seizure activity by electrical stimulation: cortical areas. Electroencephalogr Clin Neurophysiol. 38:1-12.

Racine R (1978) Kindling: the first decade. Neurosurgery. 3:234-52.

Rafiki A, Ben-Ari Y, Khrestchatisky M and Represa A (1998) Long-lasting enhanced expression in the rat hippocampus of NMDAR1 splice variants in a kainate model of epilepsy. Eur J Neurosci. 10:497-507.

Rafiq A, DeLorenzo RJ and Coulter DA (1993) Generation and propagation of epileptiform discharges in a combined entorhinal cortex/hippocampal slice. J Neurophysiol. 70:1962-74.

Rainnie DG, Asprodini EK and Shinnick-Gallagher P (1992) Kindling-induced long-lasting changes in synaptic transmission in the basolateral amygdala. J Neurophysiol. 67:443-54.

Rice A, Rafiq A, Shapiro SM, Jakoi ER, Coulter DA and DeLorenzo RJ (1996) Long-lasting reduction of inhibitory function and gamma-aminobutyric acid type A receptor subunit mRNA expression in a model of temporal lobe epilepsy. Proc Natl Acad Sci U S A. 93:9665-9.

Rivera C, Voipio J, Payne JA, Ruusuvuori E, Lahtinen H, Lamsa K, Pirvola U, Saarma M and Kaila K (1999) The K+/Cl– co-transporter KCC2 renders GABA hyperpolarizing during neuronal maturation. Nature 397, 251–255.

Robbins RJ, Brines ML, Kim JH, Adrian T, de Lanerolle N, Welsh S and Spencer DD (1991) A selective loss of somatostatin in the hippocampus of patients with temporal lobe epilepsy. Ann Neurol. 29:325-32.

Roch C, Leroy C, Nehlig A and Namer IJ (2002a) Magnetic resonance imaging in the study of the lithium-pilocarpine model of temporal lobe epilepsy in adult rats. Epilepsia. 43:325-35.

Roch C, Leroy C, Nehlig A and Namer IJ (2002b) Predictive value of cortical injury for the development of temporal lobe epilepsy in 21-day-old rats: an MRI approach using the lithium-pilocarpine model. Epilepsia. 43:1129-36.

Ronne-Engstrom E, Hillered L, Flink R, Spannare B, Ungerstedt U and Carlson H (1992) Intracerebral microdialysis of extracellular amino acids in the human epileptic focus. J Cereb Blood Flow Metab. 12:873-6.

Rudy B (1988) Diversity and ubiquity of K channels. Neuroscience. 25, 729-749.

Rutecki PA, Grossman RG, Armstrong D and Irish-Loewen SJ (1989) Electrophysiological connections between the hippocampus and entorhinal cortex in patients with complex partial seizures. J Neurosurg 70: 667–675.

Rutecki PA, Lebeda FJ and Johnston D (1985) Epileptiform activity induced by changes in extracellular potassium in hippocampus. J Neurophysiol. 54:1363-74.

Rutecki PA, Lebeda FJ and Johnston D (1987) 4-Aminopyridine produces epileptiform activity in hippocampus and enhances synaptic excitation and inhibition. J Neurophysiol. 57, 1911-1924.

Rutecki PA, Lebeda FJ and Johnston D (1990) Epileptiform activity in the hippocampus produced by tetraethylammonium. J Neurophysiol 64: 1077–1088.

Salanova V, Markand ON and Worth R (1994) Clinical characteristics and predictive factors in 98 patients with complex partial seizures treated with temporal resection. Arch Neurol. 51:1008-13.

Salmenpera T, Kalviainen R, Partanen K, Mervaala E and Pitkanen A (2000) MRI volumetry of the hippocampus, amygdala, entorhinal cortex, and perirhinal cortex after status epilepticus. Epilepsy Res. 40:155-70.

Sanabria ER, Su H and Yaari Y (2001) Initiation of network bursts by Ca2+-dependent intrinsic bursting in the rat pilocarpine model of temporal lobe epilepsy. J Physiol. 532:205-16.

Sanchez RM, Wang C, Gardner G, Orlando L, Tauck DL, Rosenberg PA, Aizenman E and Jensen FE (2000) Novel role for the NMDA receptor redox modulatory site in the pathophysiology of seizures. J Neurosci. 20:2409-17.

Sandok EK, O'Brien TJ, Jack CR and So EL (2000) Significance of cerebellar atrophy in intractable temporal lobe epilepsy: a quantitative MRI study. Epilepsia. 41:1315-20.

Sato M, Racine RJ and McIntyre DC (1990) Kindling: basic mechanisms and clinical validity. Electroencephalogr Clin Neurophysiol. 76:459-72.

Savic I, Persson A, Roland P, Pauli S, Sedvall G and Widen L (1988) In-vivo demonstration of reduced benzodiazepine receptor binding in human epileptic foci. Lancet. 2:863-6.

Scanziani M, Salin PA, Vogt KE, Malenka RC and Nicoll RA (1997) Use-dependent increases in glutamate concentration activate presynaptic metabotropic glutamate receptors. Nature 385: 630–634.

Scharfman HE (1995) Electrophysiological evidence that dentate hilar mossy cells are excitatory and innervate both granule cells and interneurons.J Neurophysiol. 74:179-94.

Scharfman HE, Kunkel DD and Schwartzkroin PA (1990) Synaptic connections of dentate granule cells and hilar neurons: results of paired intracellular recordings and intracellular horseradish peroxidase injections. Neuroscience. 90;37(3):693-707.

Schwartz-Bloom RD and Sah R (2001) gamma-Aminobutyric acid(A) neurotransmission and cerebral ischemia. J Neurochem. 77:353-71.

Schwartzkroin PA (1994) Cellular electrophysiology of human epilepsy. Epilepsy Res. 17(3):185-92.

Schwartzkroin PA and Prince DA (1977) Penicillin-induced epileptiform activity in the hippocampal in vitro prepatation. Ann Neurol. 1:463-9.

Schwartzkroin PA and Prince DA (1980) Changes in excitatory and inhibitory synaptic potentials leading to epileptogenic activity. Brain Res 183: 61–73.

Scott SK, Young AW, Calder AJ, Hellawell DJ, Aggleton JP and Johnson M (1997) Impaired auditory recognition of fear and anger following bilateral amygdala lesions. Nature. 385:254-7.

Seeburg PH (1993) The TINS/TiPS Lecture. The molecular biology of mammalian glutamate receptor channels. Trends Neurosci. 16:359-65

Seidenberg M, Kelly KG, Parrish J, Geary E, Dow C, Rutecki P and Hermann B (2005) Ipsilateral and contralateral MRI volumetric abnormalities in chronic unilateral temporal lobe epilepsy and their clinical correlates. Epilepsia. 46:420-30.

Segal M and Barker JL (1986) Rat hippocampal neurons in culture: Ca2+ and Ca2+-dependent K+ conductances. J Neurophysiol. 55, 751-766.

Sharp PE and Green C (1994) Spatial correlates of firing patterns of single cells in the subiculum of the freely moving rat. J Neurosci. 14:2339-56.

Shoji Y, Tanaka E, Yamamoto S, Maeda H and Higashi H (1998) Mechanisms underlying the enhancement of excitatory synaptic transmission in basolateral amygdala neurons of the kindling rat. J Neurophysiol. 80:638-46.

Siddiqui AH and Joseph SA (2005) CA3 axonal sprouting in kainate-induced chronic epilepsy. Brain Res. 1066:129-46.

Simantov R, Crispino M, Hoe W, Broutman G, Tocco G, Rothstein JD and Baudry M (1999) Changes in expression of neuronal and glial glutamate transporters in rat hippocampus following kainate-induced seizure activity. Brain Res Mol Brain Res. 65:112-23.

Sims KS and Williams RS (1990) The human amygdaloid complex: a cytologic and histochemical atlas using Nissl, myelin, acetylcholinesterase and nicotinamide adenine dinucleotide phosphate diaphorase staining. Neuroscience. 36:449-72.

Sloviter RS (1987) Decreased hippocampal inhibition and a selective loss of interneurons in experimental epilepsy. Science. 235:73-6.

Sloviter RS (1991) Permanently altered hippocampal structure, excitability, and inhibition after experimental status epilepticus in the rat: the "dormant basket cell" hypothesis and its possible relevance to temporal lobe epilepsy. Hippocampus. 1, 41-66.

Sloviter RS (2005) The neurobiology of temporal lobe epilepsy: too much information, not enough knowledge. C R Biol. 328:143-53.

Smith BN and Dudek FE (1997) Enhanced population responses in the basolateral amygdala of kainate-treated, epileptic rats in vitro. Neurosci Lett. 222:1-4.

Smith Y, Pare JF and Pare D (1998) Cat intraamygdaloid inhibitory network: ultrastructural organization of parvalbumin-immunoreactive elements. J Comp Neurol. 391:164-79.

Soltesz I and Jones RSG (1995) Hippocampus forum: the direct perforant path input to CA1. Hippocampus 5: 101-146.

Spencer DD and Spencer SS (1994) Hippocampal resections and the use of human tissue in defining temporal lobe epilepsy syndromes. Hippocampus. 4:243-9.

Spencer SS and Spencer DD (1994) Entorhinal-hippocampal interactions in temporal lobe epilepsy. Epilepsia 35: 721–727.

Staff NP, Jung HY, Thiagarajan T, Yao M and Spruston N (2000) Resting and active properties of pyramidal neurons in subiculum and CA1 of rat hippocampus. J Neurophysiol. 84:2398-408.

Stafstrom CE (2005) The role of the subiculum in epilepsy and epileptogenesis. Epilepsy Curr. 5:121-9.

Staley K (2004) Neuroscience. Epileptic neurons go wireless. Science. 305:482-3.

Stanton PK, Jones RS, Mody I and Heinemann U (1987) Epileptiform activity induced by lowering extracellular [Mg2+] in combined hippocampal-entorhinal cortex slices: modulation by receptors for norepinephrine and N-methyl-D-aspartate. Epilepsy Res 1: 53–62.

Stewart M and Wong RK (1993) Intrinsic properties and evoked responses of guinea pig subicular neurons in vitro. J Neurophysiol. 70:232-45.

Stoop R and Pralong E (2000) Functional connections and epileptic spread between hippocampus, entorhinal cortex and amygdala in a modified horizontal slice preparation of the rat brain. Eur J Neurosci. 12:3651-63.

Stork O and Pape HC (2002) Fear memory and the amygdala: insights from a molecular perspective. Cell Tissue Res. 310:271-7.

Sugita S, Johnson SW and North RA (1992) Synaptic inputs to $GABA_A$ and $GABA_B$ receptors originate from discrete afferent neurons. Neurosci Lett. 134:207-11.

Sutula T, Cascino G, Cavazos J, Parada I and Ramirez L (1989) Mossy fiber synaptic reorganization in the epileptic human temporal lobe. Ann Neurol. 26, 321-330.

Suzuki WA and Amaral DG (1994a) Perirhinal and parahippocampal cortices of the macaque monkey: cortical afferents. J Comp Neurol. 350:497-533.

Suzuki WA and Amaral DG (1994b) Topographic organization of the reciprocal connections between the monkey entorhinal cortex and the perirhinal and parahippocampal cortices. J Neurosci. 14:1856-77.

Swanson LW and Cowan WM (1977) An autoradiographic study of the organization of the efferent connections of the hippocampal formation in the rat. J. Comp. Neurol. 172, 49-84.

Swanson LW and Kohler C (1986) Anatomical evidence for direct projections from the entorhinal area to the entire cortical mantle in the rat. J Neurosci 6: 3010–3023.

Swanson LW and Petrovich GD (1998) What is the amygdala? Trends Neurosci. 21:323-31.

Swanson LW, Wyss JM and Cowan WM (1978) An autoradiographic study of the organization of intrahippocampal association pathways in the rat. J. Comp. Neurol. 181, 681-715.

Swartzwelder SH, Lewis DV, Anderson WW and Wilson WA (1987). Seizure-like events in brain slices: supression by interictal activity. Brain Res. 410, 362--366

Szinyei C, Heinbockel T, Montagne J and Pape HC (2000) Putative cortical and thalamic inputs elicit convergent excitation in a population of GABAergic interneurons of the lateral amygdala. J Neurosci. 20:8909-15.

Takazawa T, Saito Y, Tsuzuki K and Ozawa S (2004) Membrane and firing properties of glutamatergic and GABAergic neurons in the rat medial vestibular nucleus. J Neurophysiol. 92:3106-20.

Tanaka T, Tanaka S, Fujita T, Takano K, Fukuda H, Sako K and Yonemasu Y (1992) Experimental complex partial seizures induced by a microinjection of kainic acid into limbic structures. Prog Neurobiol. 38:317-34.

Tanaka K, Watase K, Manabe T, Yamada K, Watanabe M, Takahashi K, Iwama H, Nishikawa T, Ichihara N, Kikuchi T, Okuyama S, Kawashima N, Hori S, Takimoto M and Wada K (1997) Epilepsy and exacerbation of brain injury in mice lacking the glutamate transporter GLT-1. Science. 276:1699-702.

Tancredi V, Hwa GGC, Zona C, Brancati A and Avoli M (1990) Low magnesium epileptogenesis in the rat hippocampal slice: electrophysiological and pharmacological features. Brain Res 511: 280–290.

Taube JS (1993) Electrophysiological properties of neurons in the rat subiculum in vitro. Exp Brain Res.;96:304-18.

Tauck DL and Nadler JV (1985) Evidence of functional mossy fiber sprouting in hippocampal formation of kainic acid-treated rats. J Neurosci. 5:1016-22.

Tessler S, Danbolt NC, Faull RL, Storm-Mathisen J and Emson PC (1999) Expression of the glutamate transporters in human temporal lobe epilepsy. Neuroscience. 88:1083-91.

Thesleff S (1980) Aminopyridines and synaptic transmission. Neuroscience. 5, 1413-1419.

Thompson SM, Capogna M and Scanziani M (1993) Presynaptic inhibition in the hippocampus. Trends Neurosci. 16:222-7.

Thompson SM and Gahwiler BH (1989) Activity-dependent disinhibition. I. Repetitive stimulation reduces IPSP driving force and conductance in the hippocampus in vitro. J Neurophysiol. 61:501-11.

Traub RD, Borck C, Colling SB and Jefferys JGR (1996) On the structure of ictal events in vitro. Epilepsia, 37, 879-891.

Traub RD and Jefferys JG (1994) Simulations of epileptiform activity in the hippocampal CA3 region in vitro. Hippocampus 4: 281–285.

Traub RD, Miles R, Wong RK, Schulman LS and Schneiderman JH (1987) Models of synchronized hippocampal bursts in the presence of inhibition. II. Ongoing spontaneous population events. J Neurophysiol. 58:752-64.

Turner DA and Wheal HV (1991) Excitatory synaptic potentials in kainic acid-denervated rat CA1 pyramidal neurons. J Neurosci. 11:2786-94.

Turrigiano GG and Nelson SB (2004) Homeostatic plasticity in the developing nervous system. Nat Rev Neurosci. 5:97-107.

Turski WA, Cavalheiro EA, Bortolotto ZA, Mello LM, Schwarz M and Turski L (1984) Seizures produced by pilocarpine in mice: a behavioral, electroencephalographic and morphological analysis. Brain Res 321: 237-253.

Turski WA, Cavalheiro EA, Schwarz M, Czuczwar SJ, Kleinrok Z and Turski L (1983) Limbic seizures produced by pilocarpine in rats: behavioural, electroencephalographic and neuropathological study. Behav Brain Res. 9, 315-35.

Tuunanen J, Halonen T and Pitkanen A (1996) Status epilepticus causes selective regional damage and loss of GABAergic neurons in the rat amygdaloid complex. Eur J Neurosci. 8:2711-25.

Tuunanen J, Halonen T and Pitkanen A (1997) Decrease in somatostatin-immunoreactive neurons in the rat amygdaloid complex in a kindling model of temporal lobe epilepsy. Epilepsy Res. 26:315-27.

Tuunanen J, Lukasiuk K, Halonen T and Pitkanen A (1999) Status epilepticus-induced neuronal damage in the rat amygdaloid complex: distribution, time-course and mechanisms. Neuroscience 94: 473–495.

Vale C and Sanes DH (2000) Afferent regulation of inhibitory synaptic transmission in the developing auditory midbrain. J Neurosci. 20:1912-21.

van Elst LT, Woermann FG, Lemieux L, Thompson PJ and Trimble MR (2000) Affective aggression in patients with temporal lobe epilepsy: a quantitative MRI study of the amygdala. Brain. 123:234-43.

Van Paesschen W, Connelly A, Johnson CL and Duncan JS (1996) The amygdala and intractable temporal lobe epilepsy: a quantitative magnetic resonance imaging study. Neurology. 47:1021-31.

van Vliet EA, Aronica E, Tolner EA, Lopes da Silva FH and Gorter JA (2004) Progression of temporal lobe epilepsy in the rat is associated with immunocytochemical changes in inhibitory interneurons in specific regions of the hippocampal formation. Exp Neurol. 187:367-79.

Voipio J and Kaila K (2000) GABAergic excitation and K(+)-mediated volume transmission in the hippocampus. Prog Brain Res. 125:329-38.

von Bohlen und Halbach O and Albrecht D (1998) Tracing of axonal connectivities in a combined slice preparation of rat brains: a study by rhodamine-dextran-amine application in the lateral nucleus of the amygdala. J Neurosci Methods 81: 169–175.

von Gersdorff H and Borst JG (2002) Short-term plasticity at the calyx of held. Nat Rev Neurosci. 3:53-64.

Vreugdenhil M, Hoogland G, van Veelen CW and Wadman WJ (2004) Persistent sodium current in subicular neurons isolated from patients with temporal lobe epilepsy. Eur J Neurosci. 2004 19:2769-78.

Wada JA, Sato M and Corcoran ME (1974) Persistent seizure susceptibility and recurrent spontaneous seizures in kindled cats. Epilepsia. 15:465-78.

Walther H, Lambert JD, Jones RS, Heinemann U and Hamon B (1986) Epileptiform activity in combined slices of the hippocampus, subiculum and entorhinal cortex during perfusion with low magnesium medium. Neurosci Lett. 69:156-61.

Watanabe T, Morimoto K, Hirao T, Suwaki H, Watase K and Tanaka K (1999) Amygdala-kindled and pentylenetetrazole-induced seizures in glutamate transporter GLAST-deficient mice. Brain Res. 845:92-6.

Watson C, Jack CR Jr and Cendes F (1997) Volumetric magnetic resonance imaging. Clinical applications and contributions to the understanding of temporal lobe epilepsy. Arch Neurol. 54:1521-31.

Wellmer J, Su H, Beck H and Yaari Y (2002) Long-lasting modification of intrinsic discharge properties in subicular neurons following status epilepticus. Eur. J. Neurosci. 16, 259-266.

Whittington MA and Traub RD (2003) Interneuron diversity series: inhibitory interneurons and network oscillations in vitro. Trends Neurosci. 26:676-82.

Wiebe S (2000) Epidemiology of temporal lobe epilepsy. Can J Neurol Sci. 27, Suppl 1: S6-10.

Wiebe S, Blume WT, Girvin JP and Eliasziw M (2001) A randomized, controlled trial of surgery for temporal-lobe epilepsy. N Engl J Med. 345:311-8.

Wieser HG, Engel Jr J, Williamson PD, Babb TL and Gloor P (1993) Surgically remediable temporal lobe syndromes. In: Surgical Treatment of the Epilepsies, Engel Jr., J., Editor, Raven Press, New York, pp. 49–63.

Wilensky AE, Schafe GE and LeDoux JE (2000) The amygdala modulates memory consolidation of fear-motivated inhibitory avoidance learning but not classical fear conditioning. J Neurosci. 20:7059-66.

Williams S, Vachon P and Lacaille JC (1993) Monosynaptic GABA-mediated inhibitory postsynaptic potentials in CA1 pyramidal cells of hyperexcitable hippocampal slices from kainic acid-treated rats. Neuroscience. 52, 541-54.

Wilson CL, Maidment NT, Shomer MH, Behnke EJ, Ackerson L, Fried I and Engel J Jr (1996) Comparison of seizure related amino acid release in human epileptic hippocampus versus a chronic, kainate rat model of hippocampal epilepsy. Epilepsy Res. 26:245-54.

Wilson WA, Swartzwelder HS, Anderson WW and Lewis DV (1988) Seizure activity in vitro: a dual focus model. Epilepsy Res. 2, 289-93.

Witter MP, Groenewegen HJ, Lopes da Silva FH and Lohman AH (1989) Functional organization of the extrinsic and intrinsic circuitry of the parahippocampal region. Prog Neurobiol. 33, 161-253.

Witter MP, Ostendorf RH and Groenewegen HJ (1990) Heterogeneity in the Dorsal Subiculum of the Rat. Distinct Neuronal Zones Project to Different Cortical and Subcortical Targets. Eur J Neurosci. 2, 718-725.

Wolf HK, Aliashkevich AF, Blumcke I, Wiestler OD and Zentner J (1997) Neuronal loss and gliosis of the amygdaloid nucleus in temporal lobe epilepsy. A quantitative analysis of 70 surgical specimens. Acta Neuropathol (Berl). 93:606-10.

Wong RK and Traub RD (1983) Synchronized burst discharge in disinhibited hippocampal slice. I. Initiation in CA2-CA3 region. J Neurophysiol. 49:442-58.

Wozny C, Kivi A, Lehmann TN, Dehnicke C, Heinemann U and Behr J (2003) Comment on "On the origin of interictal activity in human temporal lobe epilepsy in vitro". Science, 301, 463.

Wuarin JP and Dudek FE (1996) Electrographic seizures and new recurrent excitatory circuits in the dentate gyrus of hippocampal slices from kainate-treated epileptic rats. J Neurosci. 16:4438-48.

Wyler AR, Ojemann GA and Ward AA Jr (1982) Neurons in human epileptic cortex: correlation between unit and EEG activity. Ann Neurol. 11:301-8.

Xi XZ and Xu ZC (1996) The effect of neurobiotin on membrane properties and morphology of intracellularly labeled neurons. J Neurosci Methods. 65:27-32.

Yaari Y and Beck H (2002) "Epileptic neurons" in temporal lobe epilepsy. Brain Pathol. 12:234-9.

Yamada N and Bilkey DK (1991) Kindling-induced persistent alterations in the membrane and synaptic properties of CA1 pyramidal neurons. Brain Res. 561:324-31.

Yilmazer-Hanke DM, Wolf HK, Schramm J, Elger CE, Wiestler OD and Blumcke I (2000) Subregional pathology of the amygdala complex and entorhinal region in surgical specimens from patients with pharmacoresistant temporal lobe epilepsy. J. Neuropathol. Exp. Neurol. 59, 907-920.

Zhang WQ, Hudson PM, Sobotka TJ, Hong JS and Tilson HA (1991) Extracellular concentrations of amino acid transmitters in ventral hippocampus during and after the development of kindling. Brain Res. 540:315-8.

APPENDIX A: Reprint of Chapter 1 and Waiver from J Neurophsyiology

J Neurophysiol
87: 634–639, 2002; 10.1152/jn.00351.2001.

RAPID COMMUNICATION

Limbic Network Interactions Leading to Hyperexcitability in a Model of Temporal Lobe Epilepsy

MARGHERITA D'ANTUONO,[1,2] RUBA BENINI,[1] GIUSEPPE BIAGINI,[1,3] GIOVANNA D'ARCANGELO,[4] MICHAELA BARBAROSIE,[1] VIRGINIA TANCREDI,[4] AND MASSIMO AVOLI[1,2]

[1]*Montreal Neurological Institute and Department of Neurology and Neurosurgery, McGill University, Montreal, Quebec H3A 2B4, Canada;* [2]*Istituto di Ricovero e Cura a Carattere Scientifico Neuromed, 86077 Pozzilli (Isernia);* [3]*Dipartimento di Scienze Biomediche, Università degli Studi di Modena e Reggio Emilia, 41100 Modena; and* [4]*Dipartimento di Neuroscienze, Università degli Studi di Roma 'Tor Vergata', 00173 Rome, Italy*

Received 30 April 2001; accepted in final form 10 October 2001

D'Antuono, Margherita, Ruba Benini, Giuseppe Biagini, Giovanna D'Arcangelo, Michaela Barbarosie, Virginia Tancredi, and Massimo Avoli. Limbic network interactions leading to hyperexcitability in a model of temporal lobe epilepsy. *J Neurophysiol* 87: 634–639, 2002; 10.1152/jn.00351.2001. In mouse brain slices that contain reciprocally connected hippocampus and entorhinal cortex (EC) networks, CA3 outputs control the EC propensity to generate experimentally induced ictal-like discharges resembling electrographic seizures. Neuronal damage in limbic areas, such as CA3 and dentate hilus, occurs in patients with temporal lobe epilepsy and in animal models (e.g., pilocarpine- or kainate-treated rodents) mimicking this epileptic disorder. Hence, hippocampal damage in epileptic mice may lead to decreased CA3 output function that in turn would allow EC networks to generate ictal-like events. Here we tested this hypothesis and found that CA3-driven interictal discharges induced by 4-aminopyridine (4AP, 50 μM) in hippocampus-EC slices from mice injected with pilocarpine 13–22 days earlier have a lower frequency than in age-matched control slices. Moreover, EC-driven ictal-like discharges in pilocarpine-treated slices occur throughout the experiment (≤6 h) and spread to the CA1/subicular area via the temporoammonic path; in contrast, they disappear in control slices within 2 h of 4AP application and propagate via the trisynaptic hippocampal circuit. Thus, different network interactions within the hippocampus-EC loop characterize control and pilocarpine-treated slices maintained in vitro. We propose that these functional changes, which are presumably caused by seizure-induced cell damage, lead to seizures in vivo. This process is facilitated by a decreased control of EC excitability by hippocampal outputs and possibly sustained by the reverberant activity between EC and CA1/subiculum networks that are excited via the temporoammonic path.

INTRODUCTION

Application of 4-aminopyridine (4AP) or Mg^{2+}-free medium to combined hippocampus–entorhinal cortex (EC) slices obtained from rodents induces ictal-like (thereafter termed ictal) epileptiform discharges that originate in EC and propagate to the hippocampus, as well as interictal activity initiating in CA3 (Avoli et al. 1996; Barbarosie and Avoli 1997; Dreier and Heinemann 1991; Wilson et al. 1988). CA3-driven interictal activity exerts an unexpected control on the EC propensity to generate ictal discharges. Accordingly, *1*) interictal discharges occur throughout the experiment, but ictal activity disappears within 1–2 h; and *2*) Schaffer collateral cut abolishes interictal activity in EC while making ictal discharge reappear in this structure (Barbarosie and Avoli 1997).

Patients suffering from temporal lobe epilepsy present seizures involving the temporal cortex and limbic structures such as the hippocampus and the EC. These patients can manifest a pattern of brain damage (termed mesial temporal sclerosis) characterized by cell loss in CA3 and CA1 subfields and in the dentate hilus (Wieser et al. 1993). A similar pattern of brain damage is reproduced in laboratory animals by injecting kainic acid (Ben Ari 1985) or pilocarpine (Cavalheiro et al. 1996; Liu et al. 1994; Turski et al. 1984) that induces an initial status epilepticus followed 2–3 wk later by recurrent, limbic-type seizures.

Limbic network hyperexcitability in temporal lobe epileptic patients and in animal models mimicking this disorder may result from seizure-induced hippocampal damage leading to synaptic reorganization such as mossy fiber sprouting (Cavazos et al. 1991; Houser et al. 1990; Sutula et al. 1989). However, recurrent limbic seizures can occur in pilocarpine-treated rats when mossy fiber sprouting (but not neuronal damage) is abolished by inhibiting protein synthesis (Longo and Mello 1997, 1998), thus suggesting that cell loss alone may cause a chronic epileptic condition. Since hippocampal output activity controls the EC propensity to generate electrographic seizures in control mouse slices (Barbarosie and Avoli 1997), we predicted that a decrease in hippocampal network activity due to cell damage may lead per se to a chronic epileptic condition in pilocarpine-treated animals and perhaps in patients with temporal lobe epilepsy. Here, we tested this hypothesis by comparing the epileptiform patterns induced by 4AP in hippocampus–EC slices obtained from pilocarpine-treated and age-matched mice.

METHODS

Twenty-two CD-1 mice (29–42 days old) were used in this study. The procedures for injecting animals (n = 12) with pilocarpine were similar to those used in our laboratories with rats (Liu et al. 1994). To

Address for reprint requests: M. Avoli, 3801 University St., Montreal, Quebec H3A 2B4, Canada (E-mail: massimo.avoli@mcgill.ca).

The costs of publication of this article were defrayed in part by the payment of page charges. The article must therefore be hereby marked "*advertisement*" in accordance with 18 U.S.C. Section 1734 solely to indicate this fact.

prevent discomfort caused by stimulation of peripheral muscarinic receptors by pilocarpine (60–100 mg/kg), mice were pretreated with subcutaneous scopolamine methylnitrate (1 mg/kg). The animals' behavior was monitored ≤4 h after pilocarpine and scored according to Racine's classification (Racine et al. 1972). Slices defined as "pilocarpine-treated" were obtained 13–24 days following pilocarpine injection from mice with a behavioral response classified as stage 6 (i.e., tonic-clonic seizures occurring for ≥1 h). Control slices were obtained from age-matched mice. Animals were decapitated under halothane anesthesia; their brains were removed and placed in cold oxygenated artificial cerebrospinal fluid (ACSF) (Barbarosie and Avoli 1997). Horizontal, hippocampus–EC slices (500 μm thick) were cut with a vibratome and transferred to a tissue chamber where they lay between oxygenated ACSF and humidified gas (95% O_2-5% CO_2) at 32–34°C. ACSF composition was as follows (mM): 124 NaCl, 2 KCl, 1.25 KH_2PO_4, 2 $MgSO_4$, 2 $CaCl_2$, 26 $NaHCO_3$, and 10 glucose. 4AP (50 μM) was bath applied. Chemicals were acquired from Sigma.

Field potential recordings were made with ACSF-filled glass pipettes (tip diameter <10 μm; resistance <5–10 MΩ) positioned in EC, dentate gyrus, CA3 or CA1, and/or the subiculum. Signals were fed to high-impedance DC amplifiers and displayed on a Gould pen recorder. Field potential profiles of the ictal discharges recorded in the CA1/subiculum were performed with two recording electrodes. One electrode was maintained at a fixed position, while the other was moved in 100 μm stepwise increments along an axis normal to the alveus. Signals from the fixed electrode were used for temporal alignment of the field potentials obtained with the moving electrode. Field potential amplitudes at different latencies from the epileptiform discharge onset were calculated by averaging two to four events and plotted in a bidimensional fashion (i.e., amplitude versus space). In any given experiment, this type of analysis was restricted to ictal events that had similar electrographic characteristics (e.g., duration >20 s) when recorded from the fixed electrode. Time delays for discharge onset in different areas of the slice were calculated by taking as reference the first deflection from the baseline in expanded traces. Electrophysiological measurements are expressed as mean ± SD and n represents the number of slices studied. Data were compared with the Student's t-test or the analysis of variance (ANOVA) test and were considered significantly different if $P < 0.05$.

At the end of the experiments, some slices were fixed in 4% paraformaldehyde/100 mM phosphate-buffered solution overnight at 4°C and then rinsed several times in 15 and 30% sucrose–phosphate-buffered solutions for cryoprotection, and frozen at −80°C. Slices were cut with a cryostat into 14 μm thick sections and processed for Nissl staining. A blinded collaborator assessed the presence of tissue damage in various hippocampal regions. In pilocarpine-treated slices processed for histology (n = 7), we found a decrease of total neuron number that ranged 36–56 and 63–80% of controls in the CA1 and CA3 area, respectively. These data are in line with previous studies of the effects of ip pilocarpine in albino mice (Cavalheiro et al. 1996; Turski et al. 1984).

RESULTS

Bath application of 4AP (50 μM) to combined hippocampus–EC slices (n = 8) obtained from control mice induced brief, interictal events at 0.5–1.1 Hz and prolonged ictal discharges with intervals of occurrence ranging 50–160 s. These two types of epileptiform activity were recorded in hippocampus and EC after 20–30 min of 4AP application (Fig. 1*A*). Time delay measurements and pathway cutting demonstrated that the interictal discharges originated in CA3 (Fig. 1*A*, *inset*), while the ictal events initiated in the EC (Barbarosie and Avoli 1997). Moreover, ictal discharges disappeared in control slices within about 2 h of continuous 4AP application, while the interictal activity occurred throughout the experiment (Fig. 1, *A* and *F*).

Hippocampus–EC slices (n = 17) from pilocarpine-treated mice also responded to 4AP application by generating interictal and ictal discharges (Fig. 1*B*). However, the interictal activity observed in these experiments had a lower rate of occurrence and a longer duration than in control slices (Fig. 1, *B*, *D*, and *E*). Moreover, ictal discharges generated by pilocarpine-treated slices continued to occur throughout the experiment (≤6 h). Thus, the percentage of slices generating ictal discharges at different times of 4AP application was different when analyzed in control and pilocarpine-treated slices (Fig. 1*F*). As reported in control slices (Barbarosie and Avoli 1997), ictal discharges in pilocarpine-treated slices initiated in EC (Fig. 1*C*).

Next, we analyzed the modalities of propagation of the interictal and ictal discharges induced by 4AP in slices obtained from control and pilocarpine-treated mice. This was done by simultaneously recording the field potential activity in the EC, the dentate gyrus, and either the CA3 or the CA1/subiculum. The epileptiform activity occurring in control slices (n = 5) at the beginning of the experiment propagated as previously reported (Barbarosie and Avoli 1997; Barbarosie et al. 2000). Namely, CA3-driven interictal discharges appeared to spread successively to CA1, subiculum, and EC from where they presumably re-entered the hippocampus via the perforant path (Fig. 2, *A* and *C*) (cf. Paré et al. 1992). Ictal discharges initiated in EC and propagated to the hippocampus through the perforant path with onset delays, suggesting the involvement of the classic trisynaptic hippocampal circuit (Fig. 2, *A* and *D*). CA3-driven interictal discharges in pilocarpine-treated slices (n = 10) also propagated to EC via the CA1-subiculum and re-entered the hippocampus via the perforant path (Fig. 2, *B* and *C*). In these experiments, however, ictal discharges initiating in EC were recorded in the dentate gyrus, CA1, and subiculum with similar time delays (Fig. 2, *B* and *D*). Hence, they presumably spread from the EC to the CA1/subiculum via the temporoammonic path.

Temporoammonic inputs to CA1/subicular neurons are localized more apically than those provided by the Schaffer collateral system (Soltesz and Jones 1995). Therefore, we analyzed the depth profile characteristics of the ictal discharges recorded in the subiculum of control (n = 5) and pilocarpine-treated slices (n = 4). In both types of tissue, the steady shift associated with the ictal discharge was positive-going at or near the alveus, inverted in polarity when the electrode was moved toward the depth, and increased in amplitude as the electrode was further lowered toward the dentate upper blade (Fig. 3*B*). However, in pilocarpine-treated slices, it displayed maximal negative values at sites that were deeper (and thus more apical) than in control slices. Moreover, the peak-to-peak amplitude of the population spikes occurring during the ictal discharge attained maximal amplitude at approximately 500 and 700 μm in control and pilocarpine-treated slices, respectively. The depth-profile data obtained from three control and four pilocarpine-treated slices are summarized in Fig. 3, *C* and *D*.

DISCUSSION

Hippocampal cell loss is found in patients with temporal lobe epilepsy (Wieser et al. 1993) and in laboratory animals

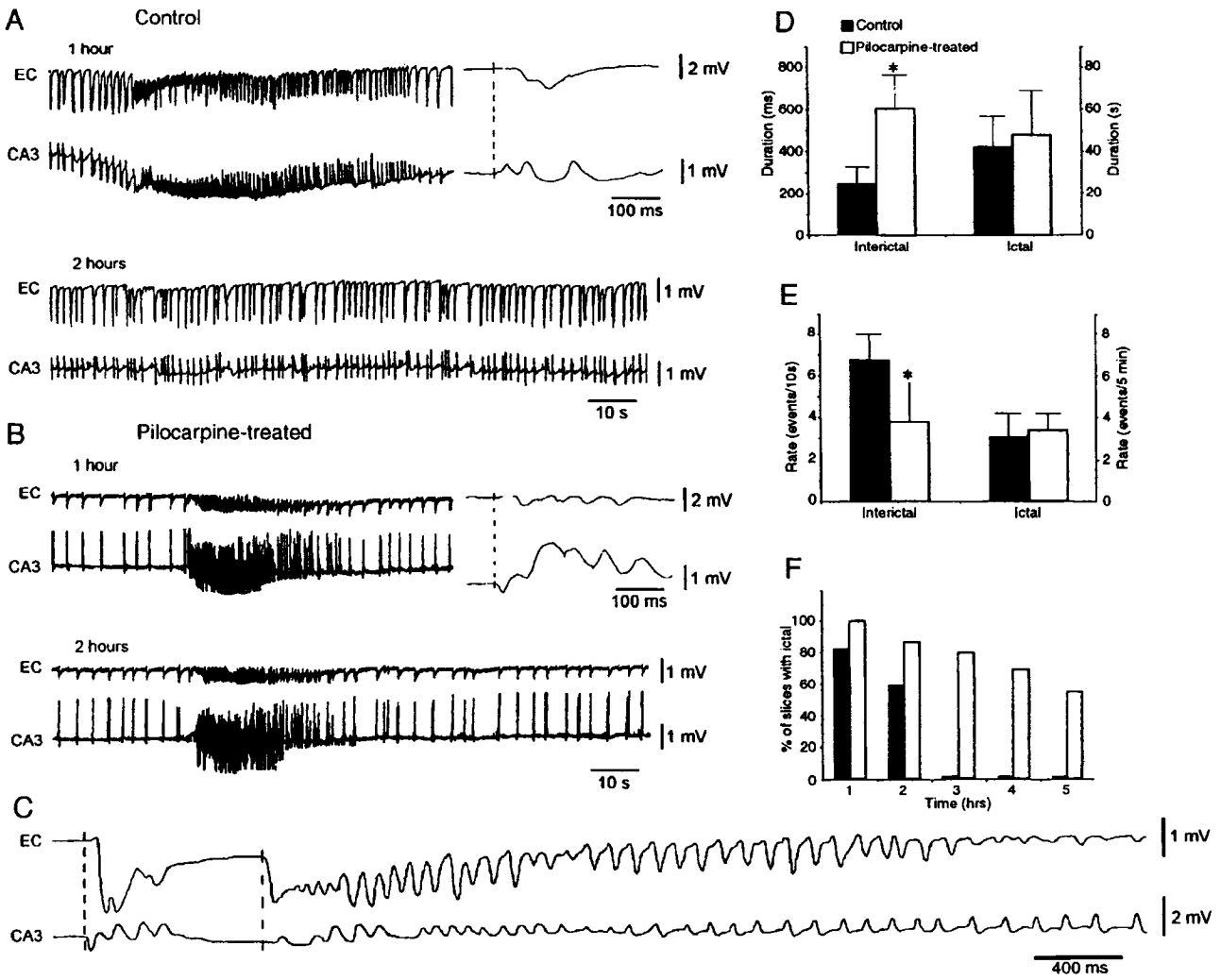

FIG. 1. 4-Aminopyridine (4AP)-induced epileptiform activities in control and pilocarpine-treated mouse hippocampus–entorhinal cortex (EC) slices. *A*: during the first hour of 4AP application, control slices generate spontaneous interictal and ictal discharges in CA3 and in EC. After 2 h of 4AP treatment, the ictal discharges are no longer recorded, while the interictal activity continues to occur. Note in the inset that the interictal discharge recorded during the first hour starts in CA3 and spreads to the EC with a 75 ms latency. *B*: similar experiment performed in a slice obtained from a pilocarpine-treated mouse. In this experiment as well both interictal and ictal discharges occur in CA3 and in EC. However, the interictal activity, which also initiates in CA3 and propagates to the EC with a 70 ms delay (*inset*), has a lower rate of occurrence and a longer duration than in the control slices. Note also that ictal discharges continue to occur after 2 h of 4AP application. *C*: expanded interictal-ictal discharge recorded in a pilocarpine-treated slice shows that the ictal event initiates in EC and propagates to CA3 with a 90 ms latency. *D* and *E*: duration and rate of occurrence of interictal and ictal discharges in control ($n = 10$) and pilocarpine-treated ($n = 11$) slices. Values that were significantly different ($P < 0.05$) are indicated by the asterisks. *F*: percentage of slices generating ictal discharges at different times of 4AP application in control and pilocarpine-treated slices. Values were obtained from 6, 5, and 4 control slices for the periods of 1, 2–3, and 4–5 h, respectively, as well as from 8, 7, and 6 pilocarpine-treated slices for the periods of 1–3, 4, and 5 h, respectively.

treated with convulsants such as kainic acid (Ben Ari 1985) or pilocarpine (Liu et al. 1994; Turski et al. 1983, 1984). The neuronal damage induced by the initial status epilepticus leads to sprouting along with synaptic reorganization (Cavazos et al. 1991; Gorter et al. 2001; Houser et al. 1990; Sutula et al. 1989). In addition, structural and functional impairment of GABA-mediated inhibition has been documented in these animal models (Doherty and Dingledine 2001; Fountain et al. 1998; Gorter et al. 2001; Williams et al. 1993). However, it is unclear how these changes in network function produce a chronic epileptic condition.

Previous work performed in nonepileptic mouse hippocampus–EC slices has revealed that CA3-driven interictal activity controls the expression of ictal discharges in the EC, presumably by perturbing the ability of EC networks to reverberate (Barbarosie and Avoli 1997). Here, we have found that CA3-driven interictal activity in pilocarpine-treated slices occurs at lower rates than in control tissue and that EC-driven ictal discharges persist throughout the experiment. Hence, we are inclined to propose that the cell damage and synapse loss seen in the CA3/CA1 areas of pilocarpine-treated slices (Cavalheiro et al. 1996; Turski et al. 1984), by reducing hippocampal

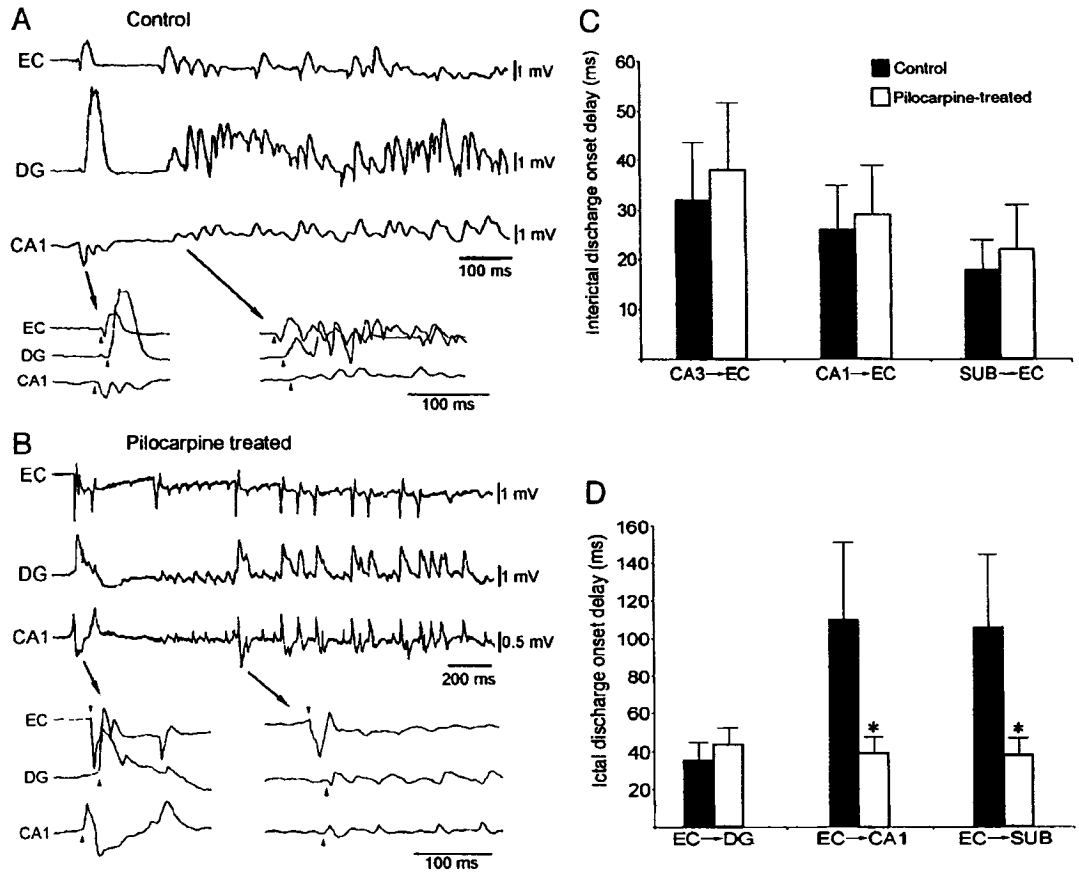

FIG. 2. Propagation modalities of the 4AP-induced epileptiform activities in control and pilocarpine-treated slices. *A*: simultaneous field potential recordings obtained from EC, dentate gyrus (DG), and CA1 in a control slice after 45 min of 4AP application. Both here and in *B*, the expanded traces in the bottom were triggered from the initial deflection seen in CA1 and in EC during the interictal and ictal discharge shown on the top recording. In this experiment, the differences in time onset suggest that interictal discharges occur first in CA1 and later spread to EC and DG, while the ictal discharges initiate in EC and spread successively to DG and to CA1. *B*: similar experimental protocol performed in pilocarpine-treated slices. Note that in this experiment as well the interictal discharge is first seen in CA1 and propagates to the EC to re-enter the hippocampus via the perforant path. However, the ictal discharge initiating in EC appears in DG and in the CA1 with similar onset latencies. *C* and *D*: quantitative summary of the differences in time onset of interictal (*C*) and ictal (*D*) events recorded in different areas of control (n = 5) and pilocarpine-treated (n = 7). Note that the time lags between EC and CA1 or subiculum (SUB) for the ictal discharges are shorter in the pilocarpine-treated slices.

output activity, may release its control on EC network excitability. In line with this view, similar data are obtained in control mouse slices by cutting the Schaffer collateral, a procedure that prevents CA3-driven interictal discharges from reaching the CA1/subiculum and thus from activating the EC (Barbarosie and Avoli 1997).

We have also found that in intact, pilocarpine-treated slices the spread of ictal discharges from the EC to the CA1-subiculum occurs through the temporoammonic path (cf. Soltesz and Jones 1995). In contrast, in control slices, this activity propagated to the CA1 through the classic trisynaptic circuit (cf. Paré et al. 1992). This conclusion is supported by the depth profile analysis of the ictal discharges recorded in the subiculum of control and pilocarpine-treated mice. We have previously shown in nonepileptic mouse slices that the temporoammonic path becomes involved in the propagation of 4AP-induced ictal discharges after cutting the Schaffer collateral and thus after blocking the activation of CA1 and subicular networks (Barbarosie et al. 2000). Under normal conditions, depressing synaptic transmission between CA3 and CA1 makes the temporoammonic projection from the EC to CA1 operative (Maccaferri and McBain 1995). In pilocarpine-treated tissue, this effect may also be contributed by a use-dependent reduction of the excitatory drive onto interneurons (Doherty and Dingledine 2001). The functional consequence of this change in modality of propagation is that the ictal activity originating in the EC short-circuits the trisynaptic hippocampal route and thus can monosynaptically activate CA1 and subicular neurons, thus ensuring a high-fidelity synaptic transfer that increases epileptiform synchronization. Indeed, it may be hypothesized that in the pilocarpine-treated brain, subicular networks play a unique role in sustaining limbic seizures.

In conclusion, we have identified some differences in the way(s) limbic networks obtained from pilocarpine-treated and age-matched control mice interact in vitro during 4AP application. Our data provide some novel explanations for why pilocarpine-treated mice, and perhaps temporal lobe epilepsy patients, are susceptible to generating seizures in vivo. In

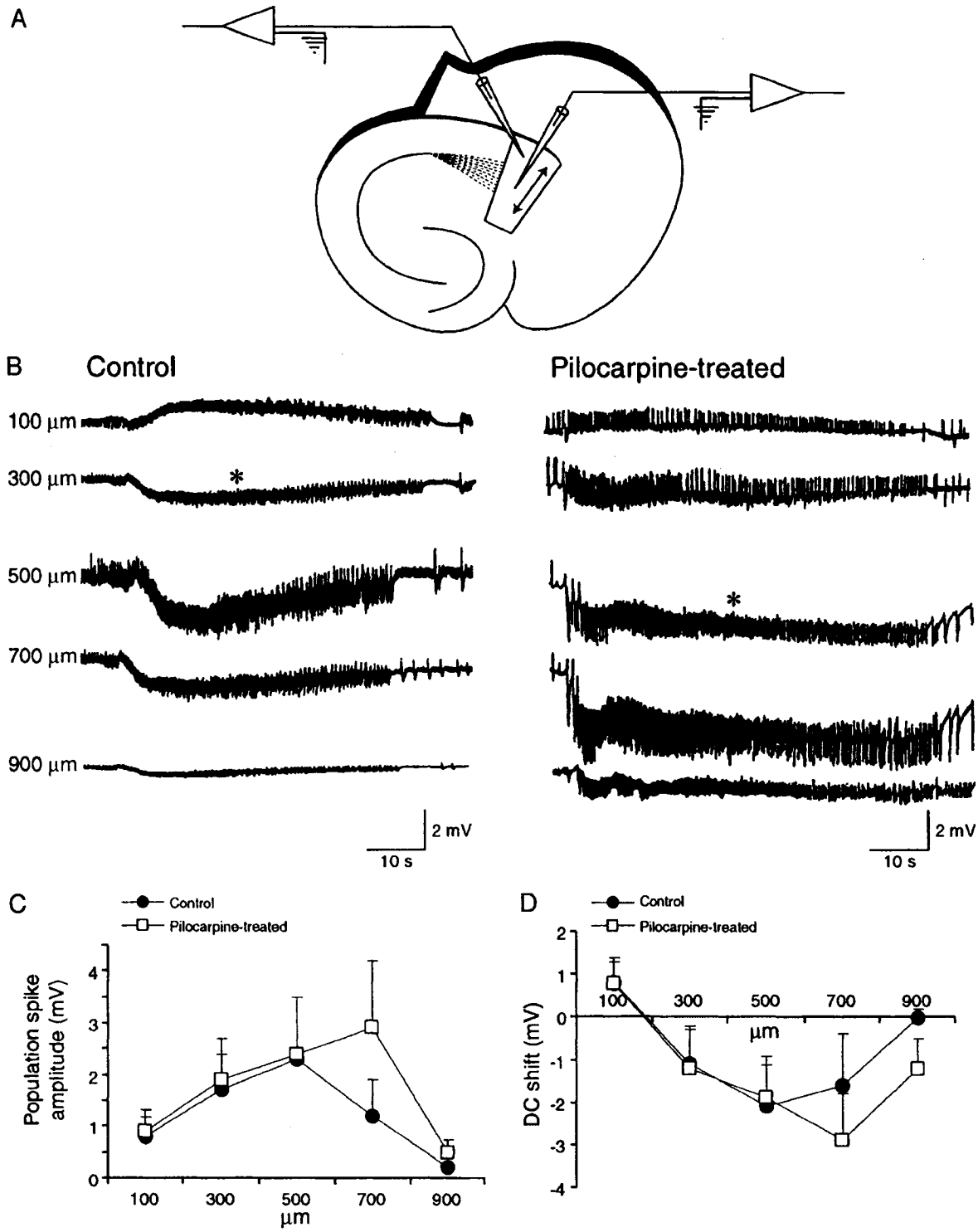

FIG. 3. Depth profile characteristics of the field potentials associated with the ictal discharges recorded in the CA1/subicular area of control and pilocarpine-treated slices. *A*: schematic representation of the experimental procedure indicating the area where recordings were obtained with two microelectrodes: one was maintained at a fixed position, while the other was moved in 100 μm stepwise increments along an axis normal to the pial aspect of the subiculum. *B*: field potential recordings obtained at different depths in control and pilocarpine-treated slices. Depth values were measured relative to the pia and are indicated on the left of each sample. Asterisks indicate the recording obtained from the stationary electrode in each of the two experiments. *C* and *D*: depth distribution of the amplitudes of the fast events and of the DC shifts associated with the ictal discharges in control ($n = 3$) and pilocarpine-treated slices ($n = 4$). Values were grouped in increments of 100 μm. Note that the amplitudes of the fast transients in pilocarpine-treated slices attain maximal values at depths that are greater than control slices ($P < 0.05$). A similar pattern of distribution is also evident for the DC shift negative values.

particular, our findings emphasize the role played by cell loss in temporal lobe epilepsy that may hamper the control of EC excitability and also make the temporoammonic path operative.

We thank Dr. D. Paré for reading an early draft of this paper and T. Papadopoulos for secretarial assistance. M. D'Antuono is a Fragile X Research Foundation of Canada fellow, G. Biagini was a North Atlantic Treaty Organization-Consiglio Nazionale delle Ricerche fellow, and M. Barbarosie a Fonds de la Recherche en Santé du Québec student.

This work was supported by the Canadian Institute of Health Research (Grant MT-8109) and the Savoy Foundation.

REFERENCES

AVOLI M, BARBAROSIE M, LÜCKE A, NAGAO T, LOPANTSEV V, AND KÖHLING R. Synchronous GABA-mediated potentials and epileptiform discharges in the rat limbic system in vitro. *J Neurosci* 16: 3912–3924, 1996.

BARBAROSIE M AND AVOLI M. CA3-driven hippocampal-entorhinal loop controls rather than sustain in vitro limbic seizures. *J Neurosci* 17: 9308–9314, 1997.

BARBAROSIE M, LOUVEL J, KURCEWICZ I, AND AVOLI M. CA3-released entorhinal seizures disclose dentate gyrus epileptogenicity and unmask a temporoammonic pathway. *J Neurophysiol* 83: 1115–1124, 2000.

BEN-ARI Y. Limbic seizures and brain damage produced by kainic acid: mechanisms and relevance to human temporal lobe epilepsy. *Neuroscience* 14: 375–403, 1985.

CAVALHEIRO EA, SANTOS NF, AND PRIEL MR. The pilocarpine model in mice. *Epilepsia* 37: 1015–1019, 1996.

CAVAZOS JE, GOLARAI G, AND SUTULA TP. Mossy fiber synaptic reorganization induced by kindling: time course of development, progression, and permanence. *J Neurosci* 11: 2795–2803, 1991.

DOHERTY J AND DINGLEDINE R. Reduced excitatory drive onto interneurons in the dentate gyrus after status epilepticus. *J Neurosci* 21: 2048–2057, 2001.

DREIER JP AND HEINEMANN U. Regional and time dependent variations of low Mg^{2+} induced epileptiform activity in rat temporal cortex slices. *Exp Brain Res* 87: 581–596, 1991.

FOUNTAIN NB, BEAR J, BERTRAM EH 3RD, AND LOTHMAN EW. Responses of deep entorhinal cortex are epileptiform in an electrogenic rat model of chronic temporal lobe epilepsy. *J Neurophysiol* 80: 230–240, 1998.

GORTER JA, VAN VLIET EA, ARONICA E, AND LOPES DA SILVA FH. Progression of spontaneous seizures after status epilepticus is associated with mossy fibre sprouting and extensive bilateral loss of hilar parvalbumin and somatostatin-immunoreactive neurons. *Eur J Neurosci* 13: 657–669, 2001.

HOUSER CR, MIYASHIRO JE, SWARTZ BE, WALSH GO, RICH JR, AND DELGADO-ESCUETA AV. Altered patterns of dynorphin immunoreactivity suggest mossy fiber reorganization in human hippocampal epilepsy. *J Neurosci* 10: 267–282, 1990.

LIU Z, NAGAO T, DESJARDINS GC, GLOOR P, AND AVOLI M. Quantitative evaluation of neuronal loss in the dorsal hippocampus in rats with long-term pilocarpine seizures. *Epilepsy Res* 17: 237–247, 1994.

LONGO BM AND MELLO LE. Blockade of pilocarpine- or kainate-induced mossy fiber sprouting by cycloheximide does not prevent subsequent epileptogenesis in rats. *Neurosci Lett* 226: 163–166, 1997.

LONGO BM AND MELLO LE. Supragranular mossy fiber sprouting is not necessary for spontaneous seizures in the intrahippocampal kainate model of epilepsy in the rat. *Epilepsy Res* 32: 172–182, 1998.

MACCAFERRI G AND MCBAIN CJ. Passive propagation of LTD to stratum oriens-alveus inhibitory neurons modulates the temporoammonic input to the hippocampal CA1 region. *Neuron* 15: 137–145, 1995.

PARÉ D, DECURTIS M, AND LLINÁS R. Role of hippocampal-entorhinal loop in temporal lobe epilepsy: extra- and intracellular study in the isolated guinea pig brain in vitro. *J Neurosci* 12: 1857–1881, 1992.

RACINE RJ. Modification of seizure activity by electrical stimulation. II. Motor seizure. *Electroencephalogr Clin Neurophysiol* 32: 281–294, 1972.

SOLTESZ I AND JONES RSG. Hippocampus forum: the direct perforant path input to CA1. *Hippocampus* 5: 101–146, 1995.

SUTULA T, CASCINO G, CAVAZOS J, PARADA I, AND RAMIREZ L. Mossy fiber synaptic reorganization in the epileptic human temporal lobe. *Ann Neurol* 26: 321–330, 1989.

TURSKI WA, CAVALHEIRO EA, SCHWARZ M, CZUCZWAR SJ, KLEINROK Z, AND TURSKI L. Limbic seizures produced by pilocarpine in rats: behavioral, electroencephalographic and neuropathological study. *Behav Brain Res* 9: 315–335, 1983.

TURSKI WA, CAVALHEIRO EA, BORTOLOTTO ZA, MELLO LM, SCHWARZ M, AND TURSKI L. Seizures produced by pilocarpine in mice: a behavioral, electroencephalographic and morphological analysis. *Brain Res* 321: 237–253, 1984.

WIESER HG, ENGEL JB JR, WILLIAMSON PD, BABB TL, AND GLOOR P. Surgically remediable temporal lobe syndromes. In: *Surgical Treatment of the Epilepsies*, edited by Engel J Jr. New York: Raven, 1993, p. 49–63.

WILLIAMS S, VACHON P, AND LACAILLE JC. Monosynaptic GABA-mediated inhibitory postsynaptic potentials in CA1 pyramidal cells of hyperexcitable hippocampal slices from kainic acid-treated rats. *Neuroscience* 52: 541–554, 1993.

WILSON WA, SWARTZWELDER HS, ANDERSON WW, AND LEWIS DV. Seizure activity in vitro: a dual focus model. *Epilepsy Res* 2: 289–293, 1988.

APPENDIX B: Reprint of Chapter 2 and Waiver from J Physiology

Rat subicular networks gate hippocampal output activity in an *in vitro* model of limbic seizures

Ruba Benini[1] and Massimo Avoli[1,2]

[1]*Montreal Neurological Institute and Departments of Neurology & Neurosurgery, and of Physiology, McGill University, Montreal, QC, H3A 2B4, Canada*
[2]*Dipartimento di Fisiologia Umana e Farmacologia, Università di Roma 'La Sapienza', 00185 Rome, Italy*

Evidence obtained from human epileptic tissue maintained *in vitro* indicates that the subiculum may play a crucial role in initiating epileptiform discharges in patients with mesial temporal lobe epilepsy. Hence, we used rat hippocampus–entorhinal cortex (EC) slices to identify the role of subiculum in epileptiform synchronization during bath application of 4-aminopyridine (4AP, 50 μM). In these slices, fast CA3-driven interictal-like events were restricted to the hippocampal CA3/CA1 areas and failed to propagate to the EC where slow interictal-like and ictal-like epileptiform discharges were recorded. However, antagonizing $GABA_A$ receptors with picrotoxin (50 μM) made CA3-driven interictal activity spread to EC. Sequential field potential analysis along the CA3–CA1–subiculum axis revealed that the amplitude of CA3-driven interictal discharges recorded in the presence of 4AP only diminished within the subiculum. Furthermore, CA1 electrical stimulation under control conditions elicited little or no subicular activation and never any response in EC; in contrast, robust subicular discharges that spread to EC could be evoked after picrotoxin. Intracellular recordings indicated that potentiation by picrotoxin was associated with blockade of hyperpolarizing IPSPs in subicular cells. Finally, when surgically isolated from adjacent structures, the subiculum generated low-amplitude synchronous discharges that corresponded to an intracellular hyperpolarization–depolarization sequence, were resistant to glutamatergic antagonists, and represented the activity of synchronized interneuronal networks. Bath application of picrotoxin abolished these 4AP-induced events and in their place robust network bursting occurred. In conclusion, our study demonstrates that the subiculum plays a powerful gating role on hippocampal output activity. This function depends on $GABA_A$ receptor-mediated inhibition and controls hippocampal–parahippocampal interactions that are known to modulate limbic seizures.

(Resubmitted 15 April 2005; accepted after revision 31 May 2005; first published online 2 June 2005)
Corresponding author M. Avoli: 3801 University, room 794, Montreal, QC, Canada H3A 2B4.
Email: massimo.avoli@mcgill.ca

Mesial temporal lobe epilepsy (MTLE) is one of the most common types of partial epilepsy in humans (Wiebe, 2000). MRI images from MTLE patients are often characterized by hippocampal atrophy which, upon histological examination, reveals extensive neuronal loss and gliosis in the dentate hilus and CA3/CA1 areas along with synaptic reorganization (Sutula *et al.* 1989; Houser *et al.* 1990). In addition, neuronal damage in this epileptic disorder is seen in limbic areas such as the entorhinal cortex (EC) and the amygdala (Du *et al.* 1993; Gloor, 1997; Pitkanen *et al.* 1998; Houser, 1999; Yilmazer-Hanke *et al.* 2000). Histopathological analysis of human epileptic tissue has also shown that subicular principal cells are relatively unaffected in MTLE (Gloor, 1997). Nevertheless, the absence of neuronal loss in the subiculum does not exclude the possibility that this area may play an active role in MTLE. Indeed, recent studies in both human (Cohen *et al.* 2002; Wozny *et al.* 2003) and animal (Behr & Heineman, 1996; D'Antuono *et al.* 2002; Wellmer *et al.* 2002) epileptic tissue suggest that cellular and synaptic reorganization in the subiculum contributes to limbic seizure generation.

The subiculum holds a strategic position within the limbic system. Not only does it serve as the major output structure of the hippocampus, getting extensive projections from the CA1 hippocampal region (Finch & Babb, 1981; Witter *et al.* 1989), but it also projects to various limbic and extralimbic areas including EC layers IV and V (Swanson & Cowan, 1977; Witter *et al.* 1989), perirhinal cortex (Swanson *et al.* 1978; Deacon *et al.* 1983), amygdala (Canteras & Swanson, 1992) and thalamus (Witter *et al.* 1990; Canteras & Swanson, 1992)

DOI: 10.1113/jphysiol.2005.088708

(see for review O'Mara *et al.* 2001). In this study, we sought to identify the role played by the subiculum in intralimbic synchronization using the 4-aminopyridine (4AP) *in vitro* model of limbic seizures. Here, we report that $GABA_A$ receptor-mediated mechanisms confer on the subiculum the ability to gate hippocampal output activity, and thus to dictate the interactions between hippocampal and parahippocampal neuronal networks.

Methods

Male, adult Sprague-Dawley rats (150–200 g) were decapitated under halothane anaesthesia according to the procedures established by the Canadian Council of Animal Care. The brain was quickly removed and a block of brain tissue containing the retrohippocampal region was placed in cold (1–3°C), oxygenated artificial cerebrospinal fluid (ACSF). The brain's dorsal side was cut along a horizontal plane that was tilted by a 10 deg angle along a postero-superior-anteroinferior plane passing between the lateral olfactory tract and the base of the brainstem (Avoli *et al.* 1996). Horizontal slices (450–500 μm) containing the EC and the hippocampus were cut from this brain block using a vibratome. Subicular minislices were prepared from these horizontal slices by using microknife cuts to isolate the subiculum from the other hippocampal and parahippocampal structures (Fig. 7*B*). Slices were then transferred into a tissue chamber where they lay at the interface between ACSF and humidified gas (95% O_2, 5% CO_2) at a temperature of 34–35°C and a pH of 7.4. ACSF composition was (mM): NaCl 124, KCl 2, KH_2PO_4 1.25, $MgSO_4$ 2, $CaCl_2$ 2, $NaHCO_3$ 26, and glucose 10. 4AP (50 μM), bicuculline methobromide (BMI, 10 μM), 6-cyano-7-nitroquinoxaline-2,3-dione (CNQX, 10 μM), 3,3-(2-carboxypiperazin-4-yl)-propyl-1-phosphonate (CPP, 10–30 μM), and picrotoxin (PTX, 50 μM) were applied to the bath. Chemicals were acquired from Sigma (St Louis, MO, USA) with the exception of BMI, CNQX and CPP, which were obtained from Tocris Cookson (Ellisville, MO, USA).

Field potential recordings were made with ACSF-filled, glass pipettes (resistance = 2–10 MΩ) that were connected to high-impedance amplifiers. The location of the recording electrodes in the combined hippocampus–EC slice is shown in Fig. 2*A*. Field responses were induced by applying single shock electrical stimuli (50–100 μs; < 200 μA) delivered through a bipolar, stainless steel electrode (Fig. 3*A*). Sharp-electrode intracellular recordings were performed in the subiculum with pipettes that were filled with 3 M potassium acetate (tip resistance = 70–120 MΩ). Intracellular signals were fed to a high-impedance amplifier with internal bridge circuit for intracellular current injection. The resistance compensation was monitored throughout the experiment and adjusted as required. The passive membrane properties of the subicular cells included in this study were measured as follows: (i) resting membrane potential (RMP) after cell withdrawal; (ii) apparent input resistance (R_i) from the maximum voltage change in response to a hyperpolarizing current pulse (100–200 ms, < −0.5 nA); (iii) action potential amplitude (APA) from the baseline; and (iv) action potential duration (APD) at half-amplitude. Intrinsic firing patterns of subicular cells were determined from responses to depolarizing current pulses of 500–1000 ms duration. Three neuronal types could be distinguished in this study: strong bursters, weak bursters and regular firing (Staff *et al.* 2000). Since no differences were observed between these classes in terms of their 4AP-induced activity, strong and weak intrinsic bursters were put together in the 'bursting' group (Fig. 5*Ab*) whilst regular firing cells were placed in the 'non-bursting' category (Fig. 6*Ab*). No fast spiking cells were ever recorded in this study.

Field potential and intracellular signals were fed to a computer interface (Digidata 1322A, Axon Instruments) and acquired and stored using the pCLAMP 9 software (Axon Instruments). Subsequent analysis of these data was made with the Clampfit 9 software (Axon Instruments). For time-delay measurements, the onset of the field potential/intracellular signals was established as the time of the earliest deflection of the baseline recording (e.g. inset traces in Fig. 1*A* and *B*). Throughout this study we arbitrarily termed as 'interictal' and 'ictal' the synchronous epileptiform events with durations shorter or longer than 2 s, respectively (cf. Traub *et al.* 1996). Measurements in the text are expressed as means ± S.D. and n indicates the number of slices or neurones studied under each specific protocol. Data were compared with Student's t test and were considered statistically significant if $P < 0.05$.

Results

Epileptiform activity induced by 4AP in combined hippocampus-EC slices

As illustrated in Fig. 1*A* (Control (4AP)) and Fig. 2*A*, the hippocampus–EC slices ($n = 110$) included in this study responded to 4AP application by generating three types of synchronous activities (cf. Avoli *et al.* 1996; Benini *et al.* 2003): (i) fast interictal discharges (interval of occurrence = 1.6 ± 0.7 s; duration 139 ± 65 ms; $n = 25$) that were restricted to the hippocampus proper (Fig. 1*A*, arrows); (ii) slow interictal events that were recorded in both hippocampal and EC regions and could initiate anywhere in the slice (interval of occurrence = 28 ± 15 s; $n = 25$; Fig. 1*A*, asterisk); and (iii) long-lasting ictal discharges (interval of occurrence = 236 ± 117 s; duration 64 ± 56 s; $n = 25$) that originated in EC and could propagate to the hippocampus via the perforant pathway

(Fig. 1*A*, bar). We termed these slices functionally disconnected due to the lack of epileptiform activity propagation from the hippocampus to the EC.

Involvement of $GABA_A$ receptors in the epileptiform activity induced by 4AP

Next, we superfused these slices with the $GABA_A$ receptor antagonist picrotoxin (50 μM) to establish the role of $GABA_A$ receptor-mediated mechanisms in 4AP-induced epileptiform discharges. As shown in Fig. 1, picrotoxin application to these functionally disconnected slices ($n = 45$) resulted in a dramatic change in the 4AP-induced electrographic activity (Figs 1 and 2). Exposure to this non-competitive $GABA_A$ receptor antagonist triggered an initial ictal burst in the EC (Fig. 2*B*, + Picrotoxin) after which the activity was replaced by robust interictal discharges that initiated in CA3 and propagated sequentially to CA1 and EC (expanded trace in the inset of Fig. 1*B*, + Picrotoxin). This phenomenon was reproduced with the competitive $GABA_A$ receptor antagonist BMI (10 μM, $n = 4$), thus suggesting that the effect observed was indeed due to hindrance of $GABA_A$ receptor function. Transformation of a functionally disconnected slice into one in which hippocampus-driven epileptiform activity could propagate to the EC was fully reversible upon washing out picrotoxin ($n = 6$) for approx. 2 h (not shown).

$GABA_A$ receptor antagonism potentiates interictal activity in the subiculum of functionally disconnected slices

To gain a better understanding of how $GABA_A$ receptor antagonism in functionally disconnected slices leads to synchronicity between hippocampus and EC, we analysed the 4AP-induced activity in neuronal networks along the CA3–CA1–subiculum axis ($n = 14$). This was achieved by obtaining simultaneous field potential recordings from CA3 and EC with two fixed electrodes while a third electrode was moved sequentially from the CA1–CA2 area towards the subiculum at the level of the stratum pyramidale. We found in six of these experiments that the CA3-driven interictal events had similar amplitudes up to the CA1–subiculum border (Fig. 2*Ab*, Control, +4AP) and then decreased as the recording electrode was placed in subiculum (Fig. 2*Ac*, Control, +4AP). Moreover, in the remaining experiments ($n = 8$) interictal events were not recorded during 4AP application in the subiculum concomitant with those seen in the CA3 and CA1 areas (Fig. 4*A*).

Following picrotoxin application (Fig. 2*B*, + Picro toxin), there was a potentiation in the amplitude of the epileptiform activity recorded within the subiculum. Moreover, such augmentation always occurred prior to the establishment of complete synchronization of the epileptiform activity between hippocampus and EC (Fig. 2*B*, + Picrotoxin, middle inset). Quantitative analysis of the picrotoxin-induced changes in field potential amplitudes in CA3, CA1 and subiculum revealed that the most drastic potentiation (314 ± 163%, $n = 6$) occurred

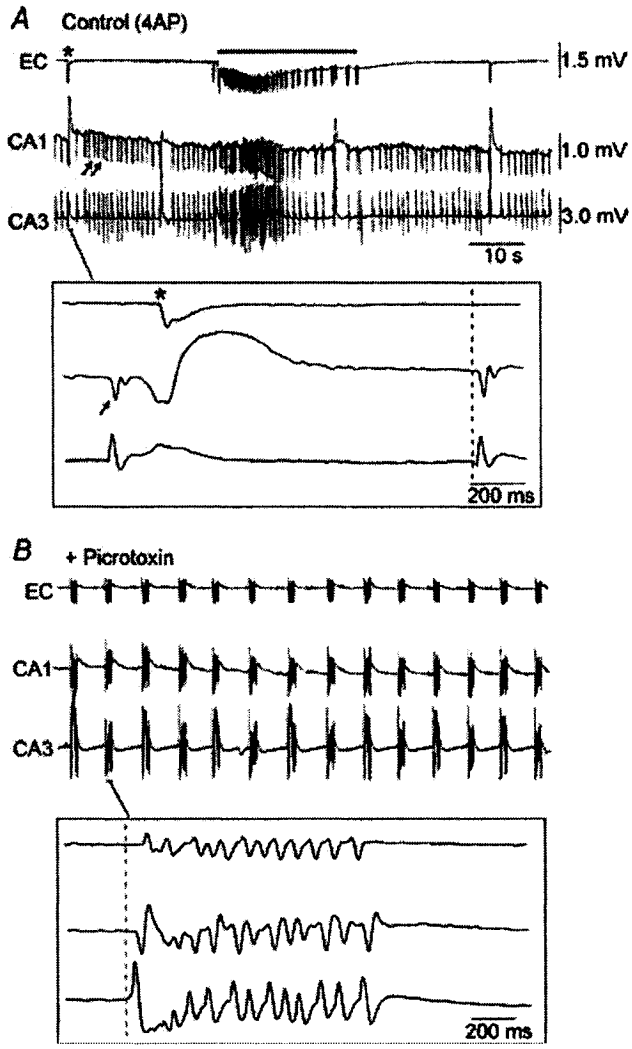

Figure 1. Effect of picrotoxin on 4AP-induced activity in a combined hippocampus–EC slice
A, simultaneous field potential recordings obtained from EC, CA1 and CA3 during bath application of 4AP. Note that fast interictal discharges (arrows in the CA1 trace) are restricted to the hippocampus (CA3 and CA1) but that slow interictal events (asterisk in the EC trace) are recorded in both hippocampus and EC. Note also the long-lasting ictal discharge (bar). *B*, picrotoxin application causes loss of ictal discharge in the EC and the appearance of robust interictal discharges that initiate in CA3 and propagate sequentially to CA1 and EC (inset). The insets in *A* and *B* show selected interictal events at faster time bases and the dashed lines demonstrate that these discharges initiate in CA3.

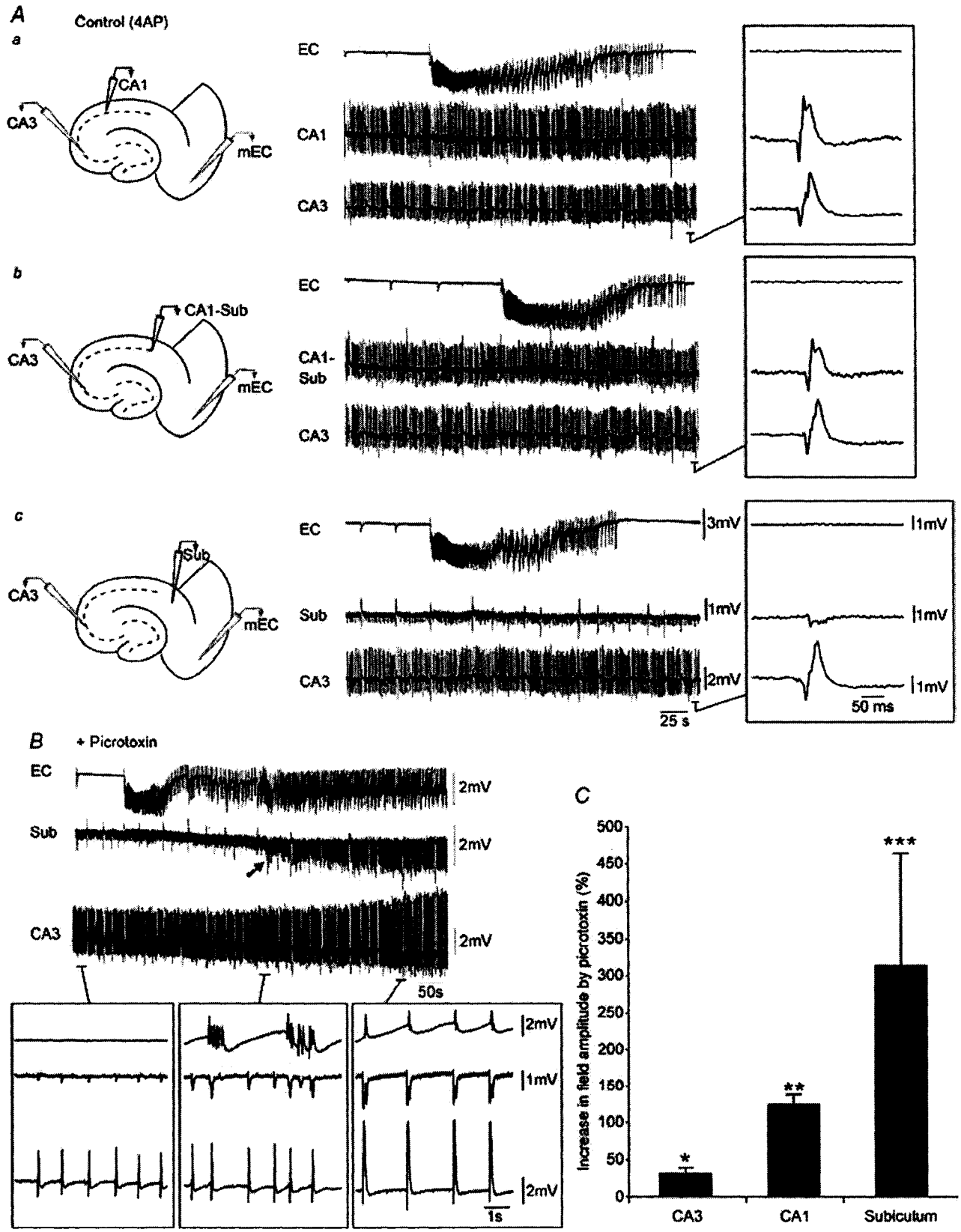

within the last structure whereas the least augmentation took place in CA3 (31 ± 8%; $n = 6$) (Fig. 2*C*).

Stimulation of hippocampal networks elicits response in EC only under $GABA_A$ receptor antagonism

To explore further the propagation of hippocampus-driven activity to the EC, we investigated the responses induced in the slice by focal electrical stimuli delivered in CA1, subiculum and EC: (i) in the absence of convulsants (i.e. normal ACSF); (ii) in the presence of 4AP; and (iii) during application of 4AP + PTX (Fig. 3*A*, *B* and *C*, respectively). In these experiments, three recording electrodes were placed in CA1 stratum pyramidale, subiculum and EC deep layers while a stimulating electrode was used to sequentially activate each of these structures.

As expected, a local field response could be recorded in any of the stimulated structures during application of normal ACSF (Fig. 3*Aa–c*, arrows); in addition, EC stimulation could also elicit some responses in subiculum and CA1. Following 4AP application (Fig. 3*B*), the local responses increased in amplitude and duration while distant activation could be clearly identified when stimuli were delivered in subiculum and EC (Fig. 3*Bb* and *c*, respectively); in contrast, as seen in normal medium, CA1 single shock stimuli (Fig. 3*Ba*) failed in eliciting subicular ($n = 12$) or EC responses ($n = 24$). Finally, during concomitant application of 4AP and picrotoxin, electrical stimuli delivered in any area of the slice induced robust epileptiform discharges in all limbic structures (Fig. 3*Ca–c* (4AP + PTX)). It should be emphasized that CA1 single-shock stimuli delivered during $GABA_A$-receptor antagonism (Fig. 3*Ca*) elicited an epileptiform response not only in subiculum, but also in EC ($n = 6$). Therefore, these observations suggest that $GABA_A$ receptor-mediated mechanisms prevent the propagation of both stimulation- and 4AP-induced hippocampal activity to the EC, thereby confirming that the functional disconnectivity between the hippocampus proper and EC was not merely an artifact of the 4AP model itself. In addition, both the potentiation of subicular responses by picrotoxin and the subsequent ability of hippocampus-driven discharges to propagate to the EC suggest that these inhibitory restrictions are most likely at play in the subiculum itself.

Picrotoxin-induced changes in connectivity do not require NMDA receptor function

We also assessed whether NMDA receptors contributed to the changes in connectivity seen during picrotoxin application. To this end we applied high concentrations of the NMDA-receptor antagonist CPP to functionally disconnected slices. As shown in Fig. 4*B* (+ 30 μM CPP, $n = 5$) CPP abolished the 4AP-induced ictal events that initiated in EC (Avoli *et al.* 1996; de Guzman *et al.* 2004). However, further addition of picrotoxin could still cause an initial ictal event followed by interictal activity in all areas of the slice (Fig. 4*C*, + 30 μM CPP + 50 μM Picrotoxin). Furthermore, NMDA receptor blockade did not avert the picrotoxin-induced potentiation of the interictal activity or its appearance in the subiculum. (Fig. 4*C*; $n = 5$).

Simultaneous field potential and intracellular recordings in the subiculum

The results obtained from the functionally disconnected slices during application of medium containing only 4AP suggest that the subiculum plays a role in gating hippocampal output activity. Furthermore, the ability of CA3-driven epileptiform discharges to propagate to the EC during picrotoxin suggests GABAergic mechanisms in the subiculum might be involved in such a control. Hence, we recorded intracellularly subicular cells along with field potential activity in CA3 and EC in the presence of 4AP and following further addition of picrotoxin.

Two main modes of subicular activity were recorded from these slices during 4AP application. The first type was seen in 20 subicular cells and consisted of bursts of action potentials that followed the interictal discharges recorded in CA3 with time lags of 21 ± 9 ms ($n = 7$) (Fig. 5). Electrophysiological characterization of these neurones revealed that 9 out of 20 cells were intrinsic non-bursters (RMP = −62.9 ± 7.2 mV, R_i = 66.4 ± 16.3 MΩ, APA = 93.5 ± 13.3 mV, APD = 1.0 ± 0.2 ms; not shown) while the remaining 11

Figure 2. Picrotoxin-induced augmentation of field amplitudes in CA3, CA1 and subiculum
A, sequential field potential recording along the CA3–CA1–subiculim (Sub)–EC axis under control (4AP) conditions. Field electrodes in CA3 and EC were kept at the same position whilst a third electrode was moved along the stratum pyramidale to CA1 (*a*), CA1–Sub border (*b*) and Sub (*c*). Note the diminished field activity recorded in the subiculum as compared to CA1 and CA1–subiculum. *B*, monitoring field potential activity in EC, subiculum and CA3 from the onset of picrotoxin application until complete synchronization of the limbic structures. Note that initially CA3-driven interictal discharges do not propagate to the EC (left lower inset), but that following potentiation of subicular network activity (arrow), CA3-driven interictal events can propagate to the EC (right lower inset). Also note that potentiation in subicular activity precedes hippocampus–EC synchronization (middle *versus* right inset). *C*, bar graph of the normalized increase in field potential amplitude recorded in different areas of the slice; note that the most drastic potentiation occurs in the subiculum.

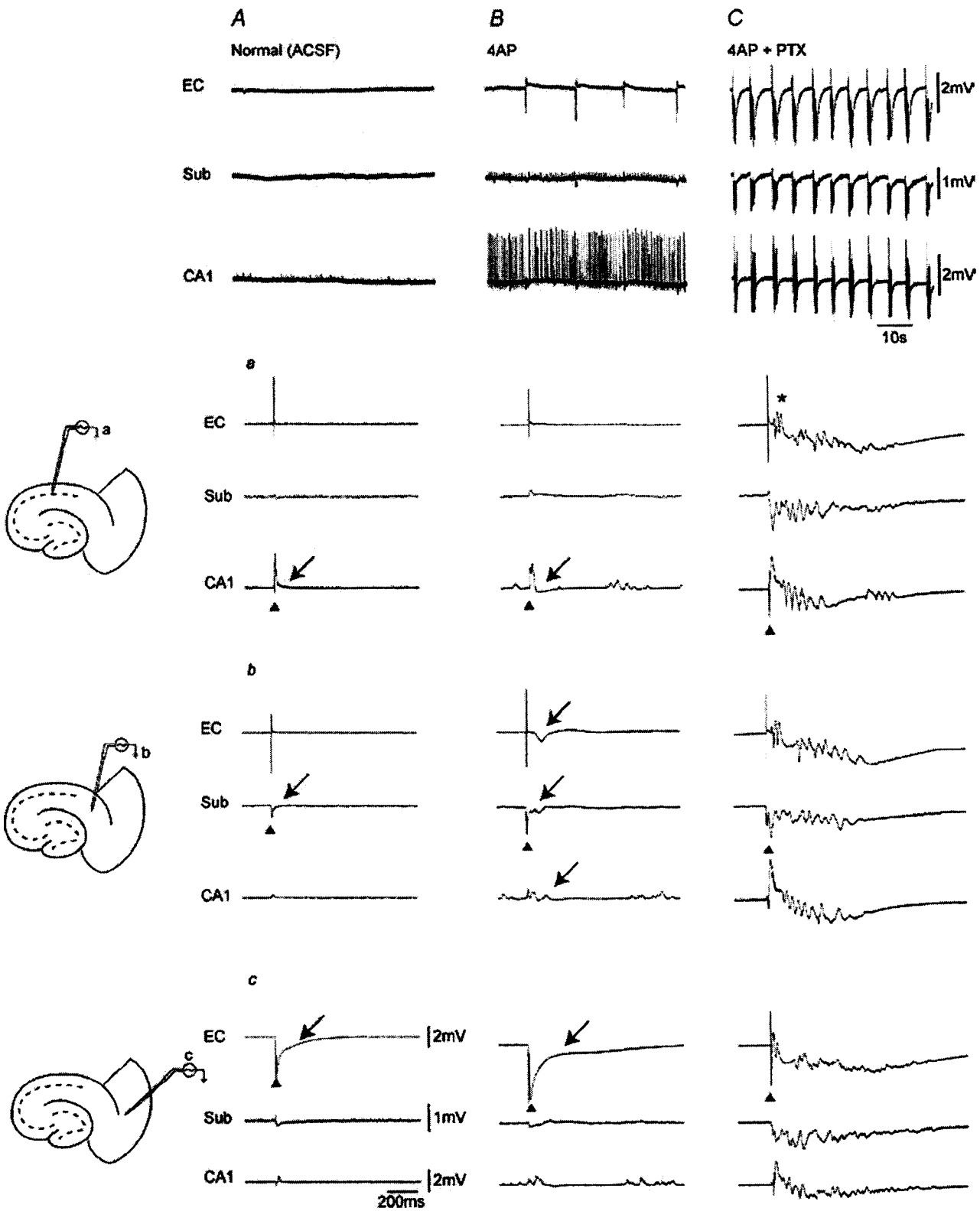

cells (RMP = −63.4 ± 7.0 mV, R_i = 60.9 ± 15.6 MΩ, APA = 94.5 ± 6.8 mV, APD = 1.0 ± 0.1 ms) discharged action potential bursts at the onset of an intracellular depolarizing pulse (Fig. 5*Ab*). Application of picrotoxin to these slices resulted in synchronous interictal discharges occurring in all areas. Furthermore, expanded traces demonstrated that these intracellular events followed CA3 field activity and preceded that of the EC (Fig. 5*B*, Picrotoxin (late), inset). Intracellular injection of depolarizing pulses indicated that picrotoxin did not modify the intrinsic firing patterns of these cells (not shown).

In contrast, the second group of subicular cells (n = 11) generated little or no spontaneous action potential firing, while producing robust postsynaptic potentials (PSPs) in association with the CA3-recorded interictal discharges (Fig. 6*Aa*, Control (4AP)). These PSPs were usually predominated by a hyperpolarizing component (Fig. 6*A*, Control (4AP), arrows in the lower inset) with a reversal value of approx. −71 mV (not illustrated) suggesting that they were $GABA_A$ receptor mediated. In addition, these neurones also generated large isolated hyperpolarizing potentials (Fig. 6*A*, Control (4AP), asterisk in the lower inset) with a similar reversal potential. Examination of the firing properties of these cells (Fig. 6*Ab*) revealed that 9 out of 11 were non-bursting elements (RMP = −67.7 ± 5.1 mV, R_i = 57.2 ± 14.3 MΩ, APA = 99.2 ± 5.4 mV, APD = 1.2 ± 0.1 ms). Superfusion of these slices with picrotoxin transformed the activity of these 'silent' cells into synchronous burst firing (Fig. 6*Aa*, Picrotoxin). Monitoring the evolution in the intracellular activity of these neurones from the onset of picrotoxin application (Fig. 6*Aa*, Picrotoxin (transition)) until the complete synchronization between hippocampal areas and EC (Fig. 6*Aa*, Picrotoxin, late) revealed a gradual decrease in the frequency of occurrence and the eventual disappearance of the robust PSPs (Fig. 6*Aa*, Picrotoxin (transition) *versus* Picrotoxin (late)) along with the complete blockade of the isolated hyperpolarizing potentials. As with the other group of subicular cells, the intrinsic firing patterns of these neurones were not changed by picrotoxin (not shown).

Picrotoxin-induced potentiation in subicular activity is not due to upstream effects

It has been well documented that GABAergic circuits exert an important inhibitory control over local networks within CA3/CA1; in addition, loss of this restraint via $GABA_A$ receptor antagonism is sufficient to unmask polysynaptic glutamatergic excitation within these structures (Miles & Wong, 1987; Miles *et al.* 1988). Hence, it can be reasonably argued that the picrotoxin-induced potentiation of subicular activity observed in our experiments might arise from enhanced, upstream hippocampal output rather than decreased gating within the subiculum. In order to clarify this issue, bath application of picrotoxin was investigated in slices in which the subiculum was isolated from CA3/CA1 by knife-cuts to the Schaffer collaterals (Fig. 7*Aa*). In this set of experiments, potentiation of subicular activity upon $GABA_A$ receptor antagonism was observed to occur in spite of the cut (n = 6, Fig. 7*Ab*, + Picrotoxin). However, epileptiform discharges in this scenario appeared to initiate sometimes in the subiculum (n = 3 slices) and at other times in the EC (n = 3 slices) (Fig. 7*Ab*, inset).

The potential gating role of subicular networks was further addressed in isolated subicular minislices (Fig. 7*B*). In the presence of 4AP, low-amplitude synchronous discharges (interval of occurrence = 142 ± 107 s; 55–450 s; n = 18) were observed to occur in all areas of the isolated subiculum and could initiate in the proximal, middle or distal regions (Fig. 7*Ba*, Control (4AP)). Subsequent addition of picrotoxin induced a drastic augmentation of activity in all subicular regions (n = 13, Fig. 7*Ba*, + Picrotoxin) thereby providing conclusive evidence that during 4AP application subicular networks, both in the combined slice and the isolated minislice preparations, are under tight $GABA_A$ receptor-mediated control.

Slow 4AP-induced interictal discharges generated in the subiculum represent the activity of synchronized interneuronal networks

Intracellular characterization of the slow-interictal discharges recorded in subicular minislices revealed a

Figure 3. Stimulation of hippocampal outputs activates EC only under conditions of $GABA_A$-receptor antagonism
Panels in the top row show the spontaneous field potential activity recorded simultaneously from CA1, subiculum and EC in the absence of convulsants (i.e. Normal ACSF) (*A*), in the presence of 4AP (*B*), and during 4AP + PTX (*C*). Slice diagrams on the left illustrate the positions of the stimulating bipolar electrode in CA1 (*a*), subiculum (*b*), and deep EC layer (*c*). Triangles indicate the structure stimulated in each set of recordings and arrows point to the subsequent response recorded. Note that single shock stimulation of CA1 networks both in the absence and presence of 4AP induces a small subicular response with no EC activation (*Aa* and *Ba*). Note in contrast the potentiated subicular response and the subsequent EC discharge (asterisk) induced by hippocampal output stimulation under $GABA_A$-receptor antagonism (*Ca*).

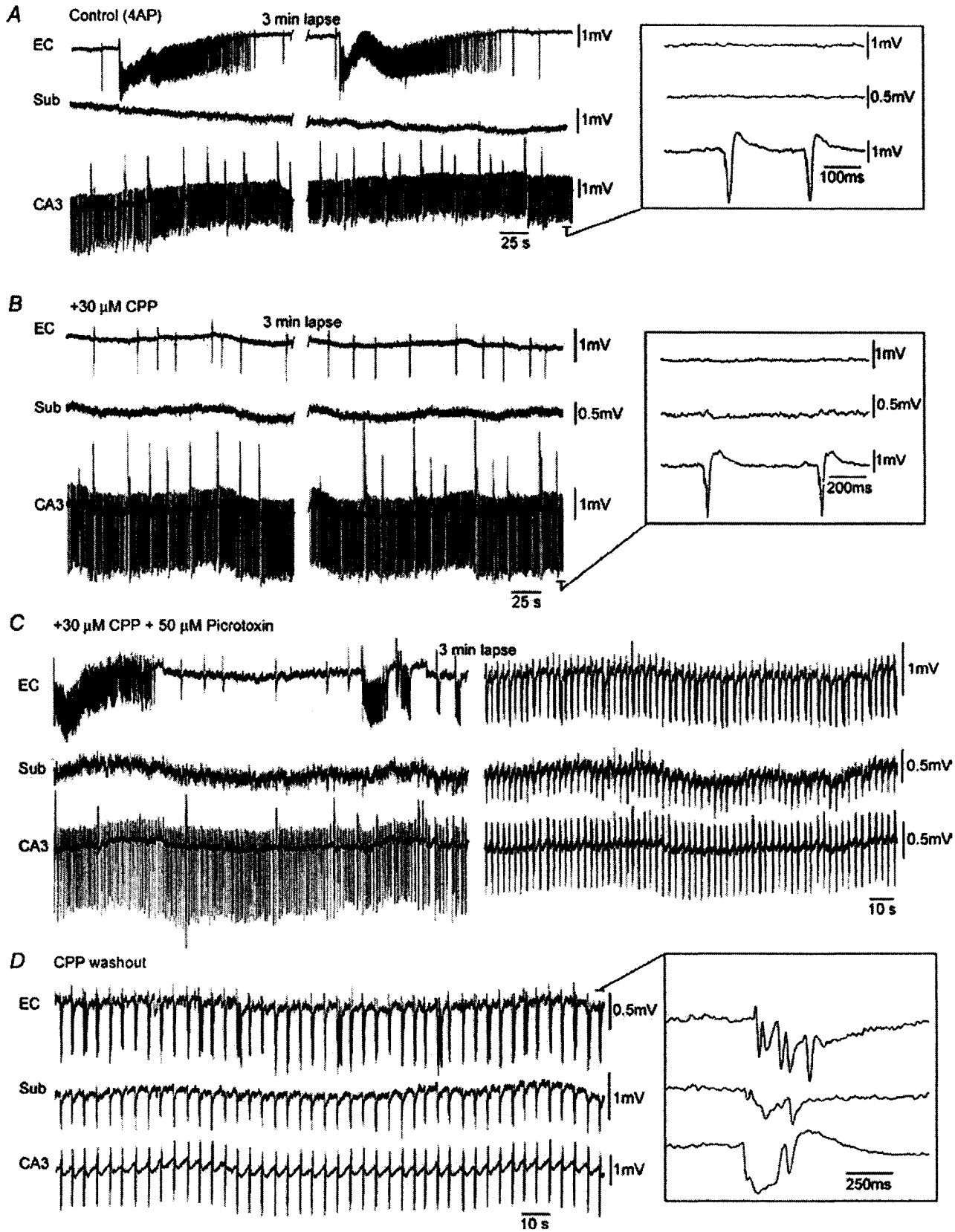

sequence of an early hyperpolarizing IPSP followed by a long lasting depolarization that could at times trigger action potential firing (Fig. 8*Aa* and *b* and *B*, Control (4AP); $n = 20$ neurones). Bath application of picrotoxin abolished these events and in their place robust network bursting was observed ($n = 6$ neurones, Fig. 8*Aa*, + Picrotoxin).

To further investigate the mechanisms underlying the generation of these 4AP-induced slow events, glutamatergic antagonists were employed. Interestingly, CPP and CNQX could not abolish these low amplitude discharges (Fig. 8*B*, + (CP P+ CNQX), $n = 8$) while further application of picrotoxin resulted in their complete loss ($n = 4$, not shown). Thus, these results indicate that as in other cortical areas (Perreault & Avoli, 1989, 1992; Avoli *et al.* 1994, 1996) the synchronous potentials recorded in the subiculum in the presence of 4AP correspond to the responses of pyramidal cells to the synchronized interneurone activity.

Discussion

We have found here that decreasing $GABA_A$ receptor function facilitates communication within the limbic networks contained in a combined hippocampus–EC slice. Accordingly, picrotoxin transformed functionally disconnected slices into ones that were functionally connected. In addition, we have discovered that this effect is mainly caused by a gating function played by the subiculum on hippocampal outputs, thus indicating that this limbic structure modulates interactions between hippocampal and parahippocampal networks.

The 4AP model revisited in the light of different patterns of epileptiform activity

We have reported that in reciprocally interconnected hippocampus–EC slices obtained from adult rat (Benini *et al.* 2003) or mouse brains (Barbarosie & Avoli, 1997; Barbarosie *et al.* 2000), application of 4AP-containing or Mg^{2+}-free medium induces CA3-driven interictal events that propagate to the EC where they control the propensity of this latter structure to generate ictal discharges resembling those seen in MTLE patients (cf. Swartzwelder *et al.* 1987; Wilson *et al.* 1988). Accordingly, cutting the Schaffer collaterals in these functionally connected slices averts CA3 outputs and discloses NMDA receptor-mediated ictal events in the EC, thus leading to a pattern of epileptiform activity similar to what is recorded in functionally disconnected slices (Avoli *et al.* 1996; Benini *et al.* 2003).

Until now, we assumed that the inability of CA3-driven interictal activity to propagate to the EC was caused by the slicing procedure that had led to damaging the connections between hippocampus proper and EC. Contrary to this view, we have discovered here that $GABA_A$ receptor antagonism can reversibly transform a disconnected slice into one that appears to be functionally connected. Hence, these findings demonstrate that the two patterns of electrographic activity may not reflect anatomical differences, but rather implicate a mechanism that rests on the gating role played by subicular networks on the propagation of epileptiform discharges originating in the hippocampus proper.

Subicular networks gate hippocampal outputs via $GABA_A$ receptor-mediated mechanisms in functionally disconnected slices

By using sequential recordings along the CA3–CA1–subiculum axis of functionally disconnected slices we have found that the amplitude of the 4AP-induced interictal activity decreases dramatically in the subiculum, where it is often non-existent. Moreover, during $GABA_A$ receptor antagonism, the subiculum undergoes the most dramatic potentiation in field activity (150–550%) signalling an increased recruitment of neurones.

It has been established that disinhibition unmasks polysynaptic excitation within CA3 neuronal networks (Miles & Wong, 1987; Miles *et al.* 1988) and it is possible that this improved synchronicity would consequently lead to an increased drive onto the subiculum. Local pharmacological activation of the subiculum would have been ideal for clarifying this issue. However, initial attempts at focal applications of picrotoxin were elusive due to the fact that in our horizontal slice preparation the subiculum lies critically close to other structures (CA1, dentate gyrus, and medial EC) and dispersion of the droplet to these areas could not be avoided.

Figure 4. NMDA receptors do not contribute to picrotoxin-induced synchronicity in a functionally disconnected slice

A, simultaneous field potential recordings in EC, subiculum (Sub) and CA3 showing that interictal discharges initiating in CA3 do not propagate to the EC where activity is characterized by robust ictal discharges. Note that in this slice no field activity was recorded in the subiculum. *B*, bath application of high concentrations of the NMDA-receptor antagonist CPP results in the loss of EC-driven ictal events. *C*, subsequent application of picrotoxin results in an initial ictal discharge in EC that is followed by a pattern of interictal discharge in all limbic structures. *D*, CPP washout causes a prolongation of the interictal events and a slow down in their frequency of occurrence. These discharges continue to initiate in CA3 and propagate sequentially to the subiculum and EC (inset).

This being said, our observations strongly suggest that although increased presynaptic release of excitatory transmitters at CA1–subiculum synapses may occur, this mechanism is unlikely by itself to explain the amplification of subicular activity observed under $GABA_A$ receptor antagonism. First, potentiation of subicular activity upon $GABA_A$-receptor antagonism was observed even when the subiculum was separated from CA3/CA1 via microknife cuts to the Schaffer collaterals. Furthermore, significant augmentation in activity was demonstrated to occur in isolated subicular minislices in the absence of either upstream or downstream factors. Altogether this is conclusive evidence that the picrotoxin-induced effect in the subiculum is not due to enhanced output of upstream structures (i.e. CA3/CA1) but rather due to the decreased control of GABAergic circuits within the subiculum itself.

Investigation into the functional role of GABAergic circuits within the subiculum was made possible by the interesting property of the 4AP model used in our study. In addition to blocking K^+ currents (Rudy, 1988) and interfering with Ca^{2+} channels (Segal & Barker, 1986), 4AP has been shown to facilitate neurotransmitter release at presynaptic terminals of both excitatory and inhibitory synapses (Thesleff, 1980; Rutecki *et al.* 1987; Aram *et al.* 1991). Previous studies have shown that the subiculum is indeed capable of generating robust interictal discharges under conditions of decreased inhibition (Harris & Stewart,

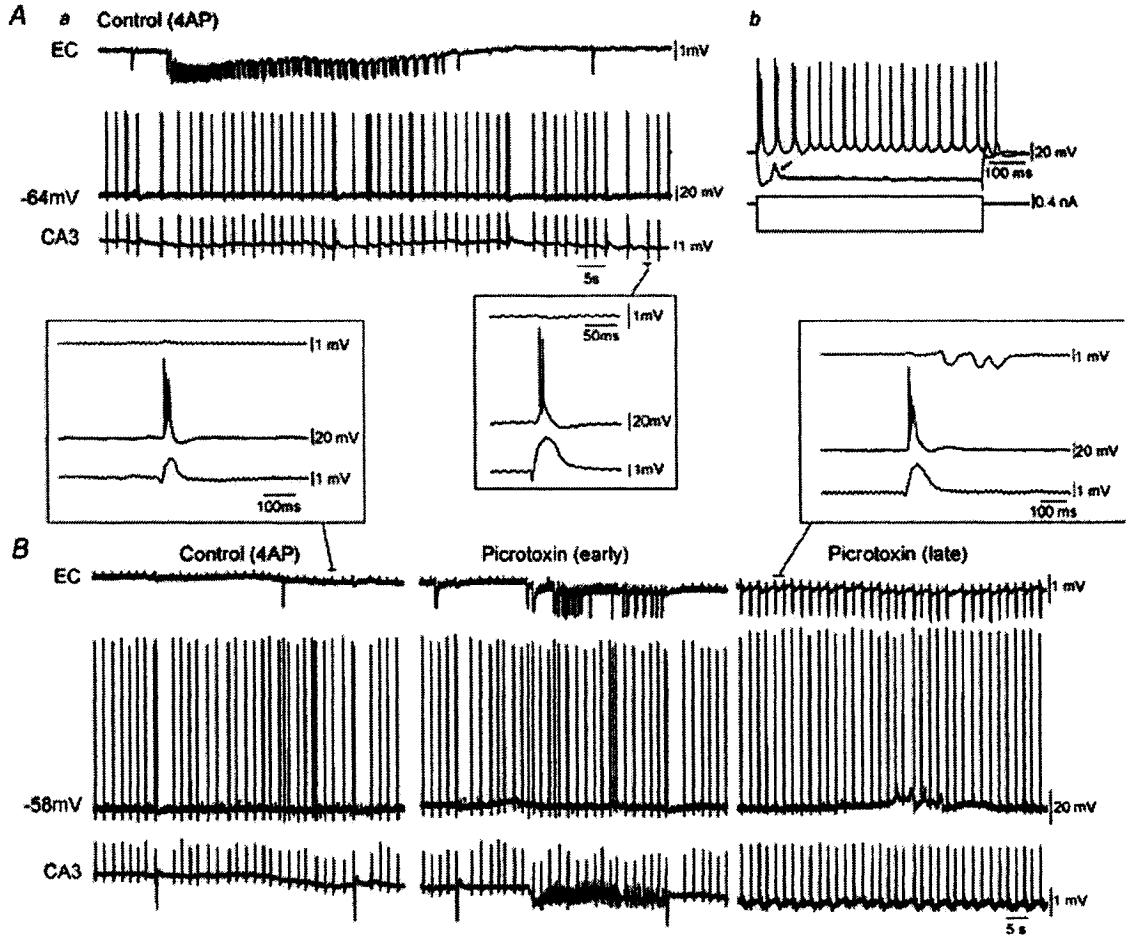

Figure 5. Simultaneous field and intracellular recordings in functionally disconnected slice
Aa, simultaneous field (EC, CA3) and intracellular (subiculum, −64 mV) recordings under control conditions (i.e. 4AP) reveal that this subicular cell is excitable at RMP. Note in the inset that the burst firing generated by this subicular neurone is synchronous with the interictal discharge recorded in CA3, but that no propagation occurs to EC. *Ab*, responses to intracellular injection of depolarizing and hyperpolarizing current pulses; note that this neurone is an intrinsic burster. Depolarizing event during hyperpolarization represents a spontaneously occurring EPSP (arrow). *B*, picrotoxin application to another functionally disconnected slice results in an initial ictal event in EC (Picrotoxin (early)) followed by synchronization of all limbic networks (Picrotoxin (late)). Note in the expanded traces that the intracellularly recorded subicular bursts follow CA3 field activity and precede that of the EC.

2001) or increased excitation (Behr & Heineman, 1996; Harris & Stewart, 2001). Using our model we have, however, shown that the subiculum does not generate robust activity when both excitatory and inhibitory mechanisms are simultaneously altered. Furthermore, we found in the isolated subiculum that under such conditions, this structure is more likely to generate slow synchronous events that are resistant to glutamatergic antagonists but sensitive to $GABA_A$ receptor blockade. These synchronous potentials, which have been reported in other hippocampal structures as well as in the neocortex, represent the activity of highly synchronized interneuronal networks (Perreault & Avoli, 1989, 1992; Michelson & Wong, 1994; Avoli *et al.* 1994, 1996; Lamsa & Kaila, 1997). Altogether, these findings indicate that the overall activity of the subiculum in the presence of 4AP is dominated by inhibitory mechanisms that control hippocampal output propagation to the EC. Blockade of $GABA_A$ receptors hampers this inhibition (as suggested by the decrease in IPSPs recorded in 'silent' subicular cells), allowing an increased recruitment of subicular networks and the consequent spread of both spontaneous and stimulus-induced activity from the hippocampus to the EC.

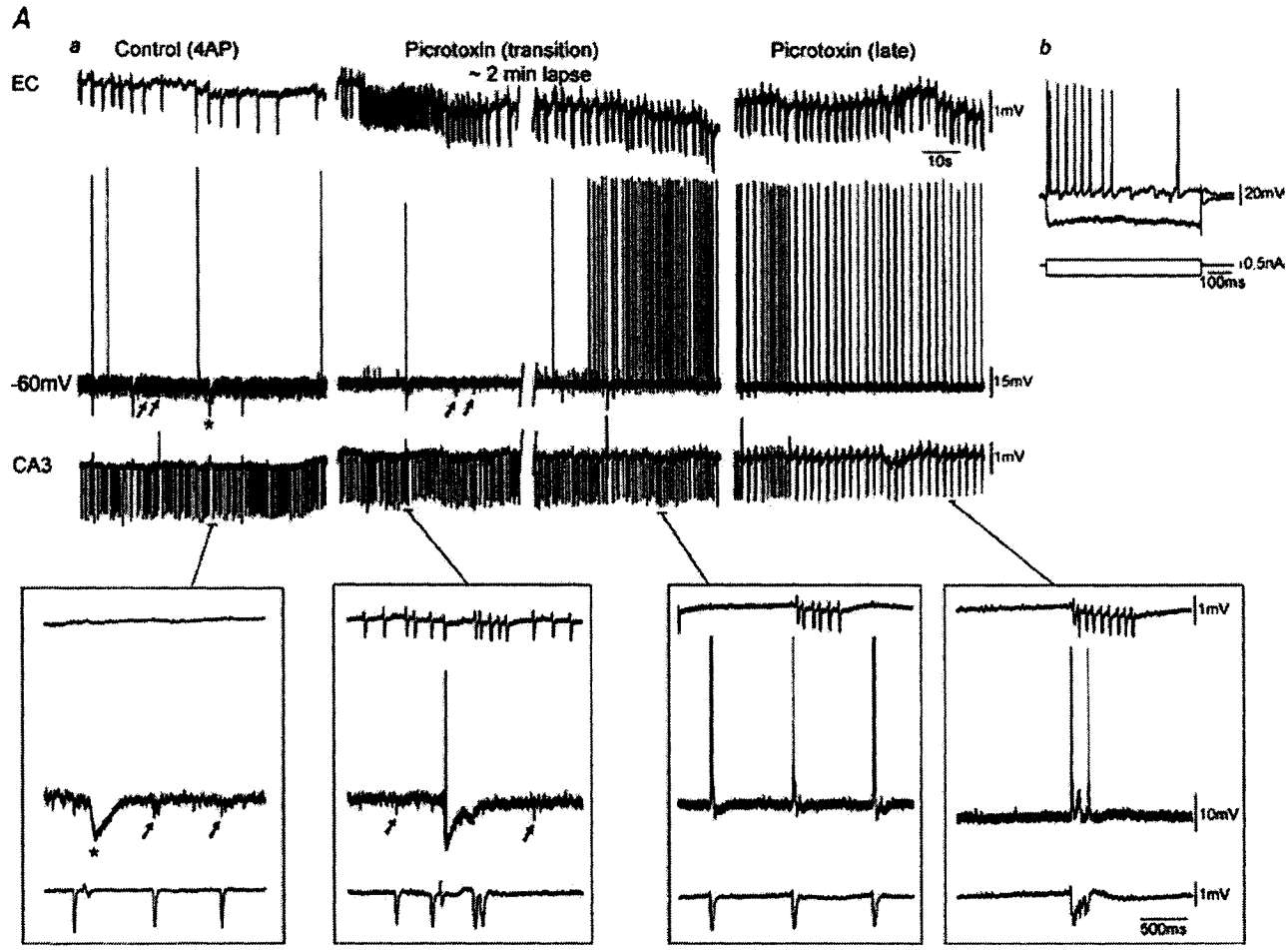

Figure 6. Field and intracellular recordings in functionally disconnected slice
Aa, simulatneous field (EC, CA3) and intracellular (subiculum, −60 mV) recordings during control (4AP) conditions reveals that this subicular cell is 'silent' at RMP. Note the presence of PSPs that are coincident with CA3 discharges (arrows) and the large isolated inhibitory postsynaptic potentials (IPSPs) (Control (4AP), asterisk). Superfusion of slices with picrotoxin discloses in these cells action potential discharges at RMP (Picrotoxin). Monitoring the evolution in the intracellular activity of these subicular neurones from the initial application of the $GABA_A$ receptor antagonist (Picrotoxin (transition)) until the complete synchronization between hippocampal and parahippocampal structures (Picrotoxin (late)) reveals IPSP disappearance. Insets below traces demonstrate expansions of selected events. Note the presence of large IPSPs (asterisk) and smaller PSPs (arrows) within the subiculum prior to complete synchronization of limbic structures. *Ab*, firing properties of this cell reveal a non-bursting neurone.

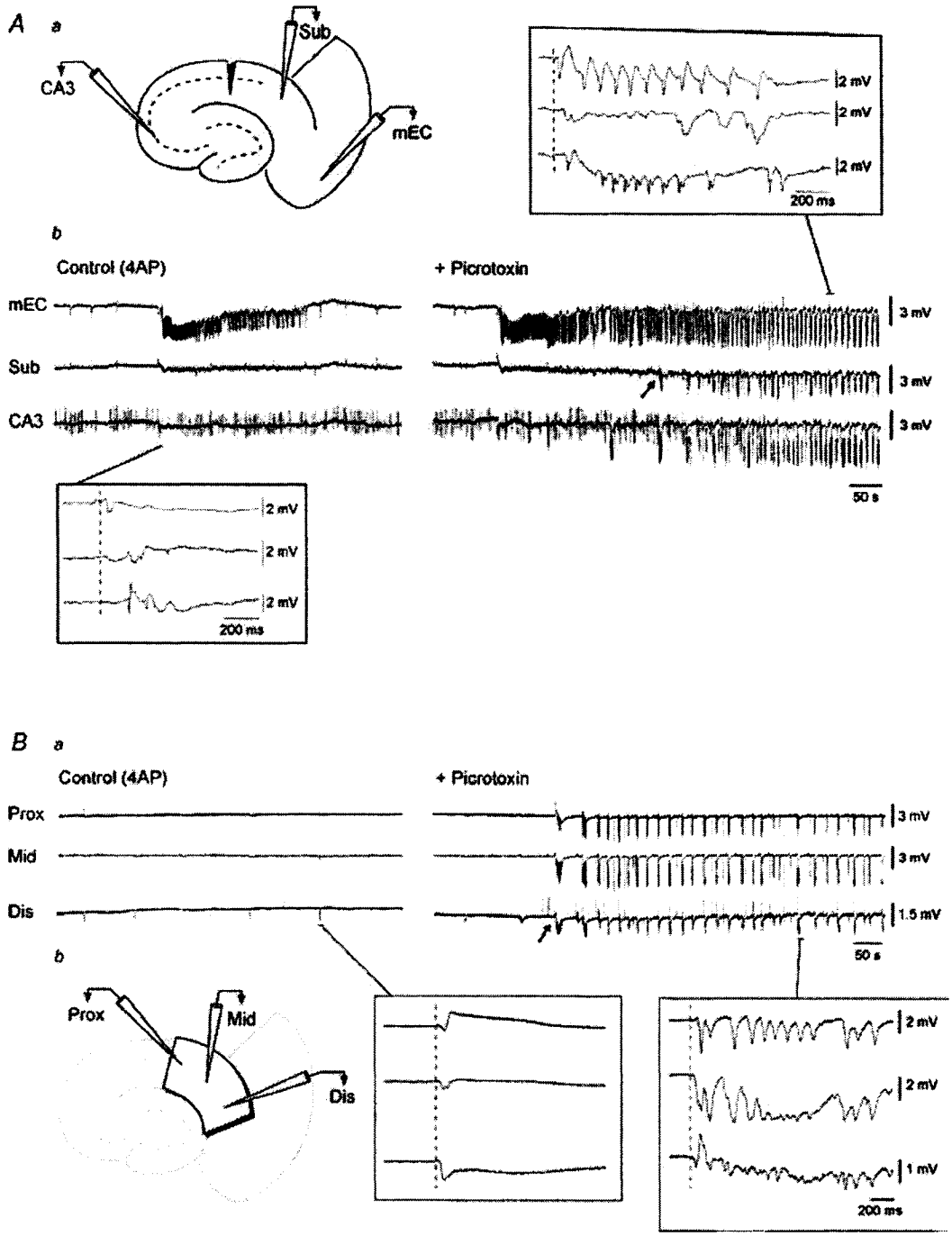

Figure 7. Picrotoxin-induced potentiation of subicular activity is not due to upstream effects
Aa, diagram illustrating a combined slice in which the Schaffer collaterals have been severed by a microknife cut at the level of CA1. *Ab*, simultaneous field potential recordings obtained from this slice preparation in EC, subiculum (Sub) and CA3 during bath application of 4AP and upon further addition of Picrotoxin. The slow interictal events observed in all structures in the presence of 4AP initiate in EC (bottom inset). Note the potentiation of subicular activity that occurs in the presence of the $GABA_A$ receptor antagonist (arrow). Also note that in the presence of picrotoxin, the epileptiform activity in this case initiates in EC and subsequently spreads to subiculum and CA3 (upper inset). *Ba*, simultaneous field potential recordings obtained from the proximal, middle and distal regions of an isolated subicular minislice preparation during 4AP application and upon further addition of Picrotoxin. Note that during 4AP, slow interictal-like events are generated in all regions of the subiculum (left inset). Also note that $GABA_A$ receptor antagonism induces potentiation of subicular activity in all regions (arrow indicates onset of picrotoxin-induced activity). Right inset illustrates expansion of picrotoxin-induced event. *Bb*, diagram illustrating the isolated minislice preparation and position of field electrodes.

Subicular cells may be under a different degree of $GABA_A$ receptor-mediated control in the same functionally disconnected slice

Neurophysiological investigations have shown that several types of GABAergic cells are present in the subiculum (Kawaguchi & Hama, 1987; Greene & Totterdell, 1997; Menendez de la Prida *et al.* 2003). We have found here that under control conditions (i.e. during application of medium containing 4AP only) subicular pyramidal neurones generate two different patterns of intracellular activity in functionally disconnected slices: one group of cells fired action potentials in coincidence with CA3-driven interictal events whilst the other generated either EPSP–IPSP sequences or isolated IPSPs. These two behaviours of subicular cells, both of which could be found in the same slice, have also been reported in the human epileptic subiculum of MTLE patients, where they reflect differences in the reversal potential of pyramidal cells for $GABA_A$ receptor-mediated conductances (Cohen *et al.* 2002).

The presence of 'silent' subicular cells in functionally disconnected slices indicates that hippocampal activity may not propagate to the EC due to local inhibitory

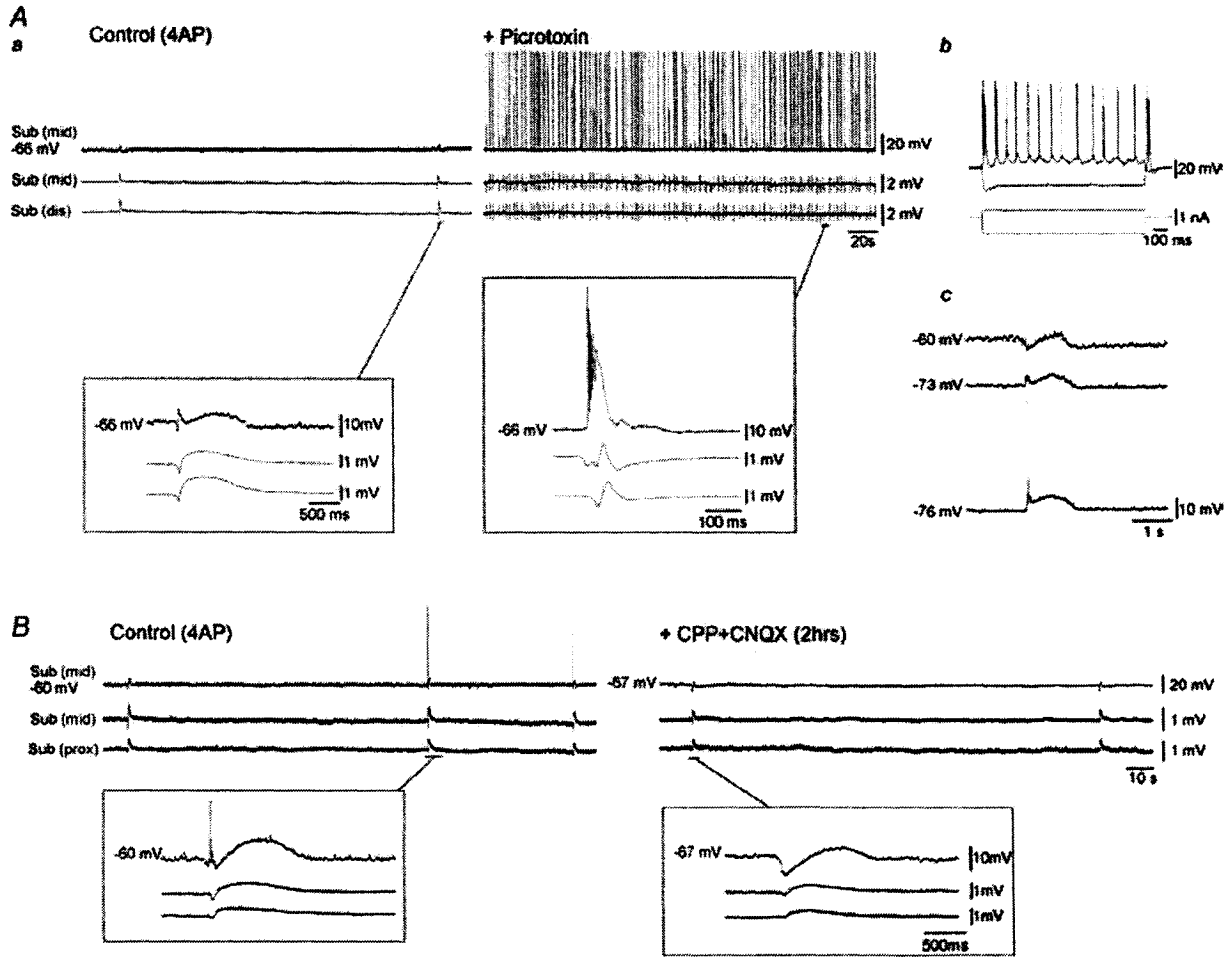

Figure 8. Pharmacological characterization of 4AP-induced activity in isolated subicular minislices
Aa, simulatneous field (middle subiculum, distal subiculum) and intracellular (middle subiculum, −66 mV) recordings during control (4AP) conditions reveals that the slow interictal events correspond intracellularly to an early hyperpolarization followed by a sustained depolarization (left inset). In the presence of picrotoxin there is increased field activity in the isolated subiculum and robust network bursting can be recorded intracellularly (right inset). *Ab*, firing properties of this cell reveals that it was an intrinsically bursting neurone. *Ac*, intracellular traces of the 4AP-induced event at different membrane potentials reveals reversal of the hyperpolarizing component at negative membrane potentials (−73 mV and −76 mV). Note the truncated action potential riding on this reversed event at −76 mV. *Ba*, simulatneous field (middle subiculum, proximal subiculum) and intracellular (middle subiculum, −60 mV and −67 mV) recordings in control (4AP) and after 2 h of further CPP + CNQX application. Note that intracellular recordings were carried out from two different cells within the same slice and in the same subicular region. Insets demonstrate expansions of the slow synchronouns event during both conditions.

control exerted on a subset of projecting subicular cells. In line with this view, previous studies have demonstrated that subicular pyramidal cells are restrained by local GABAergic networks via feedforward (Finch & Babb, 1980; Colino & De Molina, 1986; Finch *et al.* 1988; Behr *et al.* 1998) and recurrent inhibitory mechanisms (Menendez de la Prida, 2003; Menendez de la Prida & Gal, 2004). Accordingly, we have demonstrated that IPSP blockade by $GABA_A$ receptor antagonism coincides with the appearance of network-driven burst firing, thus implicating a role for subicular $GABA_A$ receptor-mediated inhibition in gating hippocampal output activity. Indeed, it has been reported that epileptiform discharges generated in the hippocampus can successfully propagate to the medial EC via the subicular complex under reduction of GABAergic mechanisms (Menendez de la Prida & Pozo, 2002).

Conclusions

Studies in various epilepsy models have identified the dentate gyrus as a gater for the spread of limbic seizures from the EC to the hippocampus proper (Collins *et al.* 1983; Heinemann *et al.* 1992). However, until this study, no investigation had addressed the role of the subiculum in controlling hippocampal outputs during epileptiform synchronization even though it was well established that this structure is in a strategic position for doing so. Our observations that blocking $GABA_A$ receptor-mediated mechanisms results in subicular hyperexcitability and subsequently intralimbic synchronization is relevant to pathological conditions such as epilepsy. Studies in slices obtained from MTLE patients indicate that both bursting pyramidal cells and interneurones contribute to the interictal activity that occurs in the subiculum (Cohen *et al.* 2002; Wozny *et al.* 2003). In addition, in chronic animal models of MTLE, alterations at the level of intrinsic and network properties of principal cells (Wellmer *et al.* 2002; Knopp *et al.* 2005) as well as a reduction in specific interneuronal subpopulations (van Vliet *et al.* 2004) have been reported in this structure. Altogether, these findings suggest that synaptic reorganization and altered inhibition contribute to subicular network hyperexcitability that may in turn play a role in the generation and spread of convulsive activity.

References

Aram JA, Michelson HB & Wong RK (1991). Synchronized GABAergic IPSPs recorded in the neocortex after blockade of synaptic transmission mediated by excitatory amino acids. *J Neurophysiol* **65**, 1034–1041.

Avoli M, Barbarosie M, Lücke A, Nagao T, Lopantsev V & Köhling R (1996). Synchronous GABA-mediated potentials and epileptiform discharges in the rat limbic system in vitro. *J Neurosci* **16**, 3912–3924.

Avoli M, Mattia D, Siniscalchi A, Perreault P & Tomaiuolo F (1994). Pharmacology and electrophysiology of a synchronous GABA-mediated potential in the human neocortex. *Neuroscience* **62**, 655–666.

Barbarosie M & Avoli M (1997). CA3-driven hippocampal-entorhinal loop controls rather than sustains in vitro limbic seizures. *J Neurosci* **17**, 9308–9314.

Barbarosie M, Louvel J, Kurcewicz I & Avoli M (2000). CA3-released entorhinal seizures disclose dentate gyrus epileptogenicity and unmask a temporoammonic pathway. *J Neurophysiol* **83**, 1115–1124.

Behr J, Gloveli T & Heinemann U (1998). The perforant path projection from the medial entorhinal cortex layer III to the subiculum in the rat combined hippocampal-entorhinal cortex slice. *Eur J Neurosci* **10**, 1011–1018.

Behr J & Heinemann U (1996). Low Mg^{2+} induced epileptiform activity in the subiculum before and after disconnection from rat hippocampal and entorhinal cortex slices. *Neurosci Lett* **205**, 25–28.

Benini R, D'Antuono M, Pralong E & Avoli M (2003). Involvement of amygdala networks in epileptiform synchronization in vitro. *Neuroscience* **120**, 75–84.

Canteras NS & Swanson LW (1992). Projections of the ventral subiculum to the amygdala, septum, and hypothalamus: a PHAL anterograde tract-tracing study in the rat. *J Comp Neurol* **324**, 180–194.

Cohen I, Navarro V, Clemenceau S, Baulac M & Miles R (2002). On the origin of interictal activity in human temporal lobe epilepsy in vitro. *Science* **298**, 1418–1421.

Colino A & Fernandez de Molina A (1986). Inhibitory response in entorhinal and subicular cortices after electrical stimulation of the lateral and basolateral amygdala of the rat. *Brain Res* **378**, 416–419.

Collins RC, Tearse RG & Lothman EW (1983). Functional anatomy of limbic seizures: Focal discharges from medial entorhinal cortex in rat. *Brain Res* **280**, 25–40.

D'Antuono M, Benini R, Biagini G, D'Arcangelo G, Barbarosie M, Tancredi V *et al.* (2002). Limbic network interactions leading to hyperexcitability in a model of temporal lobe epilepsy. *J Neurophysiol* **87**, 634–639.

Deacon TW, Eichenbaum H, Rosenberg P & Eckmann KW (1983). Afferent connections of the perirhinal cortex in the rat. *J Comp Neurol* **220**, 168–190.

Du F, Whetsell WO Jr, Abou-Khalil B, Blumenkopf B, Lothman EW & Schwarcz R (1993). Preferential neuronal loss in layer III of the entorhinal cortex in patients with temporal lobe epilepsy. *Epilepsy Res* **16**, 223–233.

Finch DM & Babb TL (1980). Inhibition in subicular and entorhinal principal neurons in response to electrical stimulation of the fornix and hippocampus. *Brain Res* **196**, 89–98.

Finch DM & Babb TL (1981). Demonstration of caudally directed hippocampal efferents in the rat by intracellular injection of horseradish peroxidase. *Brain Res* **214**, 405–410.

Finch DM, Tan AM & Isokawa-Akesson M (1988). Feedforward inhibition of the rat entorhinal cortex and subicular complex. *J Neurosci* **8**, 2213–2226.

Gloor P (1997). *The Temporal Lobe and Limbic System*. Oxford University Press, New York.

Greene JR & Totterdell S (1997). Morphology and distribution of electrophysiologically defined classes of pyramidal and nonpyramidal neurons in rat ventral subiculum in vitro. *J Comp Neurol* **380**, 395–408.

de Guzman P, D'Antuono M & Avoli M (2004). Initiation of electrographic seizures by neuronal networks in entorhinal and perirhinal cortices in vitro. *Neurosci* **123**, 875–886.

Harris E & Stewart M (2001). Intrinsic connectivity of the rat subiculum. II. Properties of synchronous spontaneous activity and a demonstration of multiple generator regions. *J Comp Neurol* **435**, 506–518.

Heinemann U, Beck H, Dreier JP, Ficker E, Stabel J & Zhang CL (1992). The dentate gyrus as a regulated gate for the propagation of epileptiform activity. *Epilepsy Res Suppl* **7**, 273–280.

Houser CR (1999). Neuronal loss and synaptic reorganization in temporal lobe epilepsy. *Adv Neurol* **79**, 743–761.

Houser CR, Miyashiro JE, Swartz BE, Walsh GO, Rich JR & Delgado-Escueta AV (1990). Altered patterns of dynorphin immunoreactivity suggest mossy fiber reorganization in human hippocampal epilepsy. *J Neurosci* **10**, 267–282.

Kawaguchi Y & Hama K (1987). Fast-spiking non-pyramidal cells in the hippocampal CA3 region, dentate gyrus and subiculum of rats. *Brain Res* **425**, 351–355.

Knopp A, Kivi A, Wozny C, Heinemann U & Behr J (2005). Cellular and network properties of the subiculum in the pilocarpine model of temporal lobe epilepsy. *J Comp Neurol* **483**, 476–488.

Lamsa K & Kaila K (1997). Ionic mechanisms of spontaneous GABAergic events in rat hippocampal slices exposed to 4-aminopyridine. *J Neurophysiol* **78**, 2582–2591.

Menendez de la Prida L (2003). Control of bursting by local inhibition in the rat subiculum in vitro. *J Physiol* **549**, 219–230.

Menendez de la Prida L & Gal B (2004). Synaptic contributions to focal and widespread spatiotemporal dynamics in the isolated rat subiculum in vitro. *J Neurosci* **24**, 5525–5536.

Menendez de la Prida L & Pozo MA (2002). Excitatory and inhibitory control of epileptiform discharges in combined hippocampal/entorhinal cortical slices. *Brain Res* **940**, 27–35.

Menendez de la Prida L, Suarez F & Pozo MA (2003). Electrophysiological and morphological diversity of neurons from the rat subicular complex in vitro. *Hippocampus* **13**, 728–744.

Michelson HB & Wong RK (1994). Synchronization of inhibitory neurones in the guinea-pig hippocampus in vitro. *J Physiol* **477**, 35–45.

Miles R, Traub RD & Wong RK (1988). Spread of synchronous firing in longitudinal slices from the CA3 region of the hippocampus. *J Neurophysiol* **60**, 1481–1496.

Miles R & Wong RK (1987). Inhibitory control of local excitatory circuits in the guinea-pig hippocampus. *J Physiol* **388**, 611–629.

O'Mara SM, Commins S, Anderson M & Gigg J (2001). The subiculum: a review of form, physiology and function. *Prog Neurobiol* **64**, 129–155.

Perreault P & Avoli M (1989). Effects of low concentrations of 4-aminopyridine on CA1 pyramidal cells of the hippocampus. *J Neurophysiol* **61**, 953–970.

Perreault P & Avoli M (1992). 4-Aminopyridine-induced epileptiform activity and a GABA-mediated long-lasting depolarization in the rat hippocampus. *J Neurosci* **12**, 104–115.

Pitkanen A, Tuunanen J, Kalviainen R, Partanen K & Salmenpera T (1998). Amygdala damage in experimental and human temporal lobe epilepsy. *Epilepsy Res* **32**, 233–253.

Rudy B (1988). Diversity and ubiquity of K channels. *Neuroscience* **25**, 729–749.

Rutecki PA, Lebeda FJ & Johnston D (1987). 4-Aminopyridine produces epileptiform activity in hippocampus and enhances synaptic excitation and inhibition. *J Neurophysiol* **57**, 1911–1924.

Segal M & Barker JL (1986). Rat hippocampal neurons in culture: Ca^{2+} and Ca^{2+}-dependent K^{+} conductances. *J Neurophysiol* **55**, 751–766.

Staff NP, Jung HY, Thiagarajan T, Yao M & Spruston N (2000). Resting and active properties of pyramidal neurons in subiculum and CA1 of rat hippocampus. *J Neurophysiol* **84**, 2398–2408.

Sutula T, Cascino G, Cavazos J, Parada I & Ramirez L (1989). Mossy fiber synaptic reorganization in the epileptic human temporal lobe. *Ann Neurol* **26**, 321–330.

Swanson LW & Cowan WM (1977). An autoradiographic study of the organization of the efferent connections of the hippocampal formation in the rat. *J Comp Neurol* **172**, 49–84.

Swanson LW, Wyss JM & Cowan WM (1978). An autoradiographic study of the organization of intrahippocampal association pathways in the rat. *J Comp Neurol* **181**, 681–715.

Swartzwelder SH, Lewis DV, Anderson WW & Wilson WA (1987). Seizure-like events in brain slices: supression by interictal activity. *Brain Res* **410**, 362–366.

Thesleff S (1980). Aminopyridines and synaptic transmission. *Neuroscience* **5**, 1413–1419.

Traub RD, Borck C, Colling SB & Jefferys JGR (1996). On the structure of ictal events in vitro. *Epilepsia* **37**, 879–891.

van Vliet EA, Aronica E, Tolner EA, Lopes da Silva FH & Gorter JA (2004). Progression of temporal lobe epilepsy in the rat is associated with immunocytochemical changes in inhibitory interneurons in specific regions of the hippocampal formation. *Exp Neurol* **187**, 367–379.

Wellmer J, Su H, Beck H & Yaari Y (2002). Long-lasting modification of intrinsic discharge properties in subicular neurons following status epilepticus. *Eur J Neurosci* **16**, 259–266.

Wiebe S (2000). Epidemiology of temporal lobe epilepsy. *Can J Neurol Sci* **27** (Suppl. 1), S6–S10.

Wilson WA, Swartzwelder HS, Anderson WW & Lewis DV (1988). Seizure activity in vitro: a dual focus model. *Epilepsy Res* **2**, 289–293.

Witter MP, Groenewegen HJ, Lopes da Silva FH & Lohman AH (1989). Functional organization of the extrinsic and intrinsic circuitry of the parahippocampal region. *Prog Neurobiol* **33**, 161–253.

Witter MP, Ostendorf RH & Groenewegen HJ (1990). Heterogeneity in the dorsal subiculum of the rat. distinct neuronal zones project to different cortical and subcortical targets. *Eur J Neurosci* **2**, 718–725.

Wozny C, Kivi A, Lehmann TN, Dehnicke C, Heinemann U & Behr J (2003). Comment on 'On the origin of interictal activity in human temporal lobe epilepsy in vitro'. *Science* **301**, 463.

Yilmazer-Hanke DM, Wolf HK, Schramm J, Elger CE, Wiestler OD & Blumcke I (2000). Subregional pathology of the amygdala complex and entorhinal region in surgical specimens from patients with pharmacoresistant temporal lobe epilepsy. *J Neuropathol Exp Neurol* **59**, 907–920.

Acknowledgements

This study was supported by the Canadian Institutes of Health Research (Grant MOP-8109). We thank Ms T. Papadopoulos for secretarial assistance.

APPENDIX C: Reprint of Chapter 3 and Waiver from Neuroscience

Neuroscience 120 (2003) 75–84

INVOLVEMENT OF AMYGDALA NETWORKS IN EPILEPTIFORM SYNCHRONIZATION *IN VITRO*

R. BENINI,[a] M. D'ANTUONO,[b] E. PRALONG[a,c] AND M. AVOLI[a,b]*

[a]*Montreal Neurological Institute and Departments of Neurology and Neurosurgery, and of Physiology, McGill University, Montreal, QC, H3A 2B4, Canada*

[b]*IRCCS Neuromed, 86077 Pozzilli, Italy*

[c]*Institute of Cellular Biology and Morphology, University of Lausanne, Lausanne, Switzerland*

Abstract—We used field potential and intracellular recordings in rat brain slices that included the hippocampus, a portion of the basolateral/lateral nuclei of the amygdala (BLA) and the entorhinal cortex (EC). Bath application of the convulsant 4-aminopyridine (50 μM) to slices (n=12) with reciprocally connected areas, induced short-lasting interictal-like epileptiform discharges that (i) occurred at intervals of 1.2–2.8 s, (ii) originated in CA3, and (iii) spread to EC and BLA. Cutting the Schaffer collaterals abolished them in both parahippocampal areas where slower interictal-like (interval of occurrence=4–17 s) and prolonged ictal-like discharges (duration=15±6.9 s, mean±S.D., n=7) appeared. These new types of epileptiform activity originated in either EC or BLA. Similar findings were obtained in slices (n=19) in which the hippocampus outputs were not connected with the EC and BLA under control conditions. Cutting the EC–BLA connections made independent slow interictal- and ictal-like activities appear in both areas (n=5). NMDA receptor antagonism (n=6) abolished ictal-like discharges and reduced the duration of the slow interictal-like events. Repetitive stimulation of BLA at 0.5–1 Hz in Schaffer collateral cut slices, induced interictal-like epileptiform depolarizations in EC and reversibly blocked ictal-like activity (n=14). Thus, CA3 outputs in intact slices entrain EC and BLA networks into an interictal-like pattern that inhibits the propensity of these parahippocampal areas to generate prolonged ictal-like paroxysms. Accordingly, NMDA receptor-dependent ictal-like events are initiated in BLA or EC once the propagation of CA3-driven interictal-like discharges to these areas is abated by cutting the Schaffer collaterals. Similar inhibitory effects also occur by activating BLA outputs directed to EC at rates that mimic the CA3-driven interictal-like pattern.

Key words: amygdala, entorhinal cortex, hippocampus, NMDA receptors, seizures.

*Correspondence to: M. Avoli, Montreal Neurological Institute and Departments of Neurology and Neurosurgery, and of Physiology, McGill University, 3801 University Street, Room 794, Montreal, QC, Canada H3A 2B4. Tel: +1-514-398-1955; fax: +1-514-398-4497.
E-mail address: massimo.avoli@mcgill.ca (M. Avoli).

Abbreviations: ACSF, artificial cerebrospinal fluid; 4AP, 4-aminopyridine; BLA, basolateral/lateral nuclei of the amygdala; CNQX, 6-cyano-7-nitroquinoxaline-2,3-dione; CPP, 3,3-(2-carboxypiperazin-4-yl)-propyl-1-phosphonate; EC, entorhinal cortex; Ri, input resistance; SUB, subiculum.

The amygdala is located in the deep, anteromedial part of the temporal lobe and is connected with many brain regions including limbic structures such as the perirhinal, entorhinal and hippocampal cortices (Lopes da Silva et al., 1990; Amaral et al., 1992; Amaral and Witter 1995; Pitkanen et al., 2000; Pikkarainen and Pitkanen, 2001). The amygdala is involved in fear conditioning and emotional learning (Gloor 1992, 1997; Scott et al., 1997; LeDoux, 2000; Wilensky et al., 2000; Davis and Whalen, 2001). Moreover, it is at the origin of some of the behavioral manifestations seen during seizures in mesial temporal lobe epilepsy patients where it is often a primary focus of seizure activity (Gloor 1992, 1997; van Elst et al., 2000). The amygdala is also the limbic area most frequently used for kindling, which is an established animal model of mesial temporal lobe epilepsy (Goddard et al., 1969).

Several studies aimed at establishing the pathophysiogenesis of mesial temporal lobe epilepsy have been carried out in brain slices in which the connections between limbic structures were, at least partially, preserved. These experiments have shown that pharmacologically induced ictal-like (thereafter termed ictal) discharges resembling electrographic limbic seizures, originate in the entorhinal cortex (EC; Stanton et al., 1987; Wilson et al., 1988; Dreier and Heinemann, 1991; Bear and Lothman, 1993; Nagao et al., 1996; Avoli et al., 1996). In line with this evidence, clinical studies have demonstrated dysfunction of EC networks in patients presenting with temporal lobe epilepsy (Rutecki et al., 1989; Deutch et al., 1991; Spencer and Spencer, 1994). In addition, we have found that CA3-driven interictal-like (thereafter termed interictal) activity in hippocampus–EC slices treated with the convulsant drug 4-aminopyridine (4AP) or with Mg^{2+}-free medium can control the EC propensity to generate ictal events (Barbarosie and Avoli, 1997; Barbarosie et al., 2000).

Coronal slices of the amygdala respond to application of 4AP or Mg^{2+}-free medium by generating interictal epileptiform discharges (Gean and Shinnick-Gallagher, 1988; Gean, 1990). However, little information is available on its participation in the epileptiform synchronization of limbic networks. In this study we addressed this issue by using horizontal, rat brain slices that contained the hippocampus proper along with the EC and a portion of the basolateral/lateral nuclei of the amygdala (thereafter referred for sake of simplicity as BLA). Recent data obtained in this *in vitro* preparation have demonstrated that interictal discharges induced by the $GABA_A$ receptor antagonist bicuculline are generated in the CA2/CA3 region of the hippocampus from where they spread to EC and BLA (Stoop and Pralong, 2000). It is however known that decreasing or abolishing

0306-4522/03$30.00+0.00
doi:10.1016/S0306-4522(03)00262-8

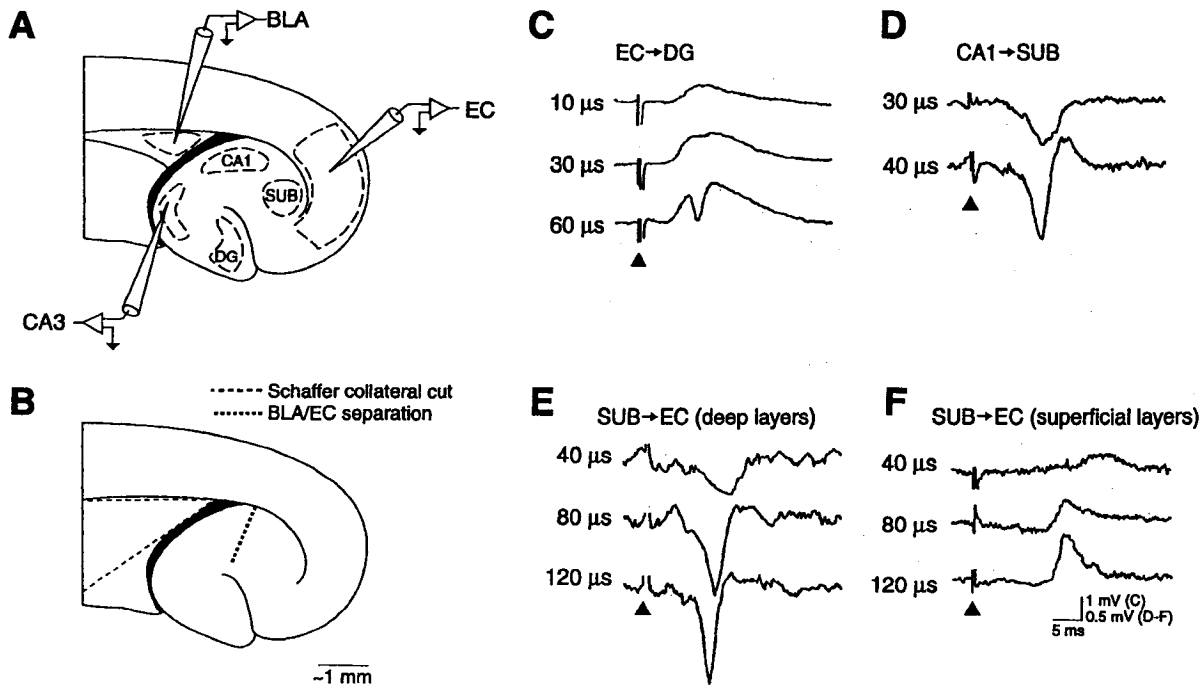

Fig. 1. Schematic drawings of the combined slice used in this study. Abbreviations in this and the following figures are CA1-3, Ammon's horn area 1–3; DG, dentate gyrus. (A) Position of the recording and stimulating electrodes that were placed in CA3, the middle layers of the medial EC and BLA. (B) Location and extension of the cuts used to lesion the Schaffer collaterals or to separate BLA from EC. (C–F) Field potential responses induced by stimuli delivered in EC (C), CA1 stratum radiatum (D) and SUB (E and F) and recorded in DG, SUB and deep or superficial EC layers, respectively. The responses illustrated in each panel were induced by stimuli of increasing strength (as obtained by changing the stimulus duration).

$GABA_A$ receptor-mediated function, reduces the ability of limbic networks to express ictal activity, at least in the *in vitro* slice preparation (Avoli et al., 1996; Lopantsev and Avoli, 1998a; Köhling et al., 2000). Therefore, we have analyzed here the role of BLA networks in the generation and in the control of epileptiform activity induced by 4AP. This drug does not interfere with GABAergic inhibition (Rutecki et al., 1987; Perreault and Avoli, 1991) and allows the appearance of both interictal and ictal discharges in combined hippocampus-EC slices obtained from rodents (Avoli et al., 1996; Lopantsev and Avoli, 1998a,b; Barbarosie and Avoli, 1997; Barbarosie et al., 2000).

EXPERIMENTAL PROCEDURES

Male, adult Sprague–Dawley rats (200–250 g) were decapitated under halothane anesthesia according to the procedures established by the Canadian Council of Animal Care. All efforts were made to minimize the number of animals used and their suffering. The brain was quickly removed and a block of brain tissue containing the retrohippocampal region was placed in cold (1–3 °C), oxygenated artificial cerebrospinal fluid (ACSF). The brain dorsal side was cut along a horizontal plane that was tilted by a 10° angle along a posterosuperior–anteroinferior plane passing between the lateral olfactory tract and the base of the brain stem (Stoop and Pralong, 2000). Horizontal slices (500 µm thick) were cut from this brain block using a vibratome and were transferred into a tissue chamber where they lay at the interface between ACSF and humidified gas (95% O_2, 5% CO_2) at a temperature of 34–35 °C and a pH of 7.4. We focused in this study on the most ventral slices that were comprised between −8.6 to −7.6 mm from the bregma (Paxinos and Watson, 1998). These slices contained the EC, the hippocampus and the BLA (Fig. 1A). Two to three of such slices could be obtained from each hemisphere. ACSF composition was (in mM): NaCl 124, KCl 2, KH_2PO_4 1.25, $MgSO_4$ 2, $CaCl_2$ 2, $NaHCO_3$ 26, and glucose 10. 4AP (50 µM), 6-cyano-7-nitroquinoxaline-2,3-dione (CNQX, 10 µM) and 3,3-(2-carboxypiperazin-4-yl)-propyl-1-phosphonate (CPP, 10 µM) were applied to the bath. Chemicals were acquired from Sigma (St. Louis, MO, USA) with the exception of CNQX and CPP that were obtained from Tocris Cookson (Langford, UK).

Field potential recordings were made with ACSF-filled, glass pipettes (resistance=2–10 MΩ) that were connected to high-impedance amplifiers. Signals were at times processed with high-pass filters set at 0.1 Hz. The location of these recording electrodes is shown in Fig. 1A. Sharp-electrode, intracellular recordings were performed in the EC with pipettes that were filled with 3 M K-acetate (tip resistance=70–120 MΩ) and were aimed at depths ranging 600–900 µm from the pia. Intracellular signals were fed to a high-impedance amplifier with internal bridge circuit for intracellular current injection. The resistance compensation was monitored throughout the experiment and adjusted as required. The fundamental electrophysiological parameters of the EC neurons included in this study were measured as follows: (i) resting membrane potential (RMP) after cell withdrawal; (ii) apparent input resistance (Ri) from the maximum voltage change in response to a hyperpolarizing current pulse (100–200 ms, <-0.5 nA); (iii) action potential amplitude from the baseline. The electrophysiological properties recorded in a representative group of EC neurons ($n=18$) during application of 4AP were: RMP=−65±12 mV (mean±S.D.), Ri=30±7.2 MΩ, and action potential amplitude=92.3±8.2 mV.

Field potential signals were displayed on a GOULD Windograf (Gould Instruments, Valley View, OH, USA) and stored on video-

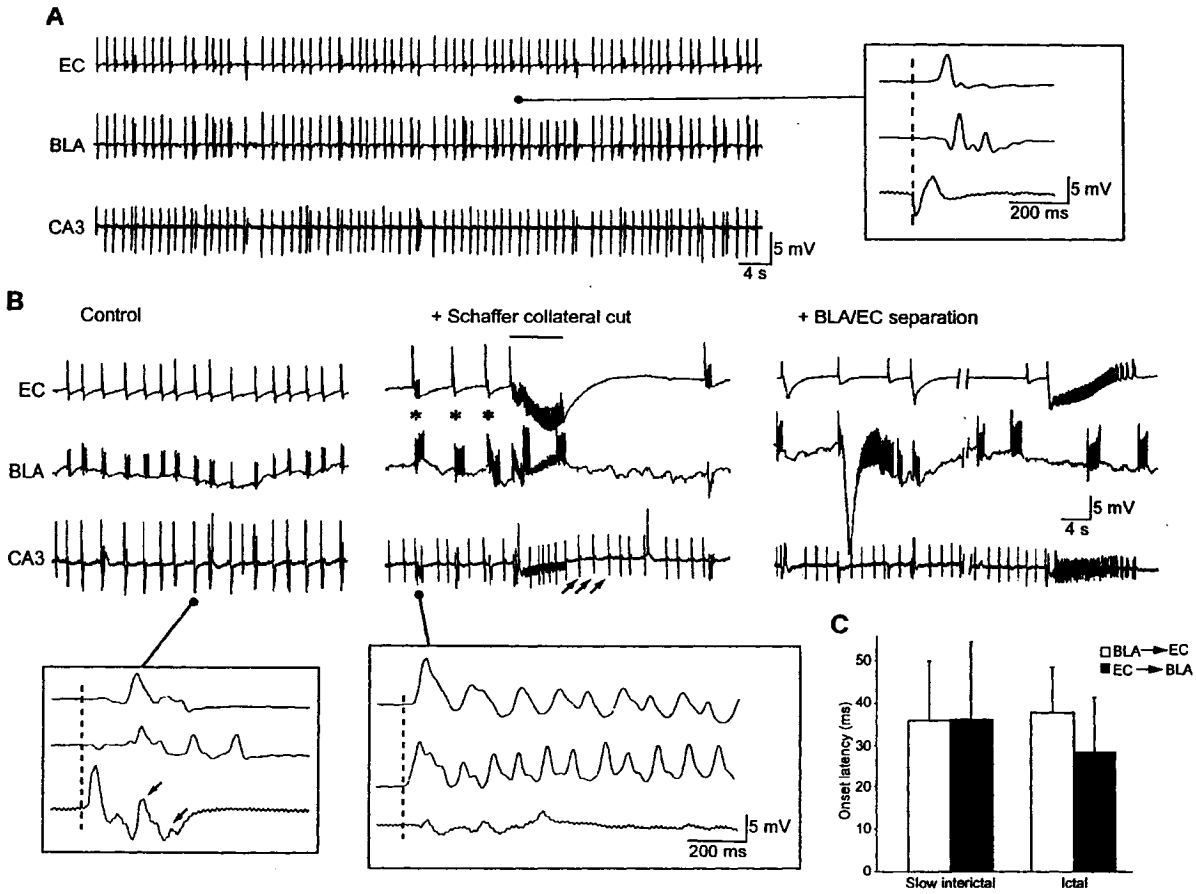

Fig. 2. (A) Simultaneous field potential recordings obtained from EC, BLA and CA3 during bath application of 4AP (50 μM). Signals in this experiment were processed with a high-pass filter at 0.1 Hz. Note that the interictal discharges occur in apparent synchronicity in all limbic areas, but when displayed at faster time base (inset) they are characterized by onset in CA3 and propagation to the EC and BLA. In this and the following insets, interrupted lines point to the time of the earliest deflection of the baseline recording, which in this case occurs in CA3. (B) Effects induced by cutting the Schaffer collaterals and the BLA–EC connections during application of 4AP; note that cutting the Schaffer collaterals abolishes the propagation of CA3-driven interictal discharges (arrows in the CA3 trace) to the EC and BLA where a new type of slow interictal activity (asterisks) along with ictal discharges (continuous line) appear; note also that both types of epileptiform activity propagate to CA3. Subsequent separation of the EC from BLA makes independent interictal and ictal discharges occur in both structures. Insets show (i) expanded traces of a CA3-driven interictal discharge under control conditions in which the CA3 origin and the population activity reentry (arrows) can be appreciated; and (ii) expanded traces of a slow interictal discharge after the Schaffer collateral cut, originating in BLA and spreading to EC and CA3. Note also in the '+BLA/EC separation' panel that only the ictal discharge occurring in EC propagates to CA3. (C) Column histogram of the time differences in the onset of slow interictal and ictal discharges measured in EC and BLA. Data were obtained from five slices and segregated according to their site of origin (i.e. BLA or EC). Values represent the mean±S.D. of onset latency of 28 and 47 slow interictal discharges for BLA→ EC and EC→ BLA propagation, and seven and 12 ictal discharges for BLA→ EC and EC→ BLA propagation, respectively. Differences were not statistically significant.

tape. Time-delay measurements were obtained with a digital oscilloscope. For each trace the onset of the 4AP-induced synchronous potentials was determined as the time of the earliest deflection of the baseline recording (e.g. insert traces in Fig. 2). Intracellular signals were fed to a computer interface (Digidata 1200B, Axon Instruments, Union City, CA, USA) and were acquired and stored by using the pClamp 8 software (Axon Instruments). Subsequent analysis of these data was made with the Clampfit8 software (Axon Instruments).

Cut of the Schaffer collateral pathway or of selected areas in the slice was accomplished under visual control with a razor blade mounted on a micromanipulator (cf, Barbarosie and Avoli, 1997). The location of these cuts is illustrated in Fig. 1B. At the beginning of each experiment (i.e. before applying 4AP), we verified the reciprocal connectivity between different structures of the slice by analyzing the field potential responses induced by single-shock, electrical stimuli (10–150 μs; <200 μA) that were delivered through bipolar, stainless steel electrodes in appropriate areas. As illustrated in Fig. 1C–F, field potential responses, with latencies ranging from 6 to 14 ms, were recorded in the dentate gyrus, subiculum (SUB) and deep or superficial EC layers following electrical stimulation of the EC, CA1 stratum radiatum and SUB, respectively. Field and intracellular responses could also be obtained under control conditions in the EC in response to single-shock electrical stimulation of the BLA (not illustrated).

Throughout this study we termed interictal and ictal discharges the synchronous epileptiform events with durations shorter or longer than 3 s, respectively. In doing so, we included the afterdischarge that could at times occur with both types of activity (e.g. BLA trace in Fig. 3, Control). Measurements in the text are expressed as mean±S.D. and *n* indicates the number of slices or neurons studied under each specific protocol. The results obtained were compared with the Student's *t*-test or the

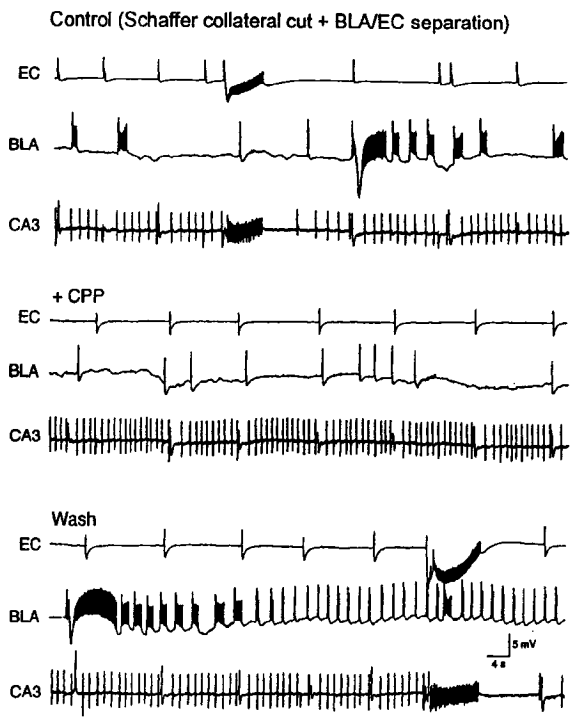

Fig. 3. Application of the NMDA receptor antagonist CPP (10 μM) reversibly blocks the ictal discharges recorded in a combined slice after Schaffer collateral cut and separation of the BLA from the EC. Note that this NMDA receptor antagonist also reduces the amount of fast events associated with each interictal event in the BLA, while the rate of occurrence of CA3-driven interictal activity increases. Note also that in the Control and Wash panels only the slow interictal and ictal discharges generated by EC networks propagate to CA3.

ANOVA test and were considered statistically significant if $P<0.05$.

RESULTS

Epileptiform activity induced by 4AP in combined hippocampus–EC–amygdala slices

A pattern of continuous interictal activity occurred synchronously in CA3, EC and BLA during steady, bath application of 4AP to 12 slices (Fig. 2A). These interictal discharges could be recorded throughout each experiment (up to 4 h) and had intervals ranging between 1.2 and 2.8 s and durations of 180–650 ms when measured in the CA3 subfield. Time-delay measurements of the onset of these interictal events demonstrated that they always initiated in CA3 from where they first spread to the EC and then to BLA with latencies of 93±8 ms and 137±44 ms ($n=12$), respectively (Fig. 2A, inset). Moreover, these epileptiform discharges could often re-enter the CA3 network as indicated by the occurrence of late population spikes at this recording site (Fig. 2B, arrows in the bottom, left inset; cf. Paré et al., 1992).

A similar pattern of interictal activity occurs in reciprocally connected, mouse hippocampus–EC slices treated with 4AP or Mg^{2+}-free medium (Barbarosie and Avoli, 1997; Barbarosie et al., 2000). We have reported there that the CA3-driven interictal activity can inhibit the expression of ictal discharges in the EC. Hence, we investigated the effects induced by cutting the Schaffer collateral, a procedure that would selectively abolish the propagation of CA3 activity to CA1 and SUB, thus preventing hippocampal output activity from reaching the EC and BLA. As illustrated in Fig. 2B, cutting the Schaffer collaterals abolished the propagation of CA3-driven interictal activity (arrows in the CA3 trace of the panel '+Schaffer collateral cut') to the EC and BLA and disclosed in both structures ictal (duration=15±6.9 s; interval of occurrence=75–300 s, $n=6$; continuous line in Fig. 2B '+Schaffer collateral cut' panel) and interictal discharges (duration=240–2100 ms; interval of occurrence=4–17 s, $n=11$; asterisks in Fig. 2B '+Schaffer collateral cut' panel). Thereafter, this interictal activity will be termed slow interictal discharge. It should be also noted that cutting the Schaffer collaterals also reduced the late population spikes associated with the CA3-driven interictal discharges in this area further suggesting that these population events reflect re-entry of activity from the EC (not shown, but see Barbarosie and Avoli, 1997).

Both ictal and slow interictal discharges recorded in EC and BLA after cutting the Schaffer collateral propagated to CA3 (Fig. 2B). Moreover, ictal events had always similar durations in BLA and EC, while the slower interictal discharges could display different durations in these two limbic areas. In any given experiment the two new types of epileptiform activity disclosed by cutting the Schaffer collaterals could initiate in either EC or BLA and spread to the other parahippocampal area with similar time delays ranging between 15 and 70 ms (Fig. 2C). Further lesion of the connections between EC and BLA ($n=5$) caused the appearance of independent slow interictal and ictal discharges in these two limbic areas (Fig. 2B, '+BLA/EC separation' panel), thus indicating that both EC and BLA networks can generate per se these two types of epileptiform synchronization.

As shown in Figs. 2B ('+BLA/EC separation' panel) and 3, only the epileptiform activity that was present in the EC did propagate to the CA3 subfield after separation of the BLA from the EC, presumably through the perforant path–dentate gyrus route. This way of propagation was further demonstrated by cutting the perforant path, a procedure that made slow interictal and ictal discharges disappear in CA3, but not in the EC ($n=3$; not illustrated). Findings similar to those seen after cutting the Schaffer collateral in reciprocally connected hippocampus–EC–BLA slices were obtained in 19 additional experiments in which the hippocampus outputs were not functionally connected with the EC-BLA networks under control conditions (cf. Avoli et al., 1996).

Involvement of NMDA receptors in epileptiform activity induced by 4AP

Next we analyzed the involvement of NMDA receptor-mediated transmission in the generation of the slow interictal and ictal discharges recorded in the EC and BLA after Schaffer collateral cut ($n=6$). Three of these slices had undergone a further lesion of the EC–BLA connections,

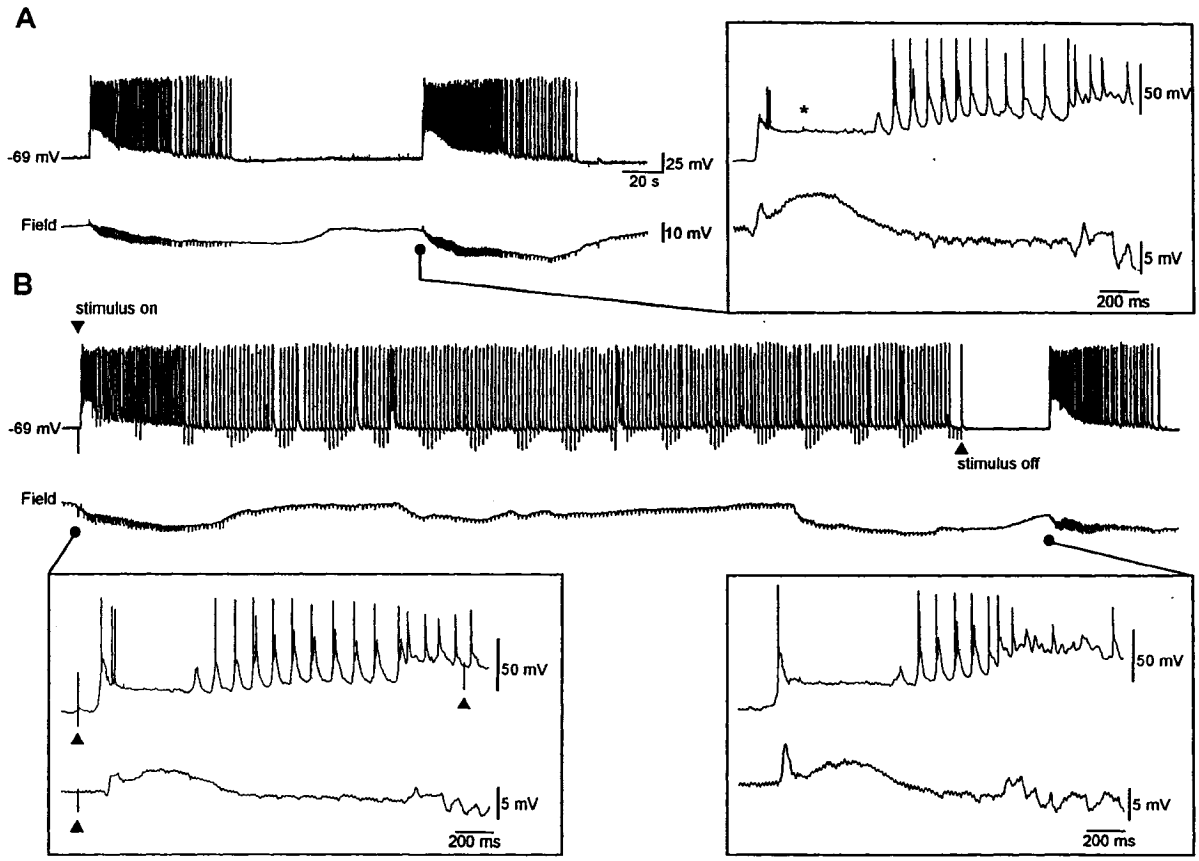

Fig. 4. Simultaneous intracellular (−69 mV) and field potential (Field) recordings obtained in the EC of a Schaffer collateral cut slice during 4AP application. A and B are continuous recordings. Note that ictal discharges are generated spontaneously under control conditions (A) as well as that repetitive stimuli delivered in BLA at 0.5 Hz induce an initial sustained response similar to the spontaneous ictal discharges, followed by a continuous pattern of interictal responses with disappearance of the ictal events. Note also that the interictal responses were barely visible in the field potential recording due to the low gain of the amplification. (B) These reappear within 40 s upon termination of repetitive stimulation. The expanded traces show the onset of an ictal discharge during the prestimulus period, the first stimulus-induced response (triangles point at the stimulus artifacts), and the ictal discharge seen at the end of the stimulation period.

and thus they generated independent epileptiform activity in these two areas.

Bath application of the NMDA receptor antagonist CPP (10 μM) abolished ictal discharges in all limbic structures (Fig. 3). This effect was accompanied by a block of the afterdischarges seen in BLA during each interictal event. Interestingly the rate of occurrence of CA3-driven interictal events increased during CPP application (from 0.9±0.3–1.1±0.3 Hz, n=4). The ictal discharges as well as the afterdischarges associated with the slow interictal events generated in BLA and EC reappeared during CPP washout with control medium containing 4AP only (Fig. 3, Wash). In three additional experiments we found that all epileptiform discharges (including those originating in CA3) were abolished by bath applying the non-NMDA receptor antagonist CNQX (10 μM; not illustrated, but cf. Avoli et al., 1996).

Slow frequency amygdala stimulation can control ictal discharges

We have previously shown that repetitive electrical stimulation of hippocampal outputs at 0.5–1 Hz reversibly blocks the occurrence of ictal discharges induced by 4AP or by Mg^{2+}-free ACSF in Schaffer collateral cut hippocampus–EC slices obtained from mice (Barbarosie and Avoli, 1997). Here, we have found that CA3-driven interictal discharges entrain both EC and BLA networks and inhibit the occurrence of ictal discharges that are otherwise seen after cutting the Schaffer collaterals. Hence, we tested whether under these experimental conditions (i.e. after lesioning the Schaffer collaterals), low-frequency (i.e. 0.1–1 Hz) stimulation of BLA, which projects to the EC (Finch et al., 1986; Pikkarainen and Pitkanen, 2001), can control 4AP-induced ictal discharges in a way similar to what was previously reported with hippocampal output stimulation.

Spontaneous ictal discharges, which were recorded extracellularly in these experiments, corresponded intracellularly to sustained membrane depolarizations that were capped by repetitive action potential bursts (Fig. 4A). As shown in the inset of Fig. 4A (asterisk), the onset of these discharges was often characterized by a sustained depolarization that triggered minimal action potential firing and

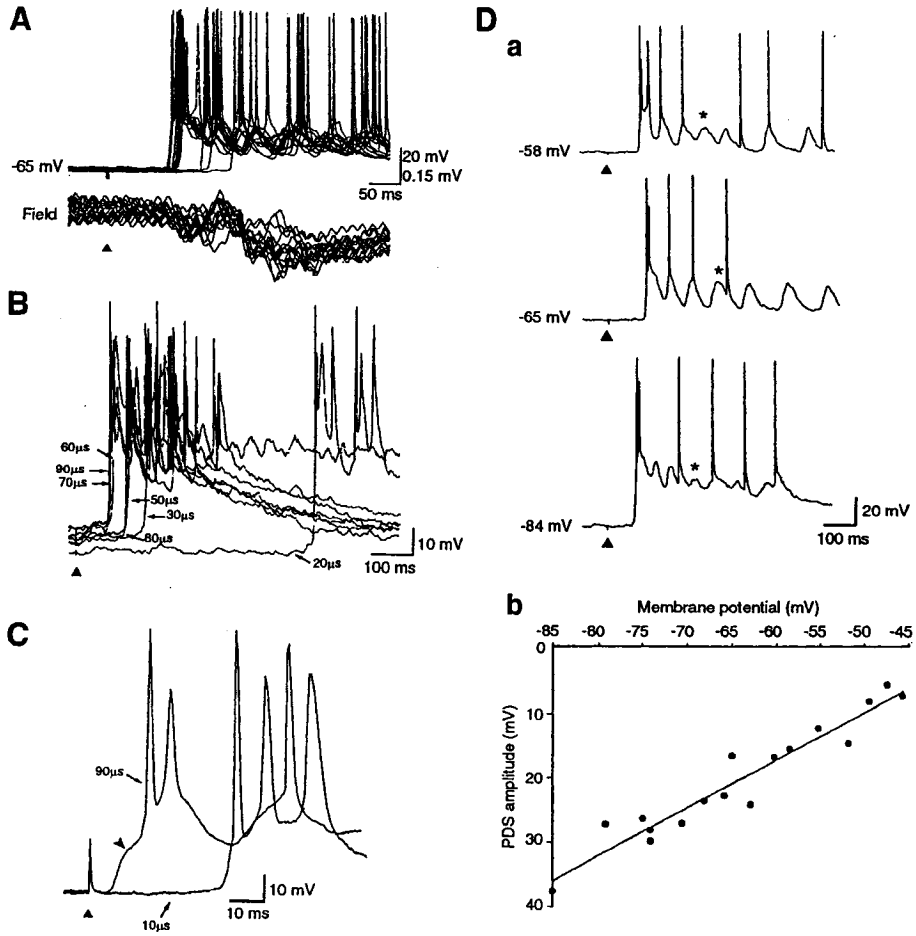

Fig. 5. Interictal-like responses induced in an EC cell by repetitive stimuli delivered at 0.5 Hz to the BLA. Triangles below each set of traces point at the stimulus. (A) Expanded intracellular (−65 mV) and field potential (Field) traces reveal that the stimulus-induced epileptiform responses have variable latency. (B) Effects induced by increasing the stimulus strength (which was varied by increasing the stimulus duration from 20 to 90 μs) on the latency of the epileptiform depolarization; note that the delay time decreases suggesting the activation of polysynaptic pathways. (C) Intracellular responses induced by stimuli delivered at low (10 μs) and high (90 μs) strength. Note that in the latter case the interictal-like response is initiated by an EPSP (arrow-head). (D) Intracellular recordings made during steady injection of depolarizing and hyperpolarizing current. In a, intracellular responses at depolarized (−58 mV), hyperpolarized (−84 mV) and RMP (−65 mV) are shown. In b, plot of the values of the epileptiform depolarizations obtained at different values of the membrane potential. These values were measured at approx. 300 ms from the stimulus during a period of the interictal depolarization that was not associated with action potential, as shown by the stars in sample a.

led, within a few hundreds of milliseconds, to the development of repetitive action potential bursting at 9–15 Hz. This modality of firing, which identified the initial 'tonic' phase of the ictal event, was followed by recurrent 'clonic' discharges that progressively slowed down during the membrane repolarization. These characteristics were remarkably similar to those reported in previous intracellular studies of the ictal activity generated by 'isolated' rat EC network during application of 4AP (Lopantsev and Avoli, 1998a,b).

The ictal discharges generated spontaneously by limbic networks in these slices were decreased and eventually abolished during repetitive stimulation of BLA. As shown in Fig. 4B, the first stimulus of the sequence could at times trigger an ictal-like response, but successive stimuli only elicited short-lasting (<1 s) epileptiform discharges that closely resembled the paroxysmal depolarizing shifts that are the typical intracellular correlate of the CA3-driven interictal activity induced by a variety of epileptogenic procedures (Schwartzkroin and Prince, 1980; Rutecki et al., 1987, 1990; Tancredi et al., 1990; Perreault and Avoli, 1991).

The short-lasting epileptiform responses induced by BLA stimuli displayed latencies that were quite variable and could range between 60 and 180 ms (Fig. 5A). Moreover, these latency values could be decreased in the same experiment by augmenting the stimulus intensity (Fig. 5B). Such a procedure could eventually induce an epileptiform response that was initiated by an EPSP with latency ranging between 6 and 10 ms (arrowhead in Fig. 5C). As shown in Fig. 5D, modifying the membrane potential with intracellular injection of steady depolarizing or hyperpolarizing current caused a decrease or an increase of the intracellular epileptiform responses, respectively (n=6 cells).

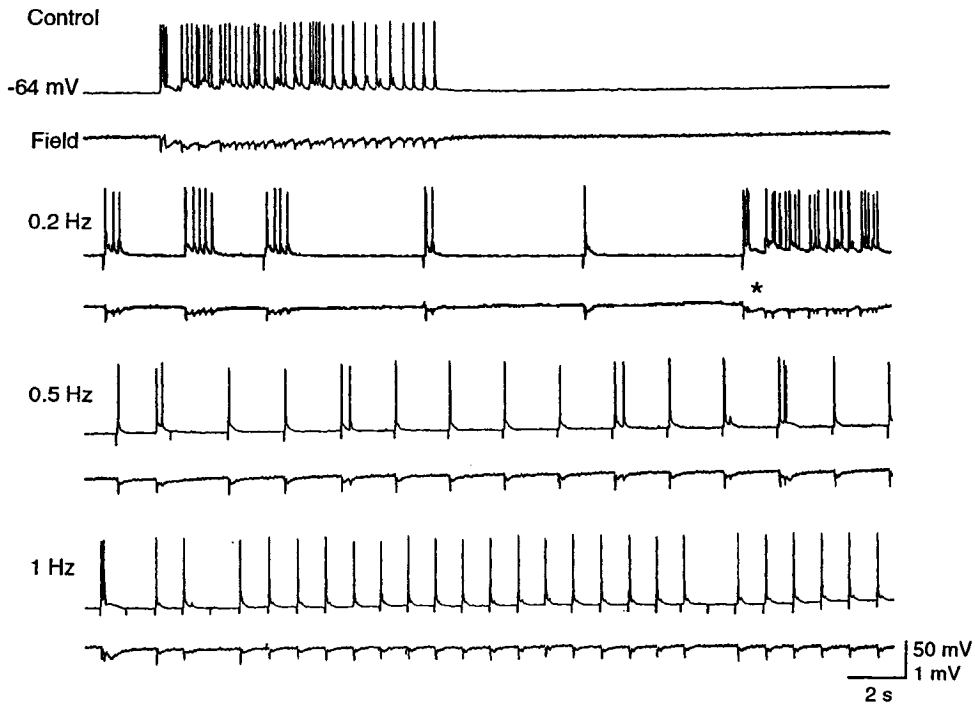

Fig. 6. Effects induced by different rates of repetitive stimuli delivered in BLA on the spontaneous ictal discharges recorded simultaneously with field potential and intracellular microelectrodes in the EC of a slice in which the Schaffer collaterals have been cut. Data were obtained during the steady state response (i.e. at least 10 s after the onset of repetitive stimulation). Note that stimuli delivered at 0.2 Hz are unable to abolish the occurrence of ictal discharges (asterisk). In contrast, repetitive stimuli at 0.5 and 1 Hz can inhibit the ictal discharges. Note also that the interictal-like responses induced by 0.2 Hz stimulation are longer than those seen with either 0.5 or 1 Hz rates.

These changes, which are quantitatively illustrated in the plot of Fig. 5Db, indicated an extrapolated reversal potential of these epileptiform depolarizations at approximately −35 mV. These values suggested that, as reported in CA3 pyramidal cells (Rutecki et al., 1987; Perreault and Avoli, 1991), $GABA_A$ receptor-mediated, inhibitory conductances contributed to the paroxysmal depolarizing shifts generated by EC neurons in response to stimuli delivered in BLA.

Fig. 6 illustrates the effects induced on the occurrence of ictal discharge by repetitive stimuli delivered at rates between 0.2 and 1 Hz in the BLA. At 0.2 Hz, EC networks responded to BLA stimuli by generating epileptiform discharges that lasted less than 2 s; however, at this rate of stimulation, ictal discharges (i.e. periods of epileptiform synchronization lasting over 3 s) continued to occur (Fig. 6, asterisk in the 0.2 Hz trace). When repetitive stimuli were delivered at 0.5 or 1 Hz, ictal discharges did not occur during the period of stimulation (with the exception of the ictal-like response that was at times seen at the stimulation onset). As illustrated in Fig. 6, stimuli at 0.5 or 1 Hz elicited paroxysmal depolarizing shifts that had shorter duration than at 0.2 Hz. Data obtained in 14 experiments indicated that repetitive stimulation at 0.2 Hz had no effect on the occurrence of ictal discharges, while it completely suppressed them at 0.5 and 1 Hz. It must be emphasized that in all cases the effects induced by BLA repetitive stimulation on ictal discharge occurrence was assessed by delivering periods of stimulation that were in any given experiment at least twice as long as the interval of occurrence of the spontaneous ictal events. Ictal discharges that were similar both in duration and in shape to those seen during the prestimulus period, reappeared in all experiments upon termination of the stimulating protocol (Fig. 4B).

DISCUSSION

Reciprocal functional connectivity between hippocampus and EC in mouse combined slices makes CA3-driven interictal discharges restrain the propensity of EC networks to generate prolonged ictal discharges resembling the electrographic limbic seizures seen in patients presenting with mesial temporal lobe epilepsy (Barbarosie and Avoli, 1997; Barbarosie et al., 2000). This characteristic, which underscores an important mechanism for activity-dependent control of limbic network excitability, was not so far obtained in rat combined slices in which only EC to hippocampus connections remained preserved after slicing (Dreier and Heinemann, 1991; Avoli et al., 1996). In this study, we have found that the hippocampus–EC loop (cf. Paré et al., 1992) can also be maintained in slices obtained from the most ventral portion of the rat brain (i.e. comprised between −8.6 and −7.6 mm from the bregma; Paxinos and Watson, 1998). In addition, these slices contained a connected portion of the BLA.

By employing such an *in vitro* preparation we have discovered that CA3 outputs can entrain EC and BLA networks into a pattern of interictal activity that restrains

the propensity of these parahippocampal areas to generate ictal activity. Accordingly, cutting the Schaffer collaterals prevented CA3-driven output activity from reaching the CA1 area and the SUB (and thus from leaving the hippocampus), and disclosed ictal discharges in EC and BLA. This ictal activity depended on the function of the NMDA receptor, could initiate in either BLA or EC networks, and could be sustained by either structure independently. In addition, we have demonstrated that activation of BLA outputs directed to the EC at a frequency that mimics that of CA3-driven interictal activity, can effectively depress ictal discharges in limbic networks. It should however, be emphasized that our findings were obtained from normal tissue to which 4AP was applied in order to disclose epileptiform synchronization. Such a situation is certainly different from what is encountered in patients with mesial temporal lobe epilepsy or in animal models mimicking this disorder.

CA3 networks as pacers of limbic network activity

We have found that 4AP treatment in extended brain slices that include the hippocampus proper, the EC and the BLA, induces CA3-driven interictal activity that spread to the EC and BLA. All these limbic regions are densely interconnected (Finch et al., 1986; Pitkanen et al., 2000; Pikkarainen and Pitkanen, 2001; cf. Amaral and Witter, 1995). Moreover, preservation of connections between the amygdala and other limbic areas has been anatomically documented in a horizontal, brain slice preparation by von Bohlen und Halbach and Albrecht (1998).

The CA3 area in isolated hippocampal slices responds readily to a variety of epileptogenic treatments by generating epileptiform discharges recurring at frequencies comprised between 0.5 and 1 Hz (Schwartzkroin and Prince, 1980; Tancredi et al., 1990; Rutecki et al., 1987, 1990; Perreault and Avoli, 1991). This pattern of interictal discharge reflects the presence of recurrent excitatory, glutamatergic synapses on neighboring CA3 pyramidal cells along with the ability of these neurons to generate dendritic Ca^{2+} spikes (Miles and Wong, 1986, 1987; for review see Traub and Jefferys, 1994). Thus, the ability of CA3 networks to generate interictal discharges is not unexpected. However, it is surprising that in intact, interconnected slices this type of epileptiform activity can consistently entrain BLA and EC networks, even though the fiber paths directed from these two parahippocampal area to CA3 area are functional, as demonstrated by the re-entry of interictal activity to CA3. Indeed, we have found here that even when BLA networks are included in the slice preparation, CA3-driven interictal discharges control rather than facilitate the occurrence of limbic seizures.

BLA and EC networks as generators of electrographic limbic seizures

When set free from the interictal activity originating from the hippocampus, EC and BLA networks generate ictal discharges, along with slow interictal events. This observation is in keeping with previous experiments in extended hippocampus–EC slices, where ictogenesis occurred in EC networks that did not receive hippocampal output activity, or it appeared after separation from the hippocampus proper (Avoli et al., 1996; Barbarosie and Avoli, 1997; Dreier and Heinemann, 1991; Wilson et al., 1988).

We have also found that the ictal activity recorded in slices after cutting the Schaffer collaterals, can originate in either EC or BLA (even in the same experiment), and propagate to the other limbic area with time delays of 15–70 ms. Similar characteristics were seen with the slow interictal events. Such a large variability in onset delay suggests that these epileptiform events may also initiate from limbic areas (e.g. the perirhinal cortex) located in between the EC and BLA. This type of initiation has been documented in preliminary experiments in which simultaneous field potential recordings were obtained from the EC, the perirhinal cortex and the BLA (de Guzman et al., unpublished data).

The evidence obtained by surgically separating the EC from the BLA, demonstrates that both limbic areas are endowed with the ability to produce similar periods of prolonged epileptiform synchronization. Interestingly, BLA and EC networks under 4AP treatment were unable per se to generate the pattern of frequent interictal discharge seen in the CA3 area. Previous studies (Gean and Shinnick-Gallagher, 1988; Gean, 1990) have shown that the epileptiform activity induced by 4AP or Mg^{2+}-free medium in coronal slices of the amygdala, consists of interictal events that recur at intervals longer than 7 s.

We have also provided evidence for a role played by NMDA receptors in the generation of ictal discharges in BLA or EC. Similar conclusions have been reached with the ictal activity recorded in the EC during several epileptogenic procedures (Avoli et al., 1996; Dreier and Heinemann, 1991; Nagao et al., 1996; Stanton et al., 1987). In addition, NMDA receptor antagonism reduced the amount of afterdischarge associated with the slow interictal activity (cf. Gean and Shinnick-Gallagher, 1988), but it failed in blocking fast CA3-driven interictal discharges (Perreault and Avoli, 1991). In line with several studies performed in limbic structures treated with convulsant drugs (Avoli et al., 1996; Nagao et al., 1996; Gean, 1990), all types of epileptiform discharge were abolished by the non-NMDA receptor antagonist CNQX.

BLA outputs can control electrographic limbic seizures

The EC and the amygdala are interconnected components of the limbic system as documented by several anatomical studies (Swanson and Kohler, 1986; Finch et al., 1986; Lopes da Silva et al., 1990; Amaral and Witter, 1995). We have found here that repetitive BLA stimulation at frequencies of 0.5–1 Hz reversibly block ictal discharge generation in limbic networks. This activity-dependent effect may result from several mechanisms that include the activation of presynaptic metabotropic receptors inhibiting glutamate release (Burke and Hablitz, 1994; Scanziani et al., 1997), or extracellular alkalization leading to a reduction of NMDA transmission (de Curtis et al., 1998). Moreover, the stimulus frequency effective in inhibiting ictal discharges is close

to what is used for eliciting long term depression of synaptic transmission in the hippocampus (Kimura and Pavlides, 2000). However, ictal discharges in our experiments reappeared shortly after the termination of the stimulating procedure thus suggesting that long-term depression was presumably not involved in this inhibitory action.

The field potential characteristics of the responses generated by EC neurons during repetitive stimuli delivered at frequencies >0.5 Hz were similar to those of the CA3-driven interictal discharges recorded in intact slices, in which ictogenesis does not occur. By employing intracellular recordings we have also found that the interictal-like responses to repetitive stimuli are characterized by depolarizing bursts that are presumably contributed by $GABA_A$ receptor-mediated conductances. Hence, repetitive stimulation may also lead to an increased release of GABA that in turn activates presynaptic $GABA_B$ receptors thus reducing glutamate release. Such a mechanism has been recently proposed to contribute to the control of ictogenesis by interictal activity (de Curtis and Avanzini, 2001). Interestingly, the latencies of the interictal-like responses induced in the EC by BLA stimulation were longer than what seen with stimulus-induced EPSPs (i.e. approximately 30 ms versus 10 ms). Further analysis is required to establish why a different latency characterizes EC neuron activation following stimulation of the same pathway. However, it is attractive to speculate that this phenomenon reflects the time required by EC networks to elaborate the synaptic interactions that lead to the interictal discharge.

Relevance for identifying the mechanisms of temporal lobe epilepsy

Mesial temporal lobe epilepsy is characterized both in humans and in animal models by a reduction in neuronal population in limbic structures such as the CA3 area of the hippocampus and the amygdala (Liu et al., 1994; Miller et al., 1994; Tuunanen et al., 1999; van Elst et al., 2000; Yilmazer-Hanke et al., 2000). The results obtained by cutting the Schaffer collaterals support the hypothesis that a decreased excitatory drive from the hippocampus onto EC or BLA may lead to ictogenesis (Barbarosie and Avoli, 1997; Barbarosie et al., 2000). Such a mechanism has been recently demonstrated to occur in slices obtained from pilocarpine-treated epileptic mice in which the increased occurrence of ictal events *in vitro* is paralleled by decreased CA3-driven output activity and presumably sustained by interactions between the EC and SUB (D'Antuono et al., 2002).

Likewise, the results obtained by stimulating the BLA indicate that a reduction of amygdala output activity, as a result of the neuronal damage associated with mesial temporal lobe epilepsy, may contribute to ictogenesis. However, evidence obtained with depth electrode EEG recordings in epileptic patients indicates that the damaged amygdala can generate (and at times initiate) electrographic discharges (Gloor, 1992). These conflicting data indicate that further experiments in animal models of mesial temporal lobe epilepsy are required in order to identify the relative contribution of cell damage versus intrinsic epileptogenicity of amygdala networks.

Acknowledgements—This study was supported by the Canadian Institutes of Health Research (grant MT-8109) and the Savoy Foundation. M.D. is a fellow of the Fragile X Research Foundation of Canada, while E.P. was supported by the Fond du 450ème and la Société Académique Vaudoise. We thank Ms T. Papadopoulos for secretarial assistance.

REFERENCES

Amaral DG, Price JL, Pitkänen A, Carmichael TS (1992) Anatomical organization of the primate amygdaloid complex. In: The amygdala: neurobiological aspects of emotion, memory and mental dysfunction (Aggleton JP, ed), pp 1–66. New York: Wiley-Liss.

Amaral DG, Witter MP (1995) Hippocampal formation. In: The rat nervous system (Paxinos G, ed), pp 443–493. San Diego: Academic Press.

Avoli M, Barbarosie M, Lücke A, Nagao T, Lopantsev V, Köhling R (1996) Synchronous GABA-mediated potentials and epileptiform discharges in the rat limbic system in vitro. J Neurosci 16:3912–3924.

Barbarosie M, Avoli M (1997) CA3-driven hippocampal-entorhinal loop controls rather than sustains *in vitro* limbic seizures. J Neurosci 17:9308–9314.

Barbarosie M, Louvel J, Kurcewicz I, Avoli M (2000) CA3-released entorhinal seizures disclose dentate gyrus epileptogenicity and unmask a temporoammonic pathway. J Neurophysiol 83:1115–1124.

Bear J, Lothman EW (1993) An *in vitro* study of focal epileptogenesis in combined hippocampal-parahippocampal slices. Epilepsy Res 14:183–193.

Burke JP, Hablitz JJ (1994) Presynaptic depression of the synaptic transmission mediated by activation of metabotropic glutamate receptors in the rat neocortex. J Neurosci 4:5120–5130.

D'Antuono M, Benini R, Biagini G, D'Arcangelo G, Barbarosie M, Tancredi V, Avoli M (2002) Limbic network interactions leading to hyperexcitability in a model of temporal lobe epilepsy. J Neurophysiol 87:634–639.

Davis M, Whalen PJ (2001) The amygdala: vigilance and emotion. Mol Psychiatry 6:13–34.

de Curtis M, Manfridi A, Biella G (1998) Activity-dependent pH shifts and periodic recurrence of spontaneous interictal spikes in a model of focal epileptogenesis. J Neurosci 18:7543–7551.

de Curtis M, Avanzini G (2001) Interictal spikes in focal epileptogenesis. Prog Neurobiol 63:541–567.

Deutch C, Spencer S, Robbins R, Cicchetti D, Spencer D (1991) Interictal spikes and hippocampal somatostatin levels in temporal lobe epilepsy. Epilepsia 32:174–178.

Dreier JP, Heinemann U (1991) Regional and time dependent variations of low Mg^{2+} induced epileptiform activity in rat temporal cortex slices. Exp Brain Res 87:581–596.

Finch DM, Wong EE, Derian EL, Chen XH, Nowlin-Finch NL, Brothers LA (1986) Neurophysiology of limbic system pathways in the rat: projections from the amygdala to the entorhinal cortex. Brain Res 370:273–284.

Gean PW (1990) The epileptiform activity induced by 4-aminopyridine in rat amygdala slices: antagonism by non-*N*-methyl-D-aspartate receptor antagonists. Brain Res 530:251–256.

Gean PW, Shinnick-Gallagher P (1988) Epileptiform activity induced by magnesium-free solution in slices of rat amygdala: antagonism by *N*-methyl-D-aspartate receptor antagonists. Neuropharmacology 27:557–562.

Gloor P (1992) Role of the amygdala in temporal lobe epilepsy. In: The amygdala: neurobiological aspects of emotion, memory and mental dysfunction (Aggleton J, ed), pp 505–538. New York: Wiley-Liss.

Gloor P (1997) The temporal lobe and limbic system. New York: Oxford University Press.

Goddard GV, McIntyre DC, Leech CKA (1969) Permanent change in brain function resulting from daily electrical stimulation. Exp Neurol 25:295–330.

Kimura A, Pavlides C (2000) Long-term potentiation/depotentiation are accompanied by complex changes in spontaneous unit activity in the hippocampus. J Neurophysiol 84:1894–1906.

Köhling R, Vreugdenhil M, Bracci E, Jefferys JG (2000) Ictal epileptiform activity is facilitated by hippocampal $GABA_A$ receptor-mediated oscillations. J Neurosci 20:6820–6829.

LeDoux JE (2000) Emotion circuits in the brain. Annu Rev Neurosci 23:155–184.

Liu Z, Nagao T, Desjardins CG, Gloor P, Avoli M (1994) Quantitative evaluation of neuronal loss in the dorsal hippocampus in rats with long term pilocarpine seizures. Epilepsy Res 17:237–247.

Lopantsev V, Avoli M (1998a) Participation of $GABA_A$-mediated inhibition in ictal-like discharges in the rat entorhinal cortex. J Neurophysiol 79:352–360.

Lopantsev V, Avoli M (1998b) Laminar organization of epileptiform discharges in the rat entorhinal cortex in vitro. J Physiol (Lond) 509:785–796.

Lopes da Silva FH, Witter MP, Boeijinga PH, Lohman AH (1990) Anatomic organization and physiology of the limbic cortex. Physiol Rev 70:453–511.

Miles R, Wong RK (1986) Excitatory synaptic interactions between CA3 neurons in the guinea-pig hippocampus. J Physiol 373:397–418.

Miles R, Wong RK (1987) Inhibitory control of local excitatory circuits in the guinea-pig hippocampus. J Physiol 388:611–629.

Miller LA, McLachlan RS, Bouwer MS, Hudson LP, Munoz DG (1994) Amygdalar sclerosis: preoperative indicators and outcome after temporal lobectomy. J Neurol Neurosurg Psychiatry 57:1099–1105.

Nagao T, Alonso A, Avoli M (1996) Epileptiform activity induced by pilocarpine in the rat hippocampal-entorhinal slice preparation. Neuroscience 72:399–408.

Paré D, de Curtis M, Llinás R (1992) Role of hippocampal-entorhinal loop in temporal lobe epilepsy: extra- and intracellular study in the isolated guinea pig brain *in vitro*. J Neurosci 12:1857–1881.

Paxinos, G, Watson, C (1998) The rat brain in stereotaxic coordinates, 4th edition. San Diego, CA, USA: Academic Press.

Perreault P, Avoli M (1991) Physiology and pharmacology of epileptiform activity induced by 4-aminopyridine in rat hippocampal slices. J Neurophysiol 65:771–785.

Pikkarainen A, Pitkanen A (2001) Projections from the lateral, basal and accessory basal nuclei of the amygdala to the perirhinal and postrhinal cortices in rat. Cereb Cortex 11:1064–1082.

Pitkanen A, Pikkarainen M, Nurminen N, Ylinen A (2000) Reciprocal connections between the amygdala and the hippocampal formation, perirhinal cortex, and postrhinal cortex in rat: a review. Ann NY Acad Sci 911:369–391.

Rutecki PA, Lebeda FJ, Johnston D (1987) 4-Aminopyridine produces epileptiform activity in hippocampus and enhances synaptic excitation and inhibition. J Neurophysiol 57:1911–1924.

Rutecki PA, Grossman RG, Armstrong D, Irish-Loewen SJ (1989) Electrophysiological connections between the hippocampus and entorhinal cortex in patients with complex partial seizures. J Neurosurg 70:667–675.

Rutecki PA, Lebeda FJ, Johnston D (1990) Epileptiform activity in the hippocampus produced by tetraethylammonium. J Neurophysiol 64:1077–1088.

Scanziani M, Salin PA, Vogt KE, Malenka RC, Nicoll RA (1997) Use-dependent increases in glutamate concentration activate presynaptic metabotropic glutamate receptors. Nature 385:630–634.

Schwartzkroin PA, Prince DA (1980) Changes in excitatory and inhibitory synaptic potentials leading to epileptogenic activity. Brain Res 183:61–73.

Scott SK, Young AW, Calder AJ, Hellawell DJ, Aggleton JP, Johnson M (1997) Impaired auditory recognition of fear and anger following bilateral amygdala lesions. Nature 385:254–257.

Spencer SS, Spencer DD (1994) Entorhinal-hippocampal interactions in temporal lobe epilepsy. Epilepsia 35:721–727.

Stanton PK, Jones RS, Mody I, Heinemann U (1987) Epileptiform activity induced by lowering extracellular $[Mg^{2+}]$ in combined hippocampal-entorhinal cortex slices: modulation by receptors for norepinephrine and *N*-methyl-D-aspartate. Epilepsy Res 1:53–62.

Stoop R, Pralong E (2000) Functional connections and epileptic spread between hippocampus, entorhinal cortex and amygdala in a modified horizontal slice preparation of the rat brain. Eur J Neurosci 12:3651–3663.

Swanson LW, Kohler C (1986) Anatomical evidence for direct projections from the entorhinal area to the entire cortical mantle in the rat. J Neurosci 6:3010–3023.

Tancredi V, Hwa GGC, Zona C, Brancati A, Avoli M (1990) Low magnesium epileptogenesis in the rat hippocampal slice: electrophysiological and pharmacological features. Brain Res 511:280–290.

Traub RD, Jefferys JG (1994) Simulations of epileptiform activity in the hippocampal CA3 region in vitro. Hippocampus 4:281–285.

Tuunanen J, Lukasiuk K, Halonen T, Pitkanen A (1999) Status epilepticus-induced neuronal damage in the rat amygdaloid complex: distribution, time-course and mechanisms. Neuroscience 94:473–495.

van Elst LT, Woermann FG, Lemieux L, Thompson PJ, Trimble MR (2000) Affective aggression in patients with temporal lobe epilepsy: a quantitative MRI study of the amygdala. Brain 123:234–243.

von Bohlen und Halbach O, Albrecht D (1998) Tracing of axonal connectivities in a combined slice preparation of rat brains: a study by rhodamine-dextran-amine application in the lateral nucleus of the amygdala. J Neurosci Methods 81:169–175.

Yilmazer-Hanke DM, Wolf HK, Schramm J, Elger CE, Wiestler OD, Blumcke I (2000) Subregional pathology of the amygdala complex and entorhinal region in surgical specimens from patients with pharmacoresistant temporal lobe epilepsy. J Neuropathol Exp Neurol 59:907–920.

Wilensky AE, Schafe GE, LeDoux JE (2000) The amygdala modulates memory consolidation of fear-motivated inhibitory avoidance learning but not classical fear conditioning. J Neurosci 20:7059–7066.

Wilson WA, Swartzwelder HS, Anderson WW, Lewis DV (1988) Seizure activity *in vitro*: a dual focus model. Epilepsy Res 2:289–293.

(Accepted 20 March 2003)

APPENDIX D: Reprint of Chapter 4 and Waiver from J Neurophysiology

J Neurophysiol 95: 2143–2154, 2006.
First published December 28, 2005; doi:10.1152/jn.01217.2005.

Altered Inhibition in Lateral Amygdala Networks in a Rat Model of Temporal Lobe Epilepsy

Ruba Benini[1] and Massimo Avoli[1,2]

[1]*Montreal Neurological Institute and Departments of Neurology and Neurosurgery, and of Physiology, McGill University, Montreal, Canada; and* [2]*Dipartimento di Fisiologia Umana e Farmacologia, Università di Roma "La Sapienza," Rome, Italy*

Submitted 17 November 2005; accepted in final form 22 December 2005

Benini, Ruba and Massimo Avoli. Altered inhibition in lateral amygdala networks in a rat model of temporal lobe epilepsy. *J Neurophysiol* 95: 2143–2154, 2006. First published December 28, 2005; doi:10.1152/jn.01217.2005. Clinical and experimental evidence indicates that the amygdala is involved in limbic seizures observed in patients with temporal lobe epilepsy. Here, we used simultaneous field and intracellular recordings from horizontal brain slices obtained from pilocarpine-treated rats and age-matched nonepileptic controls (NECs) to shed light on the electrophysiological changes that occur within the lateral nucleus (LA) of the amygdala. No significant differences in LA neuronal intrinsic properties were observed between pilocarpine-treated and NEC tissue. However, spontaneous field activity could be recorded in the LA of 21% of pilocarpine-treated slices but never from NECs. At the intracellular level, this network activity was characterized by robust neuronal firing and was abolished by glutamatergic antagonists. In addition, we could identify in all pilocarpine-treated LA neurons: *1*) large amplitude depolarizing postsynaptic potentials (PSPs) and *2*) a lower incidence of spontaneous hyperpolarizing PSPs as compared with NECs. Single-shock stimulation of LA networks in the presence of glutamatergic antagonists revealed a biphasic inhibitory PSP (IPSP) in both NECs and pilocarpine-treated tissue. The reversal potential of the early $GABA_A$ receptor–mediated component, but not of the late $GABA_B$ receptor–mediated component, was significantly more depolarized in pilocarpine-treated slices. Furthermore, the peak conductance of both fast and late IPSP components had significantly lower values in pilocarpine-treated LA cells. Finally, paired-pulse stimulation protocols in the presence of glutamatergic antagonists revealed a less pronounced depression of the second IPSP in pilocarpine-treated slices compared with NECs. Altogether, these findings suggest that alterations in both pre- and postsynaptic inhibitory mechanisms contribute to synaptic hyperexcitability of LA networks in epileptic rats.

INTRODUCTION

The amygdala complex, located in the deep anteromedial part of the temporal lobe, is composed of several nuclei that are interconnected with cortical and subcortical regions in a specific manner (Lopes da Silva et al. 1990; Pitkanen et al. 2000a,b). Under normal physiological conditions, the amygdala is involved in fear conditioning and emotional learning (LeDoux 2000; Pare et al. 2004; Scott et al. 1997; Stork and Pape 2002; Wilensky et al. 2000). The amygdala is also known to be at the origin of some of the behavioral manifestations observed during seizures in temporal lobe epilepsy (TLE) patients where it is often the primary focus of seizure activity (Gloor 1992, 1997; van Elst et al. 2000). Patients with TLE can present with unilateral or bilateral damage to this structure, and in certain instances, isolated amygdalar pathology occurs in the absence of hippocampal sclerosis (reviewed by Pitkanen et al. 1998). Histochemistry of resected human epileptic tissue has revealed that the lateral and basal nuclei are the most vulnerable to injury (Yilmazer-Hanke et al. 2000). Assessment of these nuclei has disclosed that in addition to neuronal loss and gliosis, synaptic alterations—in the form of decreased dendritic branching of surviving cells—also take place (Aliashkevich et al. 2003).

Histological examination of chronically epileptic animal tissue has confirmed an overlap with the pattern of cell loss detected in humans. Specifically, these studies have confirmed that amygdala damage is nucleus-specific and that some nuclei are more resistant to injury than others (Nissinen et al. 2000; Tuunanen et al. 1996). Furthermore, in addition to loss of principal cells, decreased density of specific interneuronal populations has been documented in chronically epileptic animals (Tuunanen 1996, 1997). The basolateral amygdalar nucleus (BLA) has been the primary focus of electrophysiological evaluation of the amygdala in chronic animal models of TLE. These studies have identified various mechanisms to account for the hyperexcitability of BLA networks observed in epileptic animals including loss of spontaneously occurring inhibitory postsynaptic potentials (IPSPs), loss of feedforward inhibition, and enhanced *N*-methyl-D-aspartate (NMDA)- and non–NMDA-mediated excitation (Gean et al. 1989; Mangan et al. 2000; Rainnie et al. 1992; Shoji et al. 1998; Smith and Dudek 1997).

Despite such an extensive assessment of the BLA, relatively few electrophysiological studies have carefully examined other amygdalar nuclei using chronic animal models of TLE. For instance, little is known about the functional changes that take place within the lateral nucleus of the amygdala (LA) where neuronal loss and gliosis have been identified in subjects with intractable TLE (Yilmazer-Hanke et al. 2000). A recent study reported that decreased excitatory transmission occurs in the LA of epileptic rodents, probably because of a decrease in glutamate release or neurodegeneration (Niittykoski et al. 2004). However, much information is still needed to fully understand the contribution of this structure to epileptogenesis. For example, although previous studies have shown the essential role of local GABAergic circuits in controlling LA excitability (Callahan et al. 1991; Lang and Paré 1997, 1998), a detailed electrophysiological examination of how these inhibitory networks are affected in epileptic animals is still lacking.

Address for reprint requests and other correspondence: M. Avoli, 3801 University, Rm. 794, Montreal, Quebec H3A 2B4, Canada (E-mail: massimo.avoli@mcgill.ca).

The costs of publication of this article were defrayed in part by the payment of page charges. The article must therefore be hereby marked "*advertisement*" in accordance with 18 U.S.C. Section 1734 solely to indicate this fact.

Assessing the contribution of the LA to hyperexcitability of limbic neuronal networks becomes essential when one considers its dense reciprocal interconnections with the hippocampus and parahippocampal cortices, structures that are highly implicated in TLE (Du et al. 1993; Pikkarainen and Pitkanen 2001; Pitkanen et al. 1995, 2000b). In this study, we assessed the electrophysiological changes that occur in the LA of epileptic rats by using the pilocarpine chronic animal model of TLE where damage to this amygdala nucleus has been reported (Cavalheiro et al. 1987; Fujikawa 1996). Our investigations were specifically aimed at assessing the functional characteristics of inhibition within this structure.

METHODS

Animal preparation

Procedures approved by the Canadian Council of Animal Care were used to induce status epilepticus (SE) in adult male Sprague-Dawley rats weighing 150–200 g at the time of injection. All efforts were made to minimize the number of animals used and their suffering. Briefly, rats were injected with a single dose of pilocarpine hydrochloride (380–400 mg/kg, ip). To reduce the discomforts caused by peripheral activation of muscarinic receptors, methyl scopolamine (1 mg/kg, ip) was administered 30 min before the pilocarpine injection. The animals' behavior was monitored for ~4 h after pilocarpine and scored according to Racine's classification (Racine et al. 1972). Only rats that experienced SE (stages 3–5) for >30 min [53.1 ± 9.3 (SE) min; n = 35 rats] were included in the pilocarpine group and used for in vitro electrophysiological studies ~4 mo (18 ± 1 wk; n = 35 rats) after pilocarpine injection. Because it has been previously established that all adult rats experiencing pilocarpine-induced SE will later exhibit spontaneous recurrent seizures (Cavalheiro et al. 1991; Priel et al. 1996), only a subset of pilocarpine-treated animals were video-monitored, and the presence of spontaneous behavioral seizures was confirmed in virtually all of them (n = 14/15). In this study, rats receiving a saline injection instead of pilocarpine were used as age-matched nonepileptic controls (NECs).

Slice preparation and maintenance

Adult rats were decapitated under halothane anesthesia; the brain was quickly removed, and a block of brain tissue containing the retrohippocampal region was placed in cold (1–3°C), oxygenated artificial cerebrospinal fluid (ACSF). The brain dorsal side was cut along a horizontal plane that was tilted by a 10° angle along a postero-superior-anteroinferior plane passing between the lateral olfactory tract and the base of the brain stem (Benini et al. 2003). Horizontal slices (400–450 μm thick) were cut from this brain block using a vibratome, and slices were transferred into a tissue chamber where they lay at the interface between ACSF and humidified gas (95% O_2-5% CO_2) at a temperature of 34–35°C and a pH of 7.4. We focused in this study on the most ventral slices that were comprised between −8.6 and −7.6 mm from the bregma (Paxinos and Watson 1998). These slices contained the hippocampus proper, the parahippocampal cortices, and the lateral nucleus of the amygdala (LA; Fig. 1*A*). Two to three of such slices could be obtained from each hemisphere. ACSF composition was (in mM) 124 NaCl, 2 KCl, 1.25 KH_2PO_4, 2 $MgSO_4$, 2 $CaCl_2$, 26 $NaHCO_3$, and 10 glucose. (2*S*)-3-{[(1*S*)-1-(3,4-Dichlorophenyl)ethyl] amino-2-hydroxypropyl}(phenyl-methyl)phosphinic acid (CGP 55845A, 10 μM), 6-cyano-7-nitroquinoxaline-2,3-dione (CNQX, 10 μM), 3,3-(2-carboxypiperazin-4-yl)-propyl-1-phosphonate (CPP, 10 μM), and picrotoxin (PTX, 50 μM) were applied to the bath. Chemicals were acquired from Sigma (St. Louis, MO) with the exception of CGP 55845A, CNQX, and CPP, which were obtained from Tocris Cookson (Ellisville, MO).

Electrophysiological recordings and stimulation protocols

Field potential recordings were made from the LA and deep layers of the perirhinal cortex (PC) with ACSF-filled, glass pipettes (resistance = 2–10 MΩ) that were connected to high-impedance amplifiers (Fig. 1*A*). Sharp-electrode intracellular recordings were performed in LA with pipettes that were filled with 3 M K-acetate or with 3 M K-acetate/75 mM lidocaine, *N*-ethyl bromide (QX314; tip resistance = 70–120 MΩ in both cases). Intracellular signals were fed to a high-impedance amplifier with internal bridge circuit for intracellular current injection. The resistance compensation was monitored throughout the experiment and adjusted as required. The passive membrane properties of LA cells included in this study were measured as follows: *1*) resting membrane potential (RMP) after cell withdrawal; *2*) apparent input resistance (R_i) from the maximum voltage change in response to a hyperpolarizing current pulse (100–200 ms, < −0.6 nA); *3*) action potential amplitude (APA) from baseline; and *4*) action potential duration (APD) at half-amplitude. Intrinsic firing patterns of LA cells were classified from responses to depolarizing current pulses of 1,000- to 2,500-ms duration. The adaptation ratio (AR), defined as the ratio of the last interspike interval (ISI) to the first ISI, was used to quantitatively compare the firing properties of cells from pilocarpine (n = 30) and NEC groups (n = 30) (cf. Takazawa et al. 2004). For each cell, AR was obtained from a 1,200-ms depolarizing pulse at a current intensity 0.2 nA larger than that which induced threshold action potential firing.

Synaptic responses to single shock stimulation (50–100 μs; <350 μA) of local LA networks was assessed using a bipolar, stainless steel electrode placed <500 μm from the recording electrodes. "Monosynaptic" IPSPs were evoked in the presence of glutamatergic antagonists (10 μM CPP + 10 μM CNQX). The stimulation parameters used to elicit these responses were not significantly different (P > 0.05) between pilocarpine (stimulus intensity = 203 ± 21 μA; duration = 100 μs; n = 22) and NEC (stimulus intensity = 175 ± 17 μA; duration = 100 μs; n = 16) groups. Reversal potential and peak conductance values for the early and late components of the IPSPs were obtained from a series of responses evoked at membrane potentials set to different levels by intracellular current injection. Reversal potentials were computed from regression plots of response amplitude versus membrane potential. Peak conductance values were estimated using the parallel conductance model (cf. Williams et al. 1993). Briefly, the membrane potential versus intensity of injected current was plotted *1*) before the stimulation and *2*) at the peak of the IPSP response. The slopes of these two regression lines were used to yield the input resistance at rest (i.e., before the stimulation) and during the response, respectively, and to ultimately determine the change in resistance that occurred during the IPSP (ΔR_{IPSP}). ΔR_{IPSP} was translated to peak conductance changes (ΔG_{IPSP}) using the following formula: $\Delta G_{IPSP} = 1/\Delta R_{IPSP}$.

Paired stimuli (100-μs duration) at intervals from 50 to 1,600 ms were used to assess changes in synaptic depression of "monosynaptic" $GABA_A$ receptor–mediated IPSPs by using K-acetate/QX314-filled electrodes. For the paired pulse protocols, the stimulus current strength giving >50% maximal response was used to stimulate LA interneuronal networks. Furthermore, cells were hyperpolarized by current injection to obtain depolarizing IPSPs. The membrane potential at which the test was conducted was not significantly different (P > 0.05) between the two experimental groups (pilocarpine-treated = −102 ± 2 mV, n = 10 and NEC = −105 ± 3 mV; n = 10); in addition, the absolute amplitude of the first response (P1) evoked at this membrane potential was not different in pilocarpine-treated (9 ± 0.5 mV, n = 10) and NEC (10 ± 0.5 mV, n = 10) neurons.

Field potential and intracellular signals were fed to a computer interface (Digidata 1322A, Axon Instruments) and were acquired and stored using the pClamp 9 software (Axon Instruments). Subsequent data analysis was made with the Clampfit 9 software (Axon Instru-

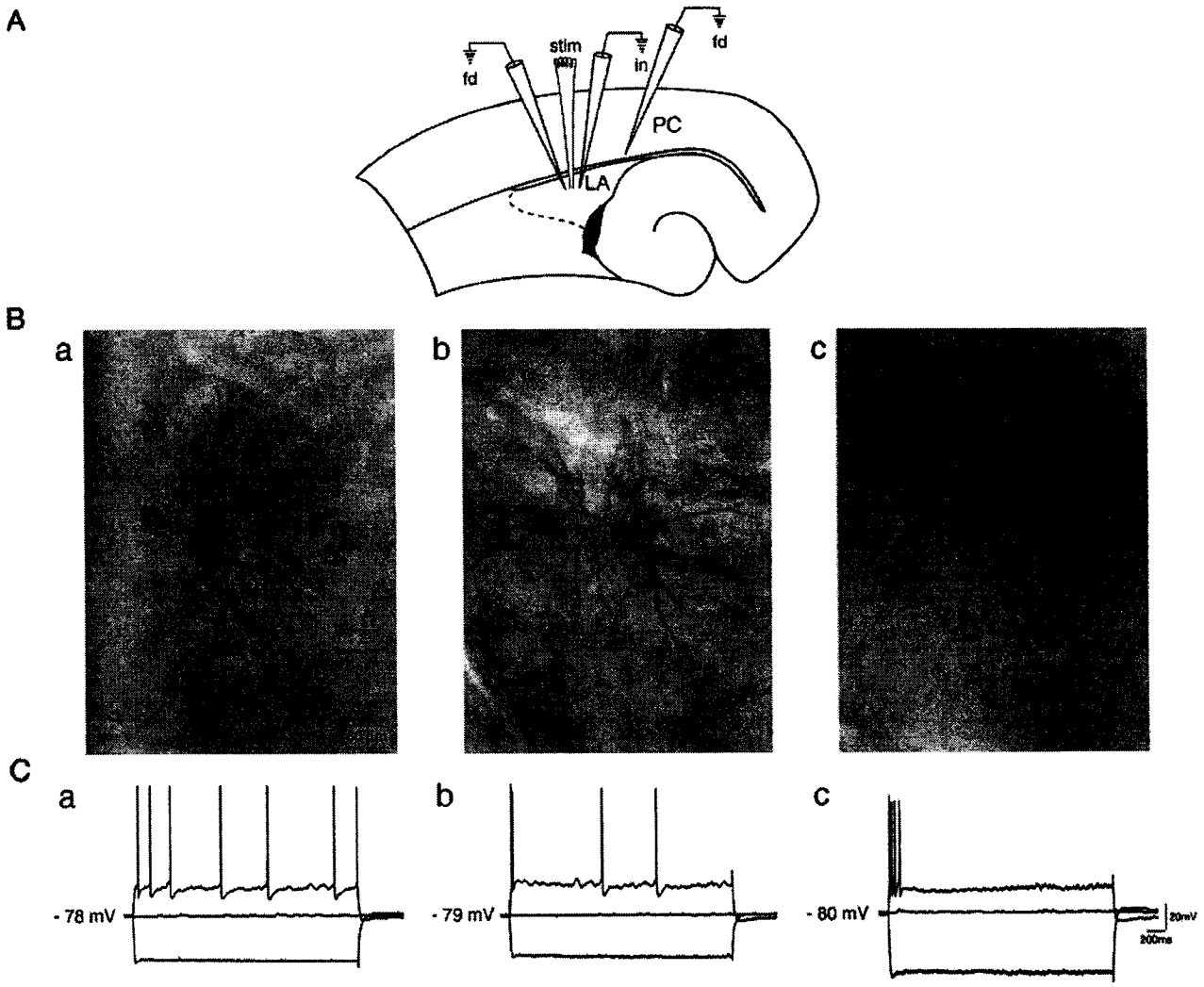

FIG. 1. Slice preparation and sites of recording. *A*: diagram of typical combined horizontal slice preparation showing position of field (fd), intracellular (in), and stimulating (stim) electrodes placed within the lateral amygdala (LA) and perirhinal cortex (PC). *B*: neurobiotin-staining identifies stellate (*a*), bipolar (*b*), and pyramidal-like (*c*) cells in pilocarpine-treated tissue. Respective firing properties of these cells are shown in *C* (*a–c*). Note that LA neurons show a range of spike frequency adaptation. Magnitude of current pulses injected include −1.0, 0, and +0.6 nA in *a* and −1.0, 0, and +0.8 nA in *b* and *c*.

ments). For time-delay measurements, the onset of the field potential/intracellular signals was determined as the time of the earliest deflection of the baseline recording (e.g., Fig. 2*Ca, inset*). Measurements in the text are expressed as means ± SE, and n indicates the number of slices or neurons studied under each specific protocol. Data were compared with the Student's t-test and were considered statistically significant if $P < 0.05$.

Neuronal labeling

Electrodes for intracellular labeling were filled with 2% neurobiotin dissolved in 2 M K-acetate. Intracellular injection of neurobiotin was accomplished by passing pulses of depolarizing current (0.5–1 nA, 3.3 Hz, 150 ms) through the recording electrode for 2–10 min. Neurobiotin injection did not have any appreciable effect on RMP, R_i, and evoked action potential properties (cf. Xi and Xu 1996). Only one neuron was filled in each slice. After the electrophysiological characterization of these neurons, slices were removed from the recording chamber and fixed in 4% paraformaldehyde and 100 mM phosphate-buffered solution overnight at 4°C. Slices were rinsed in PBS, and the endogenous peroxidase activity extinguished by incubating them in 0.1% phenylhydrazine for 20 min. After several rinses in PBS, the slices were incubated for 2 h in 1% Triton X-100 and then in vectastain ABC reagent comprising the avidin-biotinylated horseradish peroxidase complex in PBS for ≥4 h. After a wash in PBS, the sections were reacted with 0.5% 3,3′-diaminobenzidine tetrahydrochloride and 0.003% hydrogen peroxide in PBS, mounted on slides, dehydrated, and covered (Kita and Armstrong 1991). The intracellularly stained neurons were photographed using the Nomarski optics or a Zeiss Axiophot microscope. Neurobiotin and vectastain ABC were obtained from Vector Laboratories.

RESULTS

Intrinsic electrophysiological properties and morphology of lateral amygdala neurons

Intracellular recordings were carried out in the LA of brain slices obtained from pilocarpine-treated rats (n = 83 cells from 66 slices) and age-matched NECs (n = 54 cells from 41 slices). Morphological identification with intracellular injection of neurobiotin was also carried out in some neurons (n = 17 and

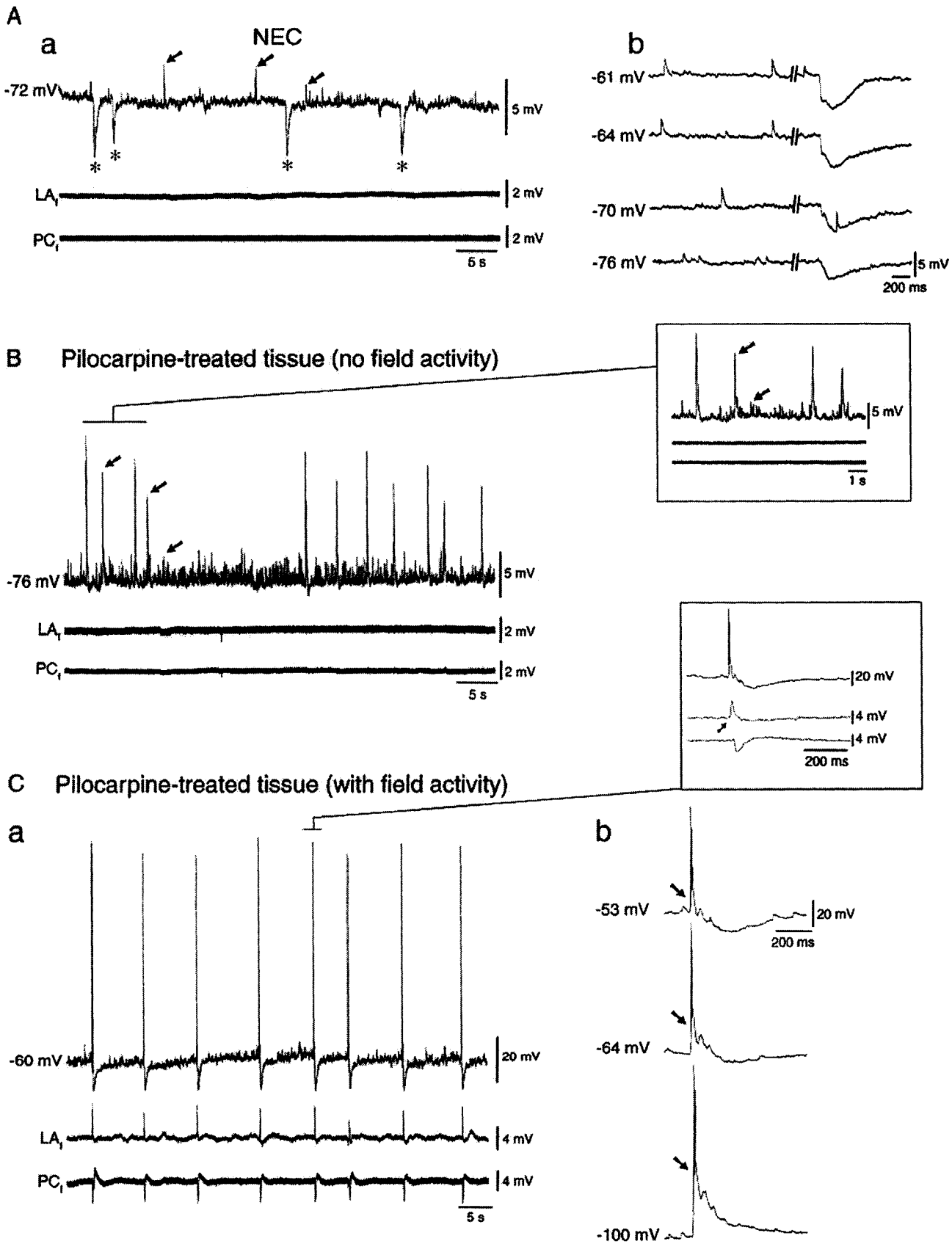

TABLE 1. *Intrinsic and regular firing properties of LA neurons in NEC and pilocarpine-treated rats*

	NEC (46)	Pilocarpine (68)
RMP, mV	−70.7 ± 1.0	−71.9 ± 0.9
Ri, MΩ	46.6 ± 1.3	47.7 ± 1.2
APA, mV	98.5 ± 1.3	99.3 ± 0.9
APD, ms	1.5 ± 0.03	1.6 ± 0.03
AR*	9.1 ± 1.8	13.5 ± 3.0

Values are RMP, resting membrane potential; Ri, input resistance; APA, action potential amplitude; APD, action potential duration at half amplitude; AR, adaptation ratio; NEC, nonepileptic control. *AR values were calculated for $n = 30$ cells from each group. Values are mean ± SE. Number in parentheses represents neurons.

TABLE 2. *Spontaneous synaptic activity recorded at rest from LA neurons in NEC and pilocarpine-treated rats*

	NEC	Neurons	Pilocarpine	Neurons
Spontaneous Bursting Activity*				14
Duration, ms			786 ± 514	
Rate of occurrence, s			13.1 ± 10.7	
Depolarizing PSPs		26		33
Amplitude, mV	1.71 ± 0.33		2.73 ± 0.05	
Rate of occurrence, s	0.72 ± 0.04		1.02 ± 0.07	
Hyperpolarizing PSPs		14		16
Amplitude, mV	−3.4 ± 0.2		−3.0 ± 0.1	
Rate of occurrence, s	18.0 ± 5.0		22.0 ± 4.0	

Values are mean ± SE. LA, lateral amygdala; NEC, nonepileptic controls; PSP, postsynaptic potentials. *These events were only observed in a subset of pilocarpine-treated tissue but never in NEC. **Indicates values significantly different ($P < 0.05$) from NEC.

11 in pilocarpine and NEC slices, respectively). Based on a gross visual examination of cell body shape and dendrite distribution, three main types of principal spiny neurons could be distinguished in both epileptic and NEC tissue: *1*) stellate-like elements (8/17 and 6/11 of pilocarpine and NEC neurons, respectively; Fig. 1*Ba*); *2*) bipolar-shaped cells (2/17 and 0/11 of pilocarpine and NEC neurons, respectively; Fig. 1*Bb*); and *3*) pyramidal-like neurons (7/17 and 5/11 of pilocarpine and NEC cells, respectively; Fig. 1*Bc*).

Analysis of the intrinsic properties of cells recorded in the two types of tissue revealed no significant differences in RMP, Ri, APD, and APA (Table 1). Moreover, as previously reported by other investigators (Faber et al. 2001; Faulkner and Brown 1999), the regular firing characteristics of LA neurons consisted of a spectrum of different spike adaptations (Fig. 1, *Ca–Cc*). The range of adaptation ratios (AR, see METHODS) varied between 1.1 and 69.0 in pilocarpine and between 1.3 and 43.5 in NEC neurons, with no significant difference in the AR distribution between the two groups ($P = 0.2$). Thus no disparity in the expression of the different modalities of repetitive firing could be identified between NEC and pilocarpine-treated neurons.

Spontaneous synaptic activity in LA of pilocarpine-treated rats is altered

Field potential recordings obtained during application of normal ACSF from the LA and the PC of NEC slices ($n = 41$) showed the absence of any spontaneous activity (Fig. 2*Aa*, *bottom*). Moreover, when analyzed with intracellular recordings, all neurons from this group exhibited at RMP depolarizing PSPs with amplitudes of 1.71 ± 0.03 mV (range = 0.5–8.4 mV, $n = 26$) and rates of occurrence of 0.72 ± 0.04 s (range = 0.01–13.5 s, $n = 26$; Fig. 2*Aa*, arrows; Table 2). In addition, spontaneous hyperpolarizing PSPs (sIPSPs; amplitude: −3.4 ± 0.2 mV; rate of occurrence: 18 ± 5 s, range = 0.2–140 s, $n = 14$) could be recorded in 53% of NEC LA neurons ($n = 25/47$; Fig. 2*Aa*,*; Table 2). Steady hyperpolarization and depolarization of the membrane potential altered the amplitude of these two types of spontaneous activities without influencing their rate of occurrence, thereby confirming their synaptic nature (Fig. 2*Ab*).

Spontaneous field activity was also absent from the majority of pilocarpine-treated slices [$n = 52/66$; Fig. 2*B*, pilocarpine-treated tissue (no field activity)]. As in NEC tissue, neurons recorded intracellularly from pilocarpine-treated slices also exhibited spontaneous depolarizing PSPs with amplitudes of 2.73 ± 0.05 mV (range = 0.7–16.6 mV, $n = 33$) and rates of occurrence of 1.02 ± 0.07 s (range = 0.01–21.8s, $n = 33$; Fig. 2*B*, arrows, *inset*; Table 2). Distribution analysis revealed that, although there was no significant difference between the two groups in their rate of occurrence, depolarizing PSPs recorded from pilocarpine-treated slices skewed toward larger amplitudes (Fig. 3*A*; $P < 0.001$; Table 2). Furthermore, in contrast to the NEC group, an appreciably lower proportion (31%) of cells ($n = 21/68$) in the epileptic group displayed sIPSPs at RMP (amplitude: −3.0 ± 0.1 mV; rate of occurrence: 22 ± 4 s, range = 1–210 s, $n = 16$; Fig. 3*B*, RMP; Table 2). This difference in the expression of sIPSPs between the two experimental groups was evident even when neurons were depolarized to approximately −60 mV to unmask any reversed inhibitory potentials (Fig. 3*B*, depolarized MP). Thus these results suggest that pilocarpine-treated LA cells display subtle differences in synaptic activity. These alterations include the presence of larger amplitude depolarizing PSPs (Figs. 2, *A* and *B*, and 3*A*) and reduced incidence of sIPSPs (Fig. 3*B*).

In addition to these differences, more significant changes were observed in 21% of slices from the pilocarpine-treated group [$n = 14/66$; Figs. 2*Ca* and 3*Da*, pilocarpine-treated tissue (with field activity)]. In these slices, spontaneous field activity (duration: 786 ± 514 ms, range: 190–2,100 ms; rate of

FIG. 2. Spontaneous synaptic activity in nonepileptic control (NEC) and pilocarpine-treated tissue. *Aa*: simultaneous field [LA_f, deep perirhinal cortex (PC_f)] and intracellular recording (−72 mV) in NEC tissue reveals *1*) depolarizing postsynaptic potentials (PSPs) indicated by arrows and *2*) robust spontaneous hyperpolarizing inhibitory PSPs (sIPSP) indicated by asterisks. *Ab*: spontaneous synaptic activity recorded during depolarization and hyperpolarization of membrane potential by steady current injection of +0.2, +0.1, −0.1, and −0.2 nA (from *top* to *bottom*). Note the larger amplitude and biphasic nature of sIPSPs at more depolarized levels (−61 to −76 mV). *B*: simultaneous field (LA_f, PC_f) and intracellular activity (−76 mV) recorded in majority of pilocarpine-treated tissue. Note absence of field activity (LA_f, PC_f) and presence of large depolarizing PSPs indicated by arrows in the intracellular trace. Expansion of these events is depicted in the *right top inset*. *Ca*: simultaneous field (LA_f, PC_f) and intracellular activity (−60 mV) recorded in a subset of pilocarpine-treated slices reveals robust network activity (LA_f, PC_f). Expansion of an event shows initiation in LA (arrow) and spread to PC (*right top inset*). *Cb*: steady hyperpolarization and depolarization of membrane potential with current injections of +0.2, −0.2, and −0.8 nA (from *top* to *bottom*) alters amplitude of underlying excitatory PSPs (EPSPs; arrow), thereby confirming the synaptic nature of the event.

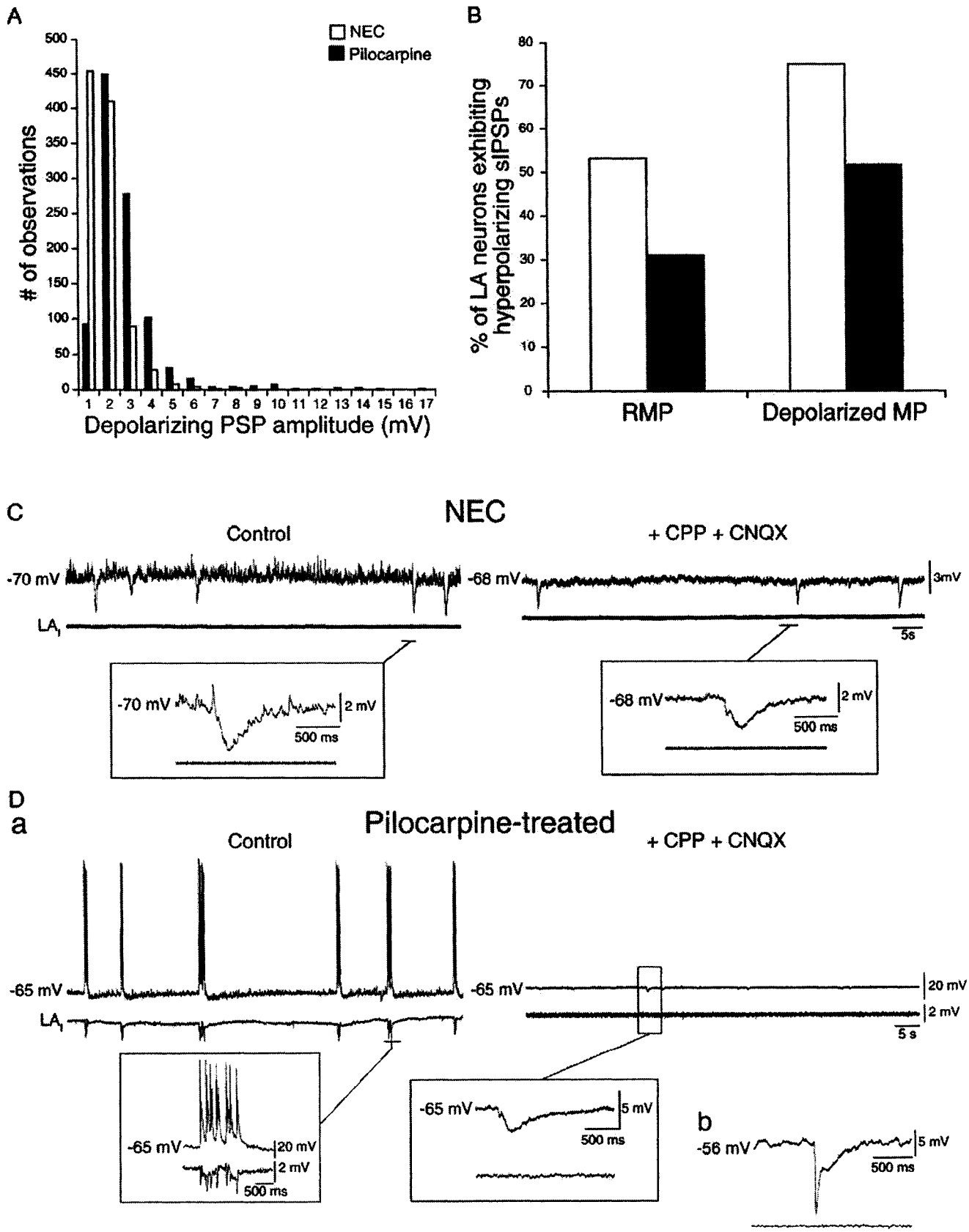

occurrence: 13.1 ± 10.7 s, 7–41 s; Table 2) could be recorded in the LA, and at times could spread to the deep layers of the PC (n = 3; Fig. 2*Ca*). Intracellularly, this network activity corresponded to robust neuronal firing at RMP (n = 14 cells), and in the majority of these cells (n = 11/14), no sIPSPs could be recorded (Figs. 2*Ca* and 3*Da*, control). The increasing amplitude of the underlying excitatory postsynaptic potential with hyperpolarization of the membrane potential confirmed the synaptic nature of these events (Fig. 2*Cb*, arrows).

Pharmacology of spontaneous activity

The NMDA receptor antagonist CPP reduced the frequency of occurrence of spontaneous depolarizing PSPs in both NEC (n = 7) and pilocarpine-treated tissue (n = 4). Further treatment with the non-NMDA receptor antagonist CNQX abolished these PSPs (n = 10 and 11 in pilocarpine and NEC slices, respectively) without affecting the occurrence of hyperpolarizing sIPSPs that were often biphasic (Fig. 3*C*, +CPP+CNQX, *inset*) and reduced by the $GABA_A$ receptor antagonist picrotoxin (n = 4, data not shown). CPP+CNQX application to pilocarpine-treated slices exhibiting spontaneous field events completely abolished this network activity (Fig. 3*Da*, +CPP+CNQX) and uncovered biphasic sIPSPs (Fig. 3, *Da* and *Db*) that were diminished with picrotoxin addition.

Evidence for alterations in inhibitory networks of LA

The incidence of sIPSPs at RMP was lower in LA neurons recorded from pilocarpine-treated slices compared with those of the NEC group (Fig. 3*B*, RMP). This difference was also evident even when the membrane potential was depolarized to approximately −60 mV to unmask any reversed sIPSPs (Fig. 3*B*, depolarized MP). This observation suggested that altered inhibition occurred in the LA of pilocarpine-treated animals.

To isolate and assess the activity of local inhibitory networks within the LA of NEC and pilocarpine-treated rats, we analyzed the intracellular responses of LA neurons to single-shock stimulation in the presence of glutamatergic antagonists (CPP+CNQX). As reported by previous studies (Heinbockel and Pape 1999), these "monosynaptic" stimulus-evoked IPSPs in the NEC group (n = 13) were biphasic in nature, with an early $GABA_A$ receptor–mediated component (Fig. 4*A*, NEC, early) and a late $GABA_B$ receptor component (Fig. 4*A*, NEC, late). Similar observations were made in the pilocarpine group (n = 13, pilocarpine-treated), thereby suggesting that postsynaptic $GABA_A$ and $GABA_B$ receptor mechanisms remained intact. However, comparison of the reversal potentials of the early IPSP component revealed a significantly ($P < 0.002$) more depolarized value in pilocarpine-treated neurons (−65.9 ± 1.5 mV, n = 13) than NEC cells (−74.5 ± 0.7 mV, n = 13; Fig. 4*B*, early phase). Peak conductance of the early IPSP component was also different ($P < 0.05$) between the two groups, with a lower peak conductance in the pilocarpine-treated tissue (7.3 ± 1.1 nS, n = 15) compared with NEC (12.1 ± 1.6 nS, n = 15; Fig. 4*C*).

Similar assessment of the late $GABA_B$ receptor–mediated component of the IPSP revealed no difference in reversal potentials between pilocarpine-treated (−95.7 ± 1.9 mV, n = 13) and NEC cells (−93.3 ± 2.0 mV, n = 11; Fig. 4*B*, late phase). However, the peak conductance of this late IPSP component was slightly lower in pilocarpine (2.2 ± 0.4 nS, n = 14) versus NEC neurons (4.6 ± 0.7 nS, n = 11; Fig. 4*C*, late phase). Altogether, these results indicate that alterations in postsynaptic GABAergic mechanisms, specifically in $GABA_A$ receptor–mediated inhibition, occur in the LA of epileptic rats.

Functional changes also involve presynaptic alterations

To determine whether modifications in presynaptic mechanisms occurred in the LA of pilocarpine-treated rats, we delivered paired stimuli (100-μs duration; <350-μA intensity) at intervals of 50–1,600 ms with a stimulating electrode placed within 500 μm from the recording electrode. Recordings were carried out with QX-314–filled microelectrodes in the presence of CPP+CNQX. In addition to its well-known effects on voltage-gated sodium channels (Connors and Prince 1982), QX-314 blocks $GABA_B$ receptors (Nathan et al. 1990), thus allowing the isolation of the fast $GABA_A$ receptor–mediated component of the IPSP. Furthermore, because of the ability of this lidocaine derivative to attenuate I_h (Perkins and Wong 1995), the corresponding IPSPs could be assessed more easily in their reversed form at hyperpolarized membrane potentials (Fig. 5, *A* and *B*).

In NEC slices, paired-pulse stimulation protocols revealed a marked depression in the amplitude of the second stimulus-induced IPSP (P2) with respect to the first (P1) at interstimulus intervals between 50 and 1,000 ms (Fig. 5, *A* and *C*; n = 10). The second IPSP amplitudes recovered to initial values at intervals of ≥1,200 ms (Fig. 5*C*). In contrast, paired IPSPs in LA neurons recorded from pilocarpine-treated tissue tended to exhibit a less pronounced depression at interstimulus intervals between 50 and 1,600 ms compared with NEC, thereby suggesting a failure in presynaptic GABAergic interneuron autoreceptors (Fig. 5, *B* and *C*; n = 10). The difference between NEC and pilocarpine-treated groups was statistically different ($P < 0.05$) at interstimulus intervals between 200 and 1,000 ms (Fig. 5*C*, *).

Presynaptic $GABA_B$ receptors have been shown to contribute to the paired-pulse depression of $GABA_A$ receptor–mediated IPSCs induced in the LA by paired stimulation of cortical and thalamic inputs in the presence of glutamatergic transmission (Szinyei et al. 2000). To determine whether the same was true for the monosynaptic IPSPs induced in our experimental

FIG. 3. Distribution and pharmacology of spontaneous activity. *A*: distribution histogram of the amplitude of depolarizing PSP events pooled from pilocarpine-treated (n = 33 neurons, 1,000 events) and NEC (n = 26 neurons, 1,000 events) groups at resting levels. Note that in pilocarpine-treated tissue, these events distribute at higher amplitudes. *B*: histogram comparing incidence of hyperpolarizing sIPSPs in NEC (n = 47 cells) vs. pilocarpine-treated tissue (n = 68 cells) at resting levels (RMP) and more depolarized membrane potentials (depolarized MP). Note lower incidence of sIPSPs in pilocarpine-treated tissue. *C*: bath application of glutamatergic antagonists (+CPP+CNQX) to NEC tissue abolishes depolarizing PSPs but does not affect sIPSPs. *Bottom insets*: expansion of sIPSP events. *Da*: in pilocarpine-treated tissue exhibiting field activity in LA (control), bath application of glutamatergic antagonists (+CPP+CNQX) abolishes spontaneously occurring network bursting (expansion in *bottom left*) and uncovers biphasic sIPSPs (expansion in *bottom right inset*). *Db*: depolarizing the membrane to −56 mV with a steady current injection of +0.5 nA increases amplitude of these sIPSPs.

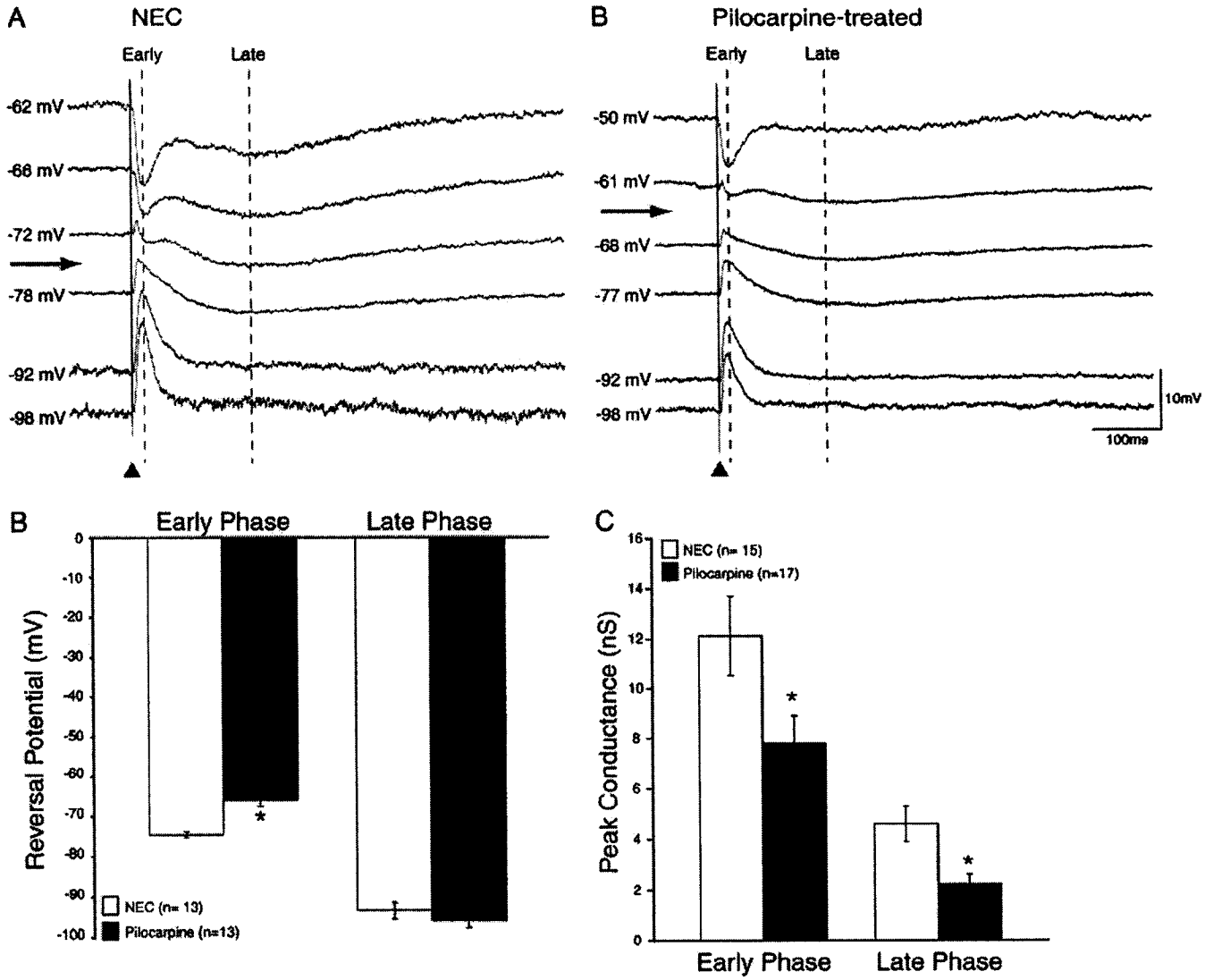

FIG. 4. $GABA_A$-mediated component of evoked IPSP in pilocarpine-treated tissue exhibits a more depolarized reversal potential and a smaller peak conductance. *A*: comparison of the monosynaptic IPSPs evoked in the presence of CPP+CNQX in NEC and pilocarpine-treated tissue at membrane potentials set to different levels by intracellular current injection (−0.6 to +0.6 nA in NEC and −0.8 to +0.6 nA in pilocarpine-treated). Note biphasic nature of these IPSPs (early and late components). Also note that reversal potential of early component (arrow) is more depolarized in NEC vs. pilocarpine-treated tissue. Triangles indicate stimulus artifact. *B*: histogram comparing reversal potential of early and late IPSP components in NEC vs. pilocarpine-treated group. *Significance at $P < 0.002$. *C*: histogram comparing peak conductance of early and late IPSP components in NEC vs. pilocarpine-treated group. *Significance at $P < 0.05$; n represents number of neurons. Error bars: means ± SE.

paradigm (i.e., in the absence of glutamatergic transmission), the effect of the $GABA_B$ receptor antagonist CGP 55845A on the magnitude of the IPSP paired-pulse depression (PPD) was tested at an interstimulus interval yielding maximal depressant effects (400 ms). In NEC tissue, CGP 55845A increased the P2/P1 ratio by 24.7 ± 4.7% in 6 of 12 neurons (Fig. 5*D*). On the other hand, PPD in pilocarpine-treated cells tended to be less affected by $GABA_B$ receptor antagonism, which increased the P2/P1 ratio in only three of nine neurons by 11.7 ± 0.9% (Fig. 5*D*). The difference in the extent of PPD attenuation by CGP 55845A was marginally significant between the NEC (24.7 ± 4.7%, $n = 6$) and pilocarpine-treated cells (11.7 ± 0.9%, $n = 3$) at $P = 0.05$. Altogether, these results suggest that presynaptic $GABA_B$ receptors may contribute to controlling neurotransmitter release from LA interneurons and point toward the possibility of altered presynaptic $GABA_B$ receptor–mediated mechanisms in chronically epileptic animals.

DISCUSSION

In this study, we sought to identify the functional changes that occur within the LA using the pilocarpine rodent model of TLE. The results obtained show that alterations in LA network excitability occur in chronically epileptic rats. Specifically, LA neurons exhibit larger PSPs and a lower incidence of hyperpolarizing sIPSPs than those observed in NEC animals. Moreover, in contrast to NEC, a subset of slices from the pilocarpine group displayed intense network bursting in LA. Finally, in

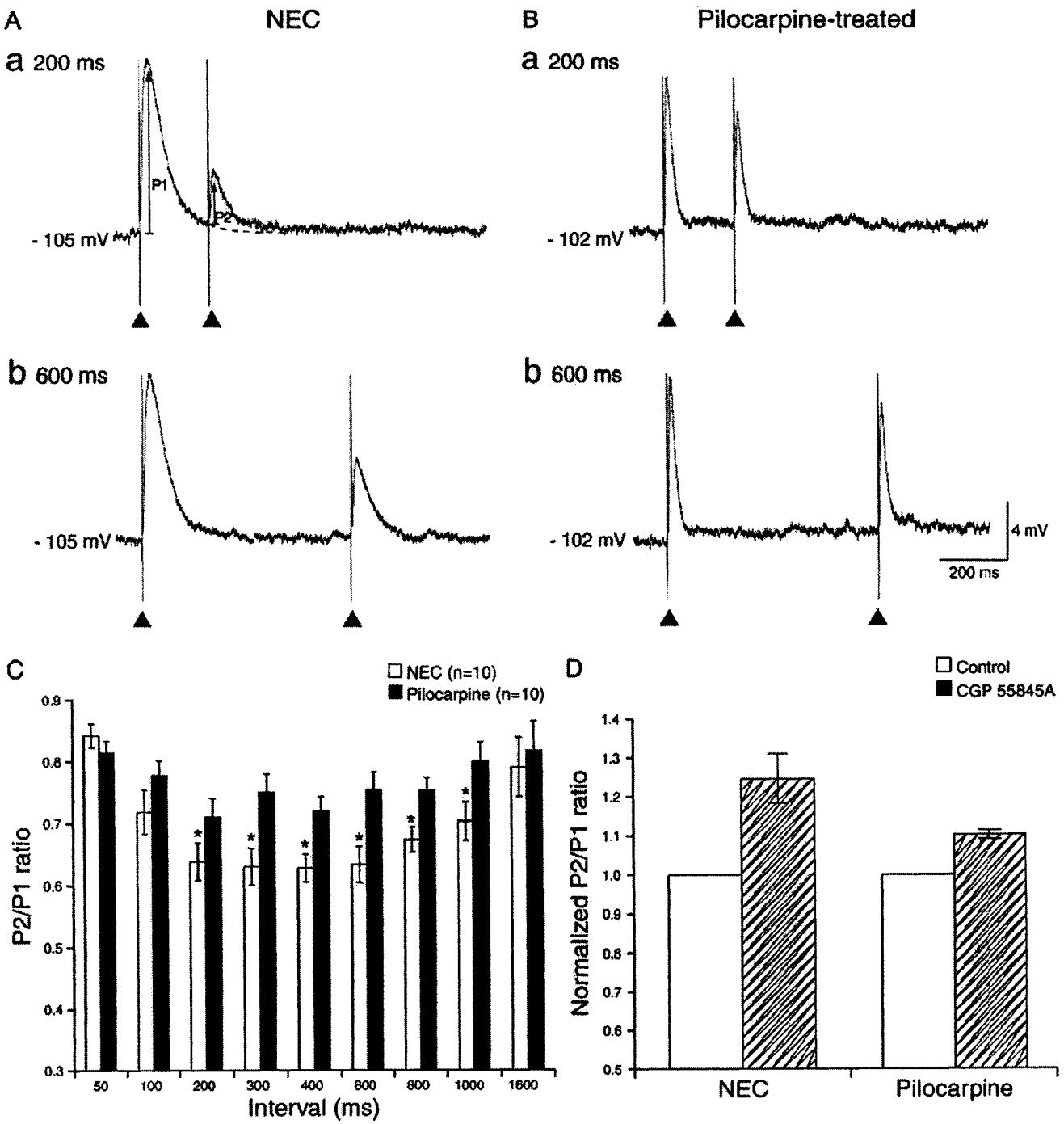

FIG. 5. Pilocarpine-treated tissue exhibits a less pronounced paired-pulse depression of monosynaptically evoked IPSPs. *A*: intracellular recording from a hyperpolarized LA neuron (−105 mV, −0.4 nA injected current) in NEC tissue showing paired IPSPs (P1 and P2) at interstimulus intervals of (*a*) 200 and (*b*) 600 ms. Note marked depression of P2 relative to P1 at both intervals. *B*: intracellular recording from a hyperpolarized LA cell (−102 mV, −0.8 nA injected current) in pilocarpine-treated tissue showing paired IPSPs (P1 and P2) at interstimulus intervals of (*a*) 200 and (*b*) 600 ms. Note that at both intervals, there is less paired-pulse depression (PPD) of the 2nd response with respect to the 1st. *C*: plot of P2/P1 ratios for interstimulus intervals between 50 and 1,600 ms. Note that pilocarpine-treated tissue exhibits less PPD than NEC. *Interstimulus intervals at which the 2 groups were significantly different from each other ($P < 0.05$). *D*: effect of CGP 55845A on the normalized P2/P1 ratio in NEC ($n = 6$) and pilocarpine-treated tissue ($n = 3$). Note the less pronounced effect of $GABA_B$ receptor antagonism in the pilocarpine-treated group ($P = 0.05$). *n* represents number of neurons. Error bars: means ± SE.

addition to the lower incidence of sIPSPs observed in the epileptic group, we provide for the first time evidence for both postsynaptic and, presumably, presynaptic modifications in GABA receptor–mediated mechanisms.

Synaptic alterations in LA of epileptic rats

Because of the overwhelming body of clinical evidence implicating the amygdala in the initiation and spread of limbic seizures, various studies have sought to identify the cellular

and network mechanisms underlying the role of this nucleated structure in epileptogenesis. In vitro studies have shown that, in the presence of convulsive agents, synaptic recruitment of amygdalar neurons through both excitatory and inhibitory mechanisms endows it with the ability to generate epileptic discharges and participate in epileptiform synchronization of limbic networks (Benini et al. 2003; Gean 1990; Gean and Shinnick-Gallagher 1988; Klueva et al. 2003; Stoop and Pralong 2000). Furthermore, studies carried out in the BLA of kindled (Gean et al. 1989; Mangan et al. 2000; Rainnie et al. 1992; Shoji et al. 1998) and kainate-treated rodents (Smith and Dudek 1997) have shown that, in addition to cellular loss and gliosis, permanent changes in synaptic transmission render this amygdaloid region epileptic. We report here similar results in the LA of pilocarpine-treated rats where spontaneous NMDA/non-NMDA–sensitive epileptiform bursting and large amplitude depolarizing PSPs occurred.

Interestingly, a reduced incidence of sIPSPs was also evident in pilocarpine-treated tissue compared with nonepileptic controls, thereby suggesting that alterations in inhibitory mechanisms had also taken place. This finding is relevant considering the extensive immunohistochemical and electrophysiological data showing that the amygdala is rich in GABAergic cells and that inhibitory processes play an underlining role in controlling the excitability of the LA (Pitkanen and Amaral 1994; Smith et al. 1998). For instance, stimulation of various afferents in vivo results in mainly inhibitory responses within the LA (Le Gal La Salle 1976; Lang and Pare 1997, 1998). Furthermore, as shown here and by other investigators, in vitro stimulation of LA networks yields biphasic IPSP responses that are mediated by $GABA_A$ and $GABA_B$ receptors (Danober and Pape 1998; Martina et al. 2001; Sugita et al. 1992). Moreover, we found that the majority of LA neurons in NEC tissue exhibit robust spontaneously occurring IPSPs that are resistant to glutamatergic antagonists but are sensitive to $GABA_A$ receptor antagonism, thus further substantiating a significant role for inhibitory networks within this nucleus.

Histological examination of epileptic tissue has shown a reduction of GABAergic neurons within the LA (Tuunanen 1996, 1997), possibly accounting for the reduced incidence of sIPSPs observed in our pilocarpine-treated tissue. It is noteworthy to mention that, in contrast to studies reporting a complete loss of sIPSPs in the BLA of epileptic animals (Gean et al. 1989; Rainnie et al. 1992), we have shown here that inhibitory inputs onto principal cells are not completely lost in the LA of pilocarpine-treated tissue. This is evident by the continued presence of sIPSPs in epileptic tissue, albeit in a smaller proportion of cells. Our findings are in line with previous reports that show a partial loss of interneurons within the LA of chronically epileptic rats, with some studies even reporting >50% of surviving interneurons (Tuunanen et al. 1996, 1997). Finally, decreased dendritic branching of surviving principal cells in the epileptic amygdala (Aliashkevich et al. 2003) also raises the possibility that interneurons make fewer contacts onto pyramidal cells and could perhaps contribute to the reduced incidence of sIPSPs in pilocarpine-treated slices. Hence, our findings suggest that, in epileptic rats, alterations in both excitatory and inhibitory synaptic transmission contribute to the hyperexcitability of LA neuronal networks.

Altered postsynaptic $GABA_A$ receptor–mediated inhibition

To further assess the changes in inhibitory inputs onto LA principal cells, IPSPs induced in the presence of glutamatergic antagonists were studied in pilocarpine-treated and NEC tissue. Interestingly, we were able to record biphasic IPSPs in the LA of both types of tissue, thereby indicating that $GABA_A$ and $GABA_B$ receptor–mediated mechanisms were present in the epileptic group. However, notable differences were observed in the reversal potential of the fast component of the IPSP. Specifically, the reversal potential of this $GABA_A$ receptor–mediated component was found to be significantly more depolarized in the pilocarpine-treated tissue compared with NECs. In fact, the reversal potential in the epileptic tissue was more positive than the mean resting membrane potential by ~6 mV. Altogether, this signifies that postsynaptic $GABA_A$ receptor–mediated potentials have a greater chance to be depolarizing at resting levels in the pilocarpine-treated group compared with NECs where the reversal potential is more negative than RMP.

GABA generally tends to induce hyperpolarization of neurons in the adult brain. However, there are several instances such as in the developing juvenile brain (Ben Ari et al. 1989) or in the adult brain under high-frequency stimulation (Lamsa and Taira 2003; Voipio and Kaila 2000) where depolarizing effects of GABA are known to occur. Furthermore, the excitatory actions of GABA have also been documented under pathological conditions such as epilepsy (Cohen et al. 2002), pain (Coull et al. 2003), and ischemia (Schwartz-Bloom and Sah 2001). Several mechanisms have been proposed to account for this polarity switch in GABA action including modified Cl^- gradients caused by a decreased expression of the K^+/Cl^- cotransporter KCC2 (Rivera et al. 1999) and deafferentiation (Vale and Sanes 2000). Thus the more depolarized reversal potential and the lower peak conductance of the $GABA_A$-mediated IPSP denotes an excitatory effect of GABA in the LA of pilocarpine-treated tissue. These changes may potentially reduce the hyperpolarizing effect of inhibitory inputs onto principal cells, bring LA neurons closer to firing threshold, and consequently facilitate epileptiform synchronization.

Reduced presynaptic depression of GABA release

Alterations in presynaptic release of neurotransmitters are known to contribute to hyperexcitability of different neuronal networks (Asprodini et al. 1992; Behr et al. 2002; Jarvie et al. 1990; Kamphuis et al. 1990). In this study, we used paired-pulse stimulation protocols in the absence of glutamatergic transmission to indirectly assess whether there were any changes in the release of GABA from LA interneurons of epileptic rats. Interneuronal inputs onto pyramidal cells generally show a frequency-dependent depression (Gupta et al. 2000). A pronounced depression in the second IPSP compared with the first would indicate that presynaptic autoreceptors are at play in controlling the release of GABA. Alternatively, additional mechanisms could include a depletion in the presynaptic vesicle pool (von Gersdorff and Borst 2002), presynaptic metabotropic receptors (Cartmell and Schoepp 2000), or even postsynaptic effects such as desensitization of receptors (Jones and Westbrooke 1996) and shifts in Cl^- gradients (Kaila 1994; Thompson and Gahwiler 1989). Interestingly, we found in NEC tissue a pronounced PPD of $GABA_A$-mediated

responses that was partially reduced by $GABA_B$ receptor antagonism. This evidence suggests that these G protein–linked receptors might play a role in controlling neurotransmitter release from LA interneurons (Miller 1998).

In contrast, we found in pilocarpine-treated tissue a depression in the paired IPSP ratio that was less pronounced and less affected by $GABA_B$ receptor antagonism compared with NEC. Altogether, these observations suggest that presynaptic $GABA_B$ receptors might be less efficient in controlling the release of GABA from LA interneurons of epileptic rodents. At first glance, these results are by themselves peculiar because less PPD in an excitatory network may imply more excitation, but in an inhibitory context may mean more inhibition caused by increased GABA at the synapse, specifically at high-frequency stimulation. However, the reduced PPD combined with the data suggesting a depolarizing effect of GABA could conceivably lead to hyperexcitability of LA neuronal networks in epileptic tissue.

In conclusion, until recently, most electrophysiological assessments of the amygdala and specifically of the BLA were carried out in coronal slices in which connections with other limbic structures are not maintained (Gean et al. 1989; Mangan et al. 2000; Rainnie et al. 1992; Shoji et al. 1998; Smith and Dudek 1997). However, the advent of the combined horizontal slice preparation (Stoop and Pralong 2000; von Bohlen und Halbach and Albrecht 2002) has enabled evaluation of the amygdala's participation in intralimbic synchronization of epileptiform activity (Benini et al. 2003; Klueva et al. 2003; Stoop and Pralong 2000). The LA is heavily interconnected with hippocampal and parahippocampal structures that are highly implicated in TLE, and it is of crucial importance to determine what significance the alterations presented in this study have on the interactions of the LA with other structures like the perirhinal and entorhinal cortices.

ACKNOWLEDGMENTS

We thank T. Papadopoulos for secretarial assistance and B. Tahvildari for help with the morphological identification of neurobiotin-stained neurons.

GRANTS

This study was supported by Canadian Institutes of Health Research Grant MOP-8109 and the Savoy Foundation. R. Benini is supported by an MD/PhD studentship from Fonds de la Recherche en Santé Québec.

REFERENCES

Aliashkevich AF, Yilmazer-Hanke D, Van Roost D, Mundhenk B, Schramm J, and Blumcke I. Cellular pathology of amygdala neurons in human temporal lobe epilepsy. *Acta Neuropathol (Berl)* 106: 99–106, 2003.

Asprodini EK, Rainnie DG, and Shinnick-Gallagher P. Epileptogenesis reduces the sensitivity of presynaptic gamma-aminobutyric acidB receptors on glutamatergic afferents in the amygdala. *J Pharmacol Exp Ther* 262: 1011–1021, 1992.

Behr J, Gebhardt C, Heinemann U, and Mody I. Kindling enhances kainate receptor-mediated depression of GABAergic inhibition in rat granule cells. *Eur J Neurosci* 16: 861–867, 2002.

Ben-Ari Y, Cherubini E, Corradetti R, and Gaiarsa JL. Giant synaptic potentials in immature rat CA3 hippocampal neurones. *J Physiol* 416: 303–325, 1989.

Benini R, D'Antuono M, Pralong E, and Avoli M. Involvement of amygdala networks in epi-leptiform synchronization in vitro. *Neuroscience* 120: 75–84, 2003.

Callahan PM, Paris JM, Cunningham KA, and Shinnick-Gallagher P. Decrease of GABA-immunoreactive neurons in the amygdala after electrical kindling in the rat. *Brain Res* 555: 335–339, 1991.

Cartmell J and Schoepp DD. Regulation of neurotransmitter release by metabotropic glutamate receptors. *J Neurochem* 75: 889–907, 2000.

Cavalheiro EA, Leite JP, Bortolotto ZA, Turski WA, Ikonomidou C, and Turski L. Long-term effects of pilocarpine in rats: structural damage of the brain triggers kindling and spontaneous recurrent seizures. *Epilepsia* 32: 778–782, 1991.

Cavalheiro EA, Silva DF, Turski WA, Calderazzo-Filho LS, Bortolotto ZA, and Turski L. The susceptibility of rats to pilocarpine-induced seizures is age-dependent. *Brain Res* 465: 43–58, 1987.

Cohen I, Navarro V, Clemenceau S, Baulac M, and Miles R. On the origin of interictal activity in human temporal lobe epilepsy in vitro. *Science* 298: 1418–1421, 2002.

Connors BW and Prince DA. Effects of local anesthetic QX-314 on the membrane properties of hippocampal pyramidal neurons. *J Pharmacol Exp Ther* 220: 476–481, 1982.

Coull JA, Boudreau D, Bachand K, Prescott SA, Nault F, Sik A, De Koninck P, and De Koninck Y. Trans-synaptic shift in anion gradient in spinal lamina I neurons as a mechanism of neuropathic pain. *Nature* 424: 938–942, 2003.

Danober L and Pape HC. Mechanisms and functional significance of a slow inhibitory potential in neurons of the lateral amygdala. *Eur J Neurosci* 10: 853–867, 1998.

Du F, Whetsell WO Jr, Abou-Khalil B, Blumenkopf B, Lothman EW, and Schwarcz R. Preferential neuronal loss in layer III of the entorhinal cortex in patients with temporal lobe epilepsy. *Epilepsy Res* 16: 223–233, 1993.

Faber ES, Callister RJ, and Sah P. Morphological and electrophysiological properties of principal neurons in the rat lateral amygdala in vitro. *J Neurophysiol* 85: 714–723, 2001.

Faulkner B and Brown TH. Morphology and physiology of neurons in the rat perirhinal-lateral amygdala area. *J Comp Neurol* 411: 613–642, 1999.

Fujikawa DG. The temporal evolution of neuronal damage from pilocarpine-induced status epilepticus. *Brain Res* 725: 11–22, 1996.

Gean PW. The epileptiform activity induced by 4-aminopyridine in rat amygdala slices: antagonism by non-N-methyl-D-aspartate receptor antagonists. *Brain Res* 530: 251–256, 1990.

Gean PW and Shinnick-Gallagher P. Characterization of the epileptiform activity induced by magnesium-free solution in rat amygdala slices: an intracellular study. *Exp Neurol* 101: 248–255, 1988.

Gean PW, Shinnick-Gallagher P, and Anderson AC. Spontaneous epileptiform activity and alteration of GABA- and of NMDA-mediated neurotransmission in amygdala neurons kindled in vivo. *Brain Res* 494: 177–181, 1989.

Gloor P. Role of the amygdala in temporal lobe epilepsy. In: *The Amygdala: Neurobiological Aspects of Emotion, Memory and Mental Dysfunction,* edited by Aggleton J. New York: Wiley-Liss, 1992, p. 505–538.

Gloor P. *The Temporal Lobe and Limbic System.* New York: Oxford, 1997.

Gupta A, Wang Y, and Markram H. Organizing principles for a diversity of GABAergic interneurons and synapses in the neocortex. *Science* 287: 273–278, 2000.

Heinbockel T and Pape HC. Modulatory effects of adenosine on inhibitory postsynaptic potentials in the lateral amygdala of the rat. *Br J Pharmacol* 128: 190–196, 1999.

Jarvie PA, Logan TC, Geula C, and Slevin JT. Entorhinal kindling permanently enhances Ca^{2+}-dependent -glutamate release in regio inferior of rat hippocampus. *Brain Res* 508: 188–193, 1990.

Jones MV and Westbrook GL. The impact of receptor desensitization on fast synaptic transmission. *Trends Neurosci* 19: 96–101, 1996.

Kaila K. Ionic basis of GABAA receptor channel function in the nervous system. *Prog Neurobiol* 42: 489–537, 1994.

Kamphuis W, Huisman E, Dreijer AM, Ghijsen WE, Verhage M, and Lopes da Silva FH. Kindling increases the K(+)-evoked Ca2(+)-dependent release of endogenous GABA in area CA1 of rat hippocampus. *Brain Res* 511: 63–70, 1990.

Kita H and Armstrong W. A biotin-containing compound N-(2-aminoethyl) biotinamide for intracellular labeling and neuronal tracing studies: comparison with biocytin. *J Neurosci Methods* 37: 141–150, 1991.

Klueva J, Munsch T, Albrecht D, and Pape HC. Synaptic and non-synaptic mechanisms of amygdala recruitment into temporolimbic epileptiform activities. *Eur J Neurosci* 18: 2779–2791, 2003.

Lamsa K and Taira T. Use-dependent shift from inhibitory to excitatory GABAA receptor action in SP-O interneurons in the rat hippocampal CA3 area. *J Neurophysiol* 90: 1983–1995, 2003.

Lang EJ and Pare D. Similar inhibitory processes dominate the responses of cat lateral amygdaloid projection neurons to their various afferents. *J Neurophysiol* 77: 341–352, 1997.

Lang EJ and Pare D. Synaptic responsiveness of interneurons of the cat lateral amygdaloid nucleus. *Neuroscience* 83: 877–889, 1998.

LeDoux JE. Emotion circuits in the brain. *Annu Rev Neurosci* 23: 155–184, 2000.

Le Gal La Salle G. Unitary responses in the amygdaloid complex following stimulation of various diencephalic structures. *Brain Res* 118: 475–478, 1976.

Lopes da Silva FH, Witter MP, Boeijinga PH, and Lohman AH. Anatomic organization and physiology of the limbic cortex. *Physiol Rev* 70: 453–511, 1990.

Mangan PS, Scott CA, Williamson JM, and Bertram EH. Aberrant neuronal physiology in the basal nucleus of the amygdala in a model of chronic limbic epilepsy. *Neuroscience* 101: 377–391, 2000.

Martina M, Royer S, and Pare D. Cell-type-specific GABA responses and chloride homeostasis in the cortex and amygdala. *J Neurophysiol* 86: 2887–2895, 2001.

Miller RJ. Presynaptic receptors. *Annu Rev Pharmacol Toxicol* 38: 201–227, 1998.

Nathan T, Jensen MS, and Lambert JD. The slow inhibitory postsynaptic potential in rat hippocampal CA1 neurones is blocked by intracellular injection of QX-314. *Neurosci Lett* 110: 309–313, 1990.

Niittykoski M, Nissinen J, Penttonen M, and Pitkanen A. Electrophysiologic changes in the lateral and basal amygdaloid nuclei in temporal lobe epilepsy: an in vitro study in epileptic rats. *Neuroscience* 124: 269–281, 2004.

Nissinen J, Halonen T, Koivisto E, and Pitkanen A. A new model of chronic temporal lobe epilepsy induced by electrical stimulation of the amygdala in rat. *Epilepsy Res* 38: 177–205, 2000.

Pare D, Quirk GJ, and Ledoux JE. New vistas on amygdala networks in conditioned fear. *J Neurophysiol* 92: 1–9, 2004.

Paxinos G and Watson C. *The Rat Brain in Stereotaxic Coordinates* (4th ed.). San Diego, CA: Academic Press, 1998.

Perkins KL and Wong RK. Intracellular QX-314 blocks the hyperpolarization-activated inward current Iq in hippocampal CA1 pyramidal cells. *J Neurophysiol* 73: 911–915, 1995.

Pikkarainen M and Pitkanen A. Projections from the lateral, basal and accessory basal nuclei of the amygdala to the perirhinal and postrhinal cortices in rat. *Cereb Cortex* 11: 1064–1082, 2001.

Pitkanen A and Amaral DG. The distribution of GABAergic cells, fibers, and terminals in the monkey amygdaloid complex: an immunohistochemical and in situ hybridization study. *J Neurosci* 14: 2200–2224, 1994.

Pitkanen A, Jolkkonen E, and Kemppainen S. Anatomic heterogeneity of the rat amygdaloid complex. *Folia Morphol (Warsz)* 59: 1–23, 2000a.

Pitkanen A, Pikkarainen M, Nurminen N, and Ylinen A. Reciprocal connections between the amygdala and the hippocampal formation, perirhinal cortex, and postrhinal cortex in rat. A review. *Ann NY Acad Sci* 911: 369–391, 2000b.

Pitkanen A, Stefanacci L, Farb CR, Go GG, LeDoux JE, and Amaral DG. Intrinsic connections of the rat amygdaloid complex: projections originating in the lateral nucleus. *J Comp Neurol* 356: 288–310, 1995.

Pitkanen A, Tuunanen J, Kalviainen R, Partanen K, and Salmenpera T. Amygdala damage in experimental and human temporal lobe epilepsy. *Epilepsy Res* 32: 233–253, 1998.

Priel MR, dos Santos NF, and Cavalheiro EA. Developmental aspects of the pilocarpine model of epilepsy. *Epilepsy Res* 26: 115–121, 1996.

Racine RJ. Modification of seizure activity by electrical stimulation. II. Motor seizure. *Electroencephalogr Clin Neurophysiol* 32: 281–294, 1972.

Rainnie DG, Asprodini EK, and Shinnick-Gallagher P. Kindling-induced long-lasting changes in synaptic transmission in the basolateral amygdala. *J Neurophysiol* 67: 443–454, 1992.

Rivera C, Voipio J, Payne JA, Ruusuvuori E, Lahtinen H, Lamsa K, Pirvola U, Saarma M, and Kaila K. The K^+/Cl–co-transporter KCC2 renders GABA hyperpolarizing during neuronal maturation. *Nature* 397: 251–255, 1999.

Schwartz-Bloom RD and Sah R. gamma-Aminobutyric acid(A) neurotransmission and cerebral ischemia. *J Neurochem* 77: 353–371, 2001.

Scott SK, Young AW, Calder AJ, Hellawell DJ, Aggleton JP, and Johnson M. Impaired auditory recognition of fear and anger following bilateral amygdala lesions. *Nature* 385: 254–257, 1997.

Shoji Y, Tanaka E, Yamamoto S, Maeda H, and Higashi H. Mechanisms underlying the enhancement of excitatory synaptic transmission in basolateral amygdala neurons of the kindling rat. *J Neurophysiol* 80: 638–646, 1998.

Smith BN and Dudek FE. Enhanced population responses in the basolateral amygdala of kainate-treated, epileptic rats in vitro. *Neurosci Lett* 222: 1–4, 1997.

Smith Y, Pare JF, and Pare D. Cat intraamygdaloid inhibitory network: ultrastructural organization of parvalbumin-immunoreactive elements. *J Comp Neurol* 391: 164–179, 1998.

Stoop R and Pralong E. Functional connections and epileptic spread between hippocampus, entorhinal cortex and amygdala in a modified horizontal slice preparation of the rat brain. *Eur J Neurosci* 12: 3651–3663, 2000.

Stork O and Pape HC. Fear memory and the amygdala: insights from a molecular perspective. *Cell Tissue Res* 310: 271–277, 2002.

Sugita S, Johnson SW, and North RA. Synaptic inputs to GABAA and GABAB receptors originate from discrete afferent neurons. *Neurosci Lett* 134: 207–211, 1992.

Szinyei C, Heinbockel T, Montagne J, and Pape HC. Putative cortical and thalamic inputs elicit convergent excitation in a population of GABAergic interneurons of the lateral amygdala. *J Neurosci* 20: 8909–8915, 2000.

Takazawa T, Saito Y, Tsuzuki K, and Ozawa S. Membrane and firing properties of glutamatergic and GABAergic neurons in the rat medial vestibular nucleus. *J Neurophysiol* 92: 3106–3120, 2004.

Thompson SM and Gahwiler BH. Activity-dependent disinhibition. I. Repetitive stimulation reduces IPSP driving force and conductance in the hippocampus in vitro. *J Neurophysiol* 61: 501–511, 1989.

Tuunanen J, Halonen T, and Pitkanen A. Status epilepticus causes selective regional damage and loss of GABAergic neurons in the rat amygdaloid complex. *Eur J Neurosci* 8: 2711–2725, 1996.

Tuunanen J, Halonen T, and Pitkanen A. Decrease in somatostatin-immunoreactive neurons in the rat amygdaloid complex in a kindling model of temporal lobe epilepsy. *Epilepsy Res* 26: 315–327, 1997.

Vale C and Sanes DH. Afferent regulation of inhibitory synaptic transmission in the developing auditory midbrain. *J Neurosci* 20: 1912–1921, 2000.

van Elst LT, Woermann FG, Lemieux L, Thompson PJ, and Trimble MR. Affective aggression in patients with temporal lobe epilepsy: a quantitative MRI study of the amygdala. *Brain* 123: 234–243, 2000.

Voipio J and Kaila K. GABAergic excitation and K(+)-mediated volume transmission in the hippocampus. *Prog Brain Res* 125: 329–338, 2000.

von Bohlen und Halbach O and Albrecht D. Reciprocal connections of the hippocampal area CA1, the lateral nucleus of the amygdala and cortical areas in a combined horizontal slice preparation. *Neurosci Res* 44: 91–100, 2002.

von Gersdorff H and Borst JG. Short-term plasticity at the calyx of held. *Nat Rev Neurosci* 3: 53–64, 2002.

Wilensky AE, Schafe GE, and LeDoux JE. The amygdala modulates memory consolidation of fear-motivated inhibitory avoidance learning but not classical fear conditioning. *J Neurosci* 20: 7059–7066, 2000.

Williams S, Vachon P, and Lacaille JC. Monosynaptic GABA-mediated inhibitory postsynaptic potentials in CA1 pyramidal cells of hyperexcitable hippocampal slices from kainic acid-treated rats. *Neuroscience* 52: 541–554, 1993.

Xi XZ and Xu ZC. The effect of neurobiotin on membrane properties and morphology of intracellularly labeled neurons. *J Neurosci Methods* 65: 27–32, 1996.

Yilmazer-Hanke DM, Wolf HK, Schramm J, Elger CE, Wiestler OD, and Blumcke I. Subregional pathology of the amygdala complex and entorhinal region in surgical speci-mens from patients with pharmacoresistant temporal lobe epilepsy. *J Neuropathol Exp Neurol* 59: 907–920, 2000.

APPENDIX E: Animal Subject Use Approval